SSC-373

PROBABILITY BASED SHIP DESIGN; LOADS AND LOAD COMBINATIONS

94 8 29   1 1 5

SHIP STRUCTURE COMMITTEE

1994

SHIP STRUCTURE COMMITTEE

The SHIP STRUCTURE COMMITTEE is constituted to prosecute a research program to improve the hull structures of ships and other marine structures by an extension of knowledge pertaining to design, materials, and methods of construction.

RADM A. E. Henn, USCG (Chairman)
Chief, Office of Marine Safety, Security
 and Environmental Protection
U. S. Coast Guard

Mr. Thomas H. Peirce
Marine Research and Development
 Coordinator
Transportation Development Center
Transport Canada

Mr. H. T. Haller
Associate Administrator for Ship-
 building and Ship Operations
Maritime Administration

Dr. Donald Liu
Senior Vice President
American Bureau of Shipping

Mr. Alexander Malakhoff
Director, Structural Integrity
 Subgroup (SEA 05P)
Naval Sea Systems Command

Mr. Thomas W. Allen
Engineering Officer (N7)
Military Sealift Command

Mr. Warren Nethercote
Head, Hydronautics Section
Defence Research Establishment-Atlantic

EXECUTIVE DIRECTOR

CDR Stephen E. Sharpe, USCG
Ship Structure Committee
U. S. Coast Guard

CONTRACTING OFFICER TECHNICAL REPRESENTATIVE

Mr. William J. Siekierka
SEA 05P4
Naval Sea Systems Command

SHIP STRUCTURE SUBCOMMITTEE

The SHIP STRUCTURE SUBCOMMITTEE acts for the Ship Structure Committee on technical matters by providing technical coordination for determinating the goals and objectives of the program and by evaluating and interpreting the results in terms of structural design, construction, and operation.

AMERICAN BUREAU OF SHIPPING

Mr. Stephen G. Arntson (Chairman)
Mr. John F. Conlon
Mr. Phillip G. Rynn
Mr. William Hanzelek

NAVAL SEA SYSTEMS COMMAND

Mr. W. Thomas Packard
Mr. Charles L. Null
Mr. Edward Kadala
Mr. Allen H. Engle

TRANSPORT CANADA

Mr. John Grinstead
Mr. Ian Bayly
Mr. David L. Stocks
Mr. Peter Timonin

MILITARY SEALIFT COMMAND

Mr. Robert E. Van Jones
Mr. Rickard A. Anderson
Mr. Michael W. Touma
Mr. Jeffrey E. Beach

MARITIME ADMINISTRATION

Mr. Frederick Seibold
Mr. Norman O. Hammer
Mr. Chao H. Lin
Dr. Walter M. Maclean

U. S. COAST GUARD

CAPT G. D. Marsh
CAPT W. E. Colburn, Jr.
Mr. Rubin Scheinberg
Mr. H. Paul Cojeen

DEFENCE RESEARCH ESTABLISHMENT ATLANTIC

Dr. Neil Pegg
LCDR D. O'Reilly
Dr. Roger Hollingshead
Mr. John Porter

SHIP STRUCTURE SUBCOMMITTEE LIAISON MEMBERS

U. S. COAST GUARD ACADEMY

LCDR Bruce R. Mustain

U. S. MERCHANT MARINE ACADEMY

Dr. C. B. Kim

U. S. NAVAL ACADEMY

Dr. Ramswar Bhattacharyya

CANADA CENTRE FOR MINERALS AND ENERGY TECHNOLOGIES
Dr. William R. Tyson

SOCIETY OF NAVAL ARCHITECTS AND MARINE ENGINEERS
Dr. William Sandberg

U. S. TECHNICAL ADIVSORY GROUP TO THE INTERNATIONAL STANDARDS ORGANIZATION
CAPT Charles Piersall

NATIONAL ACADEMY OF SCIENCES – MARINE BOARD
Dr. Robert Sielski

NATIONAL ACADEMY OF SCIENCES – COMMITTEE ON MARINE STRUCTURES
Mr. Peter M. Palermo

WELDING RESEARCH COUNCIL

Dr. Martin Prager

AMERICAN IRON AND STEEL INSTITUTE

Mr. Alexander D. Wilson

OFFICE OF NAVAL RESEARCH

Dr. Yapa D. S. Rajapakse

Ship Structure Committee

An Interagency Advisory Committee

7 April, 1994

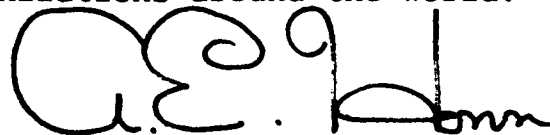## PROBABILITY-BASED SHIP DESIGN; LOADS AND LOAD COMBINATIONS

This work is the second in a five phase program planned by the Ship Structure Committee to develop a reliability based ship design methodology. Reliability methods have been developed for other fields of engineering and are in successful use today. Through their use it expected that vessel structures will be able to be designed to be less expensive, less prone to structural failure, and with possibly reduced weight.

The unique nature of marine structures field presents many difficult problems in the development of a reliability based design method, and loads and load combinations are a significant example. Here the loads problem is looked a from several angles; identification of loads, treatment of combined load effects for fatigue, and modeling errors due to loads, response, and structural analysis. Procedures are developed to address loads for different design situations. The author presents a new design oriented probabilistic load combination factor method for steady state wave induced load effects, and a time domain method suitable for combining vertical wave induced bending and transient slam effects.

Besides the five phase project this work is being coordinated with other projects; the recent SSC-371: Development of a Uniform Format for Data Reporting of Structural Material Properties for Reliability Analysis, NAVSEA Small Business Innovative Research (SBIR) project SR1344: Assessment of Reliability of Ship Structures, and ongoing work with the International Ship Structures Congress and other organizations around the world.

A. E. HENN
Rear Admiral, U. S. Coast Guard
Chairman, Ship Structure Committee

1. Report No SSC-373	2. Government Accession No. PB94-188208	3. Recipient's Catalog No.	
4. Title and Subtitle PROBABILITY-BASED SHIP DE LOADS AND LOAD COMBINAT		5. Report Date November 1993	
		6. Performing Organization Code	
7. Author(s) A. Mansour, A. Thayamballi		8. Performing Organization Report No. SR 1337	
9. Performing Organization Name and Address Mansour Engineering, Inc 14 Maybeck Twin Dr. Berkeley, CA 94708		10. Work Unit No. (TRAIS)	
		11. Contract or Grant No. DTCG23-92-R-E01086	
12. Sponsoring Agency Name and Address Ship Structure Committee U.S. Coast Guard (G-M) 2100 Second Street, SW Washington, D.C. 20593		13. Type of Report and Period Covered Final Report	
		14. Sponsoring Agency Code G-M	

15. Supplementary Notes

Sponsored by the Ship Structure Committee and its Member Agencies

16. Abstract

Several aspects of loads and load combinations for reliability based ship design are investigated. These include identification of relevant hull girder and local loads, load calculation models, procedures for extreme loads and load combinations, treatment of combined load effects for fatigue, and modeling errors related to loads, response and structural analysis. Impact of operational factors such as heavy weather countermeasures on design loads is discussed. Load combination procedures of two levels of complexity are provided: a) those suitable for design use, and b) more elaborate ones for detailed analysis. Among the procedures are a new design oriented probabilistic load combination factor method for steady state wave induced load effects, and a time domain method suitable for combining vertical wave induced bending and transient slam effects.

Distribution /
Availability Codes

Dist	Avail and / or Special
A-I	

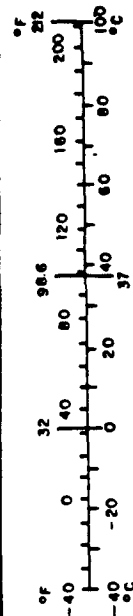| 17. Key Words Probability Loads Load Combinations Ship Design	18. Distribution Statement Available from: National Technical Information Service U.S. Department of Commerce Springfield, VA 22151		
19. Security Classif. (of this report) Unclassified	20. Security Classif. (of this page) Unclassified	21. No. of Pages 270	22. Price

Form DOT F 1700.7 (8—72) Reproduction of completed page authorized

METRIC CONVERSION FACTORS

Approximate Conversions to Metric Measures

Symbol	When You Know	Multiply by	To Find	Symbol
		LENGTH		
in	inches	*2.5	centimeters	cm
ft	feet	30	centimeters	cm
yd	yards	0.9	meters	m
mi	miles	1.6	kilometers	km
		AREA		
in²	square inches	6.5	square centimeters	cm²
ft²	square feet	0.09	square meters	m²
yd²	square yards	0.8	square meters	m²
mi²	square miles	2.6	square kilometers	km²
	acres	0.4	hectares	ha
		MASS (weight)		
oz	ounces	28	grams	g
lb	pounds	0.45	kilograms	kg
	short tons (2000 lb)	0.9	tonnes	t
		VOLUME		
tsp	teaspoons	5	milliliters	ml
Tbsp	tablespoons	15	milliliters	ml
fl oz	fluid ounces	30	milliliters	ml
c	cups	0.24	liters	l
pt	pints	0.47	liters	l
qt	quarts	0.95	liters	l
gal	gallons	3.8	liters	l
ft³	cubic feet	0.03	cubic meters	m³
yd³	cubic yards	0.76	cubic meters	m³
		TEMPERATURE (exact)		
°F	Fahrenheit temperature	5/9 (after subtracting 32)	Celsius temperature	°C

*1 in = 2.54 (exactly). For other exact conversions and more detailed tables, see NBS Misc. Publ. 286, Units of Weights and Measures, Price $2.25, SD Catalog No. C13.10:286.

Approximate Conversions from Metric Measures

Symbol	When You Know	Multiply by	To Find	Symbol
		LENGTH		
mm	millimeters	0.04	inches	in
cm	centimeters	0.4	inches	in
m	meters	3.3	feet	ft
m	meters	1.1	yards	yd
km	kilometers	0.6	miles	mi
		AREA		
cm²	square centimeters	0.16	square inches	in²
m²	square meters	1.2	square yards	yd²
km²	square kilometers	0.4	square miles	mi²
ha	hectares (10,000 m²)	2.5	acres	
		MASS (weight)		
g	grams	0.035	ounces	oz
kg	kilograms	2.2	pounds	lb
t	tonnes (1000 kg)	1.1	short tons	
		VOLUME		
ml	milliliters	0.03	fluid ounces	fl oz
l	liters	2.1	pints	pt
l	liters	1.06	quarts	qt
l	liters	0.26	gallons	gal
m³	cubic meters	35	cubic feet	ft³
m³	cubic meters	1.3	cubic yards	yd³
		TEMPERATURE (exact)		
°C	Celsius temperature	9/5 (then add 32)	Fahrenheit temperature	°F

Temperature scale:
°F -40 0 32 40 80 98.6 120 160 200 212
°C -40 -20 0 20 37 40 60 80 100

PROBABILITY BASED SHIP DESIGN – LOADS AND LOAD COMBINATIONS

Table of Contents

ii

NOMENCLATURE

Symbol	Item
A	Wave Amplitude
B	Bias (actual/predicted value)
C	Rayleigh Multiplier
D	Fatigue Damage
$E(X)$	Expected value of X
$F_X(x)$	Cumulative Distribution Function of X
I	Indicator Variable
H_s	Significant Wave Height
$H(\omega)$	Transfer Function for Frequency ω
K	Probabilistic Load Factor
K_{c1}	Probabilistic Load Factor, first load
K_{c2}	Probabilistic Load Factor, second load
K_{c3}	Probabilistic Load Factor, third load
L	Vessel Length
M_v	Vertical Bending Moment
M_h	Horizontal Bending Moment
M_t	Torsional Moment
N_T	Number of Cycles in Time T
$P, Pr.$	Probability
P_s	Probability of Slamming
S_0	Extreme Stress at $1/N_T$ exceedence
$S(\omega)$	Spectral Density for Frequency ω
SM	Section Modulus
SM_v	Section Modulus, Vertical Bending
SM_h	Section Modulus, Horizontal Bending
X	Random Variable
f	Extreme Stress
$f_X(x)$	Probability Density Function of X
$g(X)$	Limit State Function
m_0, m_2, m_4	0-th, 2nd, and 4th Moment of Spectrum
p	Local Pressure
r	Ratio of Secondary to Primary Load (Stress)
r_2	Ratio of Second to First Load (Stress)
r_3	Ratio of Third to First Load (Stress)
t_p	Duration of Slam Impulse
t_s	Seastate Persistence Time
δ	Slam Phase Angle
ε	Bandwidth Parameter
λ	Slam Stress Decay Rate

ν_0	Rate of Zero Crossings
ω	Frequency
ρ	Correlation Coefficient
σ	r.m.s. Value
ζ	Weibull Shape Parameter
Note	Other Symbols Defined Where Used

1. INTRODUCTION AND LITERATURE SURVEY

1.1 Objectives, Scope and Summary

The immediate objective of the work is to define characteristics of ship design loads suitable for use in reliability analysis, and to recommend load models and load combination procedures for use in Phase 3 of the Ship Structure Committee (SSC) Probability-Based Ship Design thrust area, titled "Implementations of Design Guidelines for Ships".

To achieve these objectives, " ndard" loads necessary for a probability-based design procedure are identified. The hull girder (i.e., global) loads include still water loads and low and high frequency wave loads. The low frequency wave loads consist of vertical, horizontal and torsional wave loads while the high frequency loads are due to slamming and springing. Procedures of extrapolation of these loads to their extreme lifetime values are reviewed and models for their combinations developed.

In addition to the hull girder loads, local loads can be important particularly in the design of local structures. These local loads consist of external and internal loads. The external loads are due to still water loads (static head), low-frequency wave loads (dynamic pressure due to waves) and high frequency local slamming loads. The internal loads can result from inertia forces of cargo associated with ship motions and accelerations and also from sloshing of liquid cargo.

Extreme local loads (external and internal) and their combinations are evaluated in the project work. In addition, combinations of local and hull girder loads are also investigated. These combinations will depend to a large extent on the location along the ship. Two locations are particularly important as noted in the project work. These are the forward part of the ship where large shear forces exist particularly when slamming occurs, and near midship section where large bending moments are likely to occur together with local loads.

In addition to the extreme loads described earlier (global and local), fatigue loads are important in the design of details. These loads need a separate treatment since they require estimation of stress ranges and number of cycles during the ship life. Many factors influence fatigue life of details. Load models and load combination procedures for fatigue in both design and analysis contexts are provided in this work.

Modeling errors in connection with extreme loads and load combinations and in fatigue loads are part of the final load models. These errors result from deficiencies and assumptions made in analytical models of estimating the loads or from lack of sufficient data when the loads are estimated empirically. They may accumulate in one direction to form a "bias" and/or can be random (uncertain) as quantified by a coefficient of variation.

Finally, a synthesis of load models and load combination procedures for ship design is considered. In addition to the loads and other considerations mentioned earlier, the question of ship routing, storm avoidance, and operator discretion become relevant. In particular, the discussion addresses questions such as: To what extent (if any at all) should design load criteria reflect current day practice of ship routing, storm avoidance and operator discretion? Recommendations are also made as to ship design load models, load data and load combination procedures to be used in Phase 3 of the SSC thrust area of probability-based ship design, and for future research.

1.2 Analysis of the Problem and Method of Approach

Probability-based ship design requires determination of extreme wave loads acting on the ship and their critical combinations. Generally, these loads are dynamic and random in nature, therefore their combinations require the difficult but important analyses for determining the degree of correlation between the individual components. These analyses may be carried out either in a frequency domain or time domain. In many cases, non-linearities become important, particularly when these individual components are calculated

1-2

in high sea states in order to determine their extreme values. These non-linearities must in principle be considered in the determination of some of the critical load combinations and may require time rather than frequency domain analyses.

Another aspect that may also need to be considered is the flexibility of the hull. Normally, a hull girder is considered to be rigid for calculating the low frequency wave loads (vertical, horizontal and torsional). This assumption cannot be made when the high frequency response due to slamming or springing is considered. These vibratory responses require modeling of the hull flexibility even if the slamming loads themselves are approximated using rigid body analysis.

One aspect that increases the degree of correlation between the different wave load components is the fact that all of them (low and high frequency components) depend on wave condition or sea state. The problem may thus be considered as an input-output system in which the input (waves) is common to all components and the sum of the individual outputs represents the sought load effect combinations. Correlation between the individual components may be determined on that basis. The fact that the slamming load component depends also on the ship motion complicates the overall treatment of load combinations.

Local loads are also correlated to hull girder or global loads since both again depend on the wave surface elevation. Similar input-output model with common input may be used to determine the degree of correlation of these loads. The location along the hull and around the hull periphery becomes a relevant factor.

A part of the work of this project is to synthesize these different aspects of the problem together with the more practical aspects such as ship routing, storm avoidance, etc., with the objective of determining final load models and load combination procedures suitable for use in probability-based ship design. The suitability of a two-level approach is considered during the performance of the work. One level is for the preliminary stages of design where simplified load models and load combinations are valuable to have. The

second level is for the later stages of design where more accurate analysis is necessary and may require the use of specialized computer programs. Both levels can be made suitable for probability-based ship design if cast in appropriate formats.

A selected reference list of the relevant work on each subject is given at the end of each chapter. Of particular interest is the work by Ochi on slamming and extreme value statistics, Buckley and Stavovy on load criteria, Kaplan on ship hull failure uncertainties, Nikolaidis and Kaplan on uncertainties in stress analyses on marine structures, Liu, Chen and Lee on statistical wave load prediction, Wirsching on probability-based fatigue design, Thayamballi on fatigue load assessments, Munse on fatigue criteria, Wen on civil engineering load combinations, Mansour on extreme wave load models; slamming load models; on combining extreme environmental loads for reliability-based design; and on probabilistic analysis of combined slamming and wave induced responses.

1.3 Review of Load Combination Methods

It is the rule rather than the exception that at any location in the vessel structure, the net effect of more than one load needs to be obtained at the same instant in time. In a probabilistic sense, the basic aim is to determine the probability density function of the combined load effect, and hence the determination of the extreme value of the combined process. The determination of the entire distribution, while difficult, is important to the solution of the problem, and to the validation of simpler approaches.

The essential feature that complicates the problem is the fact that individual process extreme do not occur at the same instant in time, i.e., correlations and phasing of loads is important. The following, then, are basic to the treatment of load combinations in ships:

- For checking structural adequacy for combined extreme load effect, using a method that is a function of the individual extreme loads, while accounting for their phasing.

• For checking fatigue performance, one needs to use additional information regarding the shape of the entire density function of the combined load effect (excluding static), and information on the number of cyclic load fluctuations.

In the simplest possible estimation of the extreme load effect one assumes that the combined extreme load effect is the sum of the extreme values from individual processes that contribute additive effects. This so-called "peak coincidence method" leads to an oversized structure, since it is not typical that extreme values from individual processes occur at the same instant in time. There are also other simplified approaches possible, two worth mentioning being Turkstra's rule (1.1), and the square root of the sum of squares (SRSS) method (1.2), both of which work best when the processes whose effects are combined are independent.

The load coincidence technique due to Wen (1.3), and Wen and Pierce (1.4) is a rather general one in that it accounts for load correlations. The method requires the use of an average coincidence rate. Central concepts of the Wen method are summarized in Appendix A of this report.

Another class of methods are those which calculate the outcrossing rate of a vector load process from a safe domain defined by load and strength variables, the outcrossing rate being related to the probability distribution function of the combined effect. Until recently, the most general use of the method was based on outcrossing rate bounds, e.g., Larrabee and Cornell (1.5), who develop an upper bound based on a "point crossing" formula, the bound being exact for certain types of random processes. A lower bound is also obtainable, and the method can be extended for nonlinear combinations and to non stationary load processes. For more than two load processes, see Ditlevsen and Madsen (1.6).

A goal programming approach to evaluating upper and lower bound failure probabilities for structures without deteriorating strength, based on the outcrossing rate technique, has been recently suggested, Shi (1.7).

Recently, Hagen and Tvedt (1.8) have proposed a method to calculate the mean outcrossing rate that is applicable to both stationary and non stationary stochastic vector processes, provided the random variables representing the process and its time derivative process can be mapped into a set of independent standard normal variates. This requirement is the same as that used in first and second order reliability calculations, and the method is thus quite general. The method is based on Madsen's formula which expresses the mean upcrossing rate of a scalar process through a given level in terms of a parallel system sensitivity measure. This method has been used for outcrossing rate calculations with limit states involving nonlinear combinations of forces, e.g., in a von Mises yield criterion, or when the threshold level is varying, e.g., due to corrosion, see Friis Hansen (1.9).

1.4 A Survey of Load Combinations for Ships

A literature survey indicates the following to be some of the problems studied in the context of ships:

(a) Combination of hull girder vertical and horizontal bending effects

(b) Combination of vertical, horizontal and torsional moment effects

(c) Combination of vertical bending and local pressure effects

(d) Combination of vertical and horizontal moment and local pressure effects

(e) Combination of vertical bending and springing moments

(f) Combination of vertical bending and slamming moments

(g) Combination of vertical and horizontal bending moments and similar whipping moments

(h) Combination of still water and wave-induced bending moments in the long term

Items (a), (c) and (e) were studied by Stiansen and Mansour (1.10). The treatment is one of load or load effect combination in the short term, i.e., within a seastate and does not include the still water moment. The long term and still water effects were included in a paper by Mansour (1.11). The methodology for short term combination assumes a Gaussian seastate process and a linear, time invariant vessel system characterized by the appropriate system transfer functions for bending moments, pressures, etc. In effect, given the sea spectrum, system transfer functions and load to load effect relationships, the variance of the combined load effect, e.g., stress is obtained using probabilistic techniques. The method is described in detail by Mansour (1.11), and was extended to any number of loads including combination of vertical, horizontal and torsional moments (item b). The combination of the effects of vertical and horizontal moment and local pressure was considered in a recent report for ABS by Mansour et al. (1.12).

Ferro and Mansour (1.13) developed a method for combining hull girder bending moment and slamming loads, using both the square root of sum of squares method and Turkstra's rule, for a ship moving in irregular seas (item f). The slam loads are considered as a train of impulses of random intensity and random arrival times, with the dependence between intensity and arrival times considered in the stochastic modeling, per Mansour and Lozow (1.14). The low frequency wave-induced vertical bending moment process is assumed Gaussian.

The same problem of combining vertical bending moment and slamming was also studied by Nikolaidis and Kaplan (1.15). Their study used computer simulations of slamming and wave bending moments and their combinations for given time histories of wave surface elevation. For each time history, the maxima of the individual and combined bending moments were found. The combined maxima were also estimated on the basis of Turkstra's rule, the square root of the sum of squares method, and from the simplified peak coincidence assumption. Biases and their Coefficients of Variation (COV) were as follows:

Method	Bias	COV
Turkstra	1.17	0.11
SRSS	1.01	0.12
Peak – coincidence	0.72	0.11

In the above, bias is defined as the ratio of the actual value to the predicted value. The COV of the bias is the ratio of its standard deviation to mean. For other statistical terminology of interest, the reader is referred to (1.21). The results indicate Turkstra's rule to be optimistic, as might be expected, and the assumption of peak coincidence to be pessimistic, again as expected. The SRSS method appears to work the best, although the authors expressed some reservations in this regard.

The combination of long term extreme values of a still water and wave-induced bending moment was studied by Guedes Soares (1.16). The still water bending moment was assumed normally distributed, but with a "truncation factor" that accounts for the possibility of exceeding an allowable (rule) value. The long term wave-induced bending moment is considered exponentially distributed by Soares. The exponential distribution has also been shown to fit long term stress measurements in the case of the SL-7 containership by Mansour et al. (1.22). On the other hand, the NAVSEA-DTMB experience in long term wave induced loads indicates them to be best characterized by the Rayleigh distribution (1.23).

The combined moment is written by Soares in the formats:

$$M_c = \phi(M_s + M_w)$$

$$M_c = M_s + \psi M_w \tag{1.1}$$

where M_s and M_w are characteristic (rule) values. The load combination factors ϕ and ψ are obtained two ways, the first using Ferry Borges-Castenhata (1.17) pulse processes to represent the time variation in the still water and wave-induced bending moments, and the second using a pulse process for the still water moment alone, together with the point

crossing formula of Larrabee and Cornell (1.5). The two methods give comparable results, sample ϕ and ψ values being 0.97 and 0.94 for laden tankers.

The combination of vertical and horizontal bending moments and whipping moments has been studied in the context of naval vessels by Engle (1.18). In the investigation, the phase relationship between bending and whipping effects was studied based on measurements, and this information was used to develop a load combination methodology. Other experimental data relevant to ship loads and load combinations that we may mention, particularly for finer form vessels such as naval ships, are those related to the SL-7 containership, widely documented in Ship Structure Committee (SSC) reports, and Canadian Navy data for the Quest and Algonquin (1.19), (1.20).

References

1.1. Turkstra, C.J., "Theory of Structural Safety," SM Study No. 2, Solid Mechanics Division, University of Waterloo, Ontario, 1970.

1.2. Mattu, R.K., "Methodology for Combining Dynamic Responses," NUREG-0484, Rev. 1, Office NRR, U.S. NRC, May 1980.

1.3. Wen, Y.K., "Statistical Combination of Extreme Loads," *J. Structural Division*, ASCE, Vol. 103, No. ST5, May 1977, pp. 1079-1093.

1.4. Wen, Y.K. and Pearce, H.T., "Combined Dynamic Effects of Correlated Load Processes," *Nuclear Engineering and Design*, Vol. 75, 1982, pp. 179-189.

1.5. Larrabee, R.D. and Cornell, C.A., "Combination of Various Load Processes," *J. Structural Division*, ASCE, Vol. 107, No. ST1, 1981, pp. 223-239.

1.6. Ditlevsen, O. and Madsen, H.L., "Transient Load Modeling: Clipped Normal Processes," *J. Engg. Mechanics Division*, ASCE, Vol. 109, No. 2, 1983, pp. 495-515.

1.7. Shi, Wei-Biao, "Stochastic Load Combinations with Particular Reference to Marine Structures," *J. Marine Structures*, Vol. 4, 1991, Elsevier Science Publishers, U.K.

1.8. Hagen, O. and Tvedt, L., "Parallel System Approach for Vector Outcrossing," Trans. ASME, *J. Offshore Mechanics and Arctic Engineering*, Vol. 114, No. 2, May 1992, pp. 122-128.

1.9. Friis Hansen, P., "Reliability Based Design of a Midship Section," ongoing dissertation work. Department of Ocean Engineering, The Technical University of Denmark, Lyngby.

1.10. Stiansen, S.G. and Mansour, A.E., "Ship Primary Strength Based on Statistical Data Analysis," *Trans. SNAME*, 1975, pp. 214-243.

1.11. Mansour, A.E., "Combining Extreme Environmental Loads for Reliability Based Designs," in *Proc. SSC SNAME Extreme Loads Response Symposium*, Arlington, VA, October 1981, pp. 63-74.

1.12. Mansour, A.E., Thayamballi, A.K., Li, M. and Jue, M., "A Reliability Based Assessment of Safety Levels in the ABS Double Skin Tanker Guide," Final Report to ABS, July 1992.

1.13. Ferro, G. and Mansour, A.E., "Probabilistic Analysis of Combined Slamming and Wave Induced Responses," *J. Ship Research*, Vol. 29, No. 3, September 1985, pp. 170-188.

1.14. Mansour, A.E. and Lozow, J., "Stochastic Theory of Slamming Response of Marine Vehicles in Random Seas," *J. Ship Research*, Vol. 26, No. 4, December 1982, pp. 276-285.

1.15. Nikolaidis, E. and Kaplan, P., "Uncertainties in Stress Analysis of Marine Structures," SSC Report 363, April 1991.

1.16. Guedes Soares, C., "Stochastic Models for Load Effects for the Primary Ship Structure." Paper presented at the Euromech 250 Colloquium on Nonlinear Structural Systems under Random Conditions, Como, Italy, June 1989.

1.17. Ferry Borges, J. and Castenhata, M., "Structural Safety," Laboratoria Nacional de Engenhera Civil, Lisbon, 1971.

1.18. Engle, A. Private communication, 1991.

1.19. Campbell, W., "CFAV Quest Trials for NATO SGE (Hydro). Part III – Ship Motions and Hull Girder Strains during Cruise Q170, March 1989," Canadian Navy Technical Memorandum 91/217, December 1991.

1.20. Ellis, W.E. and Campbell, W., "HMCS Algonquin Hull Bending Strains and Motions in Rough Weather," Canadian Navy Technical Memorandum 89/226, November 1989.

1.21. Thayamballi, A. "Structural Reliability Process Definitions," Part 3 of Final Report or Ship Structure Committee project SR-1330, September 1992.

1.22. Mansour, A., Harding, S. and Zigelman, C., "Implementation of Reliability Methods to Marine Structures," Report to ABS, University of California at Berkeley, January 1993.

1.23. Comments of the Project Technical Committee for SR-1337, August 11, 1993.

2. LOADS FOR PROBABILITY-BASED DESIGN

This chapter enumerates the various loads that need to be considered in the probability-based design of oceangoing vessels. It also identifies certain relevant characteristics of such loads, e.g., their temporal and spatial reliability and correlations. This chapter is organized as follows:

Section 2.1 Identification of Relevant Loads

Section 2.2 Load Characteristics of Interest

Section 2.3 Predictive Use of Correlation Coefficients

The intent of this chapter is to provide the reader an enumeration of the loads, their relevant characteristics, and to serve as a "lead-in" to the other chapters of this report.

It should be recognized that safety check equations in probability based design typically do not involve the loads directly, but rather the load effects. The calculation of effects (e.g., stresses) requires a structural analysis procedure, either quasistatic or dynamic. Procedures to accomplish this step of converting loads to load effects range from the sophisticated (finite element analysis) to much simpler ones (e.g., beam theory).

2.1 Identification of Relevant Loads

2.1.1 Hull Girder (Global Loads)

The loads on the hull girder consist of shear forces and bending moments arising from the following sources:

(a) Still water loading condition

(b) Low frequency, steady state, motion related wave excitation (vertical, horizontal and torsional)

(c) High frequency steady state wave excitation (also called springing)

(d) High frequency transient wave impact, resulting in slamming

The above loads are illustrated in Figures 2.1 to 2.4.

The calculation of (vertical) shear forces and bending moments for any still water condition is relatively straight forward, and involves little error insofar as the calculation accuracy is concerned. Low frequency, steady state wave induced loads (shear forces, bending moment and torsional moment) involve somewhat greater uncertainty. The calculation procedure used typically is linear strip theory based ship motion analysis, e.g., Refs. 2.1, 2.2. The shear forces and bending moments may be either vertical or horizontal. Procedures for the calculation of high frequency steady state springing (vertical) bending moments and shear forces are also relatively well developed, e.g., ABS (2.3). Calculation procedures for slam impact related vertical and horizontal bending moments and shear forces are considered elsewhere in the report.

2.1.2 Local Pressure Loads

The local loads to be considered in probability based ship design are the following:

(a) Still water loads (external static load)

(b) Low frequency wave loads (external hydrodynamic pressure due to waves)

(c) High frequency slamming loads (external pressures)

(d) Cargo inertia loads (internal, due to vessel accelerations)

(e) Liquid sloshing loads (internal, due to liquid impact in a slack tank)

The still water loads are static. The low frequency wave loads are steady state dynamic; so are the cargo inertial loads. Both are typically treated in a quasi-static manner for purposes of obtaining the load effects. The high frequency slamming loads and the liquid sloshing loads are transient and dynamic. Their effect on the structure must typically involve dynamic structural analysis.

All the local loads noted above are treated for purposes of structural design as pressures. The calculation of these local pressure loads, except in the still water case, involves considerably greater uncertainty than the hull girder global loads, and often requires specialist help. Some procedures for the calculation of local loads are referenced in Chapter 3. An often noted reason for the lesser uncertainty in global loads is that the "integration" process involved in obtaining the global loads from the local ones leads to the averaging of some of the errors involved.

2.1.3 Fatigue Loads

With ship structures becoming increasingly efficient, fatigue is fast emerging as a failure mode that needs explicit consideration in design. This is because structural efficiency and cost considerations result in a lighter structure, obtained for example by using higher strength steels, and with higher operating stresses. The reliability based design procedures of Phase 3 of the thrust of the Ship Structure Committee should address fatigue in explicit terms.

Fatigue loads in the long term arise primarily from the following sources:

(a) Loads due to overall (primary) hull girder bending

(b) Loads due to water pressure oscillation (local).

Secondary sources of fatigue damage in ships include slam effects, springing, thermal loads, and loads due to propeller and machinery vibration. Of these, in so far as the hull girder is concerned, slam effects are perhaps the most important to consider as a secondary source. In general, loads from the primary sources listed above often suffice in design as they contribute the most to fatigue damage in the long term.

The calculation of fatigue damage necessitates the establishment of the stress range versus number of associated cycles histogram for the structural detail of interest. Typically, whatever errors there are in the procedures to establish loads and load effects

get carried over into the fatigue analysis. Additional uncertainty also arises from the establishment of the number of cycles associated with a given stress range, due to inaccuracies in Miner's rule (2.13), which is used to accumulate damage from the stress fluctuations of various magnitudes and due to mean stress effects. In comparative terms, however, the stress range is the most important contributor to the fatigue damage, and any errors in it affect the damage estimates the most. This is because fatigue damage is a function of stress range raised to a power of three or greater.

In the primary hull envelope, the fatigue damage at the deck and bottom is mostly a function of the hull girder loads, at least in the midship region of the vessel. On the side shell, however, local pressure fluctuations are quite important. While there are no studies relating to local pressure related fatigue effects in the fore and aft regions of the vessel, it is likely that local pressures are a significant factor in the fore body region, in addition to slam effects. In the aft body, it is likely that loads due to propeller and machinery vibration are important.

2.1.4 Special Loads

These loads include ice loads, thermal loads, and also vibratory loads due to the propeller and machinery. Less emphasis has been placed on such special loads in this study in comparison to the other load types enumerated previously, although the procedures developed herein can be applied to special loads also, with appropriate modification of details. Nevertheless, for certain types of vessels (e.g., ice breakers), for certain parts of some vessel types (e.g., the containment structure in LNG vessels), or for reasons other than structural integrity and strength (e.g., crew comfort), it may become necessary to explicitly consider special loads and their related effects.

2.2 Load Characteristics of Interest

Important load characteristics that we may mention are:

    (i)   temporal or time variations

    (ii) spatial variations

    (iii) load correlations.

Time Variations: When dynamic analysis needs to be performed, and the loads are transient (e.g., for sloshing or for slamming) the load- versus time characteristics are important. Sometimes these characteristics may be directly available from a detailed analysis. In other cases, they may need to be estimated for the design case based on prior information. In the case of slamming, an illustration of the impact force versus time for a Mariner hull in the forward quarter body is shown in Figure 2.5, obtained from Ref. 2.7. The pulse durations, it will be noted, are in the order of 1/10 second. Because of the short duration of such loads, and because of their rapid variation in time and space, current methods in use are better suited for the integrated results than for very local analysis.

Spatial Variations: Typically, the variation of static, low frequency quasistatic or high frequency steady state dynamic loads will be obtained from the relevant load analysis. For example, conventional ship motion calculations will provide the required spatial load variation information for low frequency wave induced bending moments, shear forces, hydrodynamic pressures, or accelerations and related tank loads. As an illustration, trends for the wave induced low frequency vertical bending moment and shear force are shown in Figure 2.6. Those for low frequency wave induced accelerations and hydrodynamic pressures are shown in Figure 2.7. The information in Figures 2.6 and 2.7 are obtained from the rules of a classification society, Ref. 2.8, and are envelopes, i.e., the distributions shown are not "point-in-time" values. In the case of external hydrodynamic pressure, the variation around the hull periphery, not shown, is also relevant. The hydrodynamic

pressure around the hull periphery is maximum in way of the waterline, unlike the still water pressure load.

Load Correlations: The correlation between different load components is an important piece of information for purposes of obtaining load effects with load combinations present. In the case of low frequency wave induced loads, the required correlation coefficients between the vertical bending moment, horizontal bending moment, accelerations and external pressures can be obtained from spectral theory, considering the load processes to be stationary, and zero mean Gaussian; see Mansour, Ref. 2.9. In the case of transient loads such as slamming, the required information on phasing of the slam transient with respect to the wave induced steady state bending moment is required, and needs to be obtained either as part of a sophisticated simulation replicating the onset of slamming (which can be difficult to do) or from prior experience or data. Some relevant information in this regard is given in section 3.1.4 of this report.

In the case of the low frequency wave induced load components, the cross-spectral density for two load components, denoted 'i' and 'j' is given by

$$S_{ij}(\omega) = S(\omega)\, H_i(\omega)\, H_j^*(\omega)$$

where $S(\omega)$ is the spectral density function of the wave excitation, $H_i(\omega)$ is the transfer function for one of the load components, and $H_j^*(\omega)$ is the complex conjugate of the transfer function for the other load component. The covariance of the load components can be calculated using the cross spectral density curve. The resulting correlation coefficient, which is a measure of (linear) correlation between the two load components, is shown, for long crested seas, to be (2.9):

$$\rho_{ij} = \frac{1}{\sigma_i \sigma_j} \int_0^\infty R_e \left\{ H_i(\omega)\, H_j^*(\omega) \right\} S(\omega)\, d\omega$$

and for short crested seas with wave spreading angle μ and heading angle α

$$\rho_{ij} = \frac{1}{\sigma_i \sigma_j} \int_{\pi/2}^{\pi/2} \int_0^\infty R_e \left\{ H_i(\omega, \alpha - \mu) H_j^*(\omega, \alpha - \mu) \right\} S(\omega, \mu) d\omega d\mu$$

It will be recalled from elementary statistics that the correlation coefficient is simply the covariance divided by the product of the individual standard deviations σ_i and σ_j. The "R_e" denotes "real part" of the complex quantity within parentheses.

Information on correlation coefficients for wave induced load components for ships was obtained as part of this study, and is used in Chapter 3, but more extensive studies remain to be undertaken. The following are some illustrative values for the correlation coefficients for merchantships in head seas:

ρ_{vh}	0.5
ρ_{vp}	0.7
ρ_{vs}	0.2

where the subscripts 'v' and 'h' denote the low frequency vertical and horizontal wave induced bending moment, and 'p', the low frequency wave induced hydrodynamic pressure. The subscript 's' denotes high frequency steady state springing vertical bending moment. Correlation coefficients for the low frequency vertical and horizontal bending moments and torsional moment (denoted by subscripts 'v', 'h' and 't'), calculated for a 530 ft. cruiser hull as part of this study are shown in Table 2.1. The calculations used load transfer functions developed using the shipmotion computer program SCORES. The calculated correlation coefficients are generally small.

Table 2.1

Correlation Coefficients for a 530 ft. Cruiser Hull

Sea State	Speed (knots)	Heading (degrees)	ρ_{vh}	ρ_{vt}	ρ_{ht}
6	15	45	0.35	0.35	0
6	10	60	0.22	0.28	0
7	10	45	0.22	0.37	0

Note: (i) The 0's indicate very small values.
(ii) ISSC wave spectrum was used.

A computer program has been developed and documented which computes the probabilistic load factors for a given set of transfer functions and sea spectrum. The program has been tested on several cases of actual ships for which transfer functions are known. The program has also been tested with correlation coefficients as input and the corresponding load factors were computed. These load factors have been developed for use in design analysis and will be discussed in Chapter 3. The program is written in FORTRAN and runs on IBM PC or equivalent. Documentation of the program is attached as Appendix D.

As a further illustration of load correlations in ship structures, Figure 2.8 presents the results from a Sumitomo study related to the correlation between cargo inertial forces and external hydrodynamic pressure in the double bottom structure of a 708 ft. bulk carrier, Ref. 2.10. The calculations indicated the following:

(a) The correlation coefficient between the cargo inertial pressures P_C and the external hydrodynamic pressure P_H ranged between -0.5 and -1.0, i.e., the two opposed each other.

(b) The cargo inertial pressures were significantly greater in magnitude when compared to the external pressure.

Systematic studies of load correlation in ocean going vessels, considering vessel type, speed, heading, location along vessel length, and wave energy spreading need to be undertaken some time in the future.

2.3 Predictive Use of Correlation Coefficients

The calculation of the correlation coefficients ρ between any two wave induced steady state zero mean Gaussian processes can be carried out using linear spectral theory as outlined in Section 2.2. If ρ is large and positive (i.e., approaching +1), the values of the two load components tend to be both large or both small at the same time, whereas if ρ is large and negative (i.e., approaching -1), the value of one load component tends to be large when the other one is small and vice versa. If ρ is small or zero, there is little or no relationship between the two load components. Intermediate values of ρ (between 0 and ±1) depend on how strongly the two load components vary with one another. In general, the correlation coefficient is a measure of linear dependence. In the case of Gaussian random variables, $\rho = 0$ also implies independence.

For two random variables with zero mean bivariate Gaussian density function, the following is the predictive equation that provides the value of the variable X_2 if the value of the other variable X_1 is known (2.11):

$$E\left(X_2 | X_1\right) = \rho\left(\frac{\sigma_2}{\sigma_1}\right) X_1$$

where ρ is the correlation coefficient between the two variables, and the σ_i are the individual standard deviations. The above equation is based on the mean of the conditional probability density of X_2 given X_1. If the random variables are instantaneous values of zero mean Gaussian random processes, the above predictive (regression)

equation still holds, and the standard deviations are obtainable as the rms value of the processes. Also, the variance of X_2 given X_1 is obtained from

$$\text{Var}\left(X_2 | X_1\right) = \sigma_2^2\left(1 - \rho^2\right)$$

Note that as ρ tends to ± 1, the variance of the predicted value X_2 tends to zero, i.e., the prediction is more certain.

For zero mean Gaussian processes, the above two equations from elementary statistics can be used to provide an _estimate_ of the coexisting X_2 value and its variability when X_1 is an extreme value, as suggested in (2.11). This approach to obtaining co-existing values of loads can in fact be applied to realizations from more than two correlated zero mean Gaussian random processes, with $E(X_j | E_i)$ for any two loads i and j being given in the same form as before. While suitable for use with a load combination procedure such as Turkstra's rule (1.1), the main shortcoming of the approach is that the combined load effect resulting from it is a simple linear superposition of the individual coexisting load effects, while the actual combined load effect may bear a more complicated relationship to the individual load processes. In Chapter 3 of this report, a load combination procedure is developed, that, while based on the exact combined load effect for linear combinations of zero mean Gaussian random processes, is also eminently suitable for design.

The above discussion pertains to the probabilistic treatment of co-existing loads. A semi-deterministic treatment, based on an equivalent wave approach, is used by ABS for checking structural adequacy, see Liu et al. (2.12). The height, frequency and crest position of an equivalent regular wave that provides a maximum load (e.g., vertical bending moment or torsional moment) is found on the basis of a probabilistically calculated load extreme value and the load transfer function. For that wave and crest position, the longitudinal distribution of the hydrodynamic pressure, internal tank pressure, acceleration induced inertial load, etc. are consistently obtained using the phase

2-10

information implicit in their various transfer functions. The chosen regular wave and related co-existing loads, pressures, etc. are quasi-statically applied to the structural model to obtain the combined extreme stress.

References

2.1. Raff, A.I., "Program SCORES - Ship Structural Response in Waves," Ship Structure Committee Report SSC-230, 1972.

2.2. Meyers, W.G., Sheridan, D.J. and Salvesen, N., Manual for the "NSRDC Shipmotion and Seaload Computer Program," NSRDC Report 3376, February 1975.

2.3. "SPRINGSEA II - Springing and Seakeeping Program," American Bureau of Shipping, New York. See also "SPRINGSEA II, Program Listing and User Manual," Mansour Engineering, Inc., Berkeley, CA, 1974.

2.4. Stiansen, S.G., Mansour, A.E., Jan, H.Y. and Thayamballi, A., "Reliability Methods in Ship Structures," *The Naval Architect*, 1979. Also, *Transactions of RINA*, Vol. 122, 1980.

2.5. Stiansen, S.G. and Mansour, A.E., "Ship Primary Strength Based on Statistical Data Analysis," *Trans. SNAME*, 1975.

2.6. Clarke, J.D., "Measurement of Hull Stresses in Two Frigates During a Severe Weather Trial," *Trans. RINA*, 1981.

2.7. Ochi, M.K. and Motter, L.E., "Prediction of Slamming Characteristics and Hull Responses for Ship Design," *Trans. SNAME*, 1973.

2.8. Det norske Veritas, *Classification Rules for Oceangoing Vessels*, Part 3, Chapter 1.

2.9. Mansour, A.E., "Combining Extreme Environmental Loads for Reliability-Based Designs," *Proc. SSL-SNAME Extreme Loads Response Symposium*, Arlington, VA, October 1981.

2.10. Hattori, K. *et al.*, "A Consideration of the Phase Difference between the Wave Induced Stresses on Longitudinal and Transverse Strength," *JSNA*, Japan, Vol. 156, December 1984.

2.11. Thayamballi, A., "On Predicting Coexisting Load Values for Ship Design," Consulting Development Report, May 1993.

2.12. Liu, D., Spencer, J., Itoh, T., Kawachi, S., and Shigematsu, K., "Dynamic Load Approach in Tanker Design," SNAME Annual Meeting Paper No. 5, 1992.

2.13. Munse, W.H. et al., "Fatigue Characterization of Fabricated Ship Details for Design," Ship Structure Committee Report 318, August 1982.

List of Figures

3. EXTREME LOADS AND LOAD COMBINATIONS

The purpose of this chapter is to provide procedures for load combinations for extreme loads. Methods for the determination of individual extreme loads are also indicated where appropriate. Section 3.1 of this chapter treats hull girder loads and their combinations (still water loads, low frequency and high frequency steady state wave induced loads, and high frequency slamming loads). Section 3.2 treats local loads (low frequency dynamic wave pressure, high frequency slam pressures, and cargo inertial loads due to accelerations). Extreme sloshing loads have been de-emphasized in this work. Section 3.3 considers combined hull girder and local loads, both in the forward body region and at midships.

In all cases a simple design format pertaining to load combinations is sought. It was possible to accomplish this in closed form and design charts in the various cases except when slam loads are involved. In the case of slamming, the more involved load combination procedure presented in section 3.1.4 will be necessary.

3.1 Hull Girder Loads

The hull girder loads considered are vertical, horizontal, and torsional moments, and related shear forces. It is worth noting that while some of the procedures of this section are nominally developed for bending moments, essentially the same procedures apply to shear forces. The sources of the bending moments and shear forces considered are:

(a) Still water effects,

(b) Low frequency steady state wave excitation,

(c) High frequency steady wave excitation,

(d) Slamming.

3.1.1 Identification of Critical Load Combinations

The primary hull girder extreme loads of interest in design are the vertical bending moments and shear forces, and, in certain cases, torsional moments. The horizontal bending moment and shear force resulting from low frequency wave excitation can be significant, but the related stresses are usually small in oceangoing merchantships. Hence it is sufficient to consider the horizontal bending loads at the magnitudes that coexist with the vertical bending or torsional loads for those types of ships. For naval ships, and some merchant ships, more elaborate consideration of horizontal moments may be necessary because of higher speed or finer hull form. Torsional loads can be of primary importance in certain types of vessels of low torsional rigidity (e.g., wide hatch containerships). In vessels with closed sections (e.g., tankers), torsion related stresses are small. Such stresses are also small in most merchantships that do not have wide hatches.

Hence, insofar as hull girder loads are concerned, the following are the typical extreme loads and load combinations of interest:

(a) Extreme vertical bending loads, with coexisting values of horizontal bending and torsional loads. Vertical bending moments are important in the midship region, while shear forces are important in the forward quarter body.

(b) Extreme torsional loads, with coexisting values of vertical and horizontal bending loads. Unlike item (a) above, which applies to all ships, a primary load case addressing torsion is important in selected vessel types, namely those of relatively low torsional rigidity. Torsional effects are generally important in the forward quarter body of such vessels.

For the primary vertical bending load cases referred to in item (a), all sources of hull girder loads (i.e., still water, low and high frequency steady state wave excitation, and slamming) are important. In fact, in naval vessels, slamming can contribute not only significant

3-2

vertical bending loads, but also horizontal bending loads. In the torsional case of item (b), it is usually sufficient to consider low frequency wave excitation.

The load combination problem involving all sources of loads as a unified whole is difficult to solve. In the rest of Section 3.1, the problem is thus decomposed into the following design cases:

(i) Extreme combined vertical, horizontal and torsional wave loads due to low frequency wave excitation.

(ii) Combined extreme low frequency wave induced and slamming loads.

(iii) Combined low frequency wave induced and springing loads.

(iv) Addition of still water loads.

3.1.2 Extreme Combined Vertical, Horizontal, and Torsional Wave Loads

The following considers low frequency steady state wave induced loads and related effects, considering the correlations between them. Two cases are considered, the first with two correlated load effects, and the second with three correlated load effects. Normally, since one can often make a judgement as to which two of the three loads are significant in regard to stresses, the first case should suffice. The second case involving three correlated load effects is, however, more general.

The work assumes that the seaway and the loads are Gaussian random processes. The ship is treated as a set of multiple linear time invariant systems, each representing a particular load. The stresses from each load are additive (with the correct phase) at any location in the structure of the vessel. The set of linear time invariant systems has a common input, namely that of the seaway. The model used is shown schematically in Figure 3.1, and the theory for obtaining the variance of the combined stress is given in Mansour, Ref. 3.1. The work described here was previously developed in a more elementary form for ABS, Ref. 3.2, and further extended in this project.

It is worth noting that we consider low frequency wave induced loads and load effects (stresses) alone. To obtain the total load effect (stress), the still water load effects must also be added.

A. Two Correlated Load Effects

The following treats the combined stress at the vessel deck edge, arising from vertical and horizontal bending moments, as the illustrative case. The approach can be used for any two correlated loads/load effects with appropriate modification of detail. A probabilistic load factor (PLF), denoted K_c, is derived. One use of the probabilistic load factor, which accounts for load correlation, is to obtain the combined extreme stress f_c in the form:

$$f_c = f_v + K_c f_h$$

where f_v and f_h are the individual extreme stresses corresponding to the vertical and horizontal bending moments.

From the theory given in Ref. 3.1, the variance of a combined moment, defined as a moment which when divided by the vertical section modulus, gives the combined stress at deck edge, may be written as follows:

$$\sigma_{M_c}^2 = \sigma_{M_v}^2 + k^2 \sigma_{M_h}^2 + 2\rho_{vh} k \sigma_{M_v} \sigma_{M_h} \tag{3.1}$$

where
$$k = \frac{(SM)_v}{(SM)_h} = \text{ratio of the section moduli} \tag{3.2}$$

and
$$\sigma_{M_v}^2 = \int_{-\pi/2}^{\pi/2} \int_{0}^{\infty} |H_v(\omega, \alpha - \mu)|^2 \, S(\omega, \mu) d\omega d\mu \tag{3.3}$$

are the individual moment variances; α is the heading angle and μ is the spreading angle of the wave spectrum. The correlation coefficient between the vertical and horizontal moment is

$$\rho_{vh} = \frac{1}{\sigma_{M_v}\,\sigma_{M_H}} \int\limits_{-\pi/2}^{\pi/2} \int\limits_{0}^{\infty} R_e \left\{ H_v(\omega,\alpha-\mu) H_h^*(\omega,\alpha-\mu) \right\} S(\omega,\mu)\, d\omega\, d\mu$$

with * denoting the complex conjugate. Then the rms value of the combined stress is

$$(rms)_{cs} = \frac{\sigma_{MC}}{(SM)_v}$$

The characteristic highest $1/m^{\text{th}}$ combined stress at deck edge is

$$f_{c1/m} = C_{mc}\,(rms)_{cs}$$

where C_{mc} is a multiplier depending on m. A more appropriate form of $f_{c\,1/m}$ for use in design is:

$$f_{c1/m} \equiv f_{v1/m} + K_c\, f_{h1/m} \tag{3.5}$$

Then the probabilistic stress factor K_c is, by the above definition,

$$K_c = \frac{f_{d/m} - f_{v1/m}}{f_{h1/m}} \tag{3.6}$$

3-5

Note that

$$f_{c1/m} = C_{mc}(rms)_{cs} = C_{mc}\frac{\sigma_{Mc}}{(SM)_v}$$

$$f_{v1/m} = C_{mv}(rms)_{vs} = C_{mv}\frac{\sigma_{Mv}}{(SM)_v}$$

$$f_{h1/m} = C_{mh}(rms)_{hs} = C_{mh}\frac{\sigma_{Mh}}{(SM)_h}$$

where C_{mc}, C_{mv} and C_{mh} are multipliers.

Assume $C_{mv} = C_{mh}$, which is true if the two moment processes are narrow banded, the amplitudes being then Rayleigh distributed. In general, $C_{mc} \le C_{mv}, C_{mh}$ since the C_{mc} process is wider banded. If the band width parameter 'ε' is less than 0.65 for the combined stress process, then

$$C_{mc} \cong C_{mv} = C_{mh} \qquad (3.7)$$

Using Equation (3.7) and the previous equations, K_c from equation (3.6) above may be written

$$K_c = \frac{\sigma_{Mc} - \sigma_{Mv}}{k\,\sigma_{Mh}} \qquad (3.8)$$

Equations (3.5) and (3.8) apply to stresses, with equation (3.5) defining the combined extreme stress at deck corner in terms of extreme stresses from vertical and horizontal bending. K_c is called the probabilistic load factor (PLF).

A similar set of relationships may be proven for a combined moment defined by

$$M_{c1/m} = f_{d/m}(SM_v)$$

with

$$M_{c1/m} = M_{v1/m} + K_c\,k\,M_{h1/m} \qquad (3.9)$$

where K_c and k are as defined before. $M_{c\,1/m}$ relates a combined moment producing the extreme stress at deck corner with the extreme vertical and horizontal bending moments.

Typical Probabilistic Load Factor Values

The probabilistic load factor K_c, defined on the basis of equations (3.8) and (3.1) is

$$K_c = \frac{\left[\sigma_v^2 + k^2\sigma_H^2 + 2\rho_{vh} k\,\sigma_v\,\sigma_H\right]^{\frac{1}{2}} - \sigma_v}{k\,\sigma_h} \qquad (3.10)$$

where the symbol M has been dropped from the subscripts for convenience. K_c may also be written

$$K_c = \frac{\left[1 + k^2 r^2 + 2\rho_{vh} k r\right]^{\frac{1}{2}} - 1}{k r}$$

where $r = \sigma_h/\sigma_v$. The following "extreme" cases result:

(a) If $\rho_{vh} = 0$, i.e., the vertical and horizontal bending moments are uncorrelated, and with $k = 0.9$, and $r = 0.8$, $K_c = 0.32$.

(b) If $\rho_{vh} = 1$, i.e., the two moments are fully correlated, $K_c = 1$ independent of k or r.

For the vessel Universe Ireland, a tanker, considered by Stiansen and Mansour in their SNAME 1975 paper on "Ship Primary Strength Based on Statistical Data Analysis" (Ref. 3.3),

$$\rho_{vh} = 0.453$$
$$k = 0.88$$
$$r = 0.767$$

This gives $K_c = 0.65$. The PLF depends on the correlation coefficient assumed. In the paper cited above, it was noted that ISSC in their 1973 session recommends $\rho_{vh} = 0.32$, for which $K_c = 0.55$.

K_c may be used in equation (3.9) to get the combined moment that, when divided by the vertical section modulus, gives the combined deck corner stress or it may be used in equation (? give the combined deck corner stress directly.

The above developed procedures for the combined stress at the deck edge (up to equation (3.8)) will hold for any location if equation (3.1) is cast in terms of stresses rather than moments. In this case, k is equal to one. The probabilistic load factor K_c then becomes

$$K_c = \frac{\left[1 + r^2 + 2\rho r\right]^{\frac{1}{2}} - 1}{r}$$

Trends of K_c as a function of the correlation coefficient between a "primary" and a "secondary" stress (or load, with $k = 1$), and the ratio of secondary to primary stress (load) ratio "r" are plotted in Figure 3.2. It is seen that, for $\rho \geq 0.7$, K_c does not depend appreciably on 'r'.

Comparison with Turkstra's Rule

Turkstra (1.1) proposed that structural safety can be checked using a set of design loads, constructed with each load at its maximum value, with the other loads at their accompanying "point in time" values. In the case of two loads, each a realization of a zero mean Gaussian random process, it was noted in Section 2.3 that the accompanying load value can be estimated from

$$E(X_2|X_1) = \rho\left(\frac{\sigma_2}{\sigma_1}\right)X_1^*$$

where ρ is the correlation coefficient, and X_1^* is the value for which X_2 needs to be predicted. The σ_i are process rms values.

For stress in a given direction, denote the load to stress transformations for the two loads by a_1 and a_2. The combined total stress is then

$$f_c = a_1 X_1^* + \rho\left(\frac{\sigma_2}{\sigma_1}\right)a_2 X_1^*$$

Consider that the stress extreme values for the two loads are given by

$$f_1 = a_1 X_1^*$$
$$f_2 = a_2 X_2^*$$

where X_1^* and X_2^* are now load extreme values. Define

$$r = \frac{\sigma_2}{\sigma_1} \cong \frac{X_2^*}{X_1^*}$$

Upon substituting for r and using the equations for f_1 and f_2 in that for f_c, one can show that the following expression results for the combined extreme stress:

$$f_c = f_1 + K_c f_2$$

where $K_c = \rho$.

The corresponding K_c value obtained from the Mansour K factor approach is

$$K_c = \frac{(1 + r^2 + 2\rho r)^{\frac{1}{2}} - 1}{r}$$

The probabilistic load factor K_c from the Mansour equation is more accurate because it is correctly based on the combined extreme stress. By comparison with Figure 3.2, which shows how the Mansour K_c plots, it can be seen that a Turkstra's rule based K_c taken equal to ρ will always underestimate the combined extreme stress. The likely error increases with increasing secondary to primary load (stress) ratio $'r'$, and increases with decreasing ρ. In fact, for ρ tending to zero, the Turkstra's rule based K_c completely excludes the secondary stress, while the more exact K_c will exclude the secondary stress only if that stress itself is zero, i.e., $r = 0$.

B. Three Correlated Load Effects

Here we consider the maximum combined stress at a point, σ_c, which arises from three correlated loads, whose associated maximum stresses are σ_1, σ_2 and σ_3. The sought combined stress has the form:

$$\sigma_c = \sigma_1 + K_{c_2}\,\sigma_2 + K_{c_3}\,\sigma_3$$
$$\sigma_c = \sigma_2 + K_{c_1}\,\sigma_1 + K_{c_3}\,\sigma_3 \qquad\text{(a)}$$
$$\sigma_c = \sigma_3 + K_{c_1}\,\sigma_1 + K_{c_2}\,\sigma_2$$

where K_{c_i} are the load factors. (Note that σ denotes an extreme stress, not its r.m.s. value.) By solving the above set of equations simultaneously, the K_{c_i} may be determined, and are as follows:

$$K_{c_1} = \frac{1}{2}\left(\frac{\sigma_c}{\sigma_1} + 1 - \frac{\sigma_2}{\sigma_1} - \frac{\sigma_3}{\sigma_1}\right)$$

$$K_{c_2} = \frac{1}{2}\left(\frac{\sigma_c}{\sigma_2} + 1 - \frac{\sigma_1}{\sigma_2} - \frac{\sigma_3}{\sigma_2}\right)$$

$$K_{c_3} = \frac{1}{2}\left(\frac{\sigma_c}{\sigma_3} + 1 - \frac{\sigma_1}{\sigma_3} - \frac{\sigma_2}{\sigma_3}\right)$$

Note that in this section, the extreme stress is denoted "σ" instead of the previously used "f".

Call the stress ratios

$$r_2 = \frac{\sigma_2}{\sigma_1}$$

$$r_3 = \frac{\sigma_3}{\sigma_1}$$

Since the combined stress σ_c can be determined from any of the three equations given by we will consider the first equation only. K_{c_2} and K_{c_3} may then be written as follows, with ρ_{ij} being correlation coefficients:

$$K_{c_2} = \frac{1}{2}\left(\sigma_{c_2}{}^* + 1 - \frac{r_3 + 1}{r_2}\right)$$

$$K_{c_3} = \frac{1}{2}\left(\sigma_{c_3}{}^* + 1 - \frac{r_2 + 1}{r_3}\right)$$

where the σ^* are given from the following:

$$\sigma_{c_2}{}^* = \left[1 + \frac{1}{r_2^2} + \left(\frac{r_3}{r_2}\right)^2 + \frac{2\rho_{12}}{r_2} + 2\rho_{13}\frac{r_3}{r_2^2} + 2\rho_{23}\frac{r_3}{r_2}\right]^{\frac{1}{2}}$$

$$\sigma_{c_3}{}^* = \left[1 + \frac{1}{r_3^2} + \left(\frac{r_2}{r_3}\right)^2 + 2\rho_{12}\frac{r_2}{r_3^2} + 2\frac{\rho_{13}}{r_3} + 2\rho_{23}\frac{r_2}{r_3}\right]^{\frac{1}{2}}$$

These are derived based on the following relationship for the combined extreme stress and the individual extreme stresses:

$$\sigma_c^2 = \sigma_1^2 + \sigma_2^2 + \sigma_3^2 + 2\rho_{12}\,\sigma_1\,\sigma_2 + 2\rho_{13}\,\sigma_1\,\sigma_3 + 2\rho_{23}\,\sigma_2\,\sigma_3$$

This particular equation readily follows from the results of Ref. 3.1 for the process variances. Its use with extreme stresses involves the assumption that the maximum stress in each instance is c * rms, and the c values for all components and the combined case is the same. This assumption is valid as long as the band width parameter ε of each process is less than 0.65, which is usually the case.

The three correlated load case discussed above is an important one. While the results obtained, summarized in Figure 3.3, have been presented in the context of extreme values related to hull girder low frequency bending moments, they are considerably more general, and apply also to cases involving hull girder loads and local pressures as will be noted later.

The probabilistic load factors K_{c_2} and K_{c_3} obtained are stress based, which helps broad applicability. The sensitivity of the load factors to the correlation coefficients and stress ratios was investigated. A complete set of charts illustrating the probabilistic load factors and their sensitivities may be found in Appendix E of this report. These Mansour K charts represent a simple design treatment of load combination for steady state wave induced load effects.

3.1.3 Combined Low Frequency Wave Induced and Springing Loads

Hull vibratory loads related to springing are steady state and wave induced. They differ from low frequency wave induced loads in two respects:

(a) The hull flexibility is a factor in their calculation.

(b) They are typically of relatively higher frequency.

The second factor implies that the spectral density of response to springing is separated on the frequency scale from the low frequency response.

The probabilistic load factor procedures described in the previous section for two and three correlated loads also apply in the case of springing loads/response since one can usually assume them to be stationary and Gaussian.

Examples of Typical Load Factors

As an example, consider the case of two correlated load effects, one arising from low frequency wave induced vertical bending moment, and the other from high frequency steady state springing (vertical) bending moment. For this case, the results of Figure 3.2 may be applied, with springing load effect considered "secondary", and vertical bending load effect considered "primary". The probabilistic load factor K_c is given by:

$$K_c = \frac{\left[1 + r^2 + 2\rho_{vs} r\right]^{\frac{1}{2}} - 1}{r}$$

where r is the stress ratio σ_s/σ_v. The subscript 's' represents 'springing' and 'v' represents 'vertical bending'.

In the extreme cases, if the correlation coefficient $\rho_{vs} = 0$, which may be a realistic assumption in some cases,

$$K_c = \frac{\left(1 + r^2\right)^{\frac{1}{2}} - 1}{r}.$$

For a conservative r value of 0.5, this expression produces a K_c of 0.236. In the unrealistic case where $\rho_{vs} = 1$, the probabilistic load factor K_c is unity regardless of the stress ratio r. For a realistic case, one can use data on the Great Lakes Bulk Carrier "Stewart J. Cort", discussed in Ref. 3.3. In this case, with $\rho_{vs} = 0.2$, and if $r = 0.5$, $K_c = 0.41$, i.e., the combined extreme stress is approximately equal to the extreme wave induced vertical bending stress plus 40% of the extreme stress from springing.

3-13

3.1.4 Combined Low Frequency Wave Induced and Slamming Loads

3.1.4.1 Purpose

The primary aim of this section is to obtain the distribution of the extreme value of the combined wave induced and slamming effects in a seastate. The extreme value distribution is needed for reliability analysis. It is also useful for obtaining probabilistic load factors for design use. This section is organized as follows:

(a) In Section 3.1.4.2, the wave induced stress extreme value distribution in a seastate is obtained.

(b) In Section 3.1.4.3, the prediction of slam loads and related structural response is considered.

(c) In Section 3.1.4.4, the distribution of the combined amplitude of wave induced and slam effects is obtained.

(d) In Section 3.1.4.5, the extreme value distributions of the combined amplitudes of item (c) are obtained.

The probability distribution of the combined amplitude of slamming and wave induced effects is calculated using a deterministic load combination model which is then "randomized", i.e., distribution information for individual model variables is included, and the combined amplitude distribution is obtained by a first order reliability (FORM) method.

Additionally, an approximation to the combined amplitude distribution is also developed by fitting a three parameter Weibull density to the peaks of the combined process. This procedure can be useful in performing reliability analyses based on service stress measurements.

In this work, various concepts developed by Wen (3.18,3.19) as part of the load coincidence approach to the load combination problem are used. The load coincidence

3-14

method and related concepts, which constitute perhaps the most flexible and practical approach to load combination available today, are outlined in Appendix A.

3.1.4.2 Wave Induced Stress Extreme Value in a Seastate

The seastate duration is denoted t_s. The extreme value calculation assumes that the vessel spends all of t_s in the particular speed and heading. A weighted extreme value distribution that includes probabilities of the speed and heading pairs is calculated. We consider narrow band processes and construct the best possible estimate of the distribution of the extreme value of the low frequency wave induced stress for the seastate.

For stationary zero mean Gaussian wave surface elevations for each seastate, the response process for a linear system is also stationary zero mean Gaussian. For narrow band processes, the peaks are Rayleigh distributed, as follows:

$$F_A(a) = 1 - \exp\left(-\frac{a^2}{2m_0}\right) \tag{3.11}$$

where m_0 is the mean square value, or zero-th moment of the spectral density.

The number of peaks per unit time may be obtained from the rate of zero crossings v_0,

$$v_0 = \frac{1}{2\pi}\sqrt{\frac{m_2}{m_0}} \tag{3.12}$$

where m_n is the spectral moment of order n, typically calculated using linear shipmotion theory results. If the process is not narrow banded, the distribution of peaks is given, including both positive and negative maxima, by the well known Rice formula (3.20). A modified distribution of positive maxima alone, with associated expected number of positive maxima per unit time, has been obtained by Ochi (3.4).

To obtain the extreme value distribution $F_{X_w}|_{m,n}$ where m and n are subscripts denoting speed and heading, one can use the conventional Poisson assumption. The pulse heights are modeled as independent random variables with a distribution function $F_A(a)$. The cumulative distribution function of the maximum value F_{X_w} of the random process in the time interval $(0,t_s)$ is then given by

$$F_{X_w}(a)\Big|_{m,n} = P[X_w \le a] = \exp\left\{-[1 - F_A(a)]v_0 t_s\right\} \qquad (3.13)$$

where v_0 denotes the rate of arrival of pulses, with time units same as t_s. For a narrow band process, v_0 is defined from Eqn. 3.12 giving the expected number of $a = 0$ level crossings. With $F_A(a)$ substituted, the above equation reduces to the Wen ICP (intermittent continuous process) model, see Appendix A.

The above cumulative distribution function of the extreme value may equivalently be written as

$$F_{X_w}(a)\Big|_{m,n} = \exp\left(-v_X(a)t_s\right) \qquad (3.14)$$

where $v_X(a)$ is the expected number of a level upcrossings per unit time, given by

$$v_X(a) = v_0 \exp\left(-\frac{a^2}{2m_0}\right) \qquad (3.15)$$

The CDF estimate is known to be conservative because of "clustering", that is the tendency for a narrow-band process upcrossings to occur in clumps, particularly for the moderate threshold values of practical interest. Clustering is contrary to the basic assumption of independence of the individual outcrossings of the process used in obtaining Eqn. 3.14.

Clustering may be considered using the first passage probability of the envelope process for the given narrow band process. Usually, the Cramer-Leadbetter envelope definition is used. The upcrossing rate for the envelope process is then given by, e.g. (3.5)

$$v_R(a) = \sqrt{2\pi} \sqrt{1 - \frac{m_1^2}{m_0 m_2}} \frac{a}{\sqrt{m_0}} v_0 \exp\left(-\frac{a^2}{2m_0}\right)$$ (3.16)

This upcrossing rate needs to be corrected for the fact that envelope level crossings may occur without any upcrossings of the original process. Such envelope excursions are said to be "empty", as opposed to "qualified". The terminology is due to Vanmarcke (3.6), who obtained an estimate of the long run fraction of qualified excursions r_v for an ergodic narrow-band Gaussian process as follows:

$$r_v(a) = \frac{v_X(a)}{v_R(a)} \left\{ 1 - \exp\left(-\frac{v_R(a)}{v_X(a)}\right) \right\}$$ (3.17)

The cumulative distribution function of the maximum value of the ergodic Gaussian wave induced stress process is then given by Vanmarcke as follows:

$$F_{X_m}(a)\big|_{m,n} = \left\{ 1 - \exp\left(-\frac{a^2}{2m_0}\right) \right\} \exp\left\{ -\frac{t_r r_v(a) v_R(a)}{1 - \exp\left(-\frac{a^2}{2m_0}\right)} \right\}$$ (3.18)

The $v_R(a)$ is the upcrossing rate of the envelope process, and r_v is the Vanmarcke "empty envelope excursion" correction.

Ditlevsen and Lindgren (3.7) studied the accuracy of the Vanmarcke prediction of the long run fraction $(1 - r_v)$ of empty envelope excursions using Monte Carlo simulation. They found that while the solution has a large scatter when compared to simulations, it did

give the right order of magnitude and the practical consequence of the deviations are not likely to be serious, particularly for highly reliable structures. They have also provided an improved estimate for r_v by use of a Slepian regression technique, which reduced the deviations. The Ditlevsen and Lindgren solution has been recently proposed for use in ship structures by Cramer and Friis Hansen (3.8).

Once the wave induced stress extreme value distributions $F_{X_w}(a)|_{m,n}$ conditional on a speed and heading pair with probability $P_{m,n}$ have been obtained, the unconditional extreme value distribution for the sea state may be calculated:

$$F_{X_w}(a) = \sum_{m=1}^{n_v} \sum_{n=1}^{n_h} F_{X_w}(a)|_{m,n} P_{m,n} \tag{3.19}$$

where n_v and n_h are the number of speeds and headings.

Inclusion of a Hog-Sag Correction

A hog-sag correction may be included to represent the fact that hogging and sagging parts of a wave induced load cycle are likely to be different than that obtained by linear shipmotion analysis on which the Rayleigh parameter m_0 is based. Consider the corrected extreme value to then be

$$X_{wc} = X_w X_{hs}, \quad X_{hs} \geq 0 \tag{3.20}$$

where X_{hs} is the hog-sag correction, considered a multiplicative constant.

The constant to be applied is in general different for the hogging and the sagging parts of the wave cycle, and some related data is provided in Chapter 5. Note that

$$P[X_{wc} \leq a] = P[X_w X_{hs} \leq a] \tag{3.21}$$

3-18

Hence the distribution function of X_{wc} may be constructed knowing the distribution function of X_w.

3.1.4.3 Slam Loads and their Prediction

Slamming related local and hull girder loads arise from bottom impact or bow flare immersion. Rigorous calculation of the slam impact forces include addressing changes in fluid momentum, buoyancy and impulsive pressure variations as a function of time. The dynamic slam transient load effects are superposed on the steady state wave induced load effect. There is also a slam related deceleration which is superposed on the wave acceleration. Obtaining the stress response for slam loads requires considering hull flexibility and damping.

In obtaining combined wave bending and slam effects, the phasing between wave induced and slamming load effects is important. An explanatory sketch in this regard is shown in Figure 3.4 obtained from Ochi and Motter (3.9). The illustration is for the hull girder midship deck stress. As the wave induced stress cycle changes from hogging to sagging, the slam impact results in a compressive (sagging) stress peak on the deck. The next hogging stress is termed the "initial slam stress", and subsequent stress peaks are termed "whipping stresses". This terminology is a matter of convenience and is not unique.

The phase angle between the hogging wave induced stress peak and the start of the slam transient, δ, is a random variable, which typically lies between 0 and 50 degrees, as may be seen from Figure 3.5 obtained from Lewis et al. (3.10). It is possible for the second peak of the whipping stress, σ_s to exceed the wave induced hogging stress, if the phase lag δ is small enough. The whipping stress σ_{ss} that follows a slam will with certainty increase the next peak sagging stress, and may also increase the subsequent peak hogging stress, the magnitude of the increase depending on the phase angle, the slam

stress amplitude, and rate of decay. Usually slam transient increases the sagging part of the wave induced stress amidships, but at forward stations, there can also be an increase in the hogging stresses. Apart from bending stresses, shear stresses are also increased by slamming.

There are two established methods of obtaining slam pressures and loads, one due to Stavovy and Chuang (3.11), and another due to Ochi and Motter (3.9). The Stavovy and Chuang (SC) theory is typically preferred for high speed fine form vessels, while the Ochi and Motter (OM) theory works well for the fuller form, slower merchant ships. Both theories primarily treat impact slamming. A procedure for calculating forces due to flare entry has been developed by Kaplan (3.12). The method is based on the linear shipmotion computer program SCORES, and uses a wave elevation time history simulation procedure. A probabilistic approach to obtaining slam related bending moments using the Timoshenko beam theory has been developed by Mansour and Lozow (3.13), using the Ochi and Motter method to determine individual local slamming loads. An approach that considers the ship hull to be a set of nonuniform beams, with the response solved for using a normal mode method has been developed by Antonides (3.14).

The case of bottom slamming in ships was considered by Ochi to depend on bow emergence and a relative velocity threshold being exceeded, based on experimental observations. The number of slams per unit time λ_0 was obtained from the following expression, which combines the probability of bow emergence and the probability of a certain relative threshold velocity being exceeded:

$$\lambda_0 = \frac{1}{2\pi}\left(\frac{\sigma_{\dot{r}}}{\sigma_r}\right)\exp\left[-\left\{\frac{d^2}{2\sigma_r^2}+\frac{v_t^2}{2\sigma_{\dot{r}}^2}\right\}\right] \qquad (3.22)$$

where the $\sigma_r^2, \sigma_{\dot{r}}^2$ are the variances of the relative motion and relative velocity (with respect to the wave) at the hull cross section, d is the section draft, and v_t is the threshold

velocity. A typical value for the threshold velocity is 12 ft per second for a 520 ft long vessel, with Froude scaling applicable for other lengths. Relative velocities for slam events can vary depending on slam severity. For the Wolverine State (3.15), velocities in the range of 13 to 36 ft per second were reported, with average values about 22 for the more severe slam events. A conventional ship motion program is used to determine the relative motion and velocity. The variances of motion and velocity, and the number of slams per unit time can then be calculated. For bow flare slamming, with momentum effects considered, the bow emergence condition is not necessary.

Slamming does not occur with every wave encounter. The incidences of slamming are dependent on vessel speed, heading, and rough weather countermeasures. The master of the vessel will take measures to limit the incidences of slamming, particularly so in smaller vessels where the effect of slamming is more felt. When action is taken, the effect will be significant as slamming is very speed dependent, see related data in Chapter 5. Operational limitations on speed (3.9) based on the probability of slam impact at a forward station reaching 0.03, or the significant amplitude of vertical bow acceleration reaching 0.5g with a specified probability have been suggested. Speed can also be limited by a criterion considering local bottom damage.

3.1.4.4 Wave Stress Amplitudes Including Slam Transients

The following is a time domain based practical approach for obtaining extreme values of the combined wave induced and whipping stress in slam events assuming both exist and can be calculated. A probabilistic method to combine the resulting transient stress history with the hull girder wave induced stress is developed in the following. The procedure can, in principle, apply to both bending stress amidships and the shear force at quarter length.

A fundamental feature of the combination procedure is that the slam event occurs at a phase lag δ with respect to the hogging peak of the wave bending moment. The phase lag is measured from the hogging peak to the start of the slam transient.

Consider the combination of wave induced bending and slam effects *at deck*, as depicted in Figure 3.6. The portion of the second peak of the slam transient that is additive to the low frequency hogging wave induced stress is denoted the initial slam stress amplitude σ_*. The whipping stress that follows a slam will add to the next wave induced sagging stress peak, and the subsequent hogging stress peak. The whipping stress, additive to the sagging peak of the low frequency wave induced load cycle, is denoted σ_{**}. The whipping stress, additive to the next hogging wave induced peak, is denoted σ_{***}. Note that σ_{**} and σ_{***} do not necessarily correspond to peaks of the slam transient, but are point in time values, calculated on the decay envelope of the slam transient stress time history. The notation used is that of Ochi and Motter (3.9). In this slam stress envelope addition procedure, σ denotes a stress, not its r.m.s. value.

The magnitude of the addition to the wave induced stress will depend on the phase angle δ, the initial slam stress amplitude, and rate of decay. The additive whipping stresses referred to above are given approximately by

$$\sigma_{**} = \sigma_* \exp\left\{-\lambda\left(\frac{T_w}{2} - T_\delta - \frac{3}{4}T_{wp}\right)\right\} \tag{3.23}$$

$$\sigma_{***} = \sigma_* \exp\left\{-\lambda\left(T_w - T_\delta - \frac{3}{4}T_{wp}\right)\right\} \tag{3.24}$$

Here, T_δ is the time interval from the hogging peak to the slam initiation, which depends on the phase δ with respect to the hogging peak, and T_w is the period of the low frequency wave induced stress. The period of the slam transient is denoted T_{wp}. The values of $(T_w/2) - T_\delta - \frac{3}{4}T_{wp}$ and $T_w - T_\delta - \frac{3}{4}T_{wp}$ need to be positive. Also, $T_{wp} \ll T_w$. The variable λ is the logarithmic decrement representing the decay of the slam transient.

Hogging and Sagging Stress Amplitudes

The total stress amplitude at the time of the first hogging slam stress peak is given approximately by

$$X_{s,1} = \sigma_s + A\cos\left(\delta + \frac{2\pi}{T_w}\frac{3}{4}T_{wp}\right)\cdot X_{hs} \qquad (3.25)$$

where A is the wave induced stress amplitude calculated on the basis of line on ship motion analysis.

The combined stress at the time of the sagging peak of the wave induced stress after the slam event is given approximately by

$$X_{s,2} = \sigma_{ss} + A\cdot X_{hs} \qquad (3.26)$$

Similarly, the combined stress at the second hogging wave induced stress peak is given approximately by the following:

$$X_{s,3} = \sigma_{sss} + A\cdot X_{hs} \qquad (3.27)$$

where σ_{ss} and σ_{sss} are determined from equations (3.23) and (3.24), respectively.

In the above equations, all variables are considered positive. The variable X_{hs} *is a* correction applied to account for hog-sag nonlinearities, data related to which is provided in Chapter 5.

Probability Distribution of Combined Stress

We need to obtain the probability characteristics of the combined stress including the slam transient and wave induced stress, as defined by Eqns. 3.25, 3.26 and 3.27 above in order to determine the probability distribution of the combined stress. The following assumptions are made:

- the joint density of wave stress amplitude and frequency is given by equation (3.30) below

- initial slam stress amplitude σ_* is characterized by a shifted exponential distribution

- the phase angle δ is normally distributed

These two assumptions are based on the work of Lewis et al. (3.10). Relevant Wolverine State data from Lewis are shown in Figures 3.7 and 3.8.

The initial slam stress amplitude probability density function (p.d.f.) is then

$$f(\sigma_*) = \frac{1}{\alpha} \exp\left\{ -\left(\frac{\sigma_* - \beta}{\alpha} \right) \right\} , \quad \text{for } \sigma_* \geq \beta \tag{3.28}$$

where α (and possibly the lower limit β) can depend on the seastate, and has to be obtained from service data or time domain calculations. Note that the shifted exponential density is defined, but not continuous over the interval $(0, \infty)$.

The p.d.f. of the phase angles δ is given by

$$f(\delta) = \frac{1}{\sigma_\delta \sqrt{2\pi}} \exp\left[-\frac{1}{2} \left(\frac{\delta - \mu_\delta}{\sigma_\delta} \right)^2 \right] \tag{3.29}$$

where μ_δ and σ_δ are the mean and standard deviation. The phase angle distribution is an input to the load combination procedure, and must be separately established.

The joint probability density of the low frequency wave induced stress amplitudes and periods for a seastate, heading, and speed is given by (3.36):

$$p(\xi, \eta) = \frac{\xi^2}{\sqrt{2\pi}} \exp\left[-\xi^2 (1 + \eta^2)/2 \right] \tag{3.30}$$

where $\quad \xi = \dfrac{a}{m_0} \quad$ and $\quad \eta = \dfrac{(T_a - T_m)}{vT_m}$.

The ξ is a normalized wave amplitude, m_0 being the mean square value of the wave induced stress process. The η is a normalized period corresponding to period T_w. The following definitions apply:

$$T_m = 2\pi\frac{m_0}{m_1}$$

$$\nu = \left[\frac{m_0 m_2}{m_1^2} - 1\right]^{\frac{1}{2}}$$

$$m_i = \int_0^\infty w^i S(w)\,dw$$

Note that T_m is the spectral average period, and ν is a parameter related to the spectral bandwidth.

The above joint probability density of wave amplitudes and periods applies to a narrow band Gaussian random process, and was derived by Longuet-Higgins (3.36). The marginal p.d.f. of wave amplitude corresponding to equation 3.30 is the Rayleigh density:

$$p(\xi) = \xi\exp\left(-\frac{\xi^2}{2}\right) \tag{3.31}$$

and the marginal probability density of the wave stress process period T_w (defined as the time interval between successive upcrossings of mean level) is given by the following bell shaped curve:

$$p(\eta) = \frac{1}{2(1+\eta^2)^{\frac{3}{2}}} \tag{3.32}$$

The slam stress σ_*, the phase angle δ, the wave induced stress peak A, and wave stress period T_w are three important random variables in the combined amplitude equations. The range of important wave lengths typically range from 3L/4 to L, where L is the ship length. The whipping period T_{wp} is about 0.7 seconds for a Mariner hull, and 3 seconds

for a Great Lakes bulk carrier. Slam stress decay rate λ can vary considerably, although the applicable distribution function is unknown. For a relatively long persisting transient, λ may be about 0.05. In frigates, typical logarithmic decrements (average over five cycles from peak) are reported to be about 0.2, with maximum values in the 0.3 to 0.5 range. For a given slam, the logarithmic decrement λ decreases with decreasing σ_*, to 0.1 or less.

Stress Combination Methodology

The combined stress amplitudes $X_{s,i}$ are given by equations (3.25), (3.26), and (3.27), using equations (3.23) and (3.24). Both wave stress amplitude A and period T_w are part of these equations. A two step procedure is followed for obtaining the cumulative distribution (CDF) function of the combined stress amplitudes $X_{s,i}$:

STEP 1: Obtain the CDF of the combined stress amplitudes conditional on T_w, the wave induced stress period.

STEP 2: Obtain the unconditional CDF of the combined stress amplitudes using the results of Step 1 above, and the marginal density of wave induced stress period T_w, given by equation (3.32).

The conditional probability density of wave stress amplitudes given the period is obtained, from equations (3.30) and (3.32), as follows:

$$p\left(\xi|\eta\right) = \frac{2\xi^2}{\sqrt{2\pi}} \exp\left[-\xi^2\left(1+\eta^2\right)/2\right]\left[1+\eta^2\right]^{3/2}$$

The corresponding conditional CDFs of the combined stress amplitudes in Step 1 may be obtained by a First Order Reliability Method (FORM), once the various probability density functions of the random variables entering the combined stress equations are defined. The

unconditional CDFs of the combined stress amplitudes in Step 2 may then be obtained by standard statistical techniques.

The above load combination procedure uses a predefined joint probability density of wave induced stress amplitudes and periods. In (3.26), Friis-Hansen has developed a more sophisticated procedure wherein he determines the joint probability density of wave amplitudes and periods leading to slamming, with account of clumping of slam impacts, using a Slepian regression technique.

FORM Solution Procedure

The use of the first order reliability method for the calculation of the distribution function of any random variable X is straightforward. Define a "limit state"

$$g(X) = X - Z$$

where Z is a variable representing the value of X corresponding to which we want to calculate the cumulative distribution function

$$F_X(Z) = \Pr(X \leq Z) = \Pr[X - Z \leq 0] = \Pr[g(X) \leq 0]$$

The required CDF is obtained by calculating $\Pr[g(X) \leq 0]$ using a FORM computer program and varying the value of Z. Also, although not widely recognized, FORM can also provide probability *density* results. The pdf of $Z = X$ can be formulated based on a sensitivity factor:

$$f_X(Z) = \frac{d}{dZ}\left[\Pr\{X - Z\} \leq 0\right]$$

Also, unconditioning of probabilities can be carried out using an auxiliary variable technique due to Wen (3.33). The probability distribution functions of the combined

3-27

stress amplitude obtained above are necessary for determining the combined stress extreme values in a seastate.

Reliability Analysis using Service Data

For performing reliability analysis based on service stress measurements, a three parameter Weibull distribution, e.g., Ref. (3.16), may be fit to the histogram of the combined wave induced and slam stress amplitude, $X_{s,i}$. The determination of the distribution parameters by method of moments is described in Appendix B.

3.1.4.5 Combined Extreme Values in a Seastate

In a seastate, there are times when slamming occurs, and there are times when the steady state wave induced loads occur alone. Consider that the probability of slamming is P_s, and the probability of no slamming is $P_w = 1 - P_s$. Denote the probability distribution functions of the combined stress for a given seastate by $X_{s,i,m,n}$ and $F_{s,i,m,n}$, respectively, $i = 1...,3$. The subscripts $m = 1,...n_v$ and $n = 1,...,n_h$ denote speed and heading. The probability of a speed and heading pair for the seastate is denoted $P_{m,n}$, with

$$\sum_m \sum_n P_{m,n} = 1 .$$

The expected number of slams for a given heading and speed pair in the seastate is denoted $N_{m,n}$, with the associated slam arrival rate denoted $\lambda_{m,n}$.

The distribution function of the extreme value of the combined stress amplitudes for a given speed and heading pair may be obtained from the following:

$$F_{i,m,n}(r) = \left[F_{s,i,m,n}(r) \right]^{N_{m,n}}$$

This equation uses order statistics assuming independent, identically distributed slam effect events, to obtain the distribution of the largest value among the effects for $N_{m,n}$ slam events.

As an alternative to the above, one can also use the Poisson assumption widely used by Wen, Appendix A. If $\lambda_{m,n}$ are the rate of arrival of the Poisson pulses (i.e., the slamming rate), and the seastate duration is t_s, the probability distribution of the maximum combined stress $F_{i,m,n}$ is obtained as

$$F_{i,m,n}(r) = \exp\left[-\lambda_{m,n} t_s \left\{1 - F_{s,i,m,n}(r)\right\}\right] \quad i = 1,2,3$$

The unconditional extreme value of the combined stress amplitudes during a slam event are then obtained:

$$F_i(r) = \sum_{m=1}^{n_s} \sum_{n=1}^{n_h} P_{m,n} F_{i,m,n} \quad\quad i = 1,2,3$$

where $i = 1$ and 3 are the stresses corresponding to the hogging part of the wave induced load cycle and $i = 2$ case corresponds to the sagging part of the wave induced load cycle. For $i = 2$, the deck is in compression, which is an important design case.

The extreme value distribution of stress in the seastate needs to be obtained considering both slam and non-slam cases. The extreme value of the wave induced stress alone was previously obtained, assuming slamming does not occur. With a hog-sag nonlinearity included, the corrected stresses corresponding to the hogging and the sagging parts of the wave induced load cycle are different, and the related distribution functions are denoted $F_{wc,h}$ and $F_{wc,s}$, respectively.

In the case where the sagging part of the wave induced load cycle (deck in compression) is of interest, the cumulative distribution function of the maximum value of the combined stress, including wave and slam effects may be approximated as follows:

$$F_{wc}(r) = F_2(r) \quad\quad \text{if slamming occurs}$$

$$= F_{wc,s} \quad\quad \text{otherwise}$$

3-29

3.1.4.6 Probabilistic Load Factors for Slam Effects

The above developed procedure is useful for obtaining the extreme value distribution of the combined stress considering steady state wave induced loads and slam loads in a given seastate. This is essentially an analysis treatment of the problem. The procedure can, however, be used to develop design data in a form similar to the probabilistic load factor approach for steady state wave loads, since from it we can calculate the combined stress extreme values. The extreme values for the low frequency wave induced load effects and slam effects would also need to be obtained by appropriate procedures. Knowing the individual and combined stress extreme values, a "probabilistic load factor" for the load combination can be calculated, and from experience with several such calculations, one can develop simplified load combination rules cast in a probabilistic load factor format.

Consider the i = 2 case for the sagging part of the wave load cycle as an example. In this case, the deck is in compression, and the slam effect adds to the deck stress. The characteristic (e.g., average 1/m highest) extreme combined (wave and slam) stress is denoted f_2. Denote the characteristic extreme sagging wave induced stress alone by $f_{wc,s}$. This stress includes a hog/sag nonlinearity correction. The characteristic extreme value of the slam stress alone is denoted f_{sl}. The probabilistic load factor ψ_{sl} is obtained such that it satisfies the following equation:

$$f_2 = f_{wc,s} + \psi_{sl} f_{sl}$$

3.1.5 Consideration of Still Water Loads

Still water loads have an inherent variability, which arises from the multitude of possible loading conditions and drafts. This variability is larger in the case of merchantships than naval ships. A consequence of this variability is that the chances that the extreme wave induced effect in any seastate will occur simultaneously with the extreme still water loads

is smaller. This is another load combination problem. It is advantageous, insofar as structural efficiency is concerned, to account for it.

In this section, we describe a procedure to solve the above load combination problem and obtain the relevant probabilistic load factor representing the non-coincidence of extrema of still water and wave load effects for design. We also obtain the short term distribution of the total load effect in a sea state, considering all possible loading conditions and their variability. This short term distribution is not used in the solution of the load combination problem itself, but may be useful in other contexts.

The work considers the possibility of a number of loading conditions and seastates during vessel life. The load effect is represented by a stress. The wave load effect as a general case includes low and high frequency steady state phenomena as well as transient slam effects.

3.1.5.1 Short Term Distribution of the Total Stress Including Still Water Load

The distribution of the total stress in any given seastate is obtained as a matter of interest. We previously indicated how to obtain the distribution function of the extreme value of the combined wave induced and slamming effects, which was denoted $F_{ws}(r)$. Denote the probability density function of the still water load effect in a given loading condition (e.g., laden or ballast) $f_{ST_i}(r)$, where i is an index relating to the loading condition, whose associated probability of occurrence is P_{ST_i}.

Assuming that the wave induced and slam effect combined stress process is independent of the still water stress, we can obtain the cumulative distribution function of the total stress for the seastate by using the convolution theorem for the sum of two random variables. The CDF is given by

$$F_T(r) = \sum_{i=1}^{n_c} P_{ST_i} \int_{-\infty}^{\infty} f_{ST_i}(x) \, F_{ws}(r-x) \, dx$$

where n_c is the number of loading conditions possible during the time of the vessel life. $F_T(r)$ is the CDF of the total stress in the given seastate (still water plus extreme wave and slamming), considering all likely loading conditions the vessel may be in when it meets the particular seastate.

3.1.5.2 Long Term Distribution of the Total Stress Including Still Water Load

We obtain the long term distribution of the total stress (wave induced stress considering all wave peaks, and the long term still water stress).

Consider that there are $i = 1,...,n_c$ loading conditions and $j = 1,...,n_{SS}$ seastates during the vessel life. Also consider that the combined wave and slam stress amplitude for a seastate j, whose CDF is denoted F_{X_j}, is independent of the still water stress, of long term density $f_{ST_i}(x)$ for the loading condition i. The probabilities of occurrence of the seastates and loading conditions are denoted P_{SS_j} and P_{ST_i}, respectively. The probabilities are such that

$$\sum_{j=1}^{n_{SS}} P_{SS_j} = 1$$

$$\sum_{i=1}^{n_c} P_{ST_i} = 1$$

The cumulative distribution function of the combined wave induced and slamming stress, considering all seastates, is given, for any loading condition, by

$$F_x''(r) = \sum_{j=1}^{n_{SS}} P_{SS_j} F_{X_j}(r)$$

where the F_{X_j} are the individual CDFs of combined wave plus slam effects. For any particular loading condition, the CDF of the long term total stress consisting of the still

water stress and the wave induced and slam effects is then obtained by applying the convolution theorem:

$$F'_{T_i}(r) = \int_{-\infty}^{\infty} F'_X(r-x) f_{ST_i}(x) dx$$

3.1.5.3 Extreme Value Distribution of the Total Stress

The cumulative distribution function of the largest value of stress in a particular loading condition i can be obtained using the Ferry Borges and Castenhata model, Ref. 3.17, with pulse times representing voyages in that loading condition. The Ferry Borges process consists of pulses of uniform duration. In the present case, the duration of the pulses can be taken to be the average duration of a voyage in the loading condition i (e.g., laden or ballast). Knowing the average duration, t_i, one can obtain the number of pulses in the lifetime:

$$n_i = \frac{T_i}{t_i}$$

where T_i is the total time spent in the loading condition i.

The cumulative distribution function of the largest value of the total stress is then obtained as

$$F_{T_s}(r) = \sum_{i=1}^{n_c} \left[F'_{T_i}(r) \right]^{n_i} \cdot P_{ST_i}$$

which assumes the likely total stress pulses in the individual voyages in a loading condition to be independent of one another. The total number of loading conditions considered is n_c. Typically n_c is a small number, e.g., 2, representing, say, laden and ballast conditions.

Another approximation to the CDF above could also have been obtained using the Poisson pulse processes whose application to load coincidence analysis was pioneered by Wen, Refs. (3.18,3.19).

3.1.5.4 Probabilistic Load Factor Accounting for Still Water Loads

Denote the characteristic extreme value for the combined total stress by f_{Tc}, and those for the still water and wave load effects by f_{Sc} and f_{wc}, re: These characteristic extreme values may, for example, be values corresponding to a specified exceedence level using the applicable cumulative distribution functions.

The probabilistic load factor ψ, which accounts for the possibility of non-simultaneous occurrence of the still water and wave load effect extreme values, is obtained such that it satisfies the following relationship:

$$f_{Tc} = f_{Sc} + \psi f_{wc}$$

3.1.6 Simplified Approach to Combined Slam and Wave Induced Loads

The previously discussed detailed approach to combined slam and wave induced stress extreme values is based on a time domain approach. In the following, a simplified approach is presented, that is also consistent with a frequency domain approach to the load combination problem involving two random processes.

In the case of two zero mean Gaussian stress processes i and j, the variance of the combined stress σ_c^2 is obtained from (3.1):

$$\sigma_c^2 = \sigma_i^2 + \sigma_j^2 + 2\rho_{ij}\,\sigma_i\,\sigma_j$$

where σ_i^2 and σ_j^2 are the individual process variances, and ρ_{ij} is the correlation coefficient for the two processes. Since the extreme value of combined and individual stress processes, denoted f_c, f_i and f_j, will typically satisfy

$$f_c \simeq c \, \sigma_c$$
$$f_i \simeq c \, \sigma_i$$
$$f_j \simeq c \, \sigma_j \quad ,$$

where c is a constant. It can be shown that

$$f_c^2 \cong f_i^2 + f_j^2 + 2\rho_{ij} f_i f_j$$

In addition, if the stress processes i and j are well separated on the frequency scale, $\rho_{ij} \simeq 0$, and we have the so-called square root of Sum of Squares rule (1.2) for load combination:

$$f_c \cong \sqrt{f_i^2 + f_j^2}$$

Although derived above for Gaussian load processes, which are stationary by definition, the SRSS rule is known in practice to apply to cases involving non-stationary processes (e.g.) slam stresses as well.

In the case of slamming and wave induced stresses, the combined stress extreme value f_c for a seastate, heading, and speed, is given on the basis of the SRSS rule, by

$$f_c = \sqrt{f_w^2 + f_{sl}^2}$$

where f_w and f_{sl} are the individual (wave and slam related) extreme stresses, with the two processes considered uncorrelated because of their typical frequency separation.

As noted in Section 1.4, Nikolaides and Kaplan (1.15) provide evidence through simulations that the SRSS method may indeed be applicable to the above load combination problem. Data on combined and individual (wave and slam) bending moments provided by Mansour and Ferro (3.25) support the same conclusion. Recent work by Friis Hansen (3.26) also indicates that the correlation coefficient between wave induced stress peaks and associated point in time slam stresses to be very small (-0.12 to -0.15 for a 270m containership), thus again providing indirect support for the SRSS rule.

3.2 Local Loads

Local loads of interest in ship structures are:

    (a) still water pressure heads

    (b) extreme dynamic wave (low frequency) pressures

    (c) extreme slamming (high frequency) pressures

    (d) extreme cargo inertial loads due to accelerations

    (e) extreme sloshing pressure loads

Loads (d) and (e) above are internal. Load (e) related to sloshing is important in partially filled tanks. This section of the report considers local loads and their structural significance, with particular regard to dynamic wave pressures, slamming pressures and cargo inertial loads and their combinations. The combination of still water pressures with the other types of local pressure loads is not considered in this section. Such combination is of course necessary, and can be accomplished by the same means as in Section 3.1.

3.2.1 Structural Significance of Local Loads

In small vessels, local loads govern structural design. In the larger vessels, they govern design in selected regions of the vessel. With regard to the importance of local loads in ships, the following may be stated:

(a) In most ships, the side shell structure in way of the neutral axis is strongly influenced by local pressure loads.

(b) In most ships, the structure of the bottom in the forward body is strongly influenced by local pressure loads, primarily due to slamming.

(c) Most transverse structure in ships, e.g., transverse bulkheads and web frames, are sized to sustain local pressure loads.

(d) Tank internals and boundaries are sized in part for local pressure loads such as those from sloshing and cargo pressures.

3.2.2 Extreme (Dynamic) Low Frequency Wave Pressure

The low frequency dynamic wave induced pressures on the ship hull (also called external hydrodynamic pressures) are typically calculated based on linear strip theory, with some corrections made in way of the waterline to account for nonlinearities. The typical calculation procedures employ either conformal mapping, the Frank Close fit method, or Tasai strip theory in calculating the two dimensional added mass and damping coefficients for the strip theory calculations. It is not possible to obtain pressure information using two dimensional coefficients based on Lewis form section descriptions.

The distribution of the extreme wave pressures can be obtained from any of the extreme value prediction methods discussed in Refs. 3.20,3.23. The simplest approach is to assume that the peaks of the local pressure process are independent, and the process itself is stationary and Gaussian, similar to the sea excitation, and obtain the distribution of the largest peak in a sequence of N peaks by order statistics. As noted in Ref. 3.20, based on such an analysis, the expected value of the maximum pressure peak in a sequence of N-peaks was determined by Cartwright and Longuet-Higgins, and is approximated by

$$\frac{E\left[\max(P_1, P_2, \ldots, P_N)\right]}{\sqrt{m_0}} \cong \left[2 \ell n \left(\sqrt{1-\varepsilon^2}\ N\right)\right]^{\frac{1}{2}} + C\left[2 \ell n \left(\sqrt{1-\varepsilon^2}\ N\right)\right]^{-\frac{1}{2}}$$

where $P_1, \ldots, P_N$ are the sequence of N-peaks, m_0 is the mean square value of the pressure process, ε is its bandwidth parameter, and C is the Euler number ($C \cong 0.5772$). The first term of the equation above is the mode of the extreme value distribution. The bandwidth parameter is defined from

$$\varepsilon^2 = 1 - \frac{m_2^2}{m_0 m_4}$$

where

$$m_n = \int_{-\infty}^{\infty} \omega^n S(\omega) d\omega\ ;\quad n = 0, 2, 4$$

Here, ω is the frequency, and $S(\omega)$ is the spectral density of the pressure process. Typically, ε for the hydrodynamic pressure process in ships is small enough that the process can be considered narrow banded for practical purposes.

The number of peaks in a given time, typically the seastate persistence, may be obtained using the zero crossing period for the process, calculable from the spectral moments.

The extreme pressure peak with a probability of exceedence α is given by (3.21):

$$P_\alpha \cong \left[2 m_0 \left\{\ell n\ N + \ell n\left[\frac{1}{\ell n\left(\frac{1}{1-\alpha}\right)}\right]\right\}\right]^{\frac{1}{2}}$$

which applies for small α. Note that P_α is in general independent of ε only for small α. This particular equation does not require the peaks to be independent.

3.2.3 Extreme Accelerations and Resulting Cargo Inertial Loads

Accelerations due to vessel motion are important to ship structures for the following reasons:

(a) They result in cargo inertial loads in tanks. These loads can be large, and in some vessel types, e.g., in ore carriers, can govern the design of local structures.

(b) Internal structure in certain types of ships must be specifically designed to sustain acceleration related structural inertial loads. The most prominent example of this is the tank support structure in liquified gas carriers.

(c) Acceleration related inertial loads are relevant to cargo lashing, e.g., in containerships.

(d) Accelerations affect the performance of ship systems and crew comfort.

Resultant vertical acceleration in a vessel is usually of primary interest. Figure 3.9 (Ref. 3.22) shows trends of 10^{-8} level vertical acceleration (in g's) at the forward perpendicular, calculated for Series 60 hull forms with lengths ranging from 50 to 400 meters, and speeds up to 25 knots. As can be seen from the figure, accelerations and their effects are relatively more important in the smaller vessels; also, they increase with vessel speed. Vertical accelerations amidships, not shown in Figure 3.9, are typically lower by a factor of 2 to 2.5.

For purposes of structural design, extreme values related to vessel accelerations and related loads including pressures can be obtained in the same way as for extreme external pressures, previously described in Section 3.2.2, since the seaway related low frequency acceleration process can be considered stationary and Gaussian.

3.2.4 Extreme Slamming Pressures

As previously noted, local slam pressures can control structural design in some parts of the vessel, especially in the forward body, and the flat of bottom forward where present.

Slamming related pressures produce impulsive loads on the vessel structure. The resulting effects (stresses) typically can be characterized as being of high frequency and transient in nature.

Slam impact pressures in ships have been studied by Ochi and Motter, Ref. 3.9, in the context of bottom slamming. The impact pressure pulse is taken triangular in shape, with the time duration given by

$$t_p = 0.0044\sqrt{L} \text{ sec}$$

where L is the vessel length in feet. For a 520 ft Mariner hull, t_p is approximately 0.1 seconds. For the Mariner, the traveling time for the pressure in the longitudinal direction is said to be approximately 0.15 to 0.3 seconds from stations 2 to 5 (21 station basis) in the forward body. The traveling velocity of pressure in the longitudinal direction, for a vessel of any length L, is obtained from

$$v = 11.4\sqrt{L} \quad \text{ft / sec}$$

where L is in feet. The traveling velocity of pressure in the upward direction depends on the relative vertical velocity between the ship and waves at the location of interest. The vertical limiting depth for the impact force is typically 1/10 the design draft. The impact pressure is applied near the ship bow first and travels aft. It is worth noting that to obtain the impact force one needs to integrate pressure over the hull domain of its application. Thus, because hull (in particular, the flat of bottom area) is a factor, the location of maximum impact force resultant is not necessarily the same as the location of maximum impact pressure.

The impact pressure is indicated by Ochi to follow a truncated exponential probability distribution:

$$f(p) = \lambda \, e^{-\lambda(p - p_0)} \; ; \quad p_0 \leq p \leq \infty$$

where p = slamming impact pressure

p_0 = a threshold pressure

$\lambda = 1/(k \, R_r')$

The threshold pressure depends on a threshold velocity below which the impact pressure on the vessel is not significant. The parameter 'k' is nondimensional, and depends on section shape; R_r' is twice the variance of the relative velocity. A sample histogram of slamming pressures for a Mariner model, from Ochi's work, is shown in Figure 3.10.

The probability density function for p_n, the extreme value of slamming pressure in n impacts, can be obtained on the basis of the truncated exponential parent density and order statistics. The mode of the extreme value distribution can be shown to be

$$\bar{p}_n = p_0 + \frac{1}{\lambda} \, \ell n \, n$$

This is the most probable extreme pressure. The extreme pressure corresponding to an exceedence probability, α, where α is small, can be shown to be given by

$$\hat{p}_n(\alpha) = p_0 - \frac{1}{\lambda} \, \ell n \left\{ 1 - (1 - \alpha)^{1/n} \right\}$$

In the above equations, n is the number of slams. The value of n depends on the severity of the sea, and on vessel speed, heading and heavy weather countermeasures. The number of slams in T hours is given by

$$n = 57.3 \, T \sqrt{\frac{R_y'}{R_r'}} \; \Pr(\text{slam})$$

3-41

where R_r' and R_r' are twice the variance of the relative velocity and relative motion, respectively, obtainable using linear ship motion analysis. The probability of slam occurrence is given by

$$P_s = \exp\left\{-\left(\frac{H^2}{R_r'} + \frac{r_*^2}{R_v'}\right)\right\}$$

where H is the ship draft at the location considered, and r_* is a threshold relative velocity. The above probability of slam occurrence combines individual probabilities of bow emergence and a threshold velocity condition being met. In the case of bow-flare slamming, the above expressions will need modification.

Figure 3.11 (Ref. 3.9) shows the calculated distribution of most probable extreme pressures along ship length, for a Mariner hull in seas of 25 feet significant wave height. As may be seen, the probability of impact and extreme pressure decrease significantly with decreasing vessel speed; also, location of peak pressures moves aft with increasing speed.

3.2.5 Local Load Combinations

Impulsive local loads such as slamming impact pressures with very short pulse durations (e.g., 0.1 second) and high magnitudes must necessarily be treated individually for purposes of local structural design. It is not typically fruitful to account for their phasing with other types of local loads. Cargo inertial pressures and external hydrodynamic pressures, on the other hand, are more tractable to load combination analysis. There is also a potential benefit in considering their load combinations, since they occur over more of the vessel structure.

The consideration of the combination of external pressures and acceleration related cargo inertial pressures is straightforward, since both random processes can be considered stationary and zero mean Gaussian, with parameters obtained using ship motion analysis.

In such a case, the previously developed probabilistic load factors K_c (of Section 3.1.2) for two load components apply, and the combined extreme stress f_c can be obtained in the form

$$f_c = f_p + K_c f_s$$

where f_p and f_s are the individual extreme stresses corresponding to the "primary" and "secondary" load components. Trends of K_c for two load components are shown in Figure 3.2.

Typically in ships, the cargo inertial pressures and the low frequency wave induced pressures oppose each other. An illustration in this regard was previously given in Chapter 2; see also, Figure 2.8 which shows correlation coefficients for the two pressures acting on the double bottom structure of an ore carrier. In that illustrative case, it was concluded that extreme cargo inertial pressures, when considered alone for design, provided a safe structure.

Considering Phase Differences in Structural Analysis

Local pressures are particularly important to the design of transverse structure, as was previously pointed out. An interesting situation arises here in an analysis context, related to stresses due to the overall behavior of the transverse structure, e.g., a web frame. The essential factor that complicates the problem is the fact that local external pressures along different points on the structural periphery will have different phase angles. One way such phase differences have been handled in the past for structural analysis is to calculate, for a sufficient number of regular waves, the largest resulting bending moment (and shear force) at selected sections, i.e., the design is based on the largest probable bending moment at selected sections of the transverse web, rather than on the momentary distribution of the bending moment, see, for example, Ref. 3.24. A more exact way is to use two load cases

(in-phase and out-of-phase) for each regular wave, obtain related stresses, and thus construct a stress transfer function which is then used in the usual way.

3.3 Combined Hull Girder and Local Loads

3.3.1 Treatment of Design Load Combinations

The consideration of load combinations for design, involving hull girder and local loads, can be accomplished in much the same way as for hull girder loads. In those cases where the low and high frequency dynamic wave induced loads are steady state, and can be considered zero mean and Gaussian random processes, the methods developed in Section 3.1, using the probabilistic load factor format, directly apply. The inclusion of still water effects while not described here, can also be accomplished as per the methods of Section 3.1.

Two Correlated Loads (Hull Girder, Local)

Consider that a "primary" stress from hull girder vertical bending and a "secondary" stress from local loads such as pressure be present. The total stress may be written (3.?)

$$f_t(t) = f_0 + f_c(t)$$

where f_0 is a constant part, given by

$$f_0 = \frac{M_{sw}}{SM_v} + C\,p_{sw}$$

M_{sw} is the still water bending moment, and p_{sw} is the still water pressure, C being a pressure to stress transformation factor.

The time dependent part $f_c(t)$ is given by

$$f_c(t) = \frac{M_v(t)}{SM_v} + C\,\xi(t) = f_v + f_\xi$$

where $M_v(t)$ is the wave induced vertical bending moment, and $\xi(t)$ is a time dependent pressure. The variance of the time dependent part of the combined stress is given in terms of the stress processes by

$$\sigma_c^2 = \sigma_v^2 + \sigma_\xi^2 + 2\rho_{v\xi}\,\sigma_v\,\sigma_\xi$$

Following the same procedures as in Section 3.1, we can write

$$f_{c1/m} = f_{v1/m} + K_c\,f_{\xi1/m}$$

where

$$K_c = \frac{\left[1 + r^2 + 2\rho_{v\xi}\,r\right]^{1/2} - 1}{r}\;;\quad r = \frac{\sigma_\xi}{\sigma_v}$$

Note that the variance equation above is written in terms of stresses, i.e., the factor $K = SM_v/SM_H$ which was present in some of the developments of Section 3.1 is here unity. K_c above is the probabilistic load factor.

Typical K_c Values

Note the following extreme cases:

(a) If $\rho_{v\xi} = 0$, i.e., the bending moment and pressure are uncorrelated, which may not be a realistic assumption, and with $r = 0.2$ for the ratio of pressure to bending stresses, $K_c = 0.1$ which is small.

(b) If $\rho_{v\xi} = 1$, i.e., the two stresses are strongly correlated, $K_c = 1$ independent of r.

(c) The following data were obtained for the Universe Ireland tanker, from the previously cited paper by Stiansen and Mansour (Ref. 3.3):

$$\rho_{v\zeta} \cong 0.71 \text{ to } 0.78 \; ; \quad \text{use } 0.74$$

$$r = 0.2$$

In this case, $K_c = 0.78$.

Three Correlated Loads

The case of three correlated loads results in two probabilistic load factors, K_{c_2} and K_{c_3}, as discussed in Section 3.1. The combined extreme stress f_c is written

$$f_c = f_1 + K_{c_2} \; f_2 + K_{c_3} \; f_3$$

where f_2 and f_3 are the individual extreme stresses for loads with subscripts 2 and 3. Design charts addressing the three load case may be found in Appendix E.

To get an appreciation of the magnitudes of the factors K_{c_2} and K_{c_3} in a typical case, consider the stress arising from vertical bending f_1, horizontal bending f_2 and local pressure f_3. The K_c's can be defined if one has estimates of the stress ratios r_2 and r_3, and the correlation coefficients ρ_{12}, ρ_{13} and ρ_{23}. The following examples are based on correlation coefficients from the Stiansen and Mansour paper previously cited (Ref. 3.3):

(a) Bottom:
$r_2 = 0.4$ $\rho_{12} = 0.4$
$r_3 = 0.3$ $\rho_{13} = 0.7$
 $\rho_{23} = 0.3$

$K_{c_2} = 0.67$ $K_{c_3} = 0.56$

(b) Deck:
$r_2 = 0.4$ $\rho_{12} = 0.4$
$r_3 = 0.1$ $\rho_{13} = 0.7$
 $\rho_{23} = 0.3$

$K_{c_2} = 0.73$ $K_{c_3} \cong 0$

These values are similar to those obtained for the two variable case. Note that, for design purposes, a (small) local pressure on deck is considered above.

Also of interest are the following extreme cases of K_{c_2} and K_{c_3}:

(a) $\rho_{12} = \rho_{13} = \rho_{23} = 0$ for uncorrelated loads

$$r_2 = 0.6 \qquad K_{c_2} = 0.42$$
$$r_3 = 0.3 \qquad K_{c_3} = -0.16$$

(b) $\rho_{12} = \rho_{13} = \rho_{23} = 1$ for fully correlated loads

$$r_2 = 0.6 \qquad K_{c_2} = 1.0$$
$$r_3 = 0.3 \qquad K_{c_3} = 1.0$$

3.3.2 Identification of Critical Load Combinations

Load combinations of interest, involving hull girder and local loads, are now enumerated. Two regions of the vessel are considered, namely the midbody region and the forward quarter body. The combination identification rests on judgement and experience. There is a need for systematic evaluation of the significance of various loads and load combinations in the different parts of the structure.

Midbody Region

(i) The deck structure is governed primarily by vertical bending moment, and to a minor extent, horizontal bending moment. Sloshing loads can sometimes influence local structural strength.

(ii) The bottom structure depends primarily on the vertical bending moment, and secondarily on cargo inertial loads in tanks and the external hydrodynamic pressure.

(iii) The side shell depends primarily on the vertical bending moment and to a minor extent on the horizontal bending moment away from the waterline and toward the deck. Toward the bilge, the vertical bending moment is of primary importance, followed by the external pressures and any internal cargo inertial loads. In way of the waterlines, the structure depends primarily on the external pressures and internal cargo inertial loads.

(iv) Transverse structures, e.g., web frames and transverse bulkheads, are decided primarily by local loads (e.g., external pressure and cargo inertial pressures) and to a smaller extent by hull girder shear forces.

Note that when slam induced bending effects are large, they should be included with the vertical bending moment. Also, in naval ships, horizontal bending moment can be an important consideration. Still water effects, while not part of the above discussion, are in general pertinent for all parts of the midbody structure.

Forward Quarter Body Region

(i) The deck structure in cases where torsional effects are unimportant, is governed local loads, e.g., due to shipping of green water, which is a phenomenon that is difficult to treat except by model tests.

(ii) The bottom structure is governed by local loads, which may arise from slamming, and external pressures and internal cargo inertial pressures. Of these, slam related loads are perhaps the most significant.

(iii) The side shell structure is governed primarily by shear forces, due to wave induced low frequency hull girder bending, and due to slamming. A secondary effect on the side shell arises from external hydrodynamic pressures and internal cargo inertial loads, which tend to be significantly larger in the forward quarter body region in comparison to the midship.

(iv) Transverse structures (e.g., transverse web frame) are affected primarily by local pressures due to external pressure and cargo inertial loads, and to a smaller extent by hull girder shear forces due to low frequency wave induced loads as well as slamming.

(v) In those cases where torsional effects are important, e.g., because of wide hatches, all continuous vertical structures in the fore body region can be subject to an increase in shear stresses due to torsion. While such torsion effects are certainly important, there exist no comparative studies by which one can judge whether they, or the local pressures, or the hull girder shear forces are the dominant ones in comparative terms.

Again, while we have not discussed still water pressures in the above specification of dominant loads, they certainly are pertinent to all fore body structure.

3.4 Recommended Load Calculation Methods

The various loads to be considered in Phase 3 of the Ship Structure Committee's Reliability thrust area project include:

- Still water loads

- Low frequency steady state wave induced loads

- Slam loads

The following table summarizes the recommended methods for calculation of the individual load components.

Item	Method	Reference
still water loads	Standard, needs no elaboration	—
low frequency wave induced loads	Linear strip theory based shipmotion calculations, with correction for nonlinearities due to hog/sag differences	3.30, 3.31
slam loads	Bottom slamming method due to Ochi, bow flare effects by method due to Kaplan and Sargent, dynamic response by method due to Mansour and Lozow	3.9, 3.12, 3.13

In the case of low frequency wave induced loads, Ref. (3.30) is a 1975 vintage computer program that includes both vertical and horizontal bending moments and shear forces. Improved motion calculation technology is available in the present Navy Ship Motion Prediction Program (SMP), Ref. (3.37), which, however, does not calculate loads other than vertical bending moments and shear forces. SMP is currently being modified to include calculation of horizontal bending moment and shear force, as well as torsional moments. A good survey of existing linear strip theory programs may be found in (3.38).

References

3.1. Mansour, A.E., "Combining Extreme Environmental Loads for Reliability Based Designs," *Proc. SSC-SNAME Extreme Loads Response Symposium*, Arlington, VA, October 1981.

3.2. Mansour, A.E., Thayamballi, A.K., Li, M. and Jue, M., "A Reliability Based Assessment of Safety Levels in the ABS Double Skin Tanker Guide," Mansour Engineering Report to ABS, July 1992.

3.3. Stiansen, S.G. and Mansour, A.E., "Ship Primary Strength Based on Statistical Data Analysis," *Trans. SNAME*, 1975.

3.4. Ochi, M.K., "On the Prediction of Extreme Values," *Journal of Ship Research*, Vol. 17, No. 1, March 1973, pp. 29-37.

3.5. Madsen, H.O., Krenk, S. and Lind, N., *Methods of Structural Safety*, Prentice Hall, 1986.

3.6. Vanmarcke, E.H., "On the First Passage Time for Normal Stationary Random Processes," *J. Applied Mechanics, Trans. ASME*, March 1975, pp. 215-220.

3.7. Ditlevsen, O. and Lindgren, G., "Empty Envelope Excursions in Stationary Gaussian Processes," *J. Sound and Vibration*, Vol. 122, No. 3, 1988, pp. 571-587.

3.8. Cramer, E.H. and Friis Hansen, P., "Stochastic Modeling of the Long Term Wave Induced Responses of Ship Structures," accepted for publication in *J. Marine Structures*, 1992.

3.9. Ochi, M.K. and Motter, L.E., "Predictions of Slamming Characteristics and Hull Responses for Ship Design," *Trans. SNAME*, Vol. 81, 1973, pp. 144-190.

3.10. Lewis, E.V., Hoffman, D., Maclean, W.M., Van Hoof, R., and Zubaly, R.B., "Load Criteria for Ship Structural Design," Ship Structure Committee Report 240, May 1973.

3.11. Stavovy, A.B. and Chuang, S.L., "Analytical Determination of Slamming Pressures for High Speed Vehicles," *J. Ship Research*, Vol. 20, No. 4, Dec. 1976, pp. 190-198. Errata in Vol. 21, No. 4, December 1977, p. 254.

3.12. Kaplan, P. and Sargent, T.P., "Further Studies of Computer Simulation of Slamming and Other Wave Induced Vibratory Structural Loadings on Ships in Waves," Ship Structure Committee Report 231, 1972.

3.13. Mansour, A. and Lozow, J., "Stochastic Theory of the Slamming Response of Marine Vehicles in Random Seas," *J. Ship Research*, Vol. 26, No. 4, Dec. 1982, pp. 276-285.

3.14. Antonides, G.P., "A Computer Program for Structural Response to Ship Slamming," NSRDC Ship Acoustics Dept. Report SAD-9E, 1972.

3.15. Wheaton, J.W., "Further Analysis of Slamming Data from the S.S. Wolverine State," SSC Report 255, January 1976.

3.16. Engle, A., Private Communication, 1992.

3.17. Ferry Borges, J. and Castenhata, M., "Structural Safety," Second Edition, Laboratario Nacional de Engenharia Civil, Lisbon, 1972.

3.18. Wen, Y.K., "Structural Load Modeling and Combination for Performance and Safety Evaluation," in *Developments in Civil Engineering*, Vol. 31, Elsevier, Amsterdam, 1990.

3.19. Wen, Y.K., "Statistical Combination of Extreme Loads," *J. Structural Division, ASCE*, Vol. 103, No. ST5, May 1977.

3.20. Mansour, A.E., "An Introduction to Structural Reliability Theory," Ship Structure Committee Report 351, 1990.

3.21. Silveria, W.A. and Brillinger, D.R., "On Maximum Wave Heights of Severe Seas," OTC Paper 3232, Houston, 1978.

3.22. Abrahamsen, E., "Recent Developments in the Practical Philosophy of Ship Structural Design," DnV Reprint, circa 1967.

3.23. A. Thayamballi, "Structural Reliability Process Definitions," Part 3 of Final Report on Ship Structure Committee project SR-1330, September 1992.

3.24. Merega, F. and Squassafichi, N., "Wave Induced Stresses in Transverse Frames of Tankers," Registro Italiano Navale Technical Bulletin No. 40, 1970.

3.25. Ferro, G. and Mansour, A.E., "Probabilistic Analysis of Combined Slamming and Wave Induced Responses," *J. Ship Research*, Vol. 29, No. 3, September 1985, pp. 170-188.

3.26. Friis-Hansen, P., "On Combination of Slamming and Wave Induced Responses," Paper submitted to the *Journal of Ship Research*, April 1993.

3.27. Mansour, A. and d'Oliveira, J., "Hull Bending Moment Due to Ship Bottom Slamming in Regular Waves," *J. Ship Research*, Vol. 19, No. 2, June 1975, pp. 80-92.

3.28. Chen, Y.H., "Stochastic Analysis of Ship Dynamic Responses," Ph.D. Dissertation, Department of Naval Architecture, University of California at Berkeley, May 1977.

3.29. Chen, Y.H., "Ship Vibrations in Random Seas," *J. Ship Research*, Vol. 24, No. 3, September 1980, pp. 156-169.

3.30. Meyers, W.G., Sheridan, D.J. and Salvesen, N., "Manual for the NSRDC Ship Motion and Seaload Computer Program," NSRDC Report 3376, February 1975.

3.31. Mansour, A.E., Lin, M.C., Hovem, L.A. and Thayamballi, A., "Probability-Based Ship Design Procedures - A Demonstration," Final Report on Ship Structure Committee Project SR-1330, September 1992.

3.32. Mansour, A., Thayamballi, A. and Li, M., "Assessment of Reliability of Ship Structures - Phase I," Final Report on Ship Structure Committee Project SR-1344, August 1992.

3.33. Wen, Y.K. and Chen, H.C., "On Fast Integration for Time Variant Structural Reliability," in *Reliability and Risk Analysis in Civil Engineering*, Vol. 1, Proc. U.S.-Japan Joint Seminar on Stochastic Approaches in Earthquake Engineering, Boca Raton, Florida, May 1987. Also, *Probabilistic Engineering Mechanics*, Vol. 2, No. 3, pp. 156-162.

3.34. Kaplan, P. et al., "Analysis and Assessment of Major Uncertainties Associated with Ship Hull Ultimate Failure," Ship Structure Committee Report 332, 1984.

3.35. Rice, S.O., "Mathematical Analysis of Random Noise," in *Selected Papers on Noise and Stochastic Processes*, N. Wax, editor, Dover Publications, New York, 1954, pp. 180-181.

3.36. Longuet-Higgins, M.S., "On the Joint Distribution of the Periods and Amplitudes of Seawaves," *J. Geophysical Research*, Vol. 80, No. 18, June 1975, pp. 2688-2694.

3.37. Meyers, A.G. and Baitis, A.E.. "SMP84: Improvements to Capabilities and Prediction Accuracy of the Standard Ship Motions Prediction Program, SMP81." DTNSRDC Report 0936-04, September 1985.

3.38. Dalzell, J.F., Thomas, W.L. and Lee, W.T., "Correlations of Model Test Data with Analytic Load Predictions for Three High Speed Ships." CARDEROCKDIV/SHD-1374-02, Carderock Division, Naval Surface Warfare Center, Carderock, MD, September 1992.

List of Figures

4. FATIGUE LOADS, LOAD MODELS, AND LOAD COMBINATIONS

Consideration of load combinations in the context of fatigue design is somewhat different from that of extreme load design. In the case of fatigue, the entire long term distribution of stress ranges needs to be addressed, accounting for damage accumulation from the various stress range levels. The accumulated damage is a function, not only of the stress range levels, but also of the number of cycles of stress reversal associated with each stress level. In the case of extreme load design, the load combination treatment aims to determine design load sets. The maximum anticipated load effect for design would occur when the structure is subject to one of the design load sets. For fatigue design, in addition to governing design load set, the shape of the long term stress range distribution at any structural location is also a factor.

In the context of fatigue loads and load combinations, a two level methodology, one suitable for design, and the other for more rigorous analysis, is recommended. The first level is the Weibull approach, in which the governing stress range extreme value is determined using selected structural load cases, and the shape of the stress range distribution is taken as a "given". In the second, more elaborate level, spectral fatigue analysis is used to determine the entire stress range versus number of cycles histogram in a more rigorous manner.

4.1 Identification of Sources of Fatigue Loads

Cyclic fatigue load sources in merchantships can be classified as follows (Ref. 4.2):

Load Category	Reversals During Life
Low frequency, wave induced	10^7 - 10^8
High frequency, wave induced	10^6
Still water	300 - 500
Thermal	7000

The low frequency wave-induced loads are considered quasistatically for purposes of obtaining the fluctuating stresses, while the high frequency wave-induced loads require dynamic analysis, as these loads are often excited by slamming, whipping or springing.

Still water loading in the context of fatigue represents a change in mean load as fuel is consumed or ballast is added or shifted. Also, from voyage to voyage, there can be large changes or differences in the still water loading, because of change in the loading pattern. For example, tankers encounter very different fully laden and ballast load patterns, with the laden still water bending moment of a hogging nature while the ballast still water bending moment is of a sagging nature.

Thermal stresses in ships are induced by the presence of a non-uniform thermal gradient, which depends on the weather, the sea-air temperature differential, and exposure to the sun. Thermal load variations thus generally follow diurnal changes in air temperature. In tankers, another source of thermal loading is the intermittent use of heating coils.

In the treatment of vessel structure fatigue, the following loads and their combinations must then be considered in principle:

(a) Fatigue loads resulting from hull girder bending

(b) Fatigue loads resulting from local pressure oscillations

(c) Cargo loading and unloading (low cycle effects)

(d) Still water bending (mean level) effects

As we will later note, experience indicates items (a) and (b) above to be by far the most important.

4.2 The Design Treatment of Fatigue Loads

Central to the treatment is the lifetime maximum stress range the structural detail is subject to. Consider that there are N_T stress reversals (cycles) in the lifetime. Then

$$p(s > S_o) = \frac{1}{N_T} \qquad (4.1)$$

where S_o is the lifetime maximum stress range and 'p' denotes the probability that stress range S is greater than S_o. Assume that the stress range follows a Weibull distribution, with parameters ξ and δ, where ξ is the shape parameter, and δ is the scale parameter. The cumulative distribution function is then given by

$$F_s(S) = 1 - \exp\left[-\left(\frac{S}{\delta}\right)^{\xi} \right]; \quad S \geq 0 \qquad (4.2)$$

and, with Γ denoting the Gamma function. The expected value of S^m is given by

$$E(S^m) = \delta^m \; \Gamma\left(\frac{m}{\xi} + 1\right) \qquad (4.3)$$

Solving for S_o from (4.2) using (4.1) gives

$$S_o = \left[\ell n(N_T)\right]^{1/\xi} \delta \qquad (4.4)$$

The fatigue damage for N_T cycles, assuming a "straight line" S-N curve of the form

$$NS^m = A \qquad (4.5)$$

is given by

$$D = \frac{N_T}{A} E(S^m) \qquad (4.6)$$

Substitute Eq. (4.4) into (4.3) and (4.3) into (4.6), and eliminate δ to give the following expression for fatigue damage:

$$D_B = \frac{N_T}{A} S_o^m \left[\ell n(N_T) \right]^{-m/\xi} \Gamma\left(1 + \frac{m}{\xi}\right) \qquad (4.7)$$

The damage D (or D_B) in equations 4.6 or 4.7 is the non-dimensional ratio of N_T to the number of cycles to failure. This development assumes an S-N curve of the form $NS^m = A$. In a more general case, the S-N curves used often have a "kink", say at N_Q cycles, i.e., the curves are bilinear on a log-log scale, and are of the following form:

$$NS^m = A \qquad N \leq N_Q$$
$$NS^r = C \qquad N > N_Q$$

The fatigue damge for this two segment case may be shown to be given, e.g., Ref. 4.1, by

$$D_C = \Lambda D \qquad (4.8)$$

with the bias factor Λ given by

$$\Lambda = \frac{A \, \delta^{-m} \, \Gamma_o(b, Z)}{C \, \Gamma(a)} + \psi(a, Z)$$

where

$$\psi(a, Z) = \frac{\Gamma(a, Z)}{\Gamma(a)} \,, \quad Z = \left(\frac{S_Q}{\delta}\right)^{\xi}$$

$$a = \frac{m}{\xi} + 1 \,, \qquad b = \frac{r}{\xi} + 1$$

Here, $\Gamma(x)$ is the gamma function, and $\Gamma(a,Z)$ and $\Gamma_o(a,Z)$ are incomplete gamma functions (integrals Z to ∞ and 0 to Z). As an example,

$$\Gamma_o(a,Z) = \int_o^Z u^{a-1} \exp(-u)\, du$$

S_Q is the stress range corresponding to N_Q on the S-N curve. In this simplified approach to fatigue analysis, it is necessary to:

1. Specify the design life (number of cycles)
2. Specify the Weibull parameter ξ
3. Determine the extreme stress range the structural detail is subject to during the design life
4. Choose an appropriate S-N curve, determine relevant A, m, etc., and calculate the fatigue damage from equation (4.7) or (4.8)

The extreme stress range and the Weibull shape parameter together define the probability distribution of stress ranges, *considering the combined effect* of all loads applied to the structural detail.

4.3 Treatment of Load Combinations for Design

The stress fluctuations at any vessel location arise from some combination of hull girder bending, local pressure, cargo loading and unloading, thermal effects and still water bending. Of these, the hull girder bending and local pressure fluctuation related effects are far more significant than the others in terms of their contribution to total fatigue damage, particularly for weld fabricated ship structural details. The Weibull approach is thus typically used considering only the high cycle fatigue effects due to hull girder bending and local pressure fluctuations.

4-5

The applicable extreme stress range at any given structural detail location is obtained using suitably formulated design load cases. In the ABS Guide for Double Skin Tankers, Ref. 4.3, for example, several design load cases are specified, each consisting of a particular proportion of the following wave induced load types:

(a) Hull girder vertical bending moment

(b) Hull girder horizontal bending moment

(c) Hull girder vertical shear forces

(d) Hull girder horizontal shear forces

(e) External pressure

(f) Internal tank pressure

Load cases are defined considering different vessel headings relative to the waves. The loads to be applied are specified in terms of close-form formulae. The extreme stress range at any given location is obtained as the largest arising from structural analyses for the various load cases. The load case tables from the ABS Guide are reproduced in Figures 4.1 and 4.2.

The stress range calculated for purposes of fatigue assessment contains both hull girder and local pressure effects. Depending on the location, one of these will typically dominate. For example, at tanker deck locations, the vertical bending moment related stress fluctuation is the predominant one, while on the side shell in way of load waterline, the total stress is nearly entirely due to local pressure fluctuations. The selection of design load cases such as that of Figure 4.1 for use in fatigue design is a matter of experience and development work. Such load cases, together with additional information related to the Weibull shape parameter, subsequently discussed, constitute a simple, yet effective treatment of the effect of combined loads for purposes of fatigue assessment.

4.3.1 Shape of the Long Term Stress Distribution

Apart from the extreme stress range, the Weibull shape parameter is also a factor in the fatigue damage calculated. One way to obtain this parameter is through curve fitting the Weibull distribution to replicate damage from typical long term stress range histograms from more elaborate (spectral) fatigue analyses. In Ref. 4.4, Thayamballi developed a relationship between the Weibull shape parameter ξ and vessel length L in meters, in the form

$$\xi = 1.55 - 0.0 \quad \text{for} \quad 76 < L < 305$$

$$= 1.71 - 0.049\, L^{\frac{1}{2}} \quad \text{for} \quad L > 305$$

This expression specifically addressed a vertical bending moment controlled situation such as that of deck details. In the ABS Double Skin Tanker Guide, Ref. 4.3, the approach has been extended for refined and extended to other locations in the vessel. The Guide specifies the Weibull shape parameter in the following form:

$$\xi = 1.40 - 0.036\, \alpha\, L^{\frac{1}{2}} \quad \text{for} \quad 190 < L < 305$$

$$= 1.54 - 0.044\, \alpha^{0.8}\, L^{\frac{1}{2}} \quad \text{for} \quad L > 305$$

where

$$
\begin{aligned}
\alpha &= 1.0 && \text{for deck structures} \\
&= 0.93 && \text{for bottom structures} \\
&= 0.86 && \text{for side shell and longitudinal bulkhead structures} \\
&= 0.80 && \text{for transverse bulkhead structures}
\end{aligned}
$$

In the context of load characteristics and load combinations, certain aspects of these Weibull parameter relationships should be noted:

(a) The Weibull parameter for any given location decreases as a function of vessel length, see Figure 5.4. For a given lifetime extreme stress range, this implies that

4-7

the fatigue damage expected also reduces, or alternately, the stress range allowable increases somewhat with vessel length.

(b) Details at deck are predominantly stressed by primary bending, whereas on the bottom, there is a combination of bending and local pressure effects. On the side shell in way of waterline, the fluctuating stress is mostly (internal and external) pressure related, while on transverse bulkheads, the fluctuations arise almost entirely due to internal (cargo inertial) pressure fluctuations. For a given vessel length, the stress range allowables are comparatively less in these latter situations in comparison to deck structures.

The above relationships apply to tanker structures and not necessarily to finer form mechantships or naval vessels.

The above mentioned trends of Weibull shape parameters are the most elaborate available to date in the marine field for ship design use. The trends in the relationships discussed are consistent with those obtained from Weibull distribution fits to full scale measurement data in the case of low frequency wave-induced vertical bending moments, such as those from Ref. 4.2, shown in Figure 4.3. Experience with such studies indicates that most loading histories can invariably be fit with Weibull distributions with shape parameters in the range of 0.8 to 1.2, even with added load components such as local pressure and internal cargo loads.

4.4 Detailed Analysis by Spectral Fatigue Procedure

The various parts of a special fatigue analysis procedure for ships are as follows:

- Description of the service profile, including the loading conditions and the long term wave environment (scatter diagram).

- Calculation of ship motions, sealoads and local hydrodynamic pressures in a seaway, the related structural response, and local stress range transfer functions.

- Obtaining the stress range response spectra for each wave spectrum of the scatter diagram. The short term response statistics and the associated probability density function (pdf) of the stress range (response) are then obtained.

- The long term probability density function is obtained as the weighted sum of the various short term stress range probability density functions.

- Fatigue damage is then calculated for the structural detail situation of interest, whose fatigue performance is characterized by an appropriate S-N curve.

The above procedure is shown in a flow chart from in Figure 4.5. Note that instead of obtaining the long term distribution of stress ranges and then the fatigue damage, one can also obtain the fatigue damage for the various short term stress range probability density functions and then sum the damage.

4.4.1 Fatigue Damage in any Given Seastate

Consider an S-N curve obtained from constant amplitude fatigue tests, in the following form:

$$NS^m = A$$

where m and A are empirical constants. Also consider, as is conventional, that the stress range S in any given seastate of the scatter diagram is Rayleigh distributed. It can be shown that (see, for example, Ref. 4.5) the fatigue damage D_j in the seastate j is then given by

$$D_j = \frac{f o_j T}{A} E(S^m)$$

where

$$f_{o_j} \quad = \text{ average frequency (hertz) of the stress process}$$

$$T \quad = \text{ exposure time (seconds)}$$

$$E(S^m) \quad = \text{ expectation of } S^m$$

Upon incorporating the Rayleigh density function in the above equation and summing the damage in all J seastates, the fatigue damage is shown to be

$$D = \frac{T}{A} (2)^{m/2} \Gamma\left(\frac{m}{2} + 1\right) \sum_{j=1}^{J} f_{o_j} \, p_j \left(\sigma_j\right)^m$$

where σ_j is the rms value of stress in seastate j, and p_j is the probability of occurrence of the seastate j. The above expression is also given in (4.9) in a different form.

For those cases where the S-N curve changes slope at 10^Q cycles (the corresponding stress range on the S-N curve being S_Q), with the negative slope changing from m to $m + \Delta m$, $\Delta m \geq 0$, the expression for fatigue damage is (4.5):

$$D_c = \frac{T}{A} (2)^{m/2} \Gamma\left(\frac{m}{2} + 1\right) \sum_{j=1}^{J} \mu_j \, f_{o_j} \, p_j \left(\sigma_j\right)^m$$

where μ is the bias factor, defined as

$$\mu(v) = \mu(v; m, \Delta m)$$

$$= 1 - \frac{\Gamma_o\left(\frac{m}{2} + 1, v\right) - \left(\frac{1}{v}\right)^{\Delta m/2} \Gamma_o\left(\frac{m}{2} + \frac{\Delta m}{2} + 1, v\right)}{\Gamma\left(\frac{m}{2} + 1\right)}$$

Here,

$$v = v_j = \frac{1}{2}\left(\frac{S_Q}{\sigma_j}\right)^2$$

and the incomplete gamma function is defined by

$$\Gamma_o(a,x) = \int_a^x u^{a-1} \exp(-u)\, du$$

4.4.2 Consideration of the Wave Profile

In spectral fatigue analysis, we calculate ship motion and forces due to a sinusoidal wave of a given amplitude and frequency, and then perform a structural analysis to obtain local stresses, and hence the stress range transfer function. The vessel motions and sealoads are calculated using linear strip theory. Such a procedure, however, does not correctly consider the effect of the wave profile in way of the waterline, because of basic limitations of linear strip theory. A "quasi-static" procedure to account for the wave profile effects in way of water line, developed by Friis-Hansen (4.8), is now described.

The ship motion program used provides motion and load transfer functions considering a unit sinusoidal wave with a wave crest at the vessel center of gravity. The wave-induced pressure in way of waterline is calculated using an apparent wave height Z_{aw} at location x_l from the center of gravity, based on the heave and pitch transfer functions:

$$Z_{aw}(x_l, a, w) = a\left(Z_w(x_l, w) - Z_h(w) + Z_p(w)x_l\right)$$

where Z_w is the incoming wave with amplitude a, and Z_h and Z_p are the heave and pitch transfer functions, related to the center of gravity, with the pitch angle assumed small. The incoming wave is shifted in phase $\text{sgn}(\omega_e) \cdot (\omega_e^2/2\pi) \cdot x_l$ radians, where ω_e is the encounter frequency given by

$$\omega_e = \omega - \frac{\omega^2 v}{g} \cos\theta$$

where v is the ship velocity and θ is the vessel heading relative to the waves; sgn is the sign function, equal to +1 or -1, depending on the sign of the argument.

The water pressure at a location (x_l, z) on the side shell, z denoting the vertical coordinate, is then given by (4.8):

$$Z_p(a,w) = \gamma \{Z_m + Z_{aw}(a,w) - Z\} I$$

where Z_m is the mean water level, γ is the specific weight of water, and I is an indicator variable, defined by

$$I = 1 \quad \text{if} \quad R\{Z_m + Z_{aw} - Z\} \geq 0$$
$$= 0 \quad \text{otherwise}$$

where R denotes the real part of a complex value.

Similar profile "stretch" corrections may also be developed where the local hydrodynamic pressures are calculated by the Frank close-fit method (4.10) or the Tasai strip theory (4.11), i.e., with basic account for vessel motions. The wave profile introduces a nonlinearity in way of the water line, which, while typically not accounted for, is nevertheless an important one.

4.5 Consideration of Combined Load Effects in Analysis

In the design treatment of fatigue, as discussed in Sections 4.2 and 4.3, combined load effects were located through pre-selected design load cases, one or more of which can result in the maximum stress range at a location, and also pre-selected Weibull shape parameters. The maximum stress range and the shape parameter together defined the stress range histogram in the long term. In spectral fatigue analysis, however, the stress range rms value for each seastate needs to be estimated. The rms value is then used to define the Rayleigh distribution of stress ranges in the short term.

For any given sea condition, ship speed, heading angle and loading condition, the rms value of the stress amplitude can be obtained from a standard "input-output" procedure that involves the sea spectrum for the sea condition and the response amplitude operator for the fluctuating stress. First, the stress response spectrum is obtained as follows:

$$S_y(\omega) = |H(\omega)|^2 S_x(\omega)$$

where $H(\omega)$ is the stress transfer function, and its modulus $|H(\omega)|$ is the response amplitude operator; $S_x(\omega)$ is the sea spectrum, and $S_y(\omega)$ is the stress response spectrum, ω being the radian frequency. The mean square value of the output (stress amplitude) process is then calculated:

$$E_y = \int_o^\infty S_y(\omega) d\omega$$

i.e., the mean square value is the area under the response spectrum. The root mean square value is $\sqrt{E_y}$. The assumptions under which the above input-output equations hold can be found in Ref. 4.7. Note also that details of consideration of various ship speeds, heading angles and loading conditions have been omitted here, but may also be found in Ref. 4.7.

Consideration of load combination in spectral fatigue analysis is made at the stress amplitude transfer function calculation stage. Essentially, the fluctuating stress amplitude (and hence range) at any structural location is calculated by subjecting a structural model to loads corresponding to a unit wave amplitude at a given frequency (and heading and vessel speed). Related loads such as bending moments and local pressures for that frequency, etc. are calculated from linear ship motion analysis and applied to the structural model to determine the stresses. The phase information is preserved in the analysis by using two load cases for each frequency, corresponding to the in-phase and out-of-phase components (or real and imaginary parts) of the complex load transfer functions. In one load case, the loads applied may then correspond to a wave crest of unit amplitude at midship, while the other load case uses loads with the wave shifted 90 degrees. The stress response amplitude operator is obtained as follows:

$$|H(\omega)| = \sqrt{S_{ai}^2 + S_{ao}^2}$$

where S_{ai} and S_{ao} are the unit wave stress amplitudes from the in-phase and out-of-phase structural analyses. Load combination considerations in spectral fatigue analysis are thus

direct and explicit. Application of this method however requires the determination of a combined strap transfer function for each detail at which fatigue is to be checked. A description of spectral fatigue analysis as applied to ships can be found in Ref. 4.6.

4.6 Inclusion of Still Water and Other Loads

The previous discussion focussed mainly on low frequency wave induced bending moment and local pressure fluctuations and their contribution to high cycle fatigue. Apart from these loads, there is a certain amount of contribution to fatigue damage arising from the following sources:

(a) still water loads

(b) thermal loads

(c) springing loads

(d) slamming loads

The time scales of load reversal associated with still water and thermal loads are long, and typically, the number of load reversals is small. Except in specific cases, such as failure analysis, their consideration in fatigue design is thus not usual. Where such consideration is made, the loads and the fatigue damage accumulating from them are treated independently, i.e., it is assumed that there is no correlation between these loads and the low frequency wave-induced loads.

Fatigue contribution from springing can be important in certain vessel types such as the long and slender Great Lakes ore carriers. It is to be noted, however, that such vessels typically are not ocean-going, i.e., the wave environment they are subject to is often relatively mild. Where specific consideration needs to be made, it is assumed that the damage contribution from springing is independent of the other load types. This is reasonable because the springing related stress fluctuations occur faster than the low frequency wave-induced effects and, typically, the stress response spectra for the two load

sources are well separated on the frequency scale. Similarly, slamming fatigue damage, which is a consideration in naval vessels, can be treated independently of the lower frequency loads, much for the same reasons as for springing. Procedures for slam fatigue need to be developed.

4.7 References

4.1. Wirsching, P.H. and Chen, Y.N., "Fatigue Design Criteria for TLP Tendons," *J. Structural Engineering*, ASCE, Vol. 113, No. 7, July 1987.

4.2. Munse, W.H. et al., "Fatigue Characterization of Fabricated Ship Details for Design," Ship Structure Committee Report SSC-318, 1983.

4.3. ABS Guide for the Fatigue Strength Assessment of Tankers, June 1992.

4.4. Thayamballi, A., "Fatigue Screening for Tankers," ABS Research and Development Division Report RD-90005, May 1990.

4.5. Chen, Y.N., "A Close Form Algorithm for Fatigue Analysis of Compliant Offshore Platforms," ABS Research and Development Division Technical Report RD-85017, September 1985.

4.6. Thayamballi, A., "Fatigue Analysis of Tankers," ABS Research and Development Division Report, RD-89020-F, prepared for the ABS Far East Technical Seminars, November 1989.

4.7. Mansour, A., "An Introduction to Structural Reliability Theory," Ship Structure Committee Report 351, 1990.

4.8. Friis-Hansen, P., "Fatigue Damage in Side Shells of Ship Structures," unpublished manuscript, Department of Ocean Engineering, The Technical University of Denmark, 1992.

4.9. Mansour, A.E., Lin, M.C., Hovem, L.A., and Thayamballi, A., "Probability-Based Ship Design Procedures – A Demonstration," Final Report on Ship Structure Committee Project SR-1330, September 1992.

4.10. Frank, W., "Oscillation of Cylinders in or Below the Free Surface of Deep Fluids," NSRDC Report 2375, October 1967.

4.11. Tasai, F., "On the Damping Force and Added Mass of Ships Heaving and Pitching," Report of the Research Institute for Applied Mechanics, Japan, Vol. 7, No. 26, 1959.

List of Figures

5. MODELING ERRORS

In this chapter, information on modeling errors associated with extreme and fatigue loads and load combinations are reviewed and condensed to a useable form. It was noted that there is very little information available on modeling errors related to load combinations, and coexisting loads. Hence, most of the information developed is that related to modeling errors in loads and load effect prediction.

At the outset, we should note two facts:

(a) We deal with modeling errors. This is primarily the error in prediction methods for loads and load effects as they relate to "reality".

(b) Modeling errors can be procedure dependent, although this factor may not always be pointed out.

Modeling errors in the context of marine structures have received a fair amount of attention and have been the subject of several review and quantification studies. We may, in particular, point out the work of Mansour (5.1,5.2), Kaplan (5.4), Nikolaides and Kaplan (5.5), and Thayamballi (5.6). The Ship Structure Committee Report 363 by Nikolaides and Kaplan is the most recent among the above, and as such, has been used where appropriate in preparing this chapter, consistent with the work proposal. Reference also needs to be made to the work of Guedes Soares (5.7), whose in-depth study of load effects in ship structures provides useful insights on modeling errors. The above-mentioned references deal primarily with extreme loads and load combinations. In the case of fatigue, the primary reference we have used is that of Wirsching (5.8). Reference is also made to Thayamballi and Jan (5.9).

5.1 Sources of Uncertainties in Load Effects

In structural reliability-based design, the safety check equation involves load effects (e.g., stresses) which are compared with capacity (strength). The calculation of load effects involves the following steps, whether one considers extreme loads or fatigue damage:

(i) Environmental description (cause of loads).

(ii) Determination of loads and load combinations arising from the env   ment.

(iii) Calculation of the load effect, e.g., stresses using appropriate struct.   . analysis; in the case of fatigue, fatigue damage is typically the "demand" that enters the safety check equation.

Each of these steps involves modeling error arising from uncertainties in knowledge and inaccuracies in procedural details. In the case of ocean-going ships, our primary case of interest, two interesting sources of uncertainty in design load effects also arise:

(a) The wave environment the vessel may be subject to, in the long term, may not be known. This aspect implies that the actual load effects may be different from the load effects calculated for design purposes on the basis of a postulated design environment. In the case of ocean-going merchant ships designed for unrestricted service, a North Atlantic wave environment is used in design while the actual long term wave environment is usually likely to be (but not necessarily always) less severe.

(b) Ocean-going vessels, by their nature, can avoid rough weather. Also, in any given sea and weather, counter measures, such as speed reduction and changes in heading angles, can lead to load effect reductions.

Item (a) above, related to uncertainty due to the definition of the environment, is dealt with in this chapter. Item (b), relating to the impact of ship routing, storm avoidance and

operator action, is the subject of chapter 6 of this report, although some preliminary information is also given in this chapter.

5.2 Modeling Uncertainties in Environmental Description

The following modeling uncertainties related to the load environment may be enumerated:

(i) Uncertainty in wave spectra, due to the differences between a theoretical spectrum for a seastate, and the actual spectrum for the seastate.

(ii) Uncertainty due to inexact treatment of wave energy spreading.

(iii) Uncertainty due to nonuniformity of wave headings.

(iv) Uncertainty due to using visually observed wave data.

(v) Uncertainty due to correlations of subsequent wave peaks.

(vi) Uncertainties due to operator discretion in heavy weather.

Selected results related to the above uncertainties, obtained from Ship Structure Committee Report 363, are given in Table 5.1. The modeling errors of Table 5.1 are based on the work of Guedes Soares (5.7), and are what he terms "simplified representations". His original work provides more detailed evaluation of the uncertainties involved, although in a manner less suitable for design use in comparison to the simplified representations. While the simplified representations are a function of significant wave height for the seastate alone, the more detailed representations also account for other parameters. Since the results noted depend on procedural details, the method of approach they pertain to, and the way they were obtained, are summarized below.

Table 5.1. Model Uncertainties in Environmental Description

Source of Uncertainty	Bias	COV
Spectral shape variability	1.0 $L \leq 250$ m or $H_s > 5$ m $2 - 0.2\,H_s$ otherwise	0.1
Wave energy spreading	$1 - 0.0077\,H_s$	0.05
Non-uniform headings	$0.981 + 0.018\,H_s$	0.10
Visual wave data	$\dfrac{0.75\,H_s}{H_s - 2.33}$	0.17
Independent peaks assumption	0.9	unknown
Heavy weather countermeasures	1 to 1.25	unknown

Note: (i) H_s is the significant wave height in meters.

(ii) Bias is actual/predicted value.

Spectral Shape Variability: This uncertainty represents the effect of possible variation in spectral shape for a given seastate. The calculations were based on the mean square wave bending moment for two ships. The implication is that for long ships (L > 250 m) and small wave heights (H_s < 5 m), an underestimation occurs in the wave bending moment if an average spectrum is used to represent the seastate. The error in representing the average spectrum by a theoretical spectrum (e.g., ISSC) was not evaluated, but can be significant. As an example, for a navy cruiser, the maximum lifetime bending moment was found in (5.21) to be higher by 25% when computed with an ISSC wave spectrum than when computed with the Ochi six parameter wave spectra which fit North Atlantic wave data better. The bias of 1.0 shown for wave spectral variability in Table 5.1 does not account for such differences.

Wave Energy Spreading: The usual treatment of wave energy spreading, e.g., by a cosine-squared spreading function, assumes that the degree of spreading is independent of the seastate intensity. The tabulated modeling error pertains to the bias in the mean square bending moment, and accounts for the fact that the degree of wave energy spreading is less for the higher seastates.

Non-Uniformity of Headings: The distribution of relative wave headings along a particular route may not be uniform, but design typically assumes them to be. The tabulated value of bias pertains to the mean square bending moment for a vessel in a North Atlantic route, where the headings were assumed uniform, when in reality they are not. It may be recalled that the North Atlantic wave environment is typically used for merchantship design.

Visual Wave Data Uncertainty: The tabulated values refers to the accuracy of the significant wave height if calculated using a particular correlation equation involving the visual wave height, due to Guedes Soares. This information, developed in SSC-363, should be carefully used for several reasons. First, there are several different correlation equations available; second, not all visual data are created equal. For example, the BMT Global Wave Atlas contains enhanced visual data, rather than raw visual data. The tabulated values pertain to the wave height. The resulting bias in mean square bending moment is the tabulated value squared, with a COV of 0.34 (per Ref. 5.5).

Independent Peaks Assumption: The extreme value calculation procedures are usually based on the assumption of independent peaks in the seastate. This assumption can overestimate the maximum wave height by 10% for long return periods. The resulting loads would also show a similar overestimation.

Heavy Weather Countermeasures: The tabulated bias of 1.0 applies to large ships, where countermeasures are said to be infrequent, and 1.25 for small ships where countermeasures are more common. The countermeasures referred to relate to speed and heading changes, but do not include rough weather avoidance. The fact that the bias noted for small ships represents an <u>increase</u> in the bending moment rests on the argument that in high seastates, the likely course changes "to avoid capsizing" are such that the ship is more often aligned with head seas, resulting in larger bending moments. This result may warrant further study.

5.3 Uncertainties Related to Still Water Load Control

Given a loading pattern, the still water loads can be calculated with a good degree of certainty. Hence, the calculation related uncertainty in the still water bending moments, shear forces, and pressures is negligibly small. The inherent variability in still water loads is not the subject of our work, but considerable information on the subject may be found in SSC Report 363, based on the work of Guedes Soares and Moan (5.10).

While not strictly a "modeling error", one aspect of variability related to still water loads that is worth pointing out here is the fact that they can, with a given probability distribution, exceed the design value. In merchantships, this probability distribution can be expected to depend on the type of the vessel, the quality of the crew, constraints on vessel operation, and whether the vessel has a loading instrument or not. These aspects, which collectively affect "still water load control", were not dealt with in SSC-363.

Little data exists on this aspect of still water load variability, because the admission of such occurrence is not often desirable, making the collection of such data difficult. Some limited data on the subject, for ships with loading instruments, is available from Guedes Soares (5.11). His treatment of the subject is outlined below.

For one particular loading condition, were there perfect control on the still water load effect, a truncated normal density can be used to represent the still water effect, to account for differing loading patterns during the long term. This probability density function is given by

$$f_S(s) = \frac{\Psi^{-1}}{\sigma\sqrt{2\pi}} \exp\left(-\frac{1}{2}\left(\frac{s-\mu}{\sigma}\right)^2\right) \tag{5.1}$$

for $A \leq s \leq B$, where A and B are the lower and upper points of truncation, and Ψ is a factor that normalizes the area under the pdf to unity. This factor is defined by

$$\Psi \equiv \Phi\left(\frac{B-\mu}{\sigma}\right) - \Phi\left(\frac{A-\mu}{\sigma}\right) \tag{5.2}$$

Here, Φ is the standard normal distribution function. The lower limit of truncation can be taken to be zero, and the upper limit to be the allowable value.

Instead of using a truncated normal density, Guedes Soares (5.11) used a modified normal density together with a shifted exponential, to represent the effect of load pattern variability and the possibility of misloading beyond the allowable value S_A. A "truncation factor" T_R is proposed, such that,

$$P[S > S_A] = T_R[1 - F_S(S_A)], \quad for \quad 0 \leq T_R \leq 1 \tag{5.3}$$

where the term in parentheses is the tail area beyond S_A in the unmodified still water effect density, and T_R is a modification for the possibility that the allowable may be exceeded.

The modified pdf is related to the unmodified density $f_S(s)$ as follows:

$$f_{S_m}(s) = \frac{1 - P[S > S_A]f_S(s)}{F_S(S_A)}, \quad for \quad S \leq S_A \tag{5.4}$$

The $P[S > S_A]$ is given from Eqn. 5.3. If the allowable S_A will never be exceeded, T_R is zero, and one has a normal density truncated at S_A.

If there is a finite probability that the allowable will be exceeded, it can be shown, using a shifted exponential distribution for the upper tail of the modified distribution where $S > S_A$, that the modified density in that region is given by

$$f_{S_*}(s) = \frac{P[S > S_A]}{2} \exp\left\{-\left(\frac{S - S_A}{\sigma_e}\right)\right\}, \quad for \ S > S_A \tag{5.5}$$

Here, the $P(S > S_A)$ is again given from Eqn. 5.3. The scale parameter σ_e for the shifted exponential distribution is given by

$$\sigma_e = T_R \int_0^\infty S_e f(S_e) dS_e \tag{5.6}$$

where S_e is the load effect in excess of the allowable, that is $S_e = S - S_A$, and f is the unmodified normal density function.

Guedes Soares suggests, based on fits of the above model to two particular sets of data, the following values for the truncation factor T_R:

- Tankers, $T_R = 0.5$

- Containerships, $T_R = 0.25$

Annual probabilities Q of exceedence of design still water bending moment values for large tankers were in the order of 0.01 in the laden condition, and an order of magnitude smaller in the ballast condition, see Table 5.2. While illustrated for bending moments, the above approach can apply to any still water load or load effect.

5-8

Table 5.2. Probability of Exceeding Design Still Water Bending Moment

Ship Type	Load Condition	Q Hogging	Q Sagging
Bulk carrier	Ballast	0.0393	0.0031
	Loaded	0.0003	0.0031
Small tanker	Ballast	0.0068	0.0000
	Loaded	0.0000	0.0000
Large tanker	Ballast	0.0023	0.0000
	Loaded	0.0000	0.0105

5.4 Modeling Error in Hull Girder Wave Induced Loads

Usable data on modeling error related to hull girder wave induced vertical bending moment amidships, quantified by comparing linear strip theory predictions for the loading against model test data, are summarized in Table 5.3. The data shown in the table are selections from a more elaborate review given in SSC Report 363.

As the table clearly indicates, there are two primary sources of modeling error:

(a) Nonlinearities not included in linear strip theory, producing differences in hogging versus sagging.

(b) Other inaccuracies in linear strip theory.

The table provides modeling error data for response amplitude operators (irrespective of frequency and heading), short term root mean square bending moment, and long term extreme bending moment. In the case of the work of Guedes Soares (Ref. 5.7) shown in the table, the strip theory used is that of Salvesen, Tuck and Faltinsen (5.12); in the case of Kaplan's data, Ref. 5.4, the computer program SCORES was used.

Other less detailed trends of bias and COV considering measured and calculated rms values as a function of significant wave height, based on data in ISSC proceedings (5.18), shown plotted in Figures 5.1 and 5.2, also show similar trends. The same ISSC study

considered hog/sag nonlinearities for a particular vessel, both from measurements and by calculations. This data, shown plotted in Fig. 5.3, also indicates the effect of nonlinearities to increase with significant wave height. The ISSC study suggested the following:

(a) Use a bias factor of 0.9 to correct for over predicting the loads due to assumption of linearity in the higher seastates.

(b) In addition, use a correction factor of 1.15 to obtain sagging, and 0.85 to estimate hogging bending moments.

Corrections (a) and (b) above should be multiplied together. Nonlinearities are particularly important in finer form, higher speed, less wall sided vessels such as containerships. It is worth noting that part of the modeling error typically quoted may arise simply from amalgamation of data, e.g., lumping data related to all vessel types and block coefficients under one heading and calculating an overall bias and COV. The other trend worth mentioning is that the bias factor for a given block coefficient decreases with increasing significant wave heights.

Almost all of the data on modeling errors pertaining to hull girder loads that could be found were for midship vertical bending moments. While this is undoubtedly the most important case, there is need for similar data on other load components, e.g., horizontal bending moments amidships, hull girder shear forces at quarter points of the vessel.

Table 5.3

Item	Bias	COV	Ref.
Response amplitude operators, sagging	$(1.74 - 0.93\ C_B)$ $\times\ (1.22 - 0.005\ H_S)$	0.37	5.7
Response amplitude operators, hogging	$(0.26 + 0.93\ C_B)$ $\times\ (1.22 - 0.005\ H_S)$	0.37	5.7
Short term rms bending moment	not stated	0.10	5.4
Long term extreme bending moment	not stated	0.15 warships 0.10 merchantships	5.3
Long term extreme bending moment, tankers, $C_B = 0.80$	1.13	0.04	5.7
Long term extreme bending moment, containerships, $C_B = 0.60$	0.88 hogging 1.2 sagging	0.05 hogging 0.08 sagging	5.7
Long term extreme bending moment, any ship, any block coefficient	1.0 hogging 1.2 sagging	0.15 hogging 0.08 sagging	5.7

Note: H_S is significant wave height, meters. C_B is block coefficient.

5.5 Modeling Error in Local Pressures

We consider two seaway related steady state pressure loads. These are vessel accelerations which result in internal cargo pressures, e.g., in oil tanks, and external hydrodynamic pressures. There is no data available on modeling errors related to the former, while there is limited relevant data on external hydrodynamic pressures.

Both types of pressure loads are currently estimated based on linear strip theory based ship motion computer programs. The degree of likely error on this account is greater in the case of external pressures. Available evidence suggests that external hydrodynamic

loads are somewhat difficult to establish accurately, particularly locally. Nonlinearities, particularly in way of the waterline, contribute to the error, presumably even with wave profile related ad-hoc corrections made. Three dimensional effects neglected in strip theory also contribute to the error, especially at the vessel ends.

Using hydrodynamic pressure measurements and related calculations given in an SSC report by Chen *et al.* (5.13), Nikolaidis and Kaplan (5.5) estimated lower and upper bounds for the bias in the head seas response amplitude operator for hydrodynamic pressures for three Froude numbers. The range in the bias values is quite large, from 0.35 to 1.65. If one assumes a triangular distribution over this range, with its apex at the midrange, 1.0, one obtains, from this limited information, a mean bias of 1.0 and an associated COV of 0.27.

That a mean bias close to unity is obtained is in fact surprising. Experience with quasistatic structural analysis indicates that calculated 10^{-8} level lifetime extreme pressures typically need to be multiplied by a bias factor of less than unity (e.g., 0.7) to give reasonable combined stresses in parts of a tanker where they coexist.

In any event, additional data are needed on the modeling error related to pressure load components. Similar data are also needed on transient pressure loads resulting from slam events, and also the resulting hull girder loads.

5.6 Modeling Error in Approaches to Load Combination

Load combination approaches for purposes of structural design attempt to treat the combined effect of coexisting loads. Apart from the inaccuracies in prediction of the individual load components, such procedures are also subject to errors in the load combination techniques themselves.

The bias and COV of standard "rules" for combining loads was studied, in the context of slamming and wave induced vertical bending moments, by Nikolaides and Kaplan (5.5).

They obtained the data by comparing the rule performance against actual extreme values obtained by a SCORES based simulation method developed by Kaplan. The following were the results:

- Turkstra's rule: Bias = 1.17, COV = 0.11

- Peak coincidence: Bias = 0.72, COV = 0.11

- SRSS: Bias = 1.01, COV = 0.12

Thus while Turkstra's rule was optimistic, and the peak coincidence assumption pessimistic, the Square Root of Sum of Squares method appeared to work the best. It is to be noted that the above results pertain to the accuracy of simplified load combination rules. The accuracy of the procedures for calculating the slamming loads and the wave bending moment is not included.

The above data were obtained considering the performance of the load combination rules in the case of wave induced vertical bending and slam moment combination. Such performance need also to be evaluated for other combined load cases of interest.

5.7 Modeling Errors in Structural Analysis

In many cases, it is ultimately the load effects (e.g., stresses) rather than the loads themselves that are pertinent to structural safety. Hence, it is important to consider the modeling errors related to the accuracy of structural analysis procedures.

In ship design, simplified structural analysis procedures such as those based on beam theory, orthotropic plate theory, or grillage analysis, are used in the initial stages of design, with appropriate allowables. The design resulting from such procedures is typically (but not always) checked using finite element analysis. In this section, we review some usable data on modeling errors in finite element analysis, developed in SSC-363. The same report discusses errors in the simpler analysis procedures, which we do not review here.

Uncertainties in finite element procedures primarily arise from modeling techniques, boundary conditions, and discretization (mesh size). Hence, the modeling error information provided should be viewed with some caution. The information was obtained by comparing finite element analysis results for the SL-7 containership and model against experimental measurements. The data used were developed by Elbatouti *et al.* (5.14), Webster and Payer (5.15), and Jan *et al.* (5.16). The results obtained are summarized in Table 5.4.

The table indicates normal stresses to be predicted reasonably well by finite element analysis. In fact, the authors of SSC-368 also indicate that, for normal stresses, beam theory worked just as well, with a bias of 0.94 and a COV of 0.10. The bias of less than 1.0, implying that the finite element stresses are somewhat higher than the measured, may not be typical since in most cases the mathematical model is somewhat stiffer than the real structure. In comparison to the normal stresses, the shear and warping stresses are comparatively more difficult to predict, and exhibit higher variability. The warping stresses result partly from sudden changes in geometry and stiffness, e.g., at hatches. The average bias values associated with the shear and warping stresses for torsion loading is greater than unity, indicating that the finite element model is, in fact, stiffer than the real structure as would be expected.

The above described data pertain to quasistatic finite element analysis. Similar data need to be developed also for dynamic analyses used where the loads are transient in nature and/or when structural flexibility effects are important. Cases that one might mention in this regard are analyses related to slam effects and tank sloshing loads.

Table 5.4

Loading	Stress	Bias	COV
Pure longitudinal bending	normal	0.93	0.12 - 0.17
Distributed torsional moment	shear	1.01	0.20
Distributed torsional moment	normal warping	1.20	0.42

5.8 Modeling Errors in Fatigue Damage Prediction

In ship structures, fatigue damage calculations are based on S-N curves, and the damage is calculated using Miner's linear cumulative rule. The following are the main steps in the analysis procedure:

(a) Description of the long term wave environment, e.g., by a scatter diagram of seastates and associated probabilities.

(b) Calculating the nominal loads imposed on the structure, and

(c) Selection of appropriate S-N curves.

(d) Calculating the related nominal and local stress range histogram due to the loads imposed. This step may involve a multi-stage finite element analysis to obtain local stress information consistent with the S-N curves (nominal stress or hot spot stress) being used.

(e) Calculation of fatigue damage.

The modeling errors related to environmental description and the calculation of loads, nominal loads, and nominal stresses have been previously described. The scatter in S-N data is an important factor in fatigue reliability, but it is not a modeling error. Corrosion introduces additional uncertainty in fatigue analysis, but this aspect is not considered here. The following fatigue related modeling errors are treated in this section:

(i)   Uncertainties in the calculation of local stresses at stress concentrations.

(ii) Uncertainties due to correlation of adjacent stress peaks in a seastate, viewed in the fatigue context.

(iii) Uncertainties due to inaccuracy of Miner's linear cumulative damage rule.

Uncertainties in the Calculation of Local Stresses

Depending on the S-N curve being used, the fatigue procedure may require the estimation of very local stresses. In ships, such estimation is done primarily by finite element analysis (FEA), whereas in offshore structures, one tends more to use "canned" parametric formulae for stress concentration factors. Compared to offshore structures, the ship FEA attempts to both account for the global stress gradients in a complex structure, and also the local stress gradients as necessary.

Modeling errors related to FEA for global stresses were previously described. Ship Structure Committee Report 363 discusses some data related to FEA for local stress concentrations in a liquid fuel rocket engine, where the stress concentration factor ranges from 1.2 to 3.5, with a COV of roughly 0.15. This is also the magnitude of <u>additional</u> COV that one would expect in FEA for local stresses in ship structures, i.e., the additional uncertainty arising from finer mesh analyses that typically follow a coarse mesh FEA. If, for example, the normal stresses from the coarse mesh FEA have a COV of 0.15, the total structural analysis related modeling error COV is roughly 0.21.

Uncertainties Due to Correlation of Stress Peaks

We previously discussed the effect of correlation of adjacent wave load peaks in the context of lifetime load extreme values, and stated that the likely effect was small (less than 10%) in the extreme value magnitude. In the context of fatigue, the effect of correlation of adjacent stress peaks on the calculated cumulative fatigue damage was

investigated by Nikolaides and Kaplan (5.5). In the long term, for reasonable slopes of stress range histograms and correlation coefficients less than 0.9, the effect is negligibly small, the maximum likely COV of cumulative damage from this factor being about 0.03.

Uncertainties Due to Miner's Rule

The accuracy of Miner's rule, and the effect of any inaccuracy on fatigue reliability estimates has been extensively studied by Wirsching; see, for example, Refs. 5.8 and 5.7. Figure 5.4, obtained from Wirsching, shows a plot of the cumulative distribution function of linear cumulative damage at failure from various investigators. Wirsching and Chen (5.17) suggest the use of a bias of 1.0 and COV of 0.30 for the modeling error due to Miner's rule inaccuracies. While further refinements may be possible, it is typically not worthwhile as the effect of this source of uncertainty on fatigue reliability estimates is small compared to other sources of modeling error, particularly those related to inaccuracies in estimated stress ranges. This is because in the calculation of fatigue damage, the stress range is raised to a power that is at least 3.0, magnifying the effect of any errors in the stresses.

5.9 Equivalence of Two Approaches to Load Combination

In this section, we consider the equivalence of two approaches to load combination for wave induced effects. The load source considered is a stationary zero mean Gaussian sea state. The loads (and effects) considered can include vertical, horizontal and torsional wave induced bending moments, local hydrodynamic pressures, and also springing. Transient slam effects are specifically excluded.

Method 1: The In-Phase Out-of-Phase Method

In this method, the combined stress transfer function is computed at each location of interest in the structure for a range of frequencies. For each frequency, there are two structural analysis load cases involved, with load components that are 90 degrees apart in phase. These components include all the relevant load effects at the location, e.g., those from vertical and horizontal bending moments, local hydrodynamic pressures, etc. The stress transfer function amplitude is obtained as

$$R(\omega) = \sqrt{R_o^2(\omega) + R_i(\omega)^2}$$

where ω is the radian frequency, and R_o and R_i are the stress values corresponding to the load excitation cases 90° apart in phase. The subscripts 'o' and 'i' have been used since the corresponding load components are referred to as in-phase and out-of-phase values.

Once $R(\omega)$ is determined for the range of frequencies of interest, the stress response spectrum can be obtained by the standard input-output relationship:

$$S_R(\omega) = R^2(\omega) \, S(\omega)$$

where $S_R(\omega)$ is the response spectrum for the stress, and $S(\omega)$ is the spectral density for the seastate. The mean square value of the stress response is then

$$m_0 = \int_0^\infty S_R(\omega) \, d\omega$$

and the various combined stress fractiles (highest 1/m values) may be obtained on the basis of the Rayleigh or other applicable distribution. For example, the significant value of the combined stress amplitude is given by $2.0\sqrt{m_0}$ for the Rayleigh distribution.

As previously noted, this method requires treatment of two structural analysis load cases for each frequency for any location of interest in the structure. It is a direct

treatment of load combination and will work for any number of loads arising from a common seaway. The effect of phasing between the different load components is preserved by the consideration of the in-phase and out-of-phase load components. The method is one suitable for structural analysis. It was developed, and has been extensively used by ABS as early as 1987 for the fatigue analysis of a number of ships and SWATH vessels; see Ref. 5.19. Applications routinely considered both hull girder and local hydrodynamic pressure related stress components.

Method 2: The K Factor Method

This design oriented method was developed by Mansour (5.20). The ship is treated as a set of multiple linear time invariant systems, each representing a particular load (e.g., bending moment), the stress components from each load being additive (with the correct phase) at any location in the vessel structure.

The K factor method, dealt with in Chapter 3, can be summarized as follows.

Two load case:

$$f_c = f_1 + K f_2 \; ; \qquad f_1 > f_2$$

Three load case:

$$f_c = f_1 + K_{12} f_2 + K_{13} f_3 \; ; \qquad f_1 > f_2 > f_3$$

where f_i are the individual maximum or extreme stress components, and f_c is the combined stress. The correlation factors K_{ij} depend on the correlation coefficients (f_{ij}) between two stress components i and j and also on the ratio of the stress components $r_1 = f_2/f_1$ and $r_2 = f_3/f_1$. The factors K for the two load case and K_{12} and K_{13} for the three load case are provided in design charts (see Figure 3.2 and Appendix E).

The K-factor method and the "in-phase out-of-phase" methods for combining stresses are essentially identical since both are based on the same assumptions for linear systems. The K-factor method assumes that the band width parameter of each stress is less than 0.65 which is met in almost all practical cases. The advantage of the K-factor method however is that it is cast in a format that can be easily used in design. When the extreme stress components f_i are obtained, the combined stress f_c can be easily determined using typical values for the K-factors given in this report for each load combination case. A more accurate estimate of the combined stress can be made from the design charts provided that the correlation coefficient (ρ_{ij}) between any two load components are known. These correlation coefficients can be either determined from available information in the literature and in this report or from the transfer function of each load component (see Chapter 2). The transfer function of each load component is usually calculated by a ship motion (strip theory) computer program; and there is no need for any modification of these programs. However, the stress in the desired direction must be determined from the load using appropriate conversion factor, e.g., the section modulus in case of converting a moment to stress. The appropriate K-factor can then be determined from the provided design charts using the calculated correlation coefficients.

Currently, details of the K factor method have been developed for either two or three load components, which is adequate for practical use. The procedure can be extended to more than three load components if necessary.

References

5.1.   Mansour, A, "Probabilistic Design Concepts in Ship Structural Safety and Reliability," *Trans. SNAME*, 1972.

5.2.   Mansour, A.E., "Combining Extreme Environmental Loads for Reliability-Based Designs," Proc. SSC-SNAME Extreme Loads Response Symposium, Arlington, VA, October 1981.

5.3.   Faulkner, D., "Semi-Probabilistic Approach to the Design of Marine Structures," Proc. SSC-SNAME Extreme Loads Response Symposium, Arlington, VA, October 1981.

5.4.   Kaplan, P., "Analysis and Assessment of Major Uncertainties Associated with Ship Hull Ultimate Failure," Ship Structure Committee Report 332, 1984.

5.5.   Nikolaides, E. and Kaplan, P., "Uncertainties in Stress Analysis of Marine Structures," Ship Structure Committee Report 363, April 1991.

5.6.   Thayamballi, A., "Background to the Evaluation of Strength Uncertainties" and "Background to the Evaluation of Load Uncertainties," Appendices 1 and 2 to ABS Research and Development Report RD-85003 on "A Study to Evaluate the Cumulative Effects of Changes of ABS Rules on Ship Hull Strength," 1985.

5.7.   Guedes Soares, C., "Probabilistic Models for Load Effects in Ship Structures," The Dept. of Marine Technology, The Norwegian Institute of Technology, Trondheim, Norway, Report No. UR-84-38, 1984.

5.8.   Wirsching, P.H., "Probability Based Fatigue Design Criteria for Offshore Structures," The American Petroleum Institute, Report PRAC 80-15, Dallas, Texas, 1981.

5.9.   Thayamballi, A. and Jan, H.Y., "The Effect of Model Uncertainty on the Design Fatigue Life Estimates of Offshore Structures," *Proc. Offshore Mechanics and Arctic Engineering Symposium*, Houston, Vol. III, 1987, pp. 375-383.

5.10. Guedes Soares, C. and Moan, T., "Statistical Analysis of Still Water Load Effects in Ship Structures," *Trans. SNAME*, 1988.

5.11. Guedes Soares, C., "Influence of Human Control on the Probability Distributions of Maximum Still Water Load Effects in Ships," *J. Marine Structures*, accepted for publication, 1992.

5.12. Salvesen, N., Tuck, E.D. and Faltinsen, O., "Ship Motions and Sea Loads," *Trans. SNAME*, 1970.

5.13. Chen, H.H. *et al.*, "Correlation of Theoretical and Measured Hydrodynamic Pressures for the SL-7 Containership and the Great Lakes Bulk Carrier S.J. Cort," Ship Structure Committee Report 325, 1983.

5.14. El Batouti, A., Jan, H.Y. and Stiansen, G., "Structural Analysis of a Containership Steel Model and Comparison with Test Results," *Trans. SNAME*, 1976.

5.15. Webster, W.C. and Payer, H.G., "Structural Tests of SL-7 Ship Model," Ship Structure Committee Report SSC-269, 1977.

5.16. Jan, H.Y., Chang, K.T. and Wojnarowski, M., "SL-7 Stress Calculations Compared with Full Scale Measured Values," Ship Structure Committee Report 282, 1979.

5.17. Wirsching, P.H. and Chen, Y.N., "Consideration of Probability-Based Fatigue Design for Marine Structures," Proc. Marine Structural Reliability Symposium, Arlington, VA, 1987.

5.18. Proceedings of the International Ship Structures Congress, Committee V.1 on "Applied Design," 1991.

5.19. Thayamballi, A., "Fatigue Analysis of Tankers," ABS Research and Development Division Technical Report RD 89020-F, Prepared for the ABS Far East Technical Seminars, November 1989.

5.20. Mansour, A.E., Thayamballi, A.K., Li, M. and Jue, M., "A Reliability Based Assessment of Safety Levels in the ABS Double Skin Tanker Guide," Mansour Engineering Report to ABS, July 1992.

5.21. Engle, A., Private Communication, August 1993.

List of Figures

6. IMPACT OF OPERATIONAL FACTORS ON DESIGN LOADS

In this chapter, we consider the impact of operational factors and operator discretion on ship design loads and load criteria. Operational factors that affect loads on vessels include ship routing and storm avoidance, and heavy weather countermeasures such as changes in vessel heading and speed. Phenomena contributing to ship local loads, in particular slamming and acceleration related inertial loads, are very speed and heading sensitive. The discussion concerns primarily extreme loads.

6.1 Storm Avoidance and Ship Routing

In merchantships, a part of the effect of storm avoidance is implicitly built into today's design criteria, perhaps more unintentionally than intentionally. Consider, for example, the fact that visual data on significant wave heights and characteristic wave periods for the North Atlantic is widely used in ship design and developing structural design criteria for oceangoing merchantships. For unrestricted service, data, such as that contained in BMT's Global Wave Atlas, are for the most part obtained from voluntary reports from ships transiting the North Atlantic. Such ships can and do avoid severe storms that may develop. This leads to a "bias" in such data, which becomes evident if one compares loads developed from them with hindcast or measured data for the same routes.

Aside from wave data itself, one can argue that design criteria for merchantships, that have evolved over time, contain within them the effects of storm avoidance simply because the amalgamated ship experience base on which such data rests contains such effects. A usually benign, but unavoidable side effect of this amalgamation is that on certain routes, the calculated loads on ships in ocean service can in fact be greater than those for their nominal design environment, the North Atlantic. The margin in design criteria covers any

undesirable effects of such differences insofar as extreme loads are concerned, but the hull structure in such cases may need specific consideration for fatigue, e.g., by procedures such as in (6.11) or (6.12). One possible but undesirable way to avoid such differences is to go toward a route specific design, rather than to design vessels for "unrestricted service".

Ship routing essentially systematizes storm avoidance. Not all merchantships are routed, and, even when routing information is available, it is possible in some cases for commercial concerns to negate any benefits of it. It is also possible that errors may result in forcasting a storm severity and location. Any beneficial effects of ship routing are in a sense similar to those obtainable from hull surveillance systems, in that, where routinely and diligently used, there is a benefit to be derived provided the data are correct.

Many ships are still designed for a standard wave of length approximately equal to ship length, with a predefined height. There is a rational basis for selecting a design wave of a length close to the ship length, in that such waves result in the worst sea loads, and seas do contain waves of all periods and lengths. The height of the design wave, however, is simply an experience based "bending moment coefficient". The standard wave based design criteria are applicable to any ship, which implies that effects of storm avoidance and ship routing are again essentially an inseparable part of the load criteria.

The probabilistic design procedures of Phase 3 would aim for predefined target safety levels (nominal probabilities of failure). These target levels would, to a large extent, be based on a body of vessel experience that is considered acceptable. The design wave environment for vessels intended for unrestricted ocean transit will, following today's practice, be the North Atlantic, with no specific intention of route specific design as a general approach, and no general acceptance of storm avoidance and ship routing as factors that quantifiably reduce design requirements.

6.2 Heavy Weather Countermeasures

There are essentially three types of counteractions to heavy weather that are relevant to our study:

(a) Course changes, i.e., changes in vessel heading

(b) Voluntary reduction in speed

(c) Involuntary speed reduction.

Data on Course and Speed Changes

Course changes are made in order to ease vessel motions and avoid local damage. The primary reason course changes affect motions and loads is because of the resulting change in encounter frequency in comparison to the vessel heave, pitch and roll natural frequencies. To obtain an idea of relative headings conditional on significant wave height, we reproduce, as Tables 6.1 and 6.2, data obtained from Guedes Soares, Ref. 6.1. The first table is an amalgamation of data published by Aertssen, Refs. 6.2-6.6. This table is of interest primarily because it provides data on likely vessel headings in the more severe sea states. The table is not specific to a particular wave environment, but can be said to be characteristic of how a merchant vessel may be handled. The second table is for the North Atlantic, and is original data (for bulk carriers) collected by Soares from Moller. Both tables present an interesting fact, that in severe seas, vessels are likely to be more aligned in the head seas direction. Beam seas in particular are avoided because of the resulting (large) roll motion. Also, the headings are more uniformly distributed in the less severe sea states where the vessel spends most of its time.

Effect on Slam Loads

Course and speed changes significantly affect slamming occurrence and related effects such as hull girder stresses, and related local stresses. Some very relevant data in this

regard is available from MacLean and Lewis (6.13), for the 500 ft. long Wolverine State transiting the North Atlantic at a relatively light draft of 18 ft.; the vessel depth is 54 ft., and the design draft is about 33 ft. The following are some results from the study:

(a) There was a significant amount of speed reduction, even in the lower seastates, on account of slamming, e.g., from 17 knots to as low as 4 knots in Beaufort 4 seas. The distribution of ship speeds when slamming occurs is shown in Figure 6.1.

(b) The distribution of the frequency of slamming per unit time versus the Beaufort number is shown in Figure 6.3. The differences between the data for different Beaufort numbers is not large. There is, however, a tendency for the vessel to be handled in such a manner that slam occurrences reduce somewhat in the more severe seastates. This may be due to "occasional extra severe slams, shipping water, or excessive ship motions" in such seas, with the master responding accordingly with course and speed changes (6.13).

(c) The distribution of frequency of slamming per unit time, versus ship heading, is shown in Figure 6.3. The vessel tended to be aligned more often toward head seas when slamming occurred, but the plot shows data normalized to the same total time at each heading, from head to beam seas. No slamming occurred at other headings.

(d) The average rms values of the total stress, $\sqrt{E}$, consisting mostly of wave induced bending stress, is shown plotted in Figure 6.4 against the Beaufort number. The trend line indicates the stress to increase with Beaufort number. Figure 6.5 shows the trend of average slam stress with Beaufort number to be surprisingly flat, however, at least insofar as midship hull girder stress is concerned.

Table 6.1 Relative Headings as a function of Wave Height

H_nm	Head	Bow	Beam	Quarter	Follow	No. of Obs.
0.0–1.5	0.200	0.122	0.122	0.367	0.189	90
1.5–3.0	0.345	0.333	0.126	0.034	0.161	87
3.0–4.5	0.422	0.277	0.108	0.048	0.145	83
4.5–6.0	0.246	0.246	0.049	0.180	0.279	61
6.0–7.5	0.360	0.200	0.080	0.080	0.280	25
7.5–9.0	0.667	0.111	0.000	0.111	0.111	9
9.0–10.5	0.000	0.000	0.000	0.000	0.000	0
10.5–12.0	1.000	0.000	0.000	0.000	0.000	1
12.0–13.5	1.000	0.000	0.000	0.000	0.000	1
13.5–15.0	1.000	0.000	0.000	0.000	0.000	2
All H_e	0.326	0.234	0.100	0.150	0.189	
No. of Obs.	117	84	36	54	68	359

Note: Aertssen's Data as reported in Ref. 6.1

Table 6.2 Relative Headings vs Wave Height for the North Atlantic

H_s,m	Head	Bow	Beam	Quarter	Follow	No. of Obs.
0.5–1.5	0.750	0.000	0.250	0.000	0.000	4
1.5–2.5	0.500	0.000	0.500	0.000	0.000	4
2.5–3.5	0.406	0.156	0.063	0.000	0.375	32
3.5–4.5	0.500	0.077	0.154	0.115	0.154	26
4.5–5.5	0.591	0.273	0.045	0.000	0.091	22
5.5–6.5	1.000	0.000	0.000	0.000	0.000	1
6.5–7.5	1.000	0.000	0.000	0.000	0.000	1
All H_s	0.511	0.144	0.111	0.033	0.200	1.000
No. of Obs.	46	13	10	3	18	90

Note: Moller's data as reported in Ref. 6.1

The apparent conclusion from the above data is that the master tends to handle the vessel in such a manner that the slam frequency and the resulting stresses (or slam severity) is relatively insensitive to sea severity. The above conclusion is of interest to merchantship design, but can be criticized in the sense that it pertains only to one vessel. In naval vessels, which in some cases may have less flexibility regarding heavy weather countermeasures, the same trends may or may not apply.

Criteria for Speed Reduction and Course Changes

Regarding speed reduction, two types are possible. The first is due to added resistance and related reduction in propulsive efficiency in waves. The second is a voluntary speed reduction to ease ship motions. The first is a "natural" effect that occurs in seas of all severities. The second depends on the master's judgement, and is essentially taken in severe seas. The first is potentially calculable, e.g., Ref. 6.7. The second requires more empirical data. Figure 6.6, based on Gerritsma et al. (Ref. 6.8), shows the natural ship speed reduction as a function of wave height, derived from service data collected in the North Atlantic.

In heavy weather, the first option available to the vessel master is speed reduction. Next is to change course, and, if these do not lead to satisfactory reduction in motions or slamming, the ship may be let to heave to with the engines stopped (6.1). In so far as headings, the least preferred in severe seas is beam seas, followed by quartering seas. As previously noted, a head seas orientation is more likely to be chosen in rough weather.

From Aertsen's data on full scale trials, Refs. 6.2 to 6.6, Ochi (Ref. 6.9) notes the following criteria for voluntary speed reduction in a seaway:

(a) Vessel slams appreciably 3 times in every 100 pitch oscillations.

(b) Significant value of bow acceleration reaches 0.4 g in amplitude.

(c) Deck wetness occurs 7 times in every 100 pitch oscillations.

(d) Number of propeller emergences reaches a certain limit.

Items (a), (b) and (d) are important in light draft conditions, while (c) and also (b) are important at laden draft. The slamming referred to above are "appreciable slams", defined by Ochi to be impact at Station 3 (21 station basis); he notes that impact forward of Station 2 does not appear to cause appreciable hull response.

A method for limiting vessel speed to tolerable values based on the likelihood of bottom plating damage is also available, Ref. 6.10. The likelihood of damage depends on the margin between the extreme impact pressures and plate strength. Figure 6.7, from Ref. 6.10, indicates results of such an analysis for a Mariner hull.

Impact on Design Criteria

Heavy weather countermeasures do affect ship loads. Loads manifested as internal local pressures due to accelerations or slamming are more affected than hull girder loads. It is not altogether clear that such countermeasures necessarily reduce loads, Ref. 6.1, based on a simple similation study of the effect of course changes on the wave induced vertical bending moment indicates, for example, that in ships of 135 meters (443 feet) or less, increased alignment with head seas may in fact increase short term bending moments perhaps 25% compared to a design case that assumes uniform relative headings. The increase is negligible for vessels of 200 m (656 ft.) or more.

While countermeasures data is not available for accelerations, and local pressure loads, it is reasonable that they too may not always reduce in vessels of all sizes. This indicates a need for further study regarding the effect of speed and course changes on local and global loads, particularly in the smaller, fine form, naval vessels.

The probabilistic design criteria of Phase 3 will be based on target safety indices derives from comparable past experience. Such safety indices will then, to an extent, implicitly contain within them the effects of heavy weather countermeasures. It appears,

however, that the effect of such countermeasures is not the same for all vessel sizes. There is thus a need, particularly for the smaller, oceangoing naval vessels, to adequately study and quantify the effect of heavy weather countermeasures. Supplemental seakeeping and slamming analyses for defining the speed-heading-seastate operability envelope in such vessels is also desirable.

References

6.1. Guedes Soares, C., "Effect of Heavy Weather Maneuvering on the Wave Induced Vertical Bending Moment in Ship Structures," *Journal of Ship Research*, Vol. 34, No. 1, March 1990, pp. 60-68.

6.2. Aertsen, G., "Service Performance and Seakeeping Trials on M.V. Lukuga," *Trans. RINA*, Vol. 105, 1963, pp. 293-336.

6.3. Aertsen, G., "Service Performance and Seakeeping Trials on M.V. Jordaens," *Trans. RINA*, Vol. 108, 1966, pp. 305-333.

6.4. Aertsen, G., "Laboring of Ships in Rough Seas," *Proc. Diamond Jubilee International Meeting, SNAME*, 1968, pp. 10.1-10.16.

6.5. Aertsen, G., "Service Performance and Seakeeping Trials on a Large Ore Carrier," *Trans. RINA*, Vol. 111, 1969, pp. 217-236.

6.6. Aertsen, G. and Van Sluys, M.F., "Service Performance and Seakeeping Trials on a Large Containership," *Trans. RINA*, Vol. 113, 1971, pp. 429-439.

6.7. Strom-Tejsen, J., Yeh, H.Y.H. and Moran, D.D., "Added Resistance in Waves," *Trans. SNAME*, 1973.

6.8. Gerritsma, J., Bosch, J. van den, and Buekelman, W., "Propulsion in Regular and Irregular Waves," *International Shipbuilding Progress*, Vol. 8, No. 82, 1961.

6.9. Ochi, M.K. and Motter, L.E., "Prediction of Extreme Ship Responses in Rough Seas of the North Atlantic," Paper No. 20, *Proc. Symposium on Dynamics of Marine Vehicles and Structures in Waves*, London, April 1974.

6.10. Ochi, M.K. and Motter, L.E., "Prediction of Slamming Characteristics and Hull Responses for Ship Design," *Trans. SNAME*, Vol. 81, 1973, pp. 144-176.

6.11. Thayamballi, A., "Fatigue Analysis of Tankers," ABS Research and Development Division Technical Report RD 89020-F, prepared for the ABS Far East Technical Seminars, November 1989.

6.12. *ABS Guide for the Fatigue Strength Assessment of Tankers*, June 1992.

6.13. Maclean, W. and Lewis, E.V., "Analysis of Slamming Stresses on the S.S. Wolverine State," *J. Marine Technology*, Vol. 10, No. 1, January 1973, pp. 16-21.

6.14. Mansour, A., "Combining Extreme Environmental Loads for Reliability Based Designs," *Proc. SSC-SNAME Extreme Loads Response Symposium*, Arlington, VA, October 1981.

List of Figures

7. SUMMARY, CONCLUSIONS AND RECOMMENDATIONS

Several aspects of load combinations have been developed in this project. A lot of work still needs to be done. In particular a need exists for further research in the area of non-linear response and its impact on load combinations. Several aspects of slamming need additional research, including refined estimates of its magnitude and its impact on fatigue. Because of this and other factors, it is necessary to use reliability and probabilistic methods in design in order to analyze and reflect the uncertainties associated with design parameters.

Based on the procedures developed in this project on load combinations and on existing work in the literature, recommendations are now made. Two levels of analysis are usually required in practice, as follows:

1. Design oriented formulations: These are formulations which are used for preliminary estimates of load combinations, mostly to determine minimum scantlings and to develop the design further. These formulations must be simple and must, to a large extent, be independent of detailed or specific information which is usually not available at early stages of a design.

2. Analysis oriented procedures: These are more accurate formulations and procedures for load combinations that may be used to check the adequacy of a completed preliminary design or an existing marine structure. This "check analysis" may depend on more detailed information on the structure and the operation profile.

Our recommendations for each of these two types of formulations (design and check analysis) are summarized below. More detailed information can be found in the main part of the report.

7.1 Design Oriented Formulations for Preliminary Estimates of Load Combinations (Except Slamming and Fatigue)

The following simple K-factor formulation developed by Mansour (7.1,7.2) and further developed and simplified for design oriented estimates in this project is recommended. For two or three load combinations, the recommended format is as follows:

Two load case:

$$f_c = f_1 + K f_2 \qquad f_1 > f_2 \qquad (7.1)$$

Three load case:

$$f_c = f_1 + K_{12} f_2 + K_{13} f_3 \qquad f_1 > f_2 > f_3 \qquad (7.2)$$

where f_c is the combined load effect, i.e., stress or deflection and f_1, f_2 and f_3 are individual extreme stress (or deflection) components associated with extreme loads or bending moments acting on the structure.

The K's depend, in principle, on the stress ratios

$$r_2 = \frac{f_2}{f_1} \quad \text{and} \quad r_3 = \frac{f_3}{f_1} \qquad (7.3)$$

and the correlation coefficient ρ_{ij} between the stress components. Both r_2 and r_3 are less than one. In the absence of information on the correlation coefficients, the following typical values of the K-factor may be used for preliminary (rough) estimates of the combined load effects in ships, Tables 7.1 and 7.2. Except as noted, tabulated values apply to large oceangoing ships, e.g., tankers.

Table 7.1. Suggested Values for the K-Factors, Two Load Case – Equation 7.1

Two Load Combination Cases – Equation 7.1	K
1. Primary vertical and primary horizontal bending stresses	0.60[2]
2. Primary vertical and primary springing stresses	0.25[1]
3. Primary vertical and local plate or beam stress due to pressure	0.70[2]

Note: [1]Applies to Great Lakes Bulk Carriers.
          [2]For large oceangoing ships, e.g., tankers.

Table 7.2. Suggested Values for the K-Factors, Three Load Case – Equation 7.2

Three Load Combination Cases – Equation 7.2	K_{12}	K_{13}
1. Primary vertical, primary horizontal and primary torsional stresses	NA[1]	NA[1]
2. Primary vertical, primary horizontal and local plate or beam stress due to pressure	0.40[2]	0.55[2]

Note: [1]NA denoted "not available".
          [2]For large oceangoing ships, e.g., tankers.

If the values of the correlation coefficients "ρ_{ij}" for a specific design can be estimated at an early stage, more accurate estimates of the K-factors can be determined from the design charts provided in Figure 3.2 for the two load case, and Appendix E for the three load case. In the latter design charts $K_{C2} = K_{12}$ and $K_{C3} = K_{13}$.

The formulations given by equations (7.1) and (7.2) are best used in connection with probabilistic analysis or reliability methods since the K-factors are based on probabilistic analysis. In this case, the individual stress components should be given extreme value distributions (see reference 7.3 or 7.4) and the K-factors are to be assumed normally distributed. The modeling error associated with the K-factors which are derived on the basis of linear theory should have a bias of 0.9 and a coefficient of variation of 0.25. This

modeling error is based on past experience with reliability analysis for comparable situations. Note that it does not pertain to modeling errors in estimating the individual stress components.

7.2 Analysis Oriented Procedure for Checking Structure Under Load Combinations (Except Slamming and Fatigue)

The simple format given by equations (7.1) and (7.2) is also recommended in the analysis oriented procedure. However, a more accurate determination of the K-factor is now possible for a completed design or an existing ship using a ship motion program for determining the transfer functions of each individual load or stress. The K-factors can be determined as follows.

Two Load Case – Equation (7.1):

$$K = \frac{1}{r}\left[\left(1 + r^2 + 2\rho_{12}r\right)^{\frac{1}{2}} - 1\right] \tag{7.4}$$

where $r = f_2/f_1$ = stress ratio < 1

and ρ_{ij} for long crested seas is given by

$$\rho_{ij} = \frac{1}{\sigma_i \sigma_j} \int_0^\infty \mathrm{Re}\left\{H_i(\omega,\alpha)H_j^*(\omega,\alpha)\right\} S(\omega)d\omega \tag{7.5}$$

whereas, in short crested seas, ρ_{ij} is given by

$$\rho_{ij} = \frac{1}{\sigma_i \sigma_j} \int_{-\pi/2}^{\pi/2} \int_0^\infty \mathrm{Re}\left\{H_i(\omega,\alpha-\mu)H_j^*(\omega,\alpha-\mu)\right\} S(\omega,\mu)d\omega d\mu \tag{7.6}$$

$S(\omega)$ and $S(\omega,\mu)$ are long and short crested sea spectra, respectively, μ is wave spreading angle, $H_i(\omega,\alpha)$ is the frequency response function (transfer function) of an

individual stress component "i", α is the heading angle of ship relative to waves, ω is frequency, σ_i is the standard deviation (rms value) of stress due to load component "i", $\text{Re}\{\cdot\}$ indicates the real part and $H_j^*(\cdot)$ is the conjugate of the complex frequency response function.

The f_1 and f_2 appearing in equation (7.1) are to be taken as the most probable extreme values of individual stress components 1 and 2, respectively, in the considered design sea state, see reference (7.3) or (7.4). Here again, it is best to use this load combination model in a probabilistic rather than deterministic sense. In this case, f_1 or f_2 follows an extreme value distribution with mean equal to the most probable extreme value calculated in the design sea state, see reference (7.3). The factor K is to be taken normally distributed and the associated modeling error is to have a basis of 0.9 and a coefficient of variation of 15 percent. Modeling error associated with f_1 and f_2 due to non-linearities of the response should be accounted for separately, see reference (7.5).

Three Load Case – Equation 7.2:

The K-factors in equation (7.2) can be determined from:

$$K_{12} = \frac{1}{2}\left(\sigma_{12} + 1 - \frac{r_3 + 1}{r_2}\right) \tag{7.7}$$

$$K_{13} = \frac{1}{2}\left(\sigma_{13} + 1 - \frac{r_2 + 1}{r_3}\right) \tag{7.8}$$

where $r_2 = \dfrac{f_2}{f_1} < 1$ *and* $r_3 = \dfrac{f_3}{f_1} < 1$

and

$$\sigma_{12} = \left[1 + \left(\frac{1}{r_2}\right)^2 + \left(\frac{r_3}{r_2}\right)^2 + 2\rho_{12}\left(\frac{1}{r_2}\right) + 2\rho_{13}\left(\frac{r_3}{r_2^2}\right) + 2\rho_{23}\left(\frac{r_3}{r_2}\right)\right]^{\frac{1}{2}} \tag{7.9}$$

$$\sigma_{13} = \left[1 + \left(\frac{1}{r_3}\right)^2 + \left(\frac{r_2}{r_3}\right)^2 + 2\rho_{13}\left(\frac{1}{r_3}\right) + 2\rho_{12}\left(\frac{r_2}{r_3^2}\right) + 2\rho_{23}\left(\frac{r_2}{r_3}\right)\right]^{\frac{1}{2}} \quad (7.10)$$

The ρ_{12}, ρ_{13} and ρ_{23} are to be determined by equation (7.5) for long crested seas or (7.6) for short crested seas. Note that σ_{12} is equal to σ_{C2}^* and σ_{13} is the same as σ_{C3}^* given in Figure 3.3.

The discussion at the end of the two load case regarding the distributions of the stress components f_i and the K factors is valid for the three load case also.

The two and three load cases discussed above should cover all load combinations shown in Tables 7.1 and 7.2, respectively.

It should be noted that the frequency response function is readily computed in many ship motion computer programs for individual load (rather than stress) components, e.g., primary vertical, horizontal and torsional moments as well as external dynamic pressure. These individual "load" frequency response functions must be converted to stress frequency response functions by multiplying by an appropriate conversion factor, e.g., by one over a section modulus, to convert a moment to a stress. All stress components must be at the same location and in the same direction. In the case of a stress component due to external pressure, only the dynamic part of the pressure (i.e., excluding still water pressure) is to be used as outlined in more detail in Section 3.3.1 of the report.

An important factor in the above load combination procedure is the correlation coefficient ρ between the various load components. Systematic studies of load correlation in oceangoing vessels need to be undertaken, considering vessel type, speed, heading, location along vessel length, and wave energy spreading.

7.3 Combination of Slamming and Wave Induced Vertical Bending Stresses

It is also important to consider two levels of analysis when combining slamming with vertical wave bending stresses. The first is a design oriented formulation to be used for

preliminary estimates, whereas the second is an analysis oriented procedure that may be used to check the adequacy of a design or an existing ship.

7.3.1 Design Oriented Formulation for Combining Slamming and Vertical Wave Bending Stresses

Based on the work and example given by Ferro and Mansour (7.6) and on the recent work and example given by Friis-Hansen (7.7) and on the simulation comparisons conducted by Nikolaides and Kaplan (7.8), the following simple formulation is recommended for rough estimates of the combined effect of slamming and primary vertical bending stresses:

$$f_c = f_1 + K f_2 \qquad\qquad f_1 > f_2 \qquad\qquad (7.11)$$

where f_1 is an extreme wave bending stress and f_2 is an extreme slamming stress. The factor K depends only on the stress ratio r, in effect considering f_1 and f_2 to be uncorrelated:

$$K = \frac{1}{r}\left[\sqrt{1+r^2} - 1\right] \qquad\qquad (7.12)$$

and

$$r = \frac{f_2}{f_1} < 1$$

Thus for:

r = 0.1	K = 0.05
r = 0.2	K = 0.10
r = 0.4	K = 0.19
r = 0.6	K = 0.28

Equations (7.11) and (7.12) are best used in probabilistic rather than deterministic analysis. In this case f_1 and f_2 should be given extreme value distributions and the factor K is taken normally distributed with a bias of 1.0 and a coefficient of variation of 25 percent.

7.3.2 Analysis Oriented Procedure for Combining Slamming and Vertical Wave Bending Stresses

A time history based analysis may be necessary for more accurate estimates of the combined stress. A proposed procedure has been developed in this project and is described in detail in Section 3.1.4 of this report.

The basic procedure involves the determination of the combined stress based on typical time histories of the wave induced and slam induced stress. The total stress is formulated as the wave bending stress amplitude (peak) plus a slamming contribution given by the magnitude of the decay envelope of the slamming stress at the instant of time when the bending stress has a peak value, see Section 3.1.4. This formulation is likely to overestimate the magnitude of the combined stress and some calibration with experimental data may be necessary. The probability distribution of the combined stress should be determined using first order reliability methods (FORM) via a procedure outlined in Section 3.1.4. Procedures for obtaining the extreme value distribution of stress in a seastate have also been developed. The resulting combined stress distributions may be used directly in reliability analysis.

Current technology is lacking in many areas of slamming, particularly as to slam induced whipping and the joint probability density of slam and wave induced stresses. Research is recommended in these areas.

7.4 Fatigue Loads and Load Combinations

Two levels of analysis are also proposed for the treatment of fatigue in ship structure. The first is a simple design oriented formulation, while the second is a more elaborate analysis procedure.

7.4.1 Design Oriented Fatigue Assessment

In this simple method, the Weibull distribution is used to characterize the total stress range at a detail. The Weibull shape parameter can be taken to depend on ship length and location of the detail in the ship, following Ref. 4.4 and an ABS Guide (Ref. 4.3). The extreme stress range the structure is likely to be subjected to during the design life can be then calculated using appropriate design load cases. An estimate of the number of stress cycles during design life is made. An appropriate S-N curve is then selected and the fatigue damage is then easily calculated from equation (4.7) or (4.8). Full details of the procedure are given in Sections 4.2 and 4.3 of the report.

7.4.2 Analysis Oriented Procedure Using Spectral Fatigue Analysis

This more accurate analysis procedure entails the following steps:

- Description of the service profile, including the loading conditions and the long term wave environment (scatter diagram).

- Calculation of ship motions, sealoads and local hydrodynamic pressures in a seaway, the related structural response, and local stress range transfer functions.

- Obtaining the stress range response spectra for each wave spectrum of the scatter diagram. The short term response statistics and the associated probability density function (pdf) of the stress range (response) are then obtained.

- The long term probability density function is obtained as the weighted sum of the various short term stress range probability density functions.

- Fatigue damage is then calculated for the structural detail situation of interest, whose fatigue performance is characterized by an appropriate S-N curve.

The above procedure is shown in a flow chart form in Figure 4.5. Full details of the procedure are given in Sections 4.4 and 4.5 of the report.

References

7.1. Mansour, A.E., Thayamballi, A., Li, M. and Jue, M., "A Reliability Based Assessment of Safety Levels in the ABS Double Skin Tanker Guide," Mansour Engineering Report to ABS, July 1992.

7.2. Mansour, A.E., "Combining Extreme Environmental Loads for Reliability Based Designs," *Proc. SSC-SNAME Extreme Loads Response Symposium*, Arlington, VA, October 1981.

7.3. Mansour, A.E., Lin, M.C., Hovem, L.A. and Thayamballi, A., "Probability Based Ship Design Procedures - A Demonstration," Final Report on Ship Structure Committee Project SR-1330, September 1992.

7.4. Mansour, A.E., "An Introduction to Structural Reliability Theory," Ship Structure Committee Report 351, 1990.

7.5. Mansour, A., Thayamballi, A. and Li, M., "*Assessment of Reliability of Ship Structures – Phase I*," Final Report on Ship Structure Committee Project SR-1344, August 1992.

7.6. Ferro, G. and Mansour, A.E., "Probabilistic Analysis of the Combined Slamming and Wave Induced Responses," *J. Ship Research*, Vol. 29, No. 3, September 1985, pp. 170-188.

7.7. Friis-Hansen, P., "On Combination of Slamming and Wave Induced Responses," Paper submitted to the *Journal of Ship Research*, April 1993.

7.8. Nikoloides, E. and Kaplan, P., "Uncertainties in Stress Analysis of Marine Structures," Ship Structure Committee Report 363, April 1991.

Acknowledgments
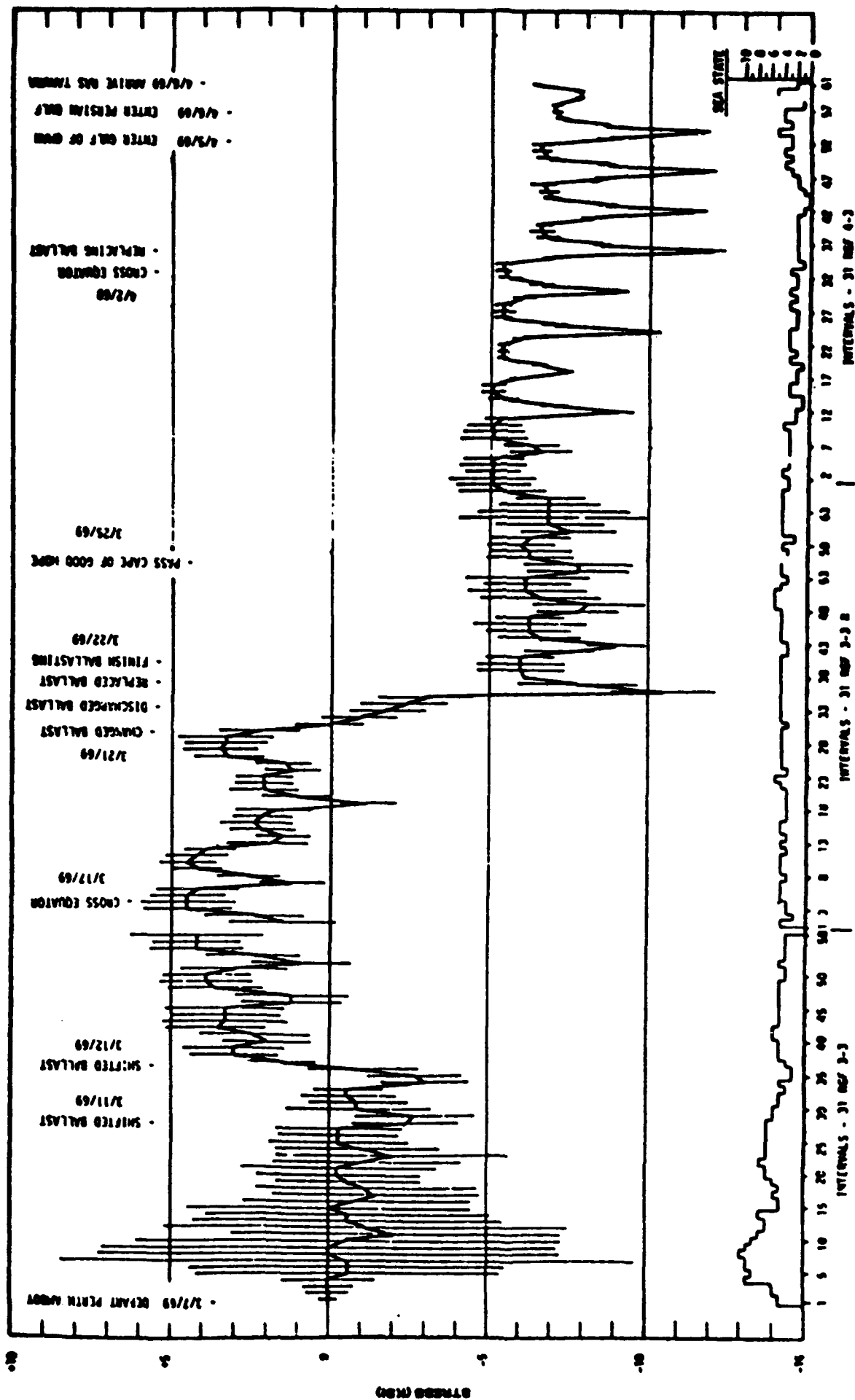
FIGURES

FIGURES

Figure 2.1 Voyage Variation of Still Water Stress in a Bulk Carrier (ref 2.4)
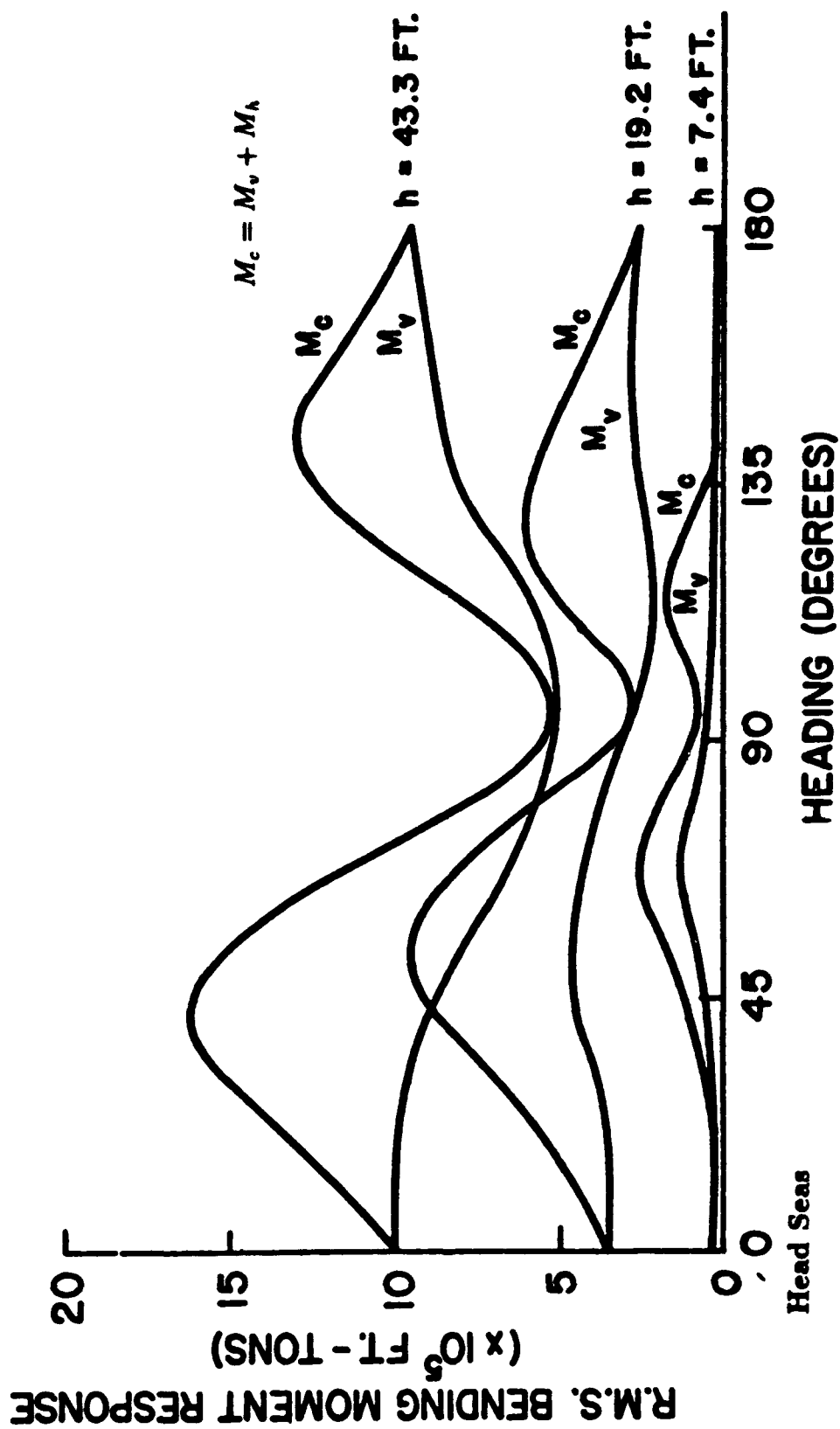
Figure 2.2 RMS value of Wave Bending Moment, Tanker (ref 2.8)

$M_c = M_v + M_h$

h = 43.3 FT.

h = 19.2 FT.

h = 7.4 FT.

HEADING (DEGREES)

R.M.S. BENDING MOMENT RESPONSE ($\times 10^5$ FT.-TONS)

Head Seas

VOYAGE NO. 7FLI-3
INTERVAL 22

12.5 SECONDS

TOTAL STRESS

5000 P.S.I.

HIGH FREQUENCY COMPONENT

LOW FREQUENCY COMPONENT

Sample of stress time hstory—*Fotini L.*

BALLAST

R.A.O. (P.S.I./FT.)

—— R.A.O. HULL FLEXI-
BILITY INCLUDED

——— R.A.O. RIGID BODY

FREQUENCY OF ENCOUNTER (HERTZ)

Stress RAO of *Fotini L.*
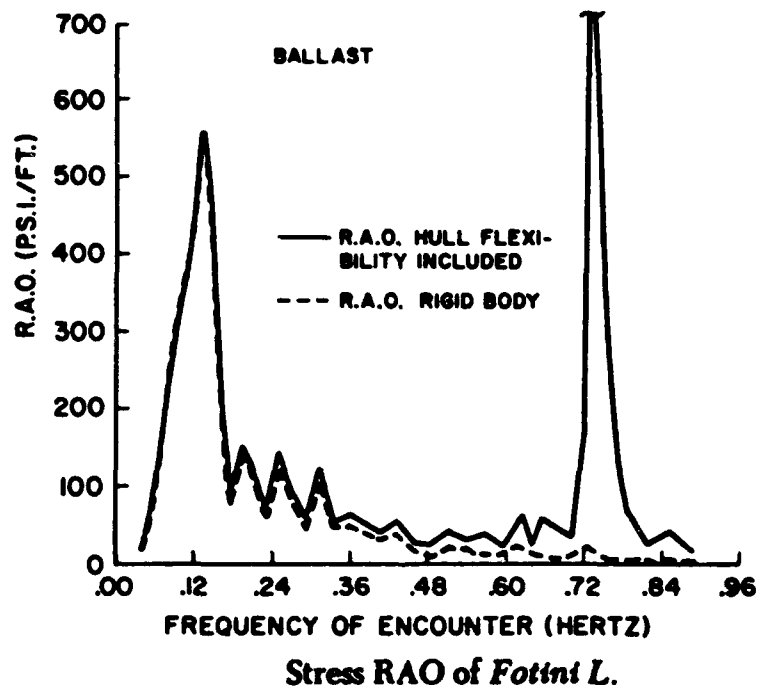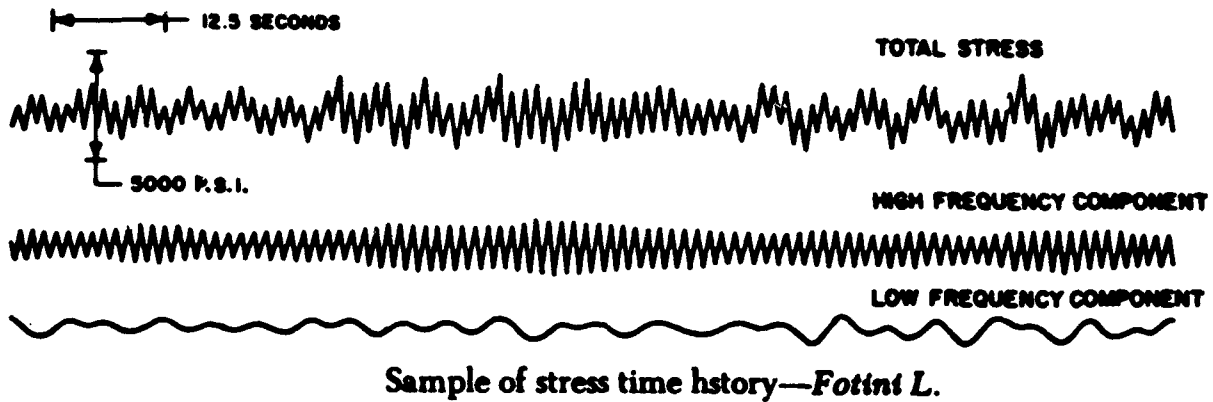
Figure 2.3 Stress Transfer Function including Springing (ref 2.5)

F-3
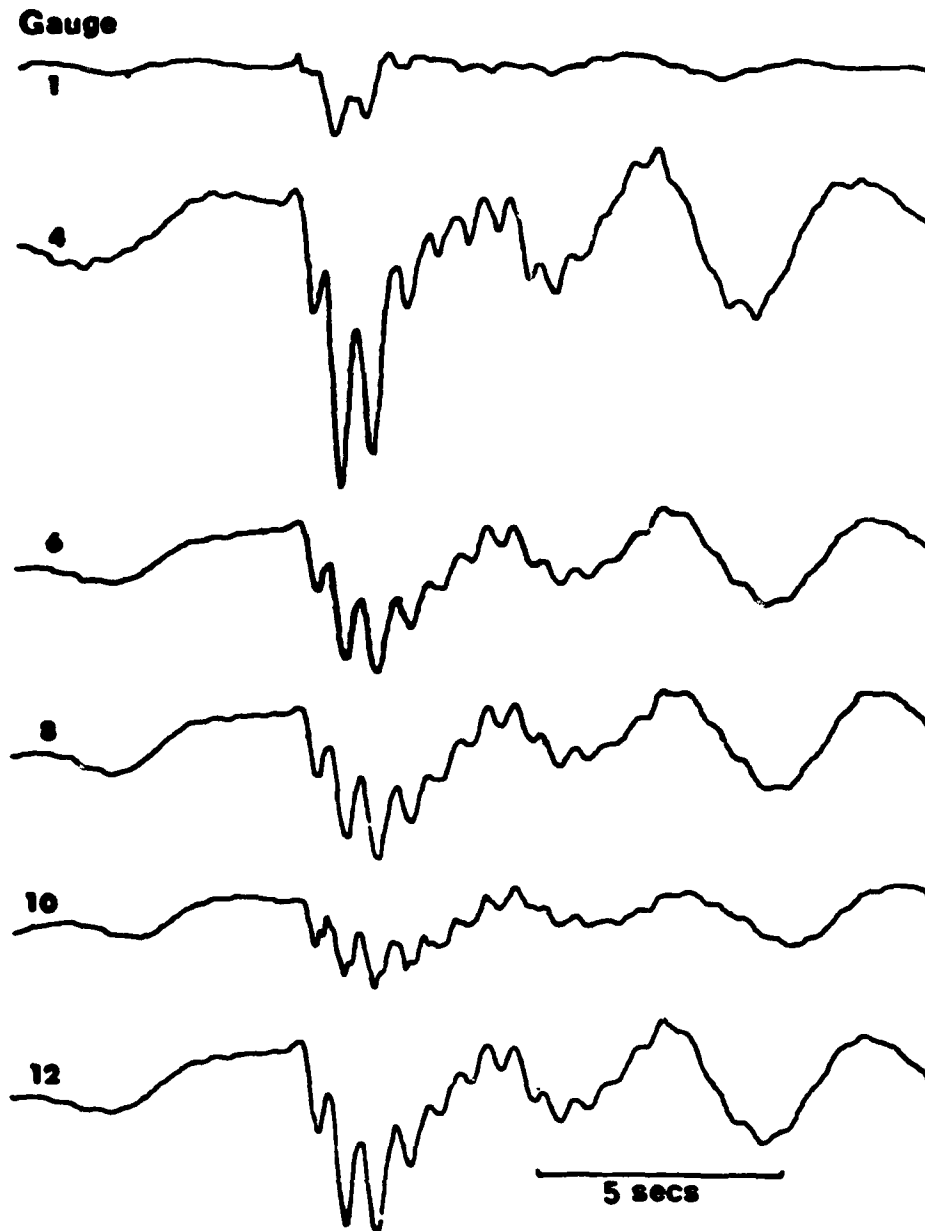
Figure 2.4 Frigate Bending Stress History, with Slamming (ref 2.6)
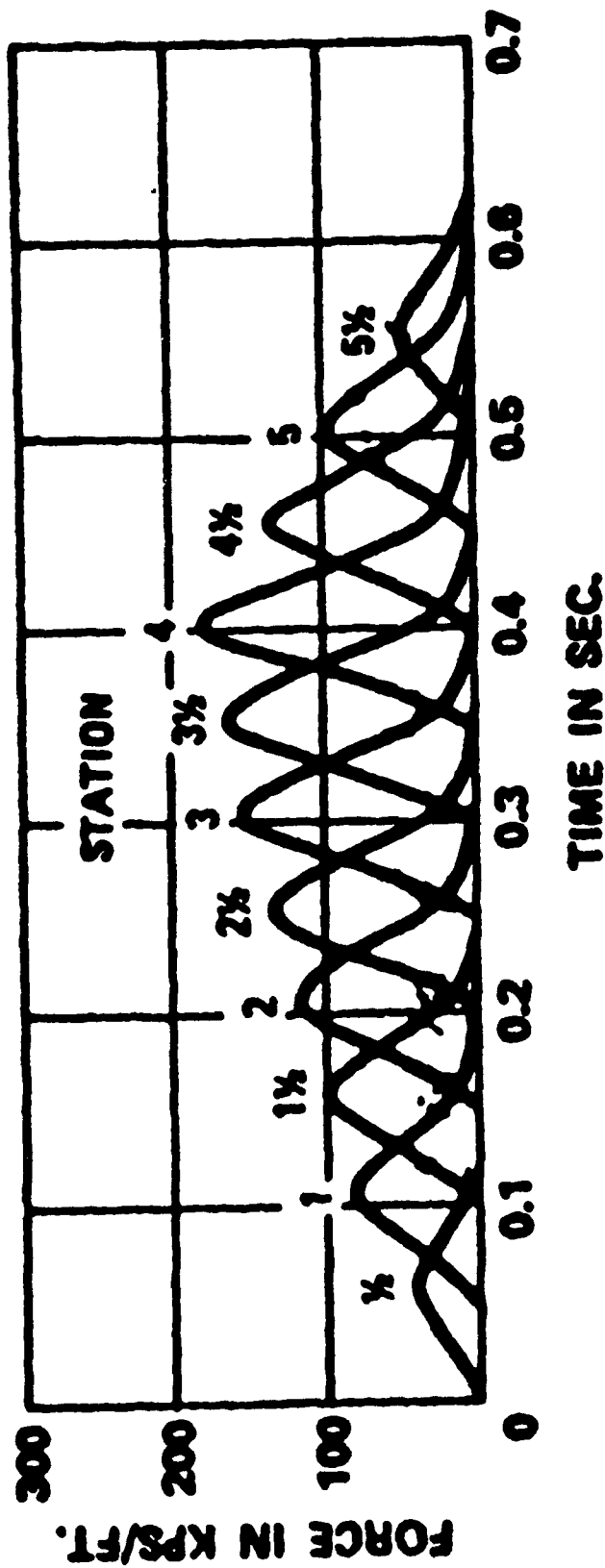
Impact force applied at various stations as a function of time; Mariner, Sea State 7, significant wave height 25 ft, ship speed 7.4 knots, light draft

Figure 2.5 Travel of Slam Impact Force (Mariner, ref 2.7)

Wave bending moment.

Wave shear force.
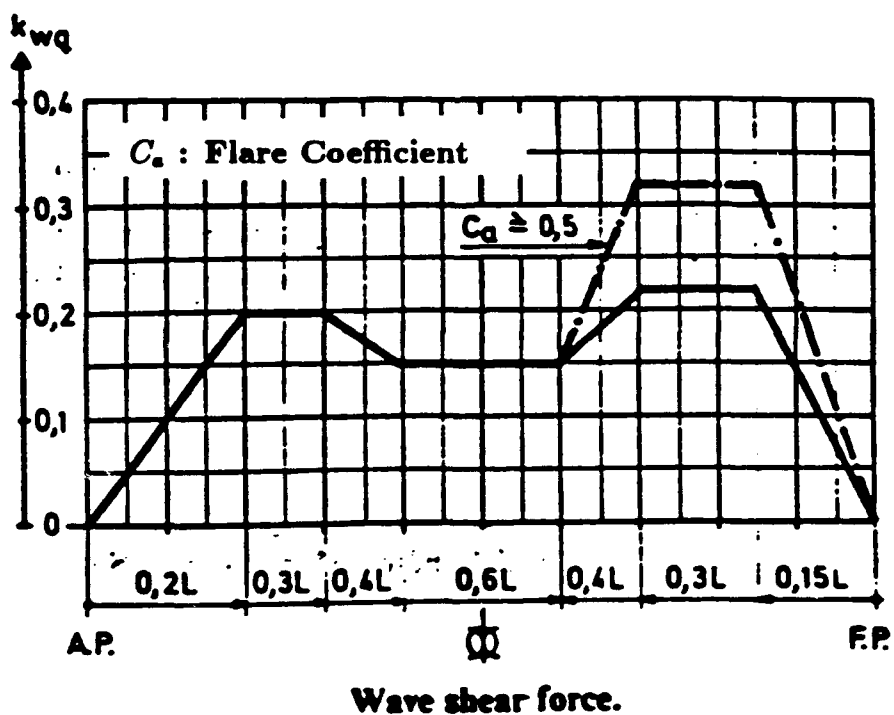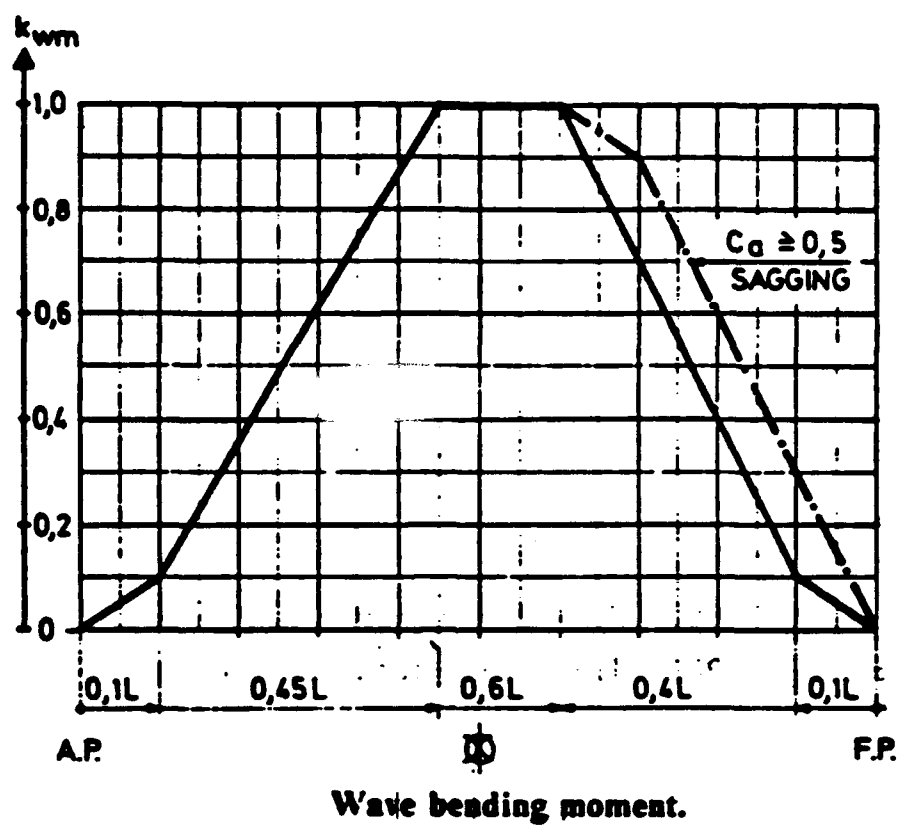
Figure 2.6 Longitudinal Variation of Wave Bending Moment and Shear
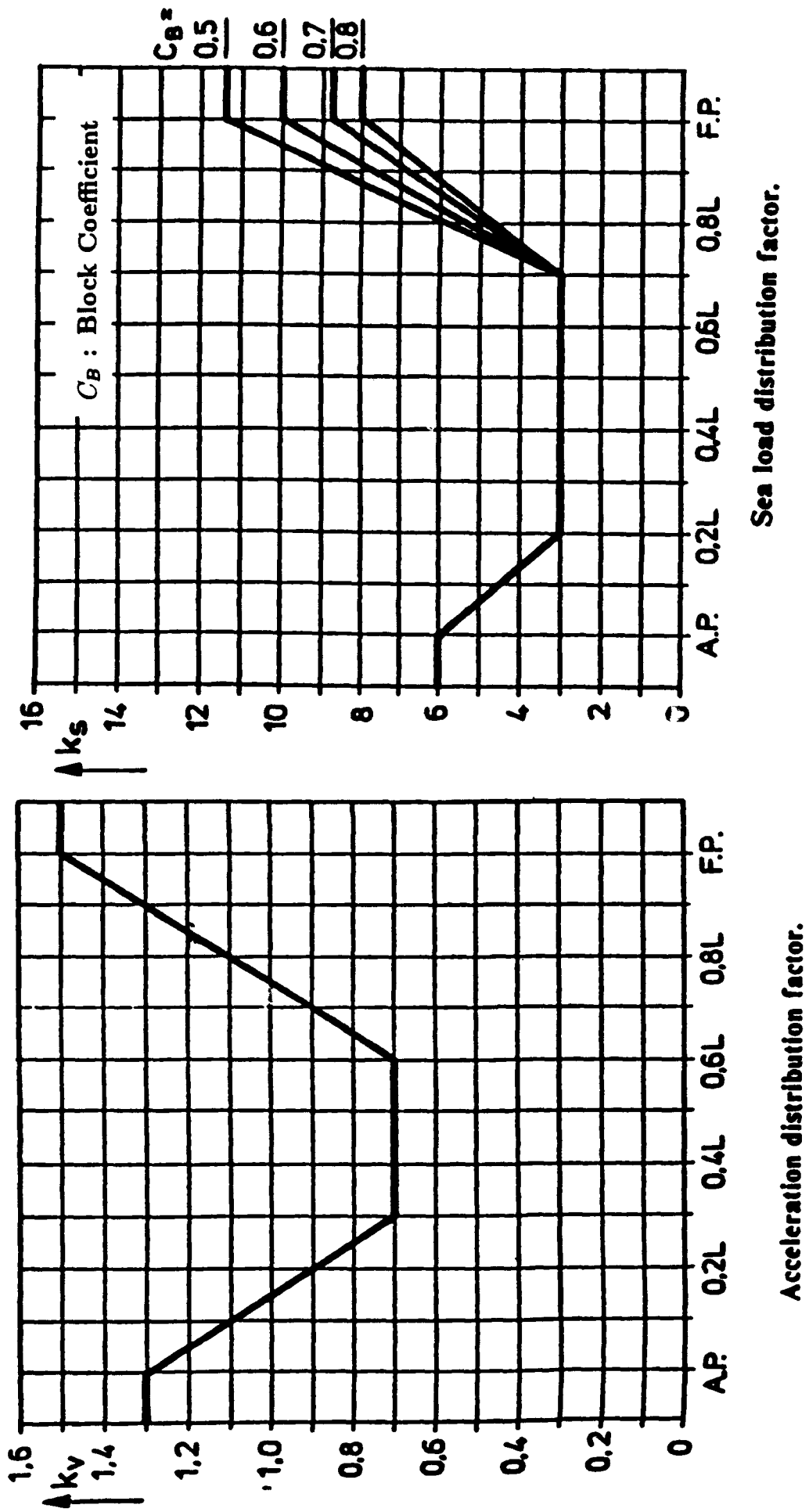
Figure 2.7 Longitudinal Variation of Acceleration and Pressure
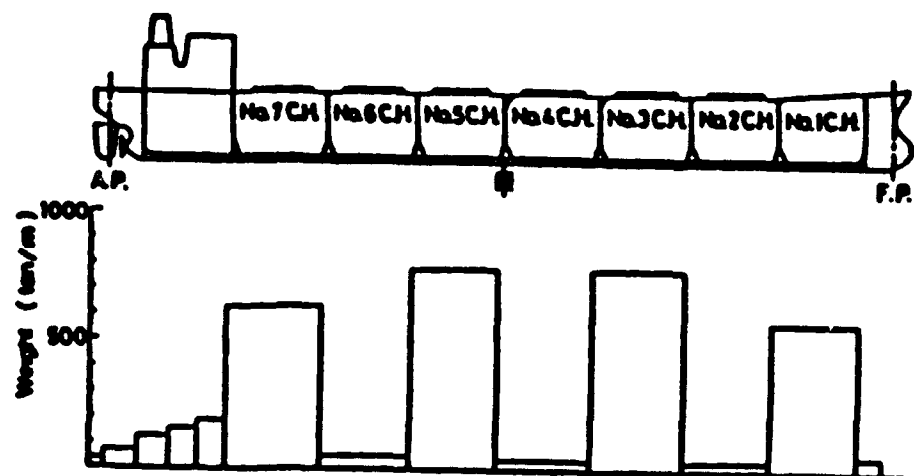
Loading condition
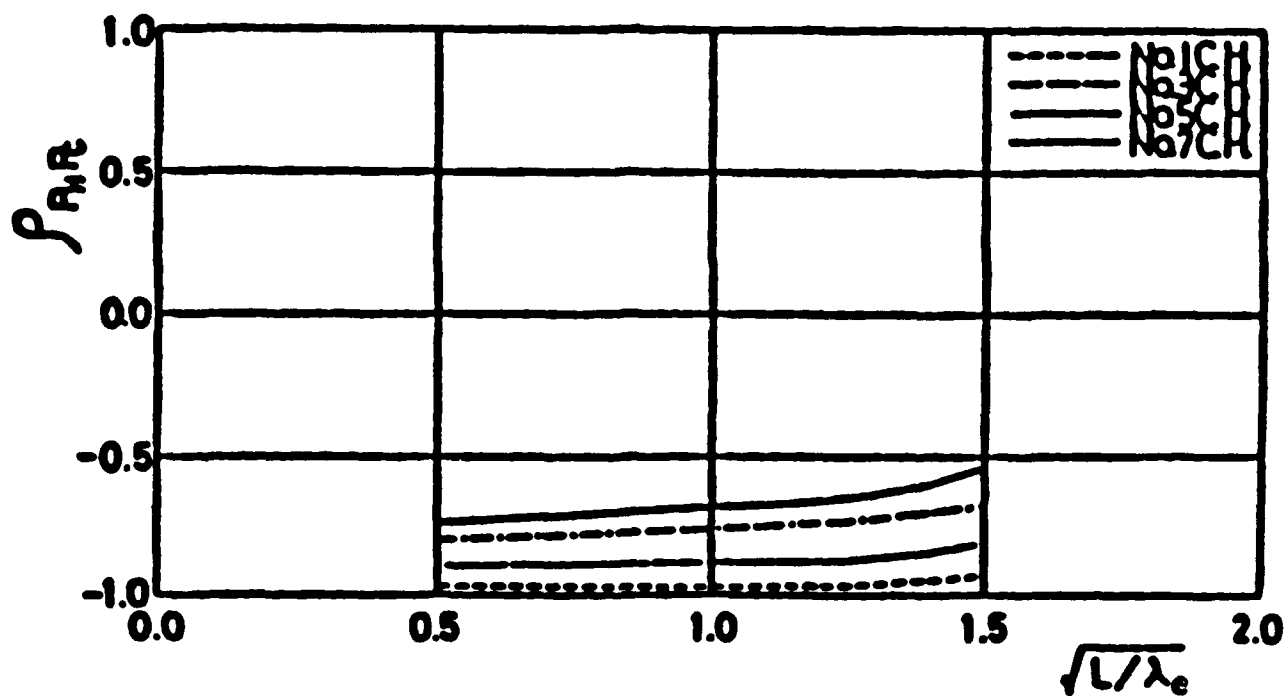
Correlation coefficent between P_H and P_c

Figure 2.8 Correlation of Inertial Loads and External Pressure
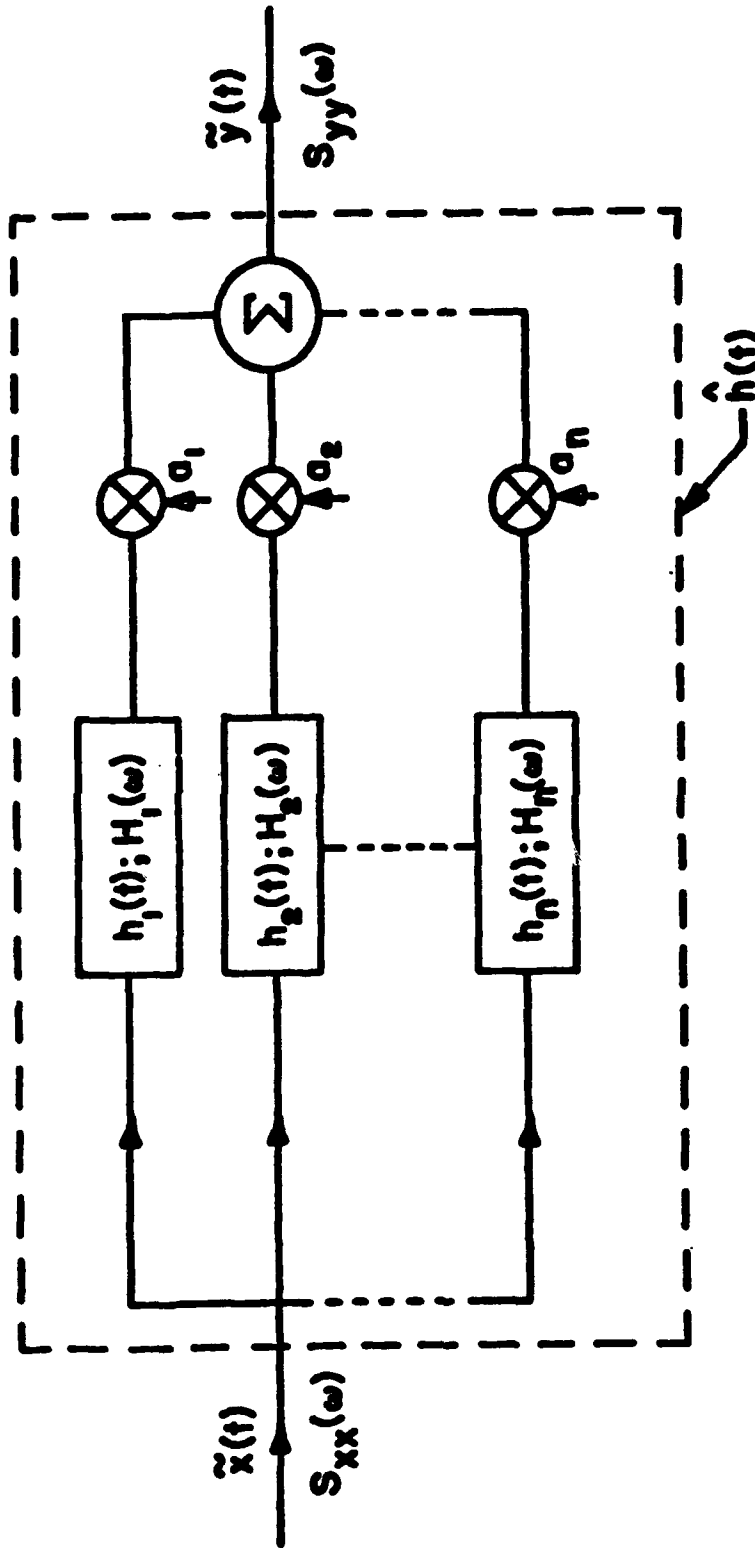
Figure 3.1 Ship System Model for Correlated Wave Loads

$$\boxed{f_c = f_p + K_c \cdot f_s}$$

$$K_c = \frac{1}{r}\left[(1 + r^2 + 2 \rho_{ps} r)^{1/2} - 1\right]$$

$$r = \frac{f_s}{f_p} = \quad \text{Secondary to Primary Stress Ratio}$$

$$\rho_{ps} = \quad \text{Correlation Coefficient}$$

$$= \frac{1}{\sigma_p \sigma_s} \int_{0}^{\infty} H_p(\omega) \, \dot{H}_s(\omega) \, S(\omega) \, d\omega$$
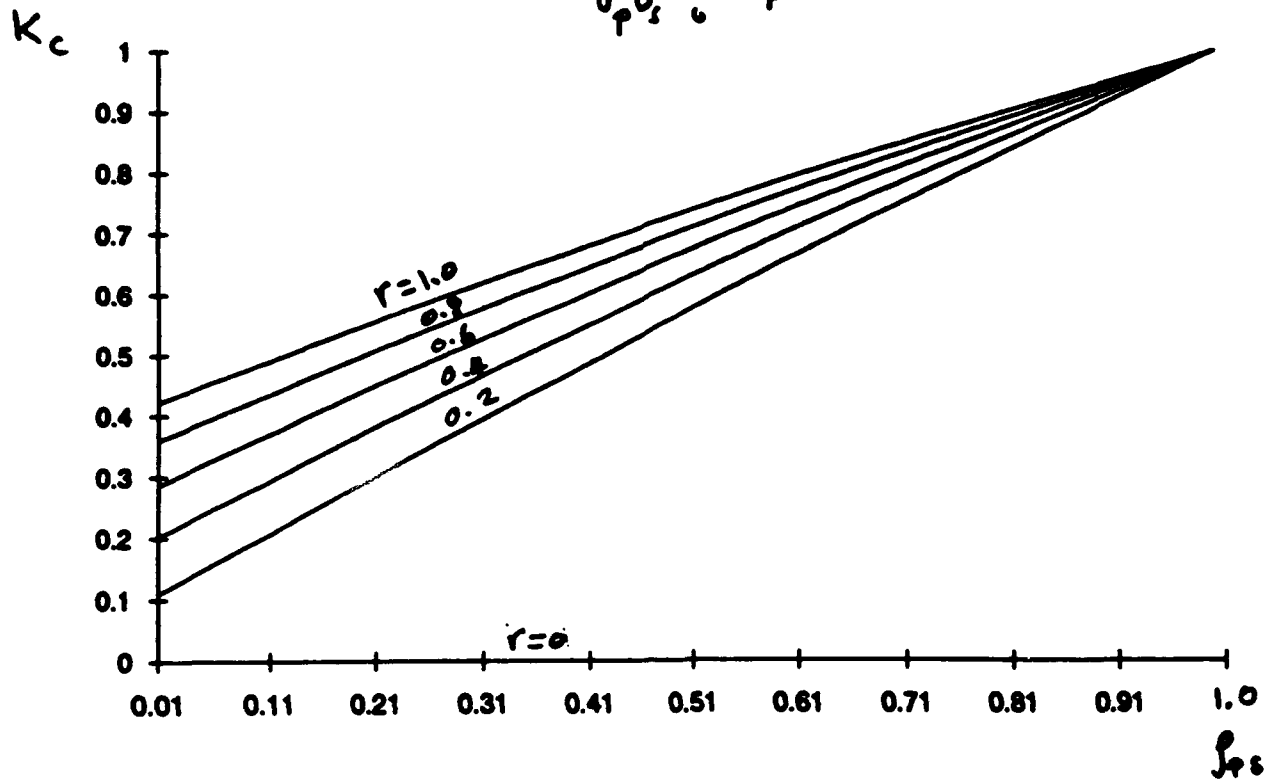
Figure 3.2 Probabilistic Load Factors for Two Correlated Wave Loads

$$\boxed{f_c = f_1 + K_{c_2} f_2 + K_{c_3} f_3}$$

Where:

f_c = combined stress

f_1, f_2, f_3 = maximum individual stresses

$$K_{c_2} = \text{correlation factor} = \frac{1}{2}\left(\overset{*}{\sigma}_{c_2} + 1 - \frac{r_3+1}{r_2} \right)$$

$$K_{c_3} = \text{correlation factor} = \frac{1}{2}\left(\overset{*}{\sigma}_{c_3} + 1 - \frac{r_2+1}{r_3} \right)$$

$$\overset{*}{\sigma}_{c_2} = \left(1 + \frac{1}{r_2^2} + \left(\frac{r_3}{r_2}\right)^2 + \frac{2\rho_{12}}{r_2} + 2\rho_{13}\frac{r_3}{r_2^2} + 2\rho_{23}\frac{r_3}{r_2} \right)^{\frac{1}{2}}$$

$$\overset{*}{\sigma}_{c_3} = \left(1 + \frac{1}{r_3^2} + \left(\frac{r_2}{r_3}\right)^2 + \frac{2\rho_{13}}{r_3} + 2\rho_{12}\frac{r_2}{r_3^2} + 2\rho_{23}\frac{r_2}{r_3} \right)^{\frac{1}{2}}$$

$r_2 = f_2/f_1$ = stress ratio

$r_3 = f_3/f_1$ = stress ratio

ρ_{12}, ρ_{13}, and ρ_{23} are correlation coefficients that are determined as in the two load case.

The correlation factors K_c are function of ρ_{12}, ρ_{13}, ρ_{23}, r_2, and r_3.

Figure 3.3 Summary of Approach, Three Correlated Wave Loads
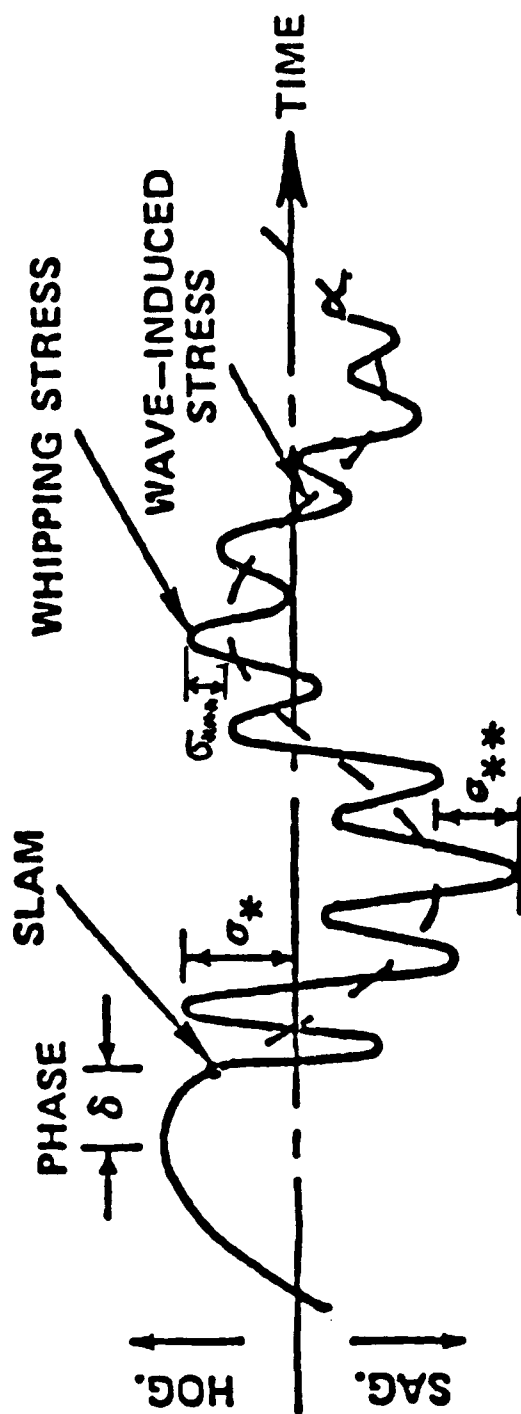
Figure 3.4 Stress Time History including Slamming

TELEDYNE DATA
(12 FEB. 72 REPORT)
LINE 14

WEBB DATA

NO.
OF
OCCURRENCES

20

15

10

5

−60° −40° −20° 0° 20° 40° 60° 80°
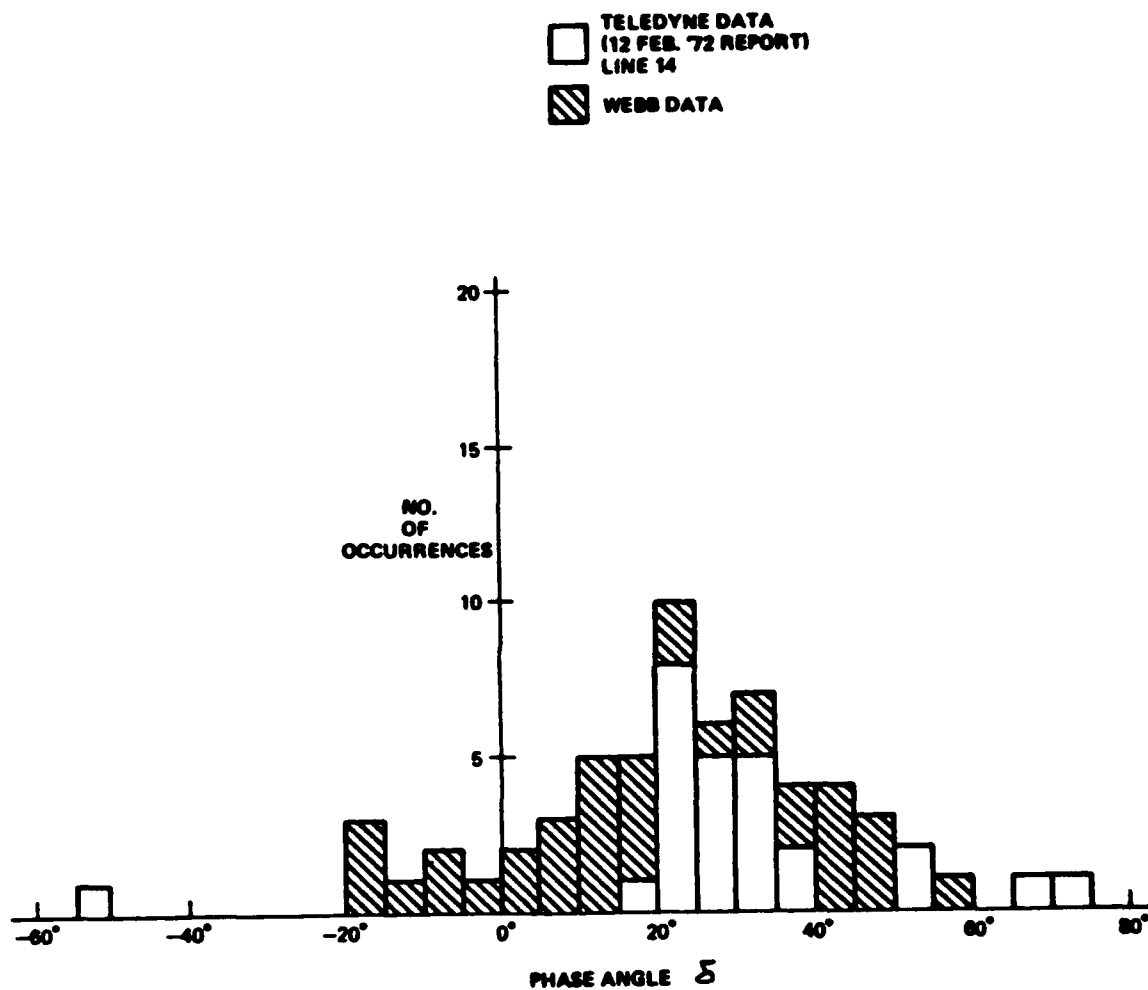
PHASE ANGLE δ

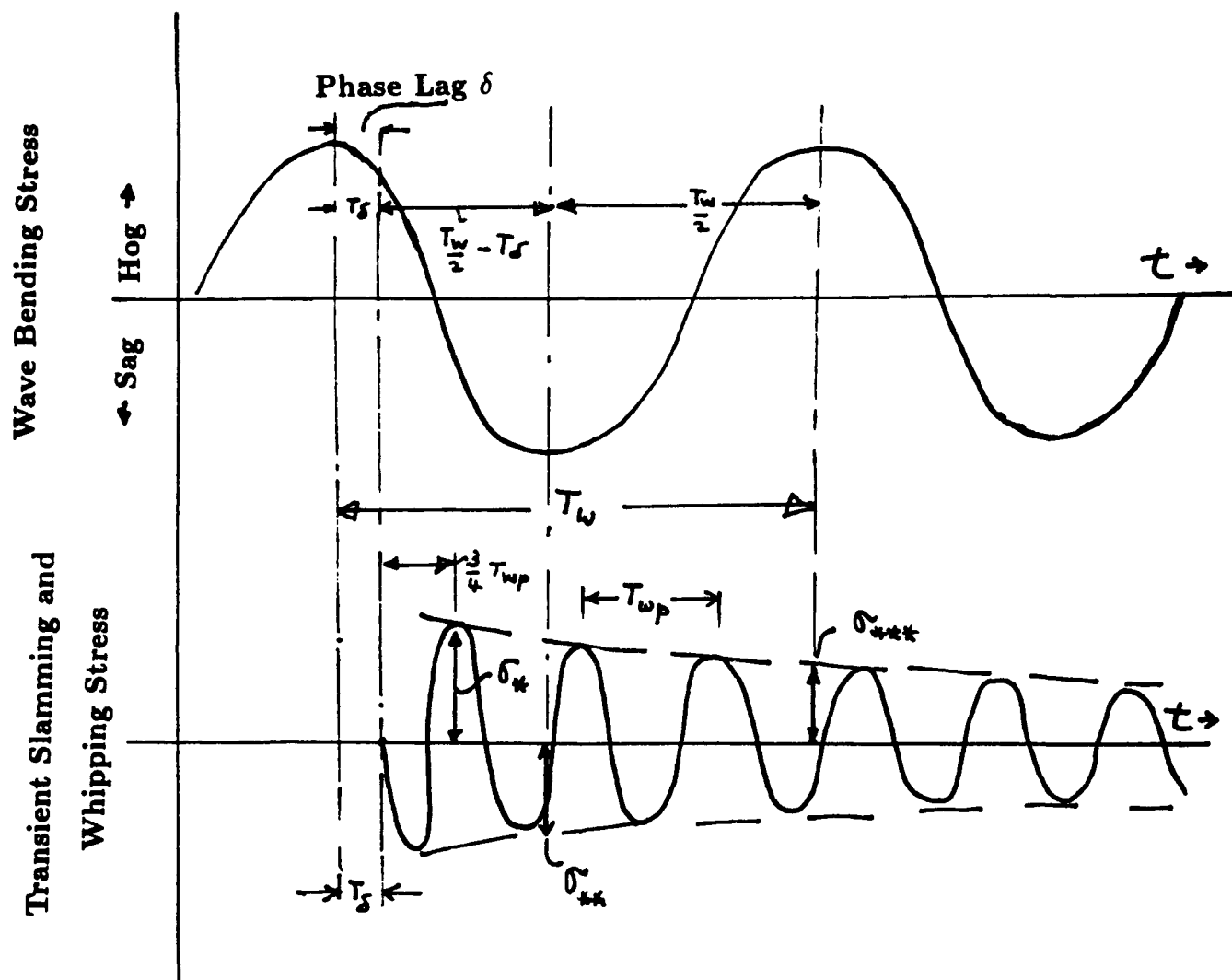Figure 3.5 Distribution of Slam Phase Angle, Wolverine State

F-13

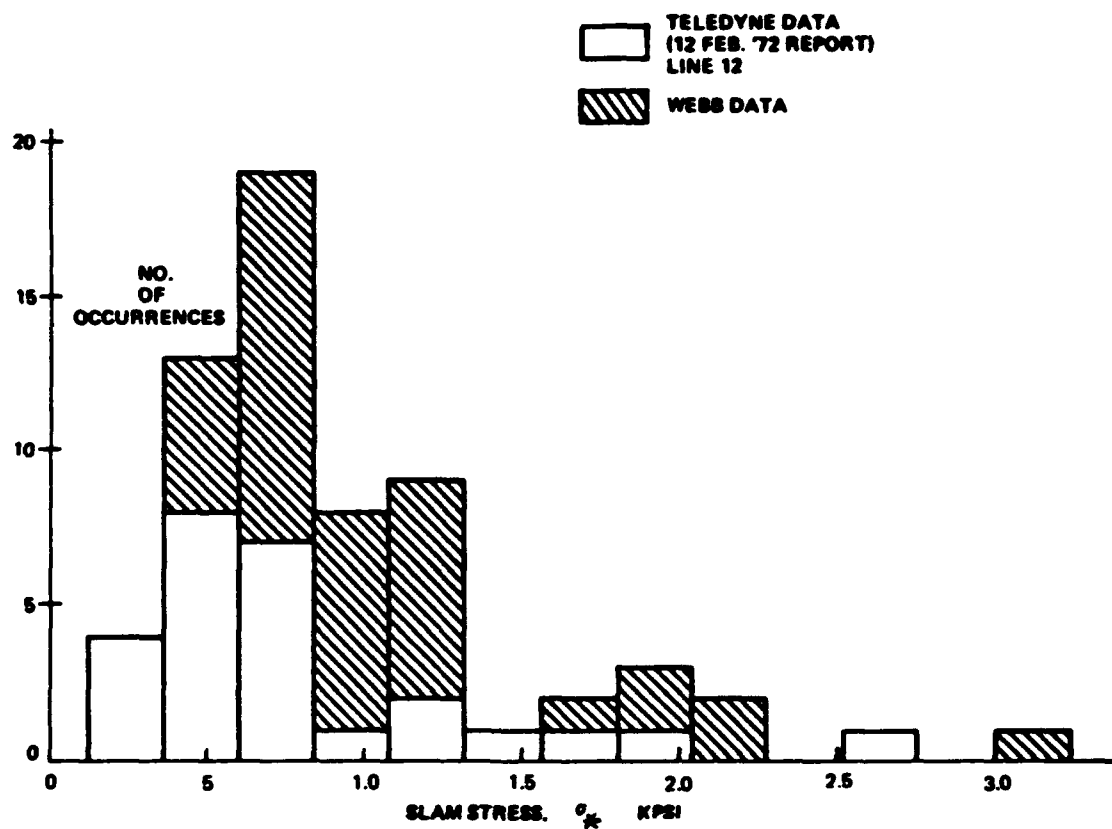Figure 3.6 Combination of Slam Transient with Wave Induced Stress

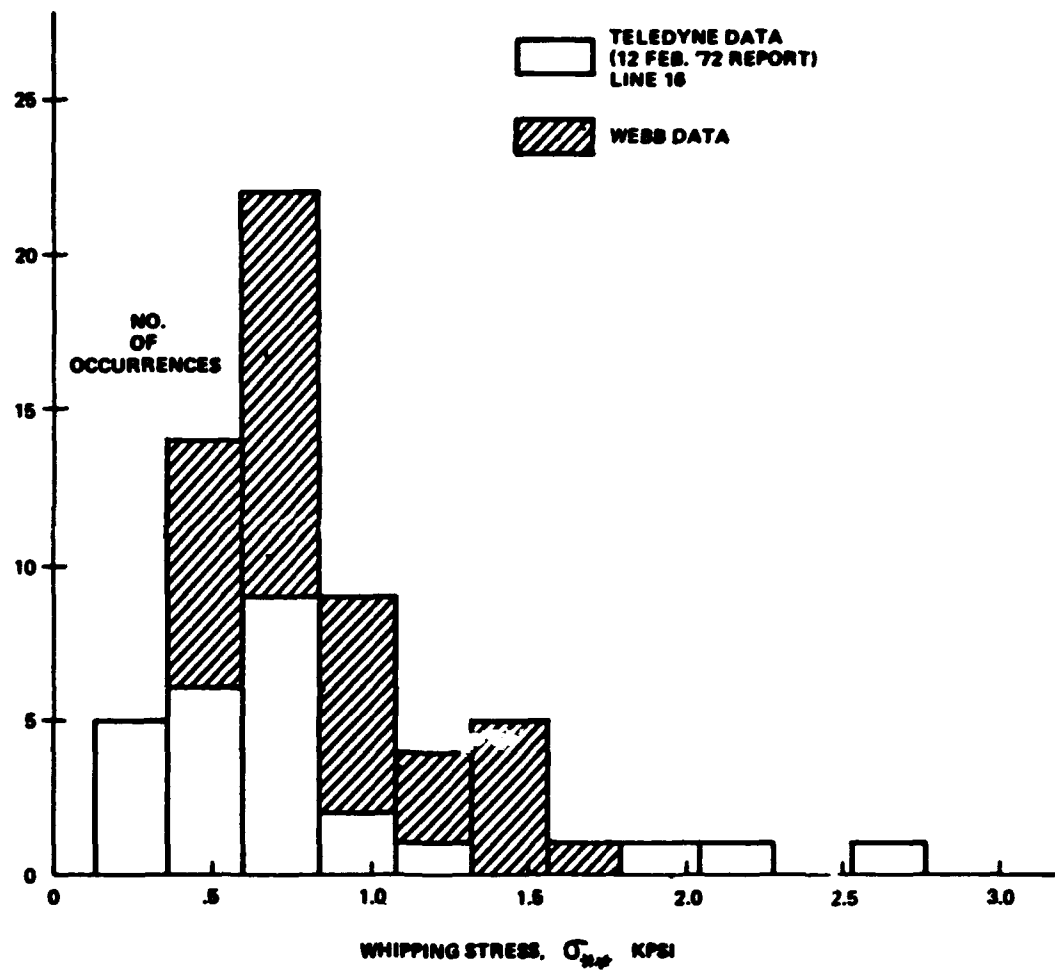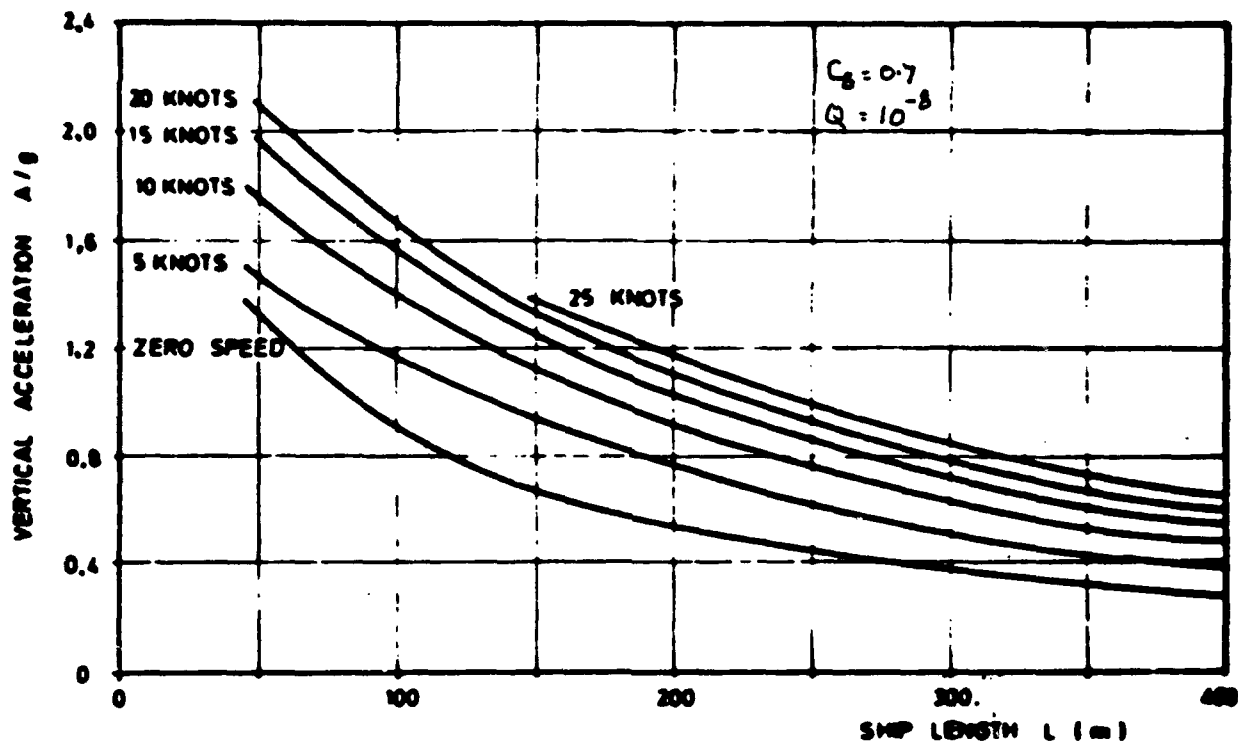F-14

Figure 3.7 Distribution of Slam Stress, Wolverine State

F-15

Figure 3.8 Distribution of Whipping Stress, Wolverine State

F-16

Calculated largest expected vertical acceleration at
forward perpendicular on Series 60. All headings included. Speed
reduction in heavy weather considered

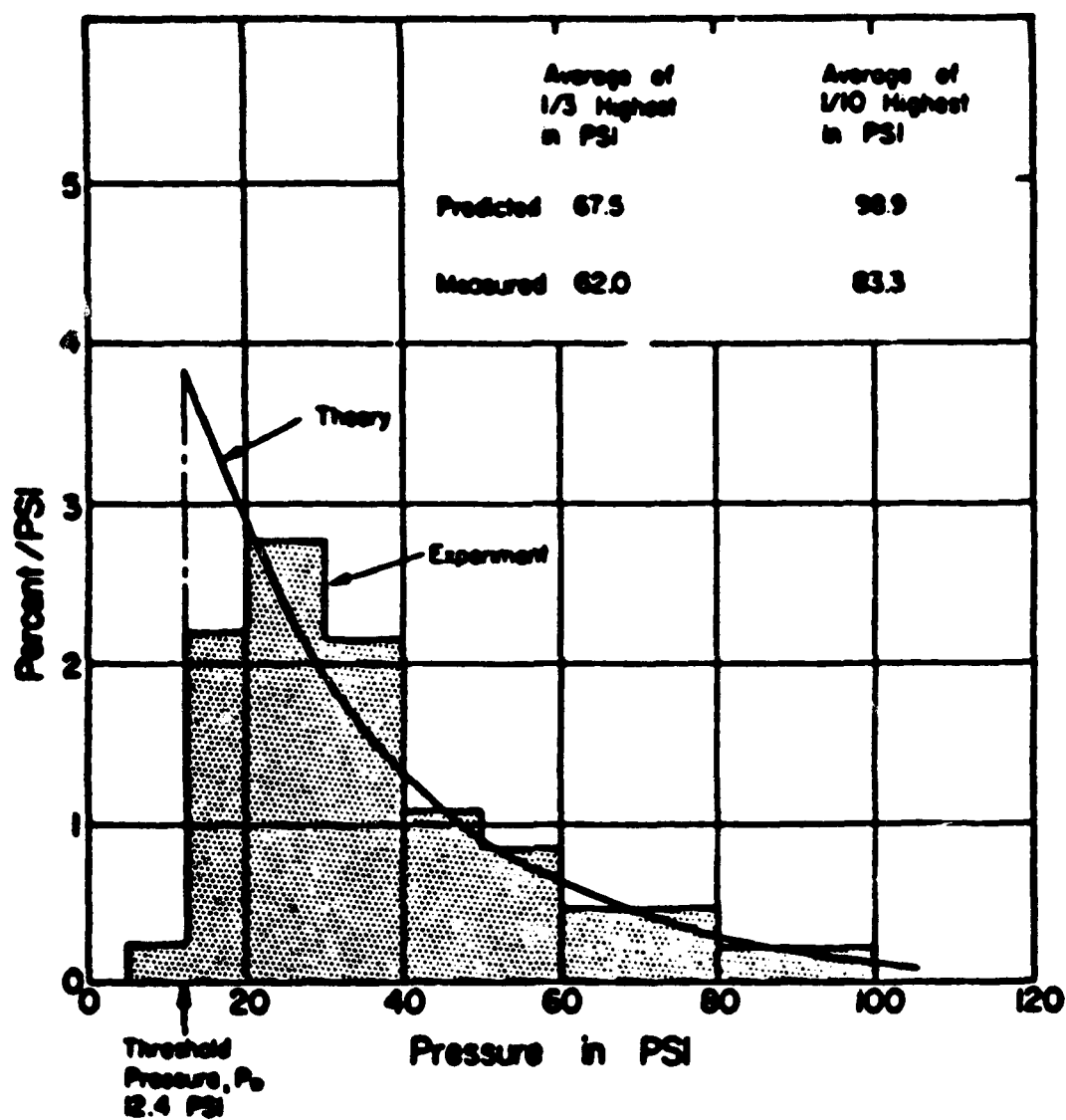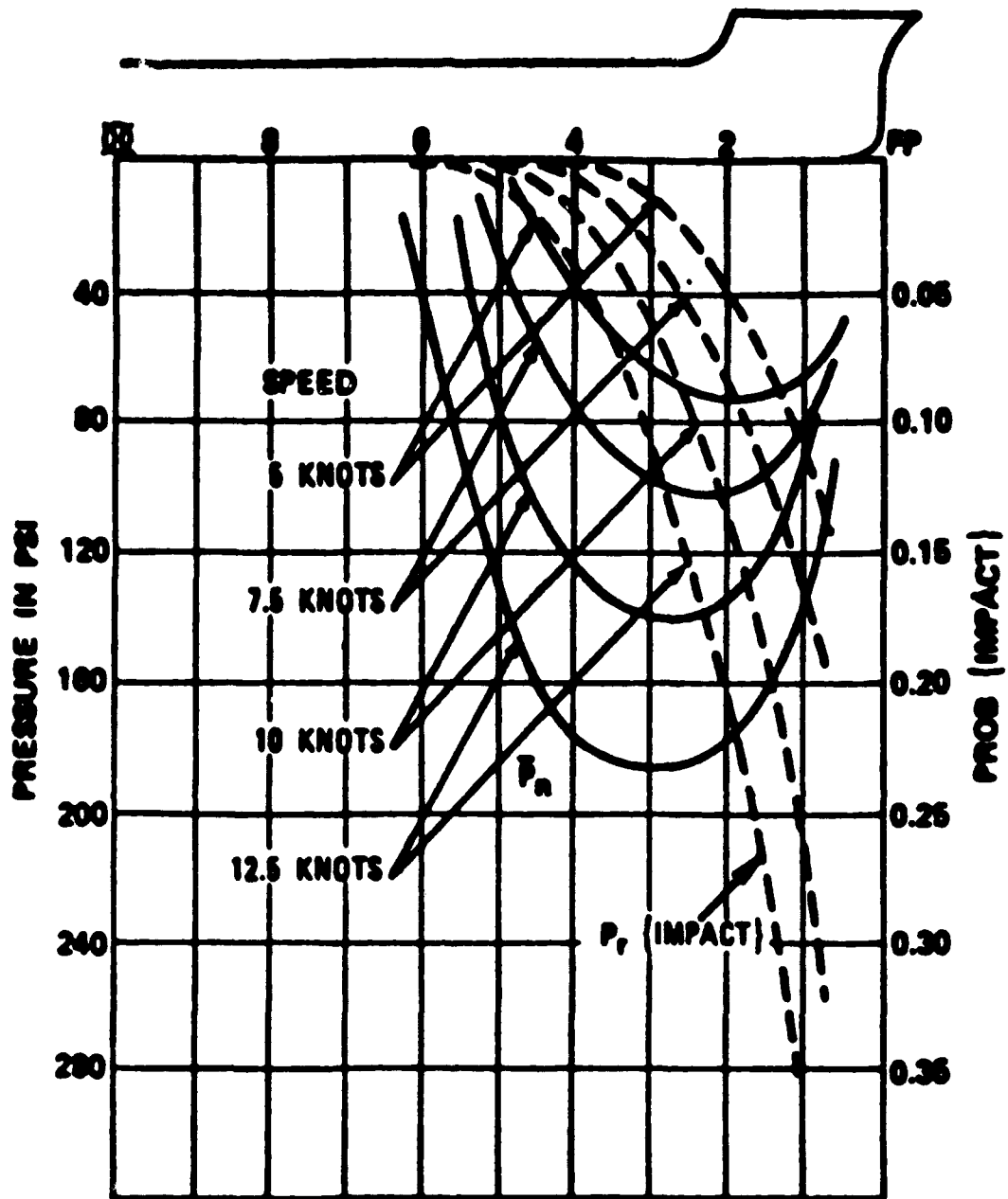Figure 3.9 Extreme Vertical Accelerations, Series 60, North Atlantic

Figure 3.10 Histogram of Slamming Pressures, Mariner Model

Distribution of extreme pressure and frequency of
impacts along the ship length; Mariner, Sea State 7,
significant wave height 25 ft, ship operation time 35 hr,
light draft

Figure 3.11 Extreme Pressures and Impact Frequency, Mariner , ref. 3.9

Table A1 Load Combinations*

|	L.C. 1	L.C. 2	L.C. 3	L.C. 4	L.C. 5	L.C. 6	L.C. 7	L.C. 8
A. HULL GIRDER LOADS (See A.2, A.3) **								
Vertical B.M. k_c	Sag (-) 1.0	Sag (+) 1.0	Sag (-) 0.7	Sag (+) 0.7	Sag (+) 0.3	Sag (-) 0.3	Sag (-) 0.4	Sag (+) 0.4
Vertical S.F. k_c	(+) 0.5	(-) 0.5	(-) 1.0	(+) 1.0	(-) 0.3	(+) 0.3	(-) 0.3	(+) 0.3
Horizontal B.M. k_c	0.0	0.0	0.0	0.0	0.3	0.3	0.3	0.3
Horizontal S.F. k_c	0.0	0.0	0.0	0.0	0.3	0.3	0.3	0.3
B. EXTERNAL PRESSURE (See A-4.1)								
k_c	0.5	0.5	0.5	1.0	0.5	1.0	0.5	1.0
k_{f0}	-1.0	1.0	-1.0	1.0	-1.0	1.0	-1.0	1.0
C. INTERNAL TANK PRESSURE								
k_c	See A.4.2 0.4 0.75	See A.4.2 0.4 -0.75	See A.4.2 1.0 0.75	See A.4.2 0.5 -0.75	See A.4.2 1.0 0.25	See A.4.2 0.5 -0.25	See A.4.2 1.0 0.4	See A.4.2 0.5 -0.4
k_f	Fwd BHD 0.25 Aft BHD -0.25	Fwd BHD -0.25 Aft BHD 0.25	Fwd BHD 0.25 Aft BHD -0.25	Fwd BHD -0.25 Aft BHD 0.25	PORT BHD -0.75 STBD BHD 0.75	PORT BHD 0.75 STBD BHD -0.75	Fwd BHD 0.2 Aft BHD -0.2	Fwd BHD -0.2 Aft BHD 0.2
							PORT BHD -0.4 STBD BHD 0.4	PORT BHD 0.4 STBD BHD -0.4
c_ϕ, Pitch	-1.0	1.0	-1.0	1.0	0.0	0.0	-0.7	0.7
c_θ, Roll	0.0	0.0	0.0	0.0	1.0	-1.0	0.7	-0.7
D. REFERENCE WAVE HEADING AND MOTION OF SHIP								
Heading Angle	0	0	0	0	90	90	60	60
Heave	Down	Up	Down	Up	Up	Down	Down	Up
Pitch	Bow Down	Bow Up	Bow Down	Bow Up	—	—	Bow Down	Bow Down
Roll	—	—	—	—	STBD Down	STBD Up	STBD Down	STBD Up

* k_c = 1.0 for all load components.
** Boundary forces should be applied to produce the above specified hull girder loads at the middle of the structural model.

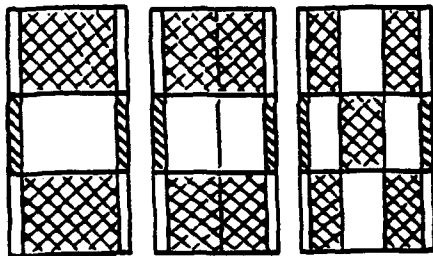Figure 4.1 Fatigue Loads Cases, ABS Guide

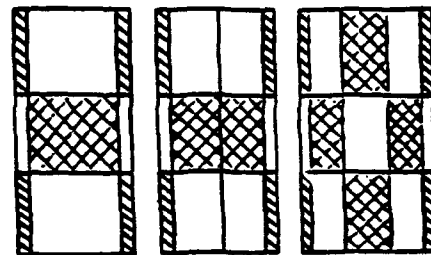Figure A.4: Tank Loading Patterns
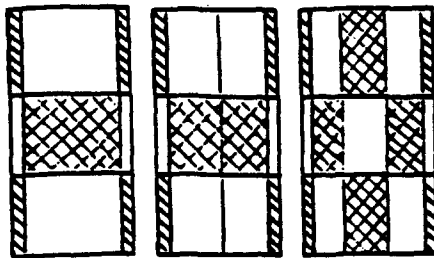
a. Load Cases #1, 3 & 7, 2/3 Design Draft
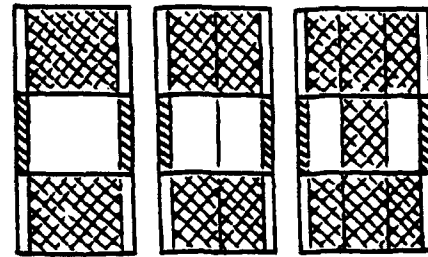
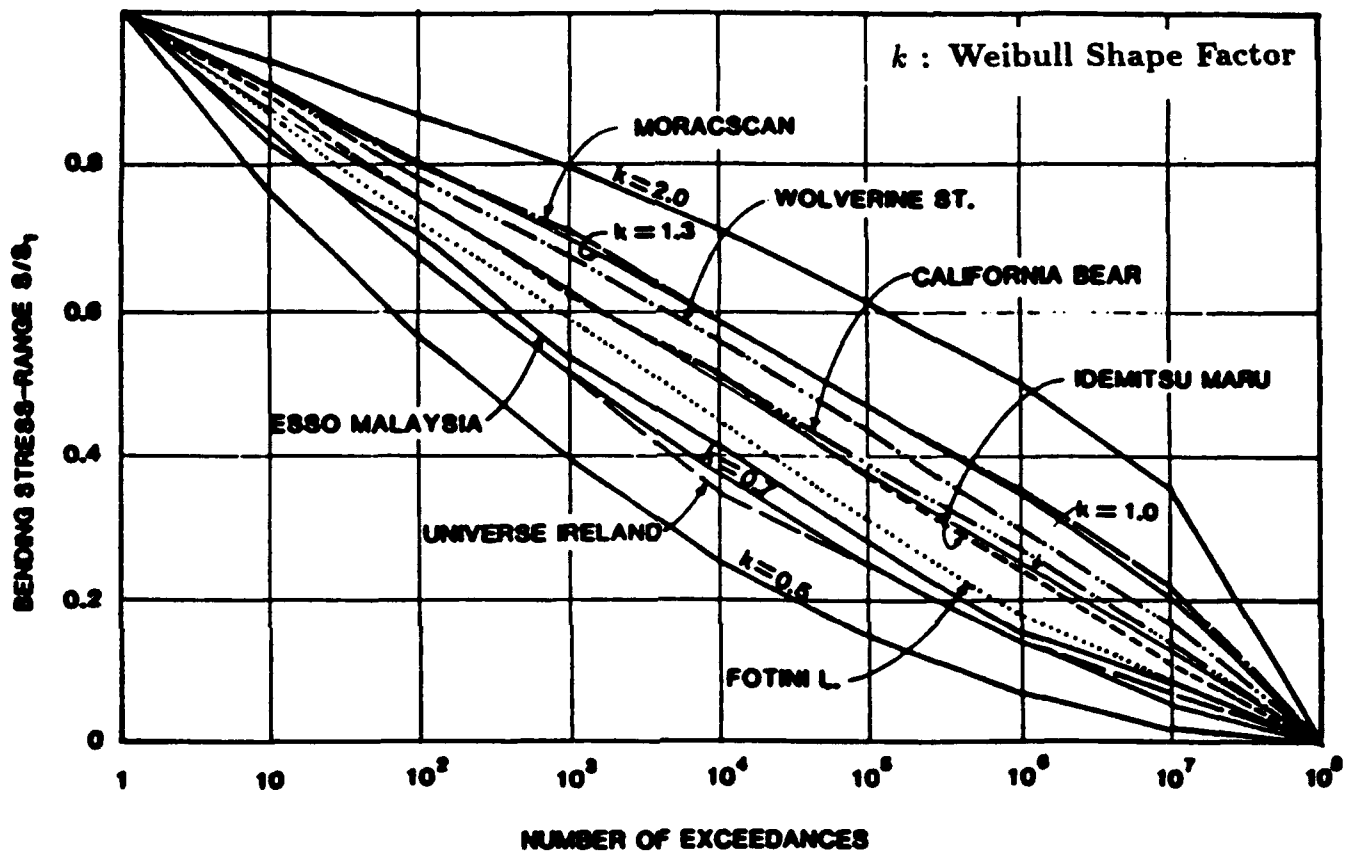b. Load Cases #2, 4 & 8 Design Draft

c. Load Case #5, 2/3 Design Draft

d. Load Case #6, 2/3 Design Draft

Figure 4.2 Still Water Load Cases, ABS Guide

Long-term distribution of stress range of large tankers, bulk carriers and dry cargo vessels

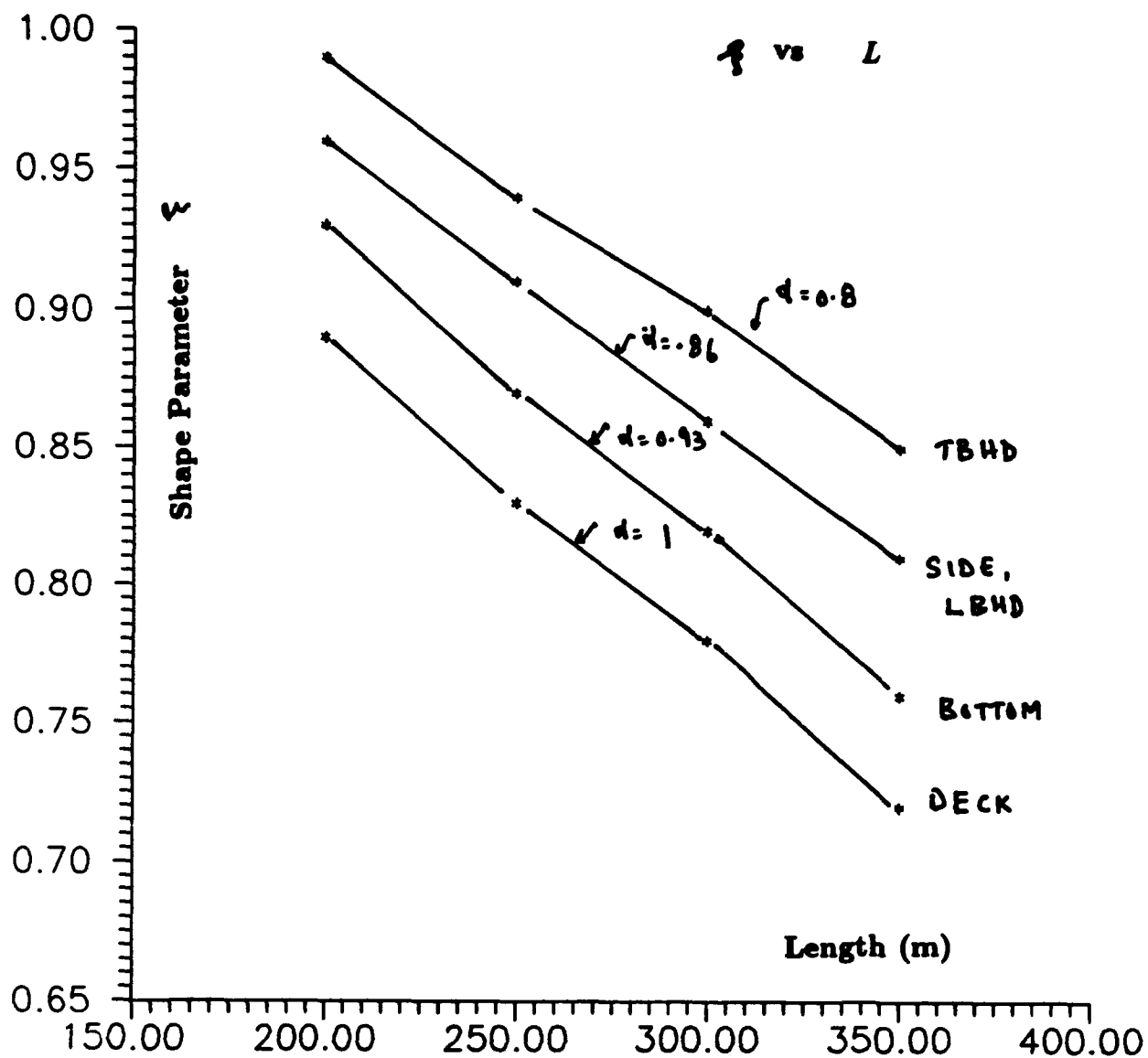Figure 4.3 Weibull Distribution fit to Service Data, from Munse

Figure 4.4 Weibull Shape Factor as a Function of Ship Length
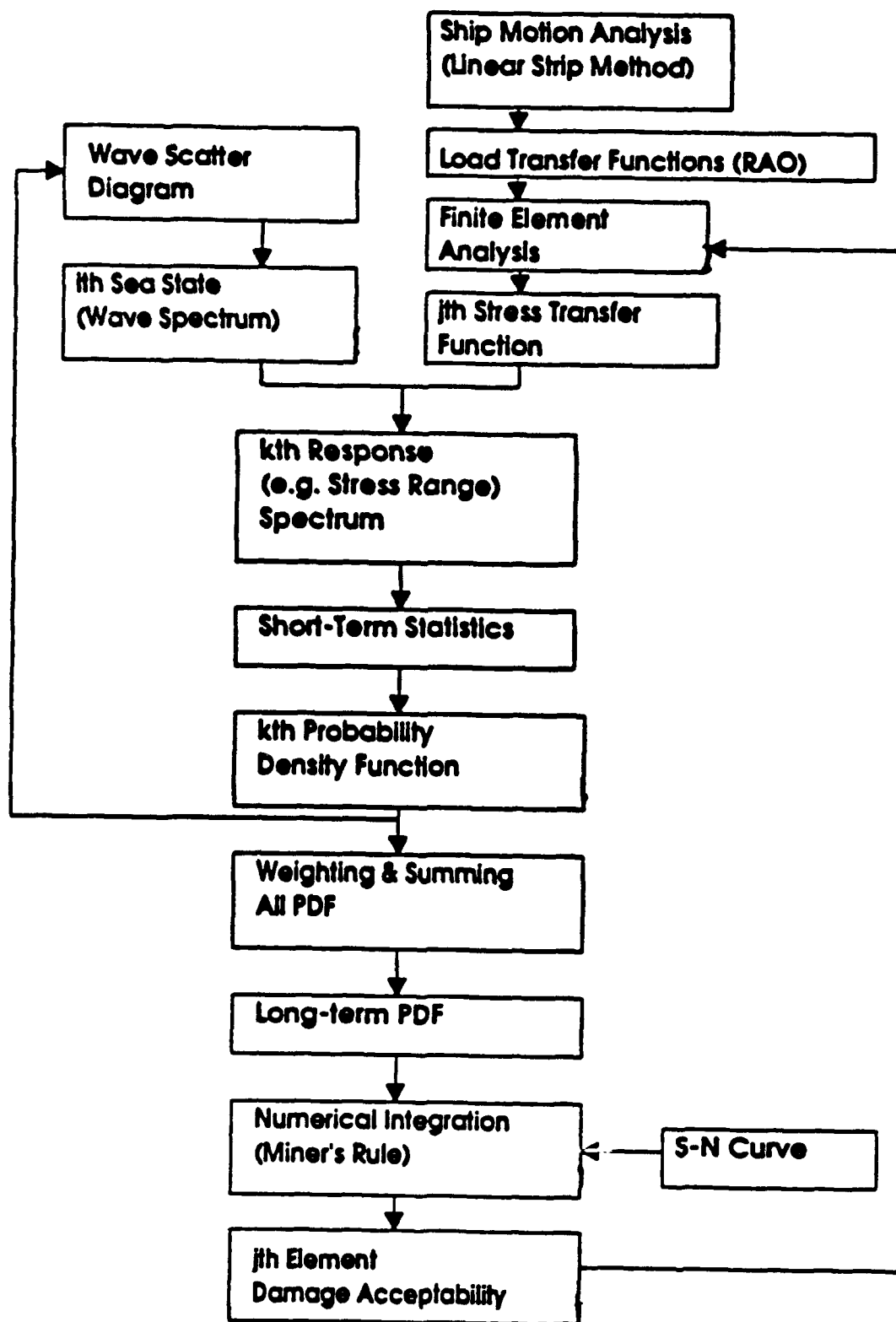
Figure 4.5 Flow Chart for Spectral Fatigue Analysis
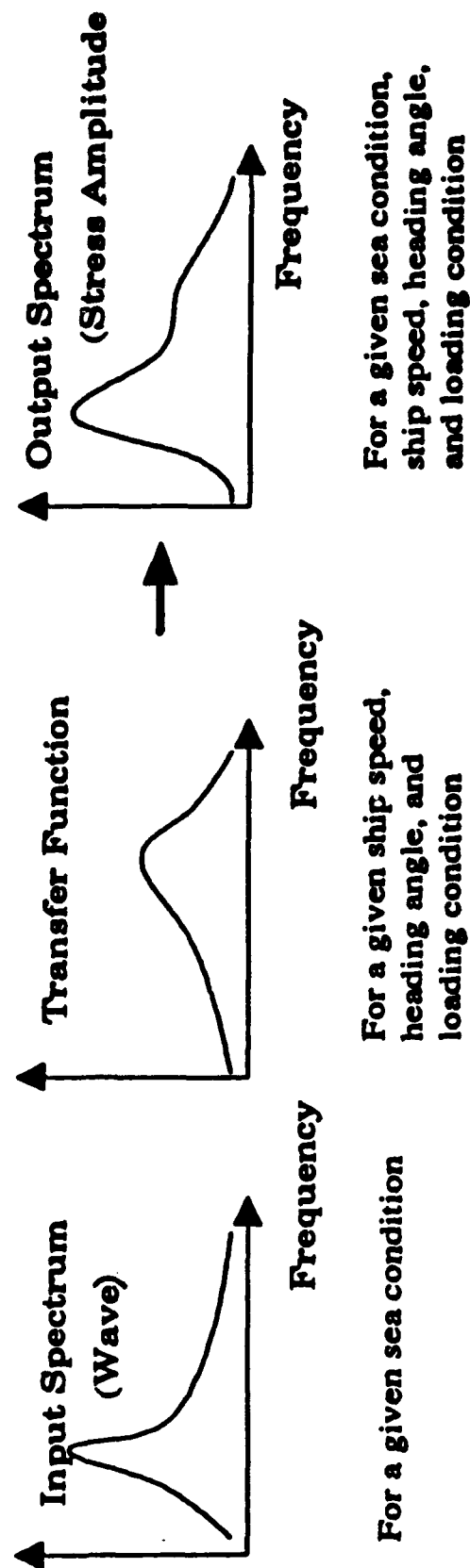
Figure 4.6 Input-Output Procedure for the Stress Amplitude Spectrum
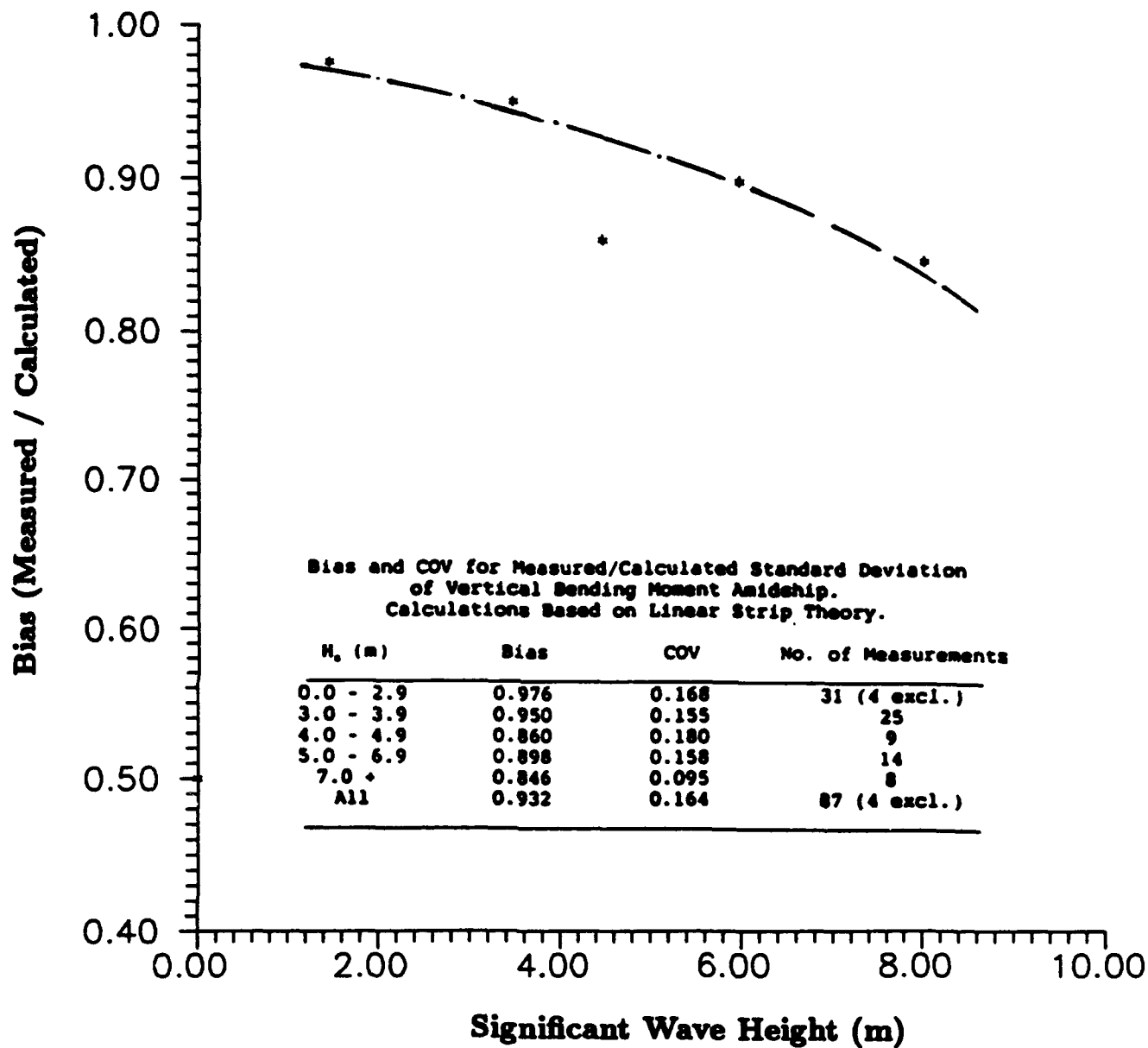
Figure 5.1 Bias in Calculated Wave Bending Moment, ISSC, ref. 5.18
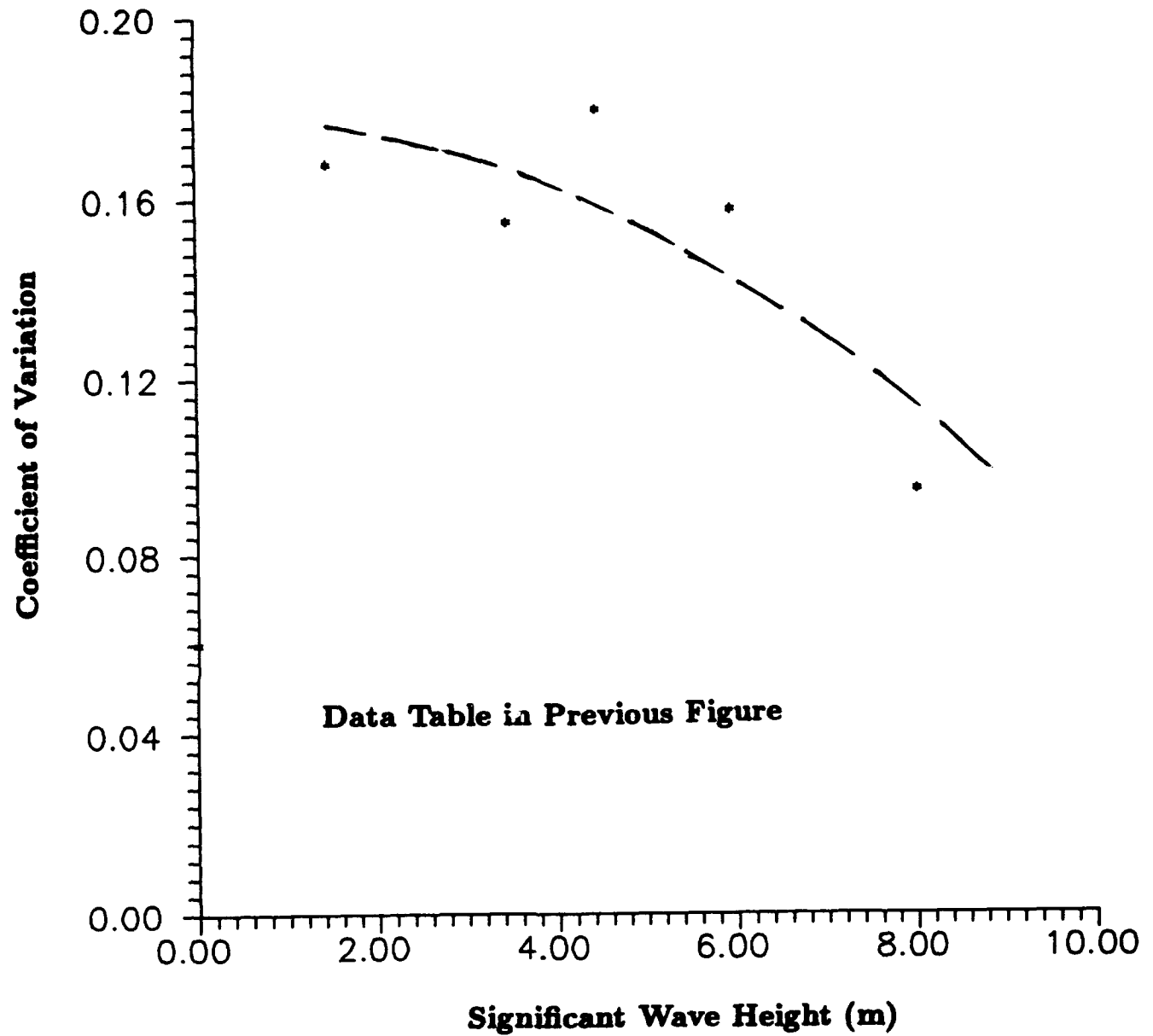
Figure 5.2 COV of bias in Wave Bending Moment
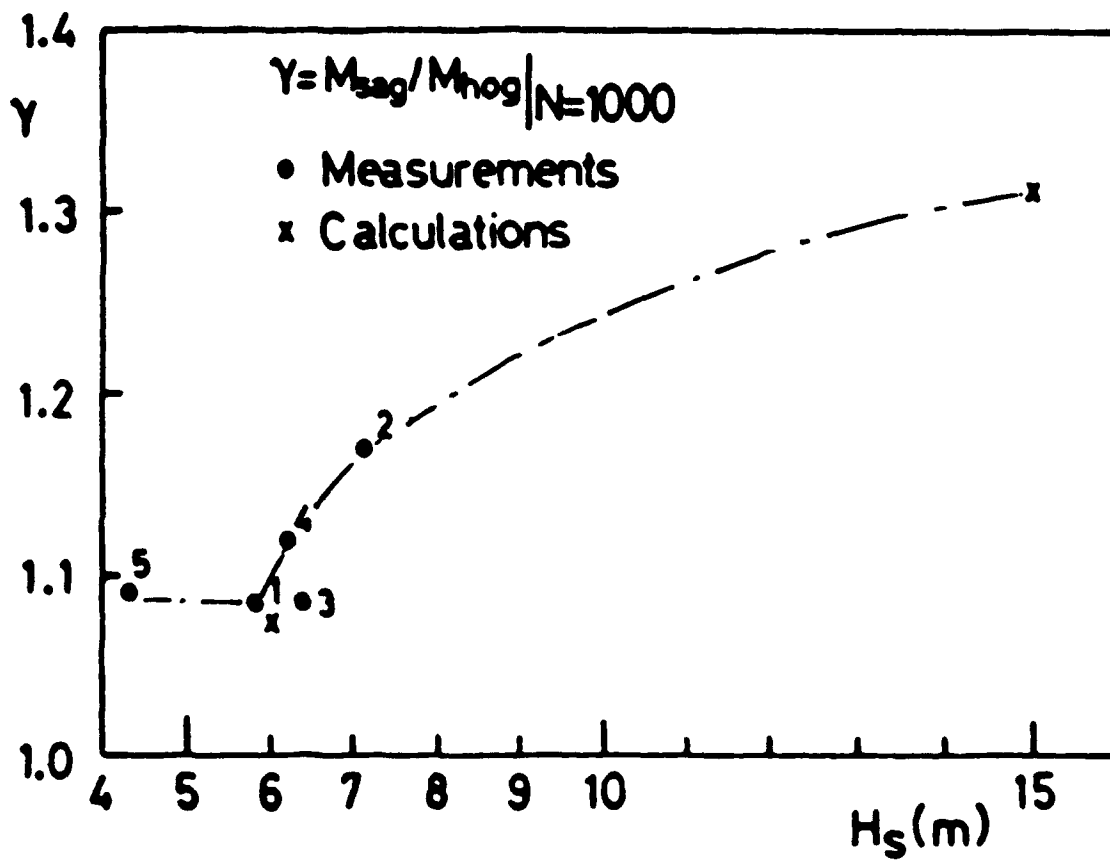
Figure 5.3 Hog/Sag Nonlinearities in Wave Bending Moment

F-28
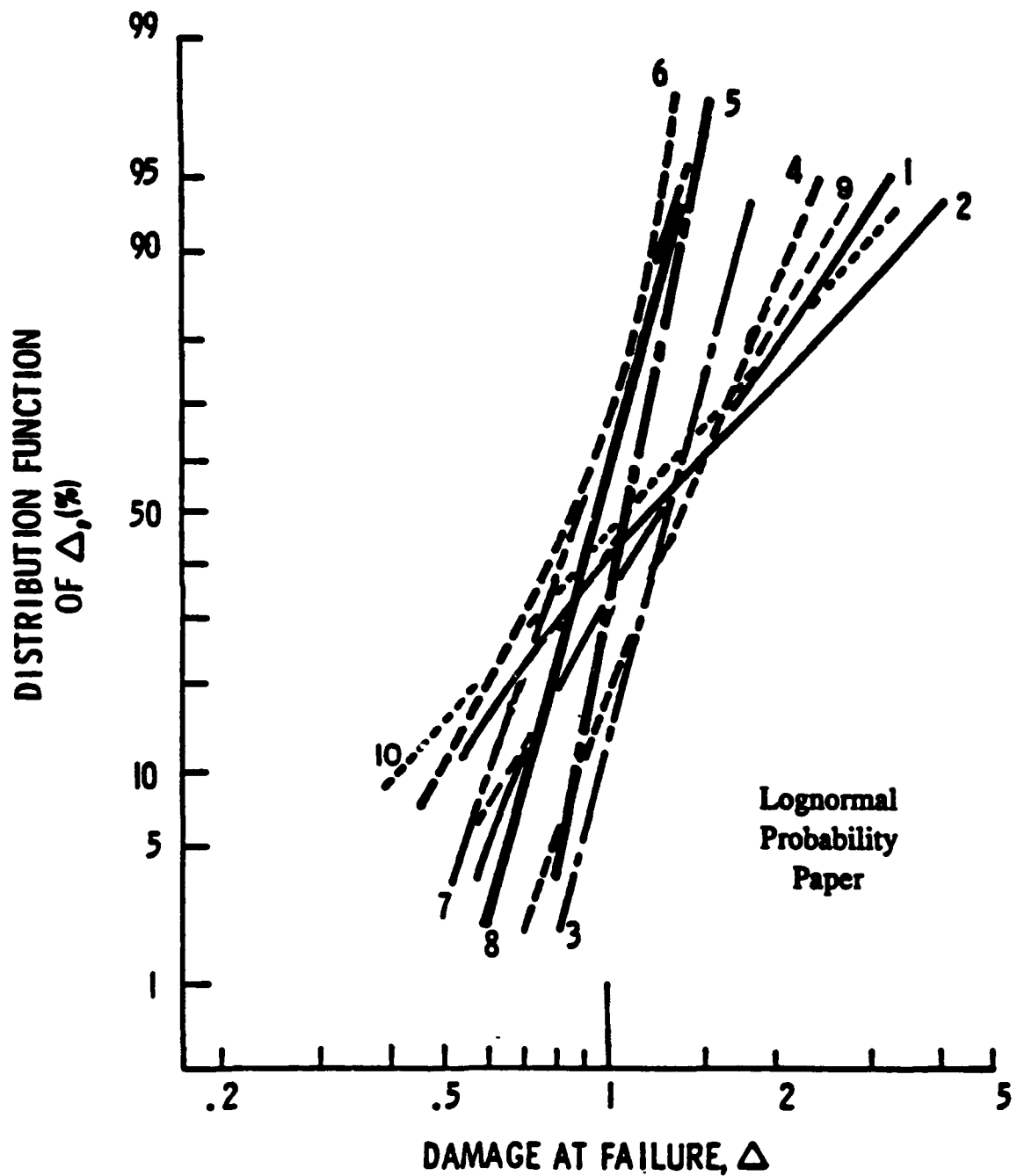
Figure 5.4 Uncertainty in Miner's Rule, from study by Wirsching
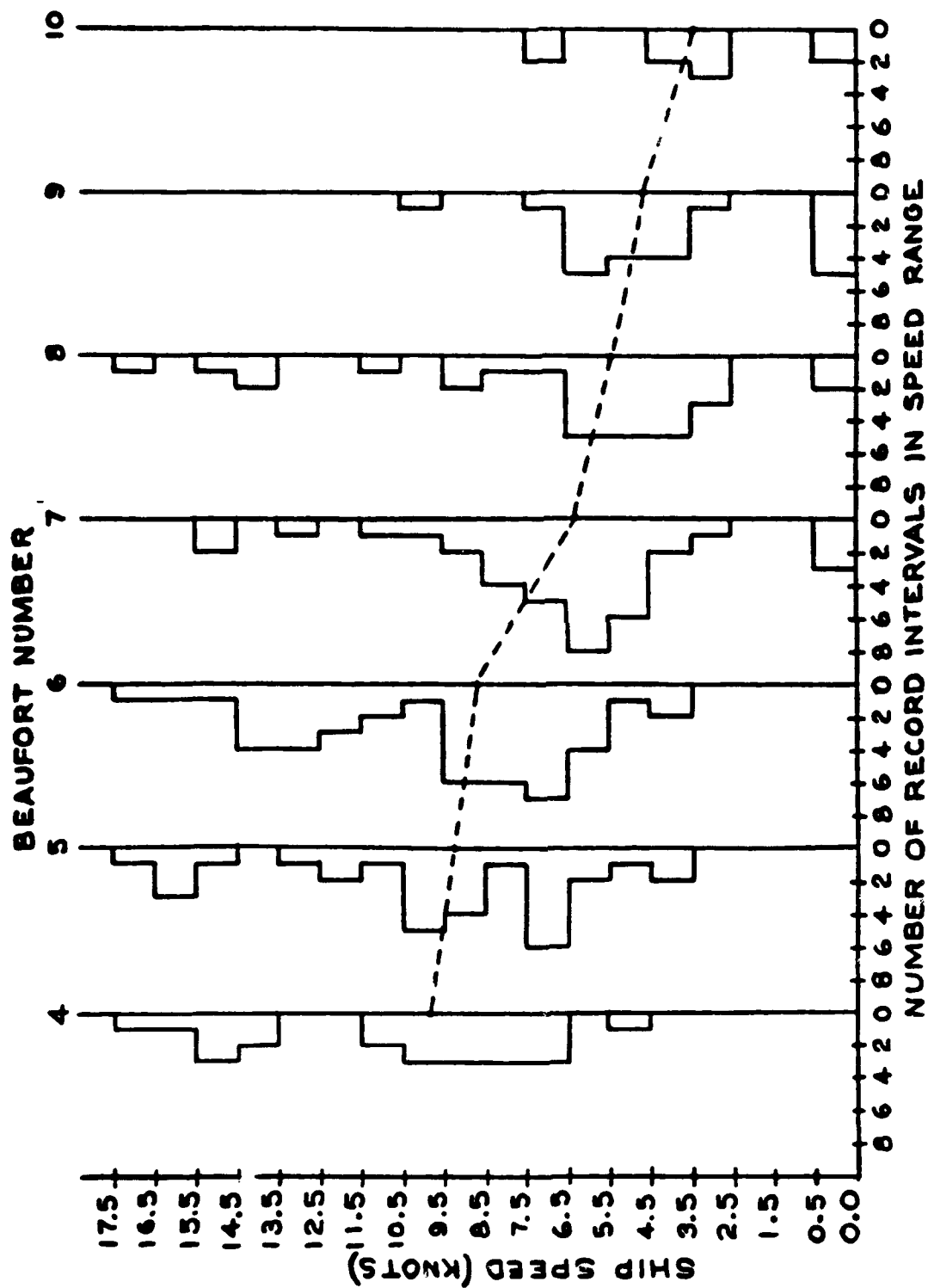
Figure 6.1 Ship Speed While Slamming, Wolverine State
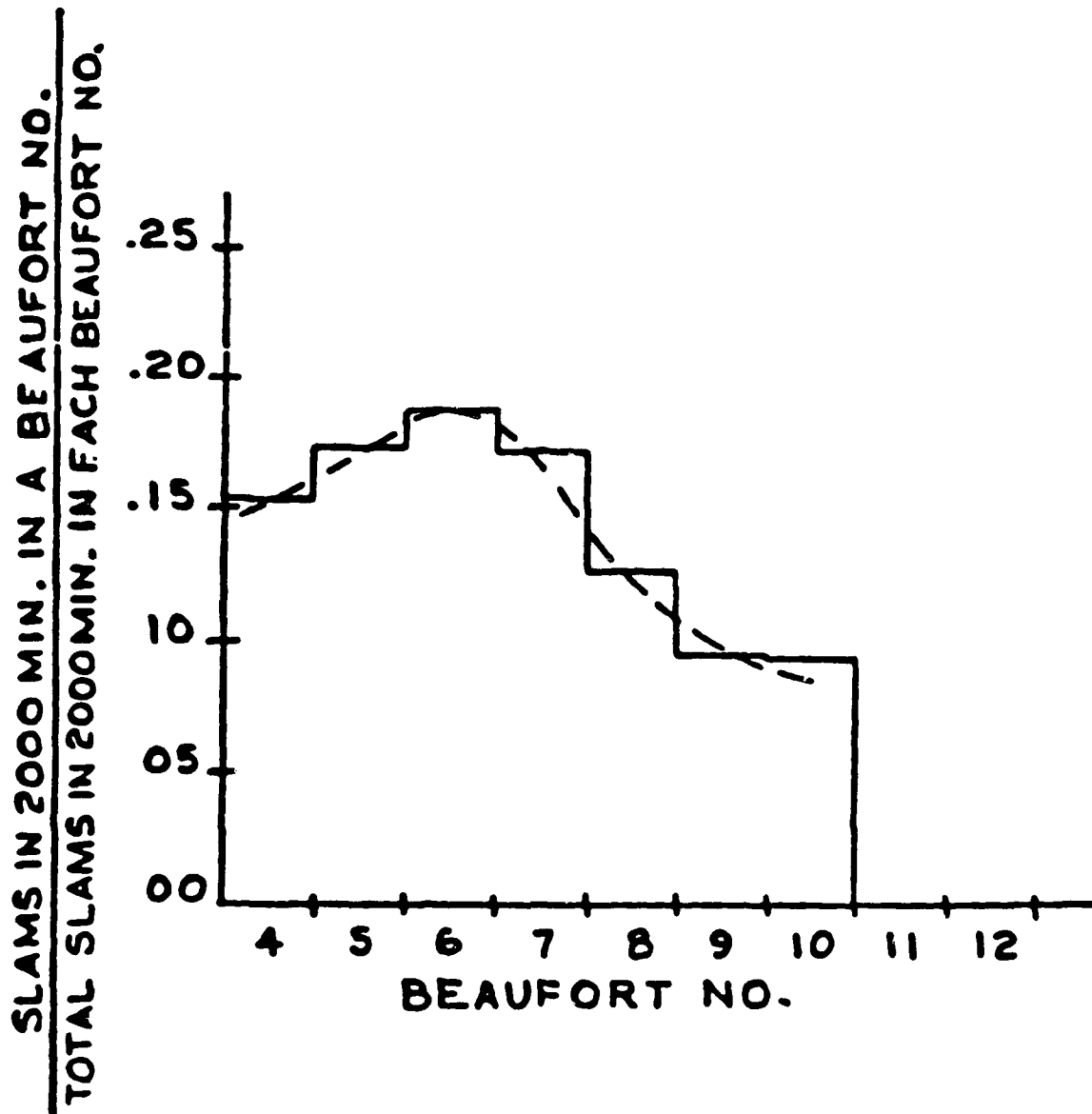
Distribution of frequency of slamming per unit time
Beaufort number

Figure 6.2 Slam Frequency, Wolverine State

F-31
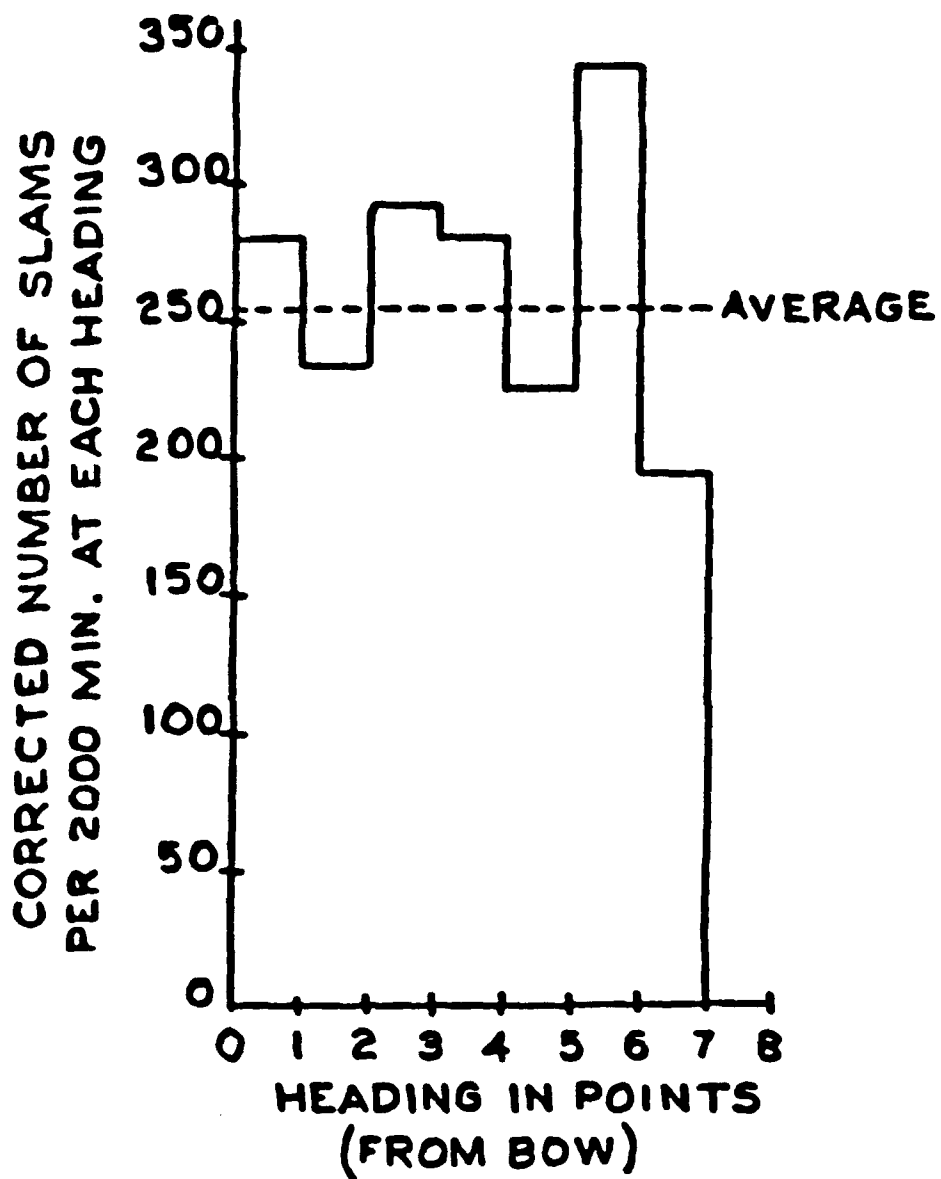
Distribution of frequency of slamming per unit time versus ship heading

Figure 6.3 Slam Frequency versus Heading, Wolverine State
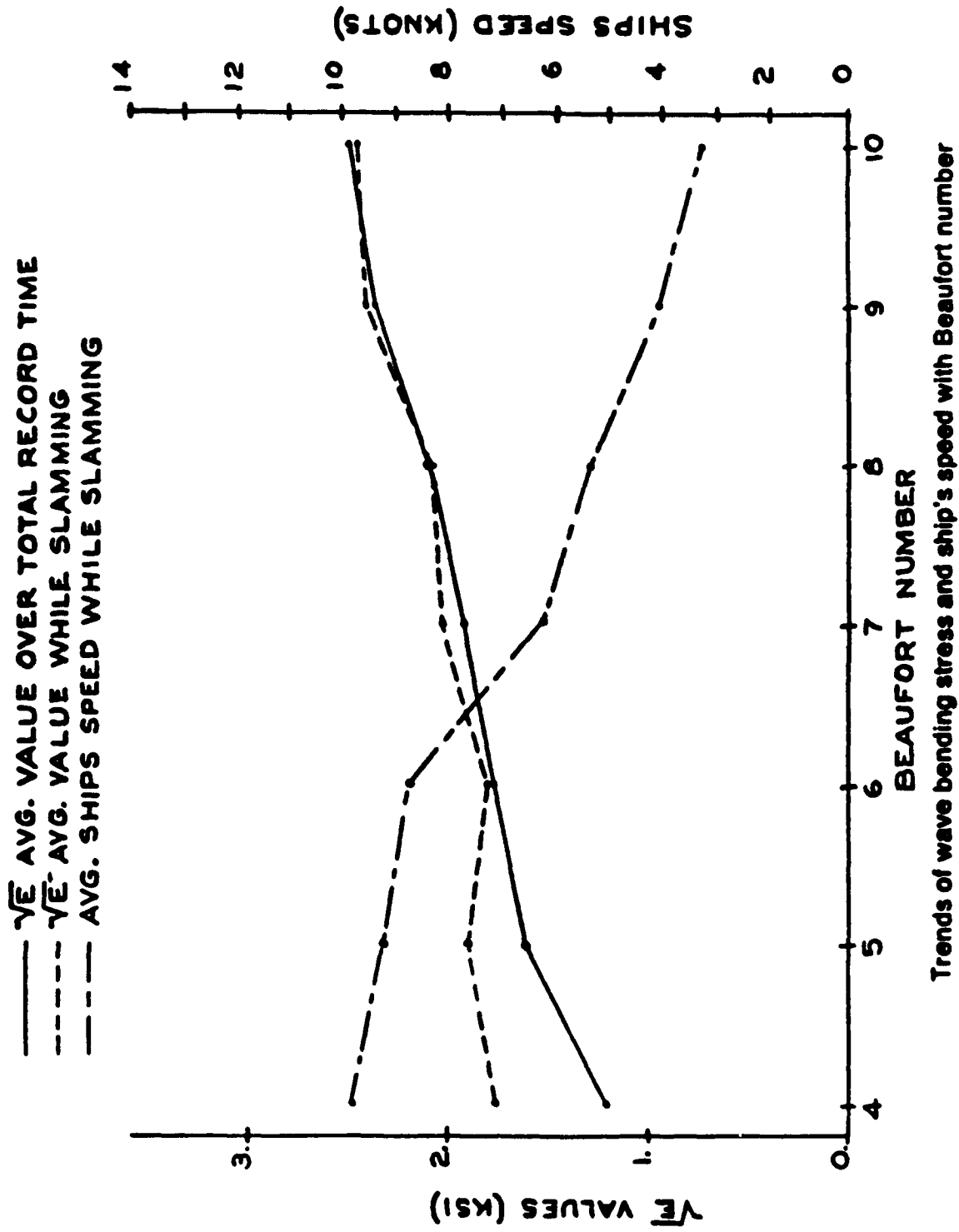
Figure 6.4 Fluctuating Bending Stress during Slamming, Wolverine State

Trends of wave bending stress and ship's speed with Beaufort number

F-33
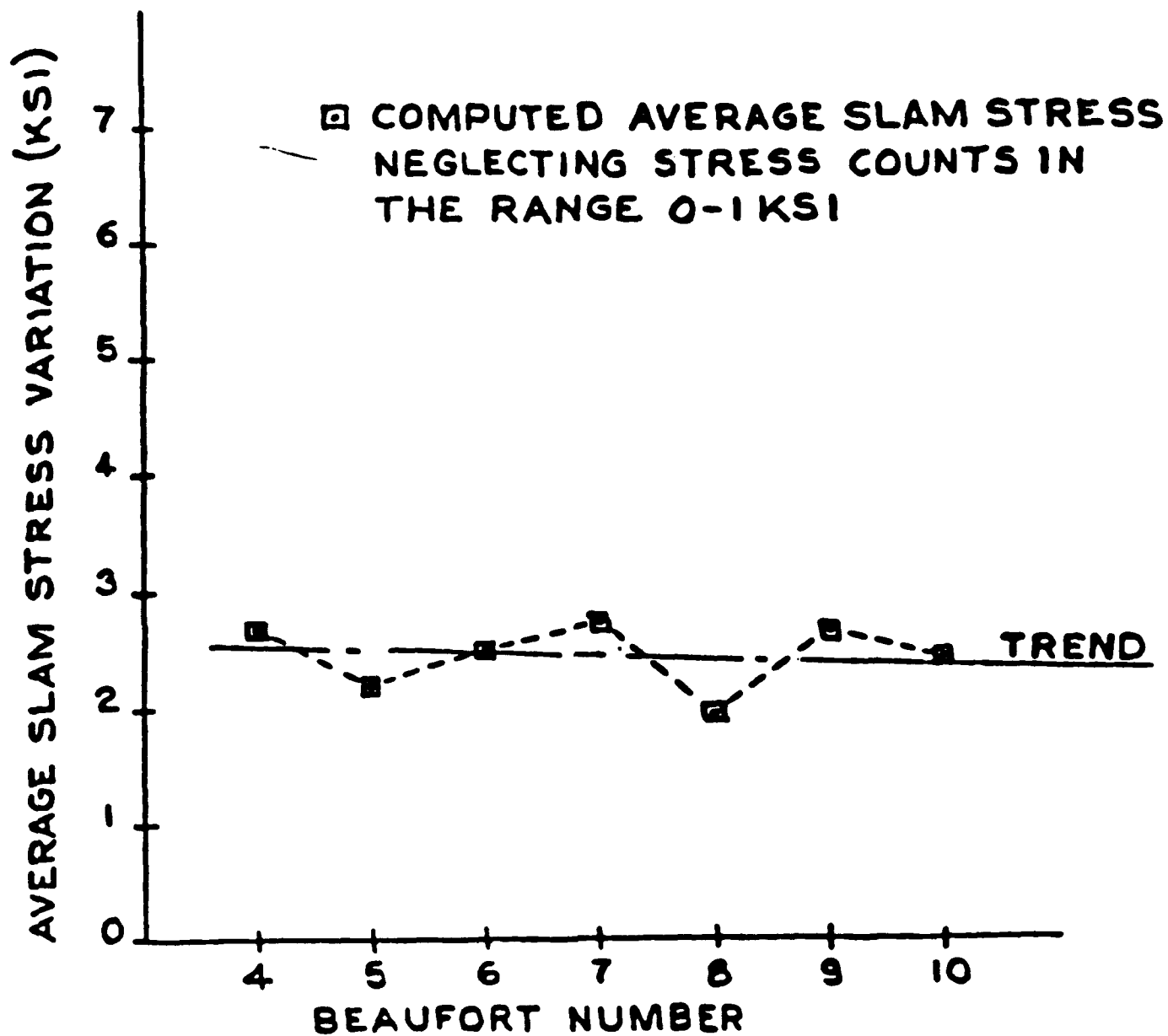
Figure 6.5 Slam Stress, Wolverine State
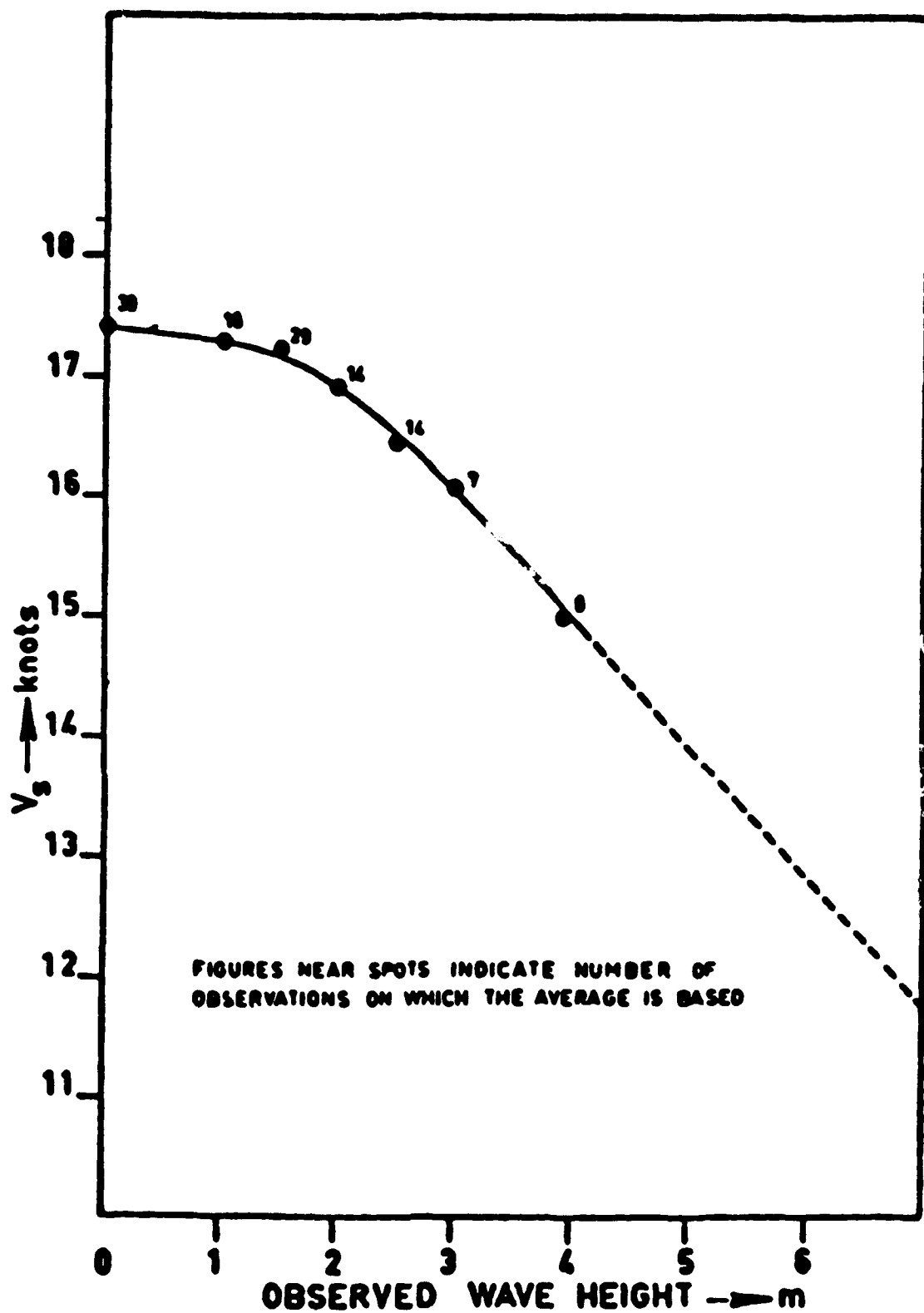
Figure 6.6 Natural Speed Reduction as a function of Wave Height

SHIP SPEED IN KNOTS

SIGNIFICANT WAVE HEIGHT IN FT.

SEA STATE

DAMAGE MOST LIKELY TO OCCUR

FREE FROM DAMAGE WITH 1 – α = 0.98

TOLERABLE SPEED

SAFE ZONE
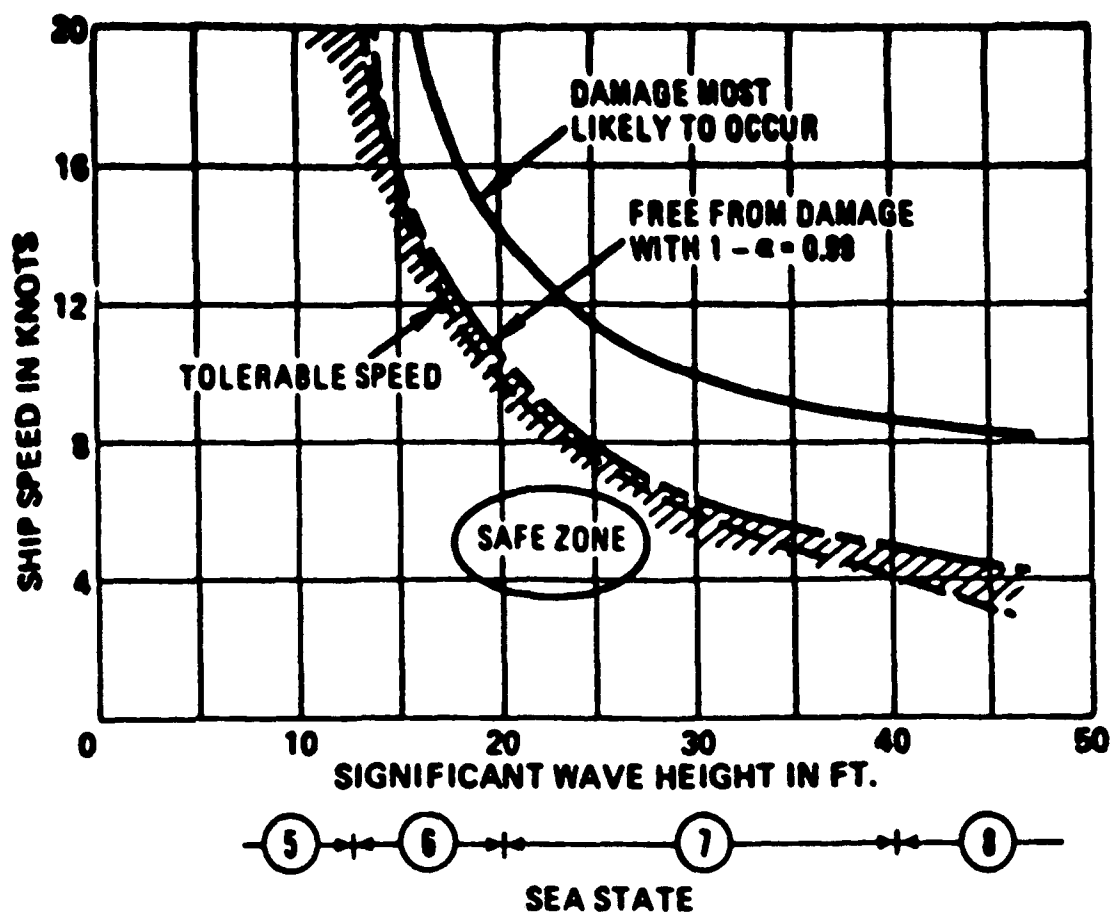
Comparison between speeds for (i) damage most likely to occur, (ii) free-from-slam damage, and (iii) tolerable limit for slam impact; Mariner, light draft

Figure 6.7 Likelihood of Slamming Damage as a function of Speed

APPENDIX A

THE WEN LOAD COINCIDENCE METHOD

APPENDIX A

THE WEN LOAD COINCIDENCE METHOD

The load coincidence method and related concepts developed by Y. K. Wen constitute a powerful approach to the treatment of load combinations. In this section we discuss two relevant concepts central to the load coincidence approach, namely the Poisson pulse process and the intermittent continuous random process (ICP). The load coincidence method as applied to two Poisson pulse processes is then described. The approach adopted herein is to present relevant concepts and results. A detailed treatment may be found in Ref. A.1.

1. POISSON PULSE PROCESS

In a Bernoulli sequence of load occurrences, if the time interval tends to zero and number of intervals tends to infinity, what results is a Poisson process. There are three characteristics to such a process:

    (i)   Any given load occurrence time is equally likely (i.e., the process is stationary).

    (ii) One occurrence is independent of another, i.e., the process is memoryless.

    (iii) Only one occurrence is possible at any given time.

For a simple Poisson process, the interarrival times are exponentially distributed with a mean rate λ per unit time. The exponential density is given by

$$f_T(t) = \lambda \exp[-\lambda t] \tag{1}$$

The duration of the pulses is exponentially distributed, with mean value μ_d. The probability that the process is 'on' at any given time is characterized by $\lambda \mu_d$. If $\lambda \mu_d = 1$, the process reduces to a Poisson square wave that is always "on"; if $\lambda \mu_d \ll 1$, load pulses

A-1

are brief; if λ is finite, but $\mu_d = 0$, we have a spike process. Thus $\lambda\mu_d$ is a measure of process sparseness.

The pulse height within any occurrence ('on' time) has a probability density $f_x(x)$. The CDF of the maximum value of a rectangular pulse process over time (O,T) is given approximately by

$$F_R(r) \cong \exp\left\{-\lambda T\left(1 - F_x(r)\right)\right\} \tag{2}$$

for large r, $F_x(x)$ being the CDF of the pulse height density.

2. INTERMITTENT CONTINUOUS PROCESS

We consider a special case of the intermittent continuous process (ICP), where, if the pulse is "on", we have a stationary Gaussian process with a given power spectral density superimposed on the rectangular pulse intensity, i.e., the pulse height is the mean of a Gaussian process. The distribution of the maximum value of the ICP is given, from Ref. A.1, by

$$F_R \cong \exp\left\{\lambda T\left(1 - F_{X_m}(r)\right)\right\} \tag{3}$$

for large r. Here $F_{X_m}(r)$ is the CDF of the within occurrence maximum value X_m. The above expression gives the maximum value over the time (O,T), λ being the rate of arrival of the composite ICP pulses over the given time T.

For a within-occurrence piecewise stationary Gaussian process, the maximum value over a given period of time d is given, based on a Poisson assumption, by:

$$F_{X_m}(r) \cong \exp\left\{-v_0\, d\exp\left[-\frac{1}{2}\left(\frac{r-\mu_x}{\sigma_x}\right)^2\right]\right\} \tag{4}$$

The above equation assumes large 'r' and that upcrossings of high levels by the "within occurrence" Gaussian random process is a Poisson process. The parameters v_0, d, μ_x and σ_x are defined as follows:

v_0: arrival rate of the Gaussian process peaks with positive slope

d: duration of the ICP pulse; can be a random variable, or a constant mean value

μ_x: mean of the Gaussian random process

σ_x: standard deviation of the Gaussian random process.

The above parameters can depend on a variable "Y", e.g., the seastate significant wave height which has its own probability distribution in the long term, although as written above, the equation for $F_{X_m}(r)$ does not include that possibility.

3. EXTENSION TO NON-STATIONARY PROCESSES

The Poisson approximation may be extended to a non-stationary process using a time dependent upcrossing rate:

$$F_{max}(r) \cong \exp\left[-\int_0^t v(x, \tau)d\tau\right]$$

where $v(x,\tau)$ is the rate of upcrossing corresponding to level x at time τ. For a zero mean Gaussian process, $v(x,\tau)$ is obtainable in close form (A.3).

4. LOAD COINCIDENCE OF TWO PULSE PROCESSES

Consider two independent Poisson pulse processes, $S_1(t)$ and $S_2(t)$. Define, over the time interval (O,T),

$$R(t) = S_1(t) + S_2(t)$$
$$R_1 = \max\left[S_1(t)\right]$$
$$R_2 = \max\left[S_2(t)\right]$$
$$R_{12} = \max\left[S_{12}(t)\right]$$

Note that $S_{12}(t)$ is the coincidence process, representing parts of the combined process where coincidence occurs.

In Ref. A.1 it is shown that since $S_1(t)$ and $S_2(t)$ are independent, and since the coincidence process is a random sampling from a pooled process consisting of $S_1(t)$ and $S_2(t)$, the coincidence pulse process $S_{12}(t)$ is also a Poisson pulse process with mean occurrence rate

$$\lambda_{12} \cong \lambda_1 \lambda_2 \left(\mu_{d_1} + \mu_{d_2}\right) \tag{5}$$

where the λ_i are the individual mean occurrence rates, and μ_{d_i} are the individual mean durations. The validity of this equation has been checked using Monte Carlo simulations by Wen, Ref. A.2 and the equation appears to work well in most engineering situations of interest. It may also be noted that if $\lambda_i \mu_{d_i} = 1$, i.e., when we have Poisson square wave processes that are always "on", the given mean rate equation is exact. Wen has also shown that the mean duration of the coincidence pulses is

$$\mu_{d_{12}} \cong \frac{\mu_{d_1} \mu_{d_2}}{\left(\mu_{d_1} + \mu_{d_2}\right)} \tag{6}$$

With the mean occurrence rate and mean duration defined, the CDF of the maximum of the coincidence process over time (O,T) is given by

$$F_{R_{12}} \cong \exp\left[-\lambda_{12}\, T\left(1 - F_{X_{12}}(r)\right)\right] \tag{7}$$

for large r. Here $F_{X_{12}}(r)$ is the conditional probability that r is not exceeded given the coincidence.

The cumulative distribution function of the maximum value of the combined process $R(t) = S_1(t) + S_2(t)$ over the time interval (O,T) is obtained from

$$F_{R_m}(r) = P(R_m < r) = P[(R_1 < r) \cap (R_2 < r) \cap (R_{12} < r)]$$
$$= P(R_1 < r)\, P(R_2 < r)\, P(R_{12} < r) \tag{8}$$

where $R_m = \max[S_1(t) + S_2(t)]$, and assuming independence of R_1, R_2 and R_{12} processes. Since R_{12} is in reality positively correlated with R_1 and R_2, the equation for $F_{R_m}(r)$ given above overestimates the probability of threshold exceedence, i.e., it is conservative. For large r,

$$F_{R_m}(r) \cong \exp\left\{-T\left[\lambda_1 F_{X_1}^*(r) - \lambda_2 F_{X_2}^*(r) - \lambda_{12} F_{X_{12}}^*(r)\right]\right\} \tag{9}$$

in which $F_X^*(r)$ is the conditional threshold exceedence probability, $1 - F_X(r)$, given occurrence or coincidence. This equation for $F_{R_m}(r)$ follows from the previous equation.

If the two processes are sparse, the CDF of R_m is generally dominated by the first two terms of the equation at low threshold levels and the third at high thresholds. If one of the processes is always "on", e.g., if $\lambda_1 \mu_{d_1} = 1$, S_2 never occurs alone, and coincidence always occurs. In this case,

$$F_{R_m} \cong P(R_1 < r)\, P(R_{12} < r)$$
$$\cong \exp\left[-\lambda_1\, T\, F_{X_1}^*(r) - \lambda_{12}\, T\, F_{X_{12}}^*\right] \tag{10}$$

If for both processes, $\lambda \mu_d = 1$, i.e., both processes are always "on", then

$$F_{R_m}(r) \cong P(R_{12} < r) \cong \exp\left[-\lambda_{12} \, T \, F_{X_{12}}^*(r)\right] \qquad (11)$$

The accuracy of the CDF of R_m as given by the above equations has been verified by Wen using Monte Carlo simulation and other available analytical results. Accuracy is good regardless of the sparsity of the processes, and always on the conservative side. Wen's studies also confirm that neglecting load coincidence can lead to significant errors at high threshold levels.

The above load coincidence analysis considered two Poisson pulse processes. Such analyses have also been developed for linear combinations of intermittent continuous processes, and for linear combinations of pulse and intermittent processes. Further, the load coincidence method has been extended by Wen, Ref. A.1, for the consideration of multiple load and load effect combination, and for load dependencies including clustering within loads and also correlations among loads. Methods for the treatment of within occurrence load nonstationarity have also been developed by Wen. In summary, for an engineering treatment of load combination for extreme loads, the Wen load coincidence method offers perhaps the most comprehensive treatment available.

References

A.1. Wen, Y.K., *Structural Load Modeling and Combination for Performance and Safety Evaluation, Developments in Civil Engineering*, Vol. 31, Elsevier, Amsterdam, 1990.

A.2. Wen, Y.K., "Statistical Combination of Extreme Loads," *J. Structural Division*, ASCE, Vol. 103, No. ST5, May 1977.

A.3. Cramer, H. and Leadbetter, M.R., *Stationary and Related Stochastic Processes*, John Wiley, New York, 1967.
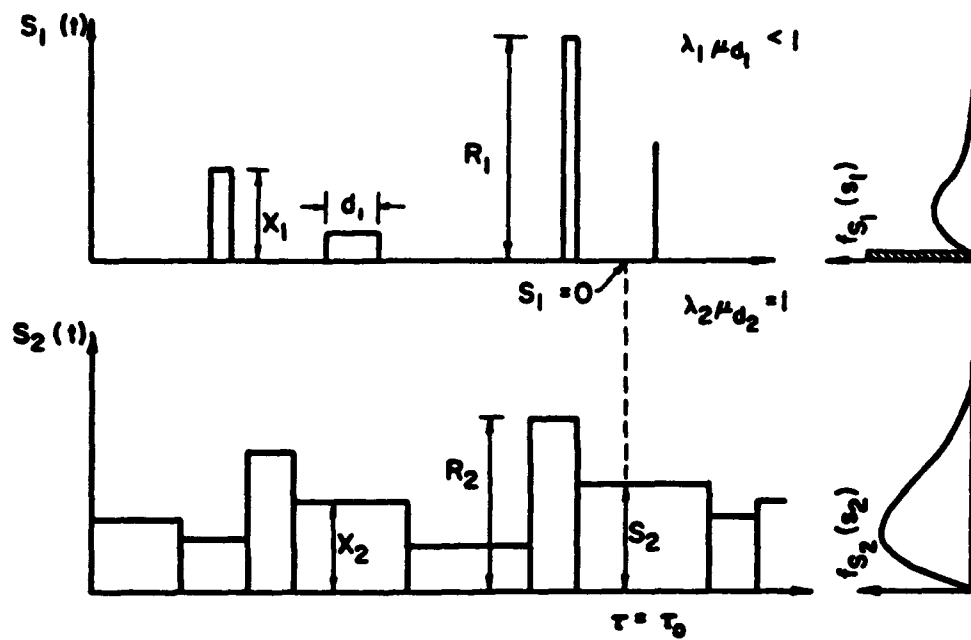
Figure A.1 The Rectangular Poisson Pulse Process

A-8
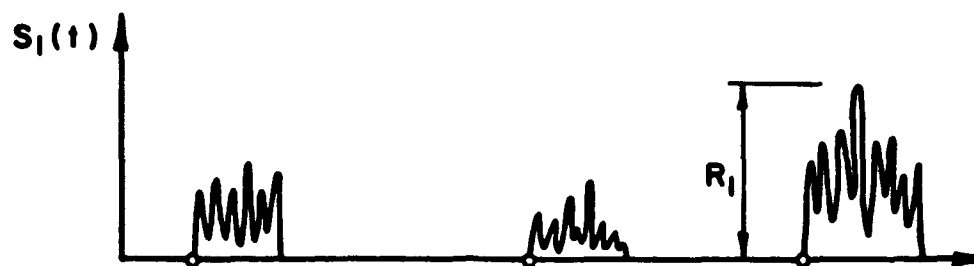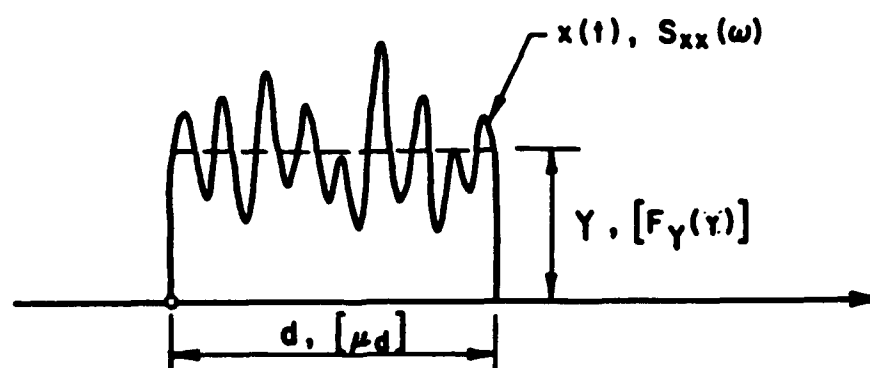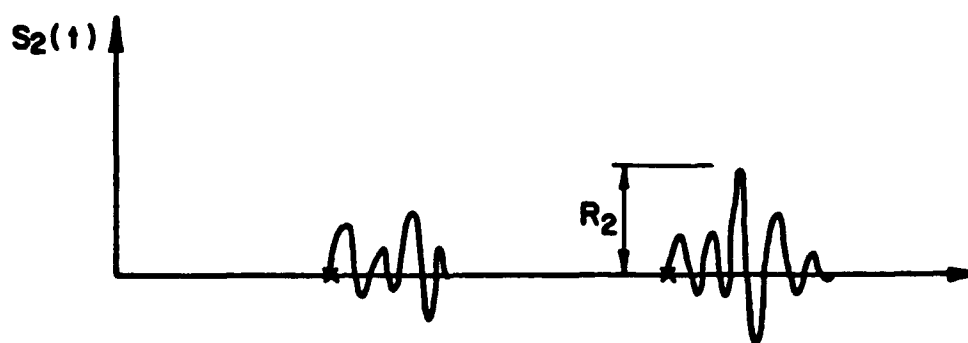
Figure A.2 The Wen Intermittent Continuous Process
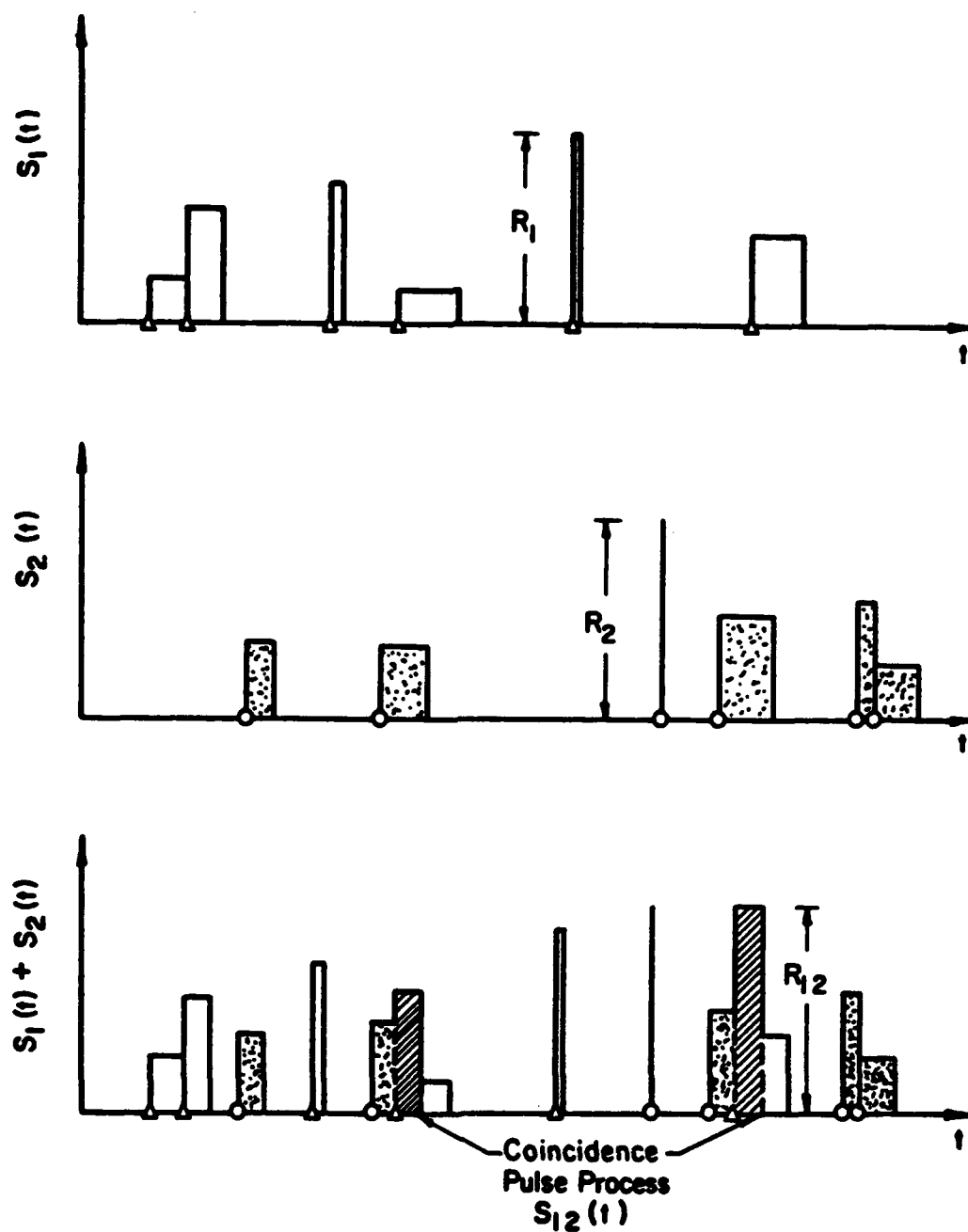
Figure A.3 Load Coincidence for Rectangular Pulse Processes

APPENDIX B

COMBINING SLAMMING AND WAVE INDUCED STRESSES BY THREE PARAMETER WEIBULL FITS

APPENDIX B

COMBINING SLAMMING AND WAVE INDUCED STRESSES
BY THREE PARAMETER WEIBULL FITS

To perform reliability analysis on the basis of service measurements, a three parameter Weibull probability density function may be fitted to the histogram of stress peaks (amplitudes). The histogram may represent

- Combined stresses (slam plus wave)

- Wave induced stress alone

- Slam stress alone

Figure B.1 from Ref. B.1 illustrates the combined stress and the slam and wave induced stresses for a bulk carrier. The following text illustrates fitting the Weibull distribution using the combined stress $X_{S,i}$ as an example. Two cases are considered, with the three parameter Weibull lower limit ξ_0 either *known* or *unknown*.

CASE: Known Lower Limit ξ_0

In this case, the probability density function and distribution function for $X_{S,i}$ is given by

$$f_{X_{S,i}} = \frac{\ell}{k}\left[\frac{x-\xi_0}{k}\right]^{\ell-1} \exp\left[-\left(\frac{x-\xi_0}{k}\right)^{\ell}\right], \quad x > \xi_0$$

$$F_{X_{S,i}}(x) = 1 - \exp\left[-\left(\frac{x-\xi_0}{k}\right)^{\ell}\right], \quad x > \xi_0$$

$$= 0 \qquad\qquad \text{otherwise}$$

From the first two moments of the three parameter Weibull distribution, it is possible to determine the values of ℓ and k. To obtain the first two moments, we may use the fact, derived in text books on statistics, that if the Weibull density were of the form

$$p_{x'}(x') = \ell x'^{k-1} \exp(-x'^{\ell}) , \quad x > 0$$

the r-th moment about zero of the variable x' above is given by

$$\mu_r' = E(x'^r) = \Gamma\left(\frac{r}{\ell}+1\right)$$

Note that moments for the three parameter Weibull density we are interested in may be obtained from the moments for the above single parameter Weibull density by using the transformation $x = \xi_0 + k\, x'$.

The first moment about zero for the three parameter Weibull is then

$$E(x) = \xi_0 + k\, E(x')$$
$$= k\, \Gamma\left(\frac{1}{\ell}+1\right) + \xi_0$$

The second moment about zero is

$$E(x^2) = E(\xi_0 + k\, x')^2$$
$$= \xi_0^2 + k^2\, E(x'^2) + 2\, k\, \xi_0\, E(x')$$
$$= \xi_0^2 + k^2\, \Gamma\left(\frac{2}{\ell}+1\right) + 2\, k\, \xi_0\, \Gamma\left(\frac{1}{\ell}+1\right)$$

The variance is then

$$\sigma^2 = E(x^2) - [E(x)]^2$$
$$= k^2\, \Gamma\left(\frac{2}{\ell}+1\right) - k^2\left[\Gamma\left(\frac{1}{\ell}+1\right)\right]^2$$

which is the same as that for a conventional two parameter Weibull density with $\xi = 0$.

The two different Weibull parameters k and ℓ must be obtained by equating E(x) and E(x²) of it to the corresponding moments for the combined stress histogram and solving

the resulting equations iteratively. The mean and variance may also be equivalently used for the purpose. Note that the conventional two parameter Weibull density ($\xi = 0$) reverts to the Rayleigh if $k = \sqrt{2m_0}$ and $\ell = 2$, and to the exponential density if $k = \lambda$ and $\ell=1$.

CASE: Unknown Lower Limit ξ_0

this more general case, the lower limit ξ_0 must also be estimated. This necessitates a condition where either the $E(x^3)$ or the skewness of the three parameter Weibull density is equated to the corresponding quantity for the combined stress histogram.

The third moment about zero, for the three parameter Weibull density, is given by

$$E(x^3) = E(\xi_0 + kx')^3$$
$$= \xi_0^3 + k^3 E(x'^3) + 3k^2 \xi_0 \, E(x'^2) + 3k\xi_0^2 E(x')$$

where x' is related to x by $x = \xi_0 + kx'$. Substituting for $E(X'')$

$$E(x^3) = \xi_0^3 + k^3 \, \Gamma\!\left(\frac{3}{\ell}+1\right) + 3k^2 \, \xi_0 \, \Gamma\!\left(\frac{2}{\ell}+1\right) + 3k \, \xi_0^2 \, \Gamma\!\left(\frac{1}{\ell}+1\right)$$

To obtain the skewness, the third moment about the mean value is determined:

$$E(x-\mu)^3 = E(x^3) - 3E(x)E(x^2) + 2[E(x)]^3$$

which may be evaluated by substituting for E(x), $E(x^2)$ and $E(x^3)$ from previous expressions. The skewness, which is a measure of symmetry of the distribution about the mean value (skew = 0 is symmetric) is given by

$$\delta = \frac{E(x-\mu)^3}{\sigma^3}$$

B-3

where σ is the standard deviation.

The three conditions obtained by equating the first three moments of the combined stress histogram to those of the three parameter Weibull density may then be solved to obtain the parameters of the Weibull density, namely ξ_0, k and ℓ. An aspect worth noting is that fitting a three parameter Weibull density, while a reasonable choice, is not an exact one. Within this limitation, the approach does lead to simple solutions suitable for rapid computation.

References

B.1 Stiansen, S.G. and Mansour, A.E., "Ship Primary Strength Based on Statistical Data Analysis," *Trans. SNAME*, 1975.
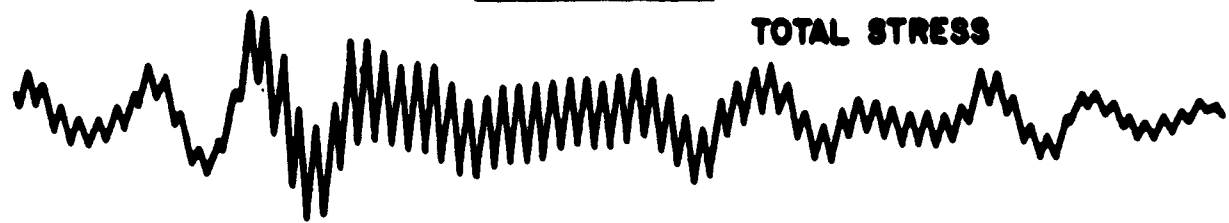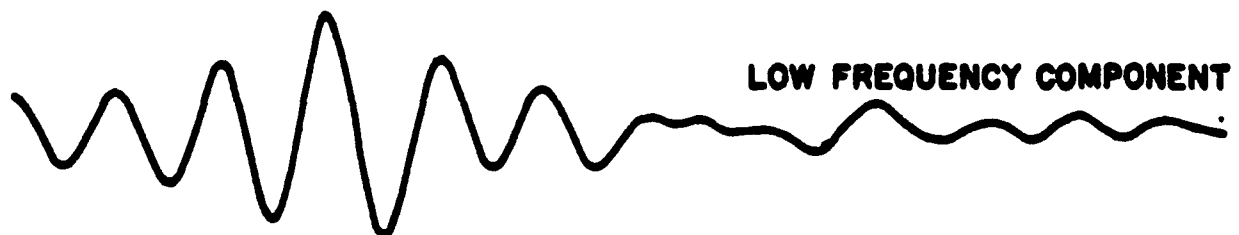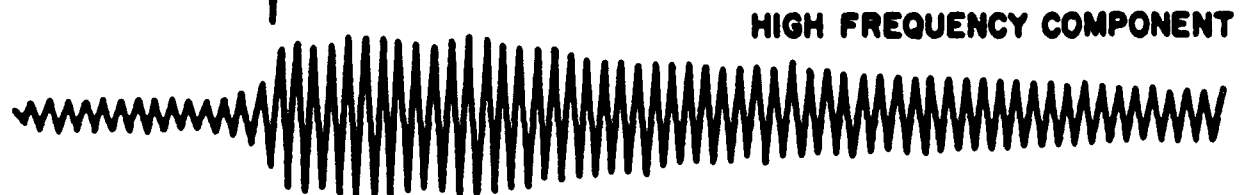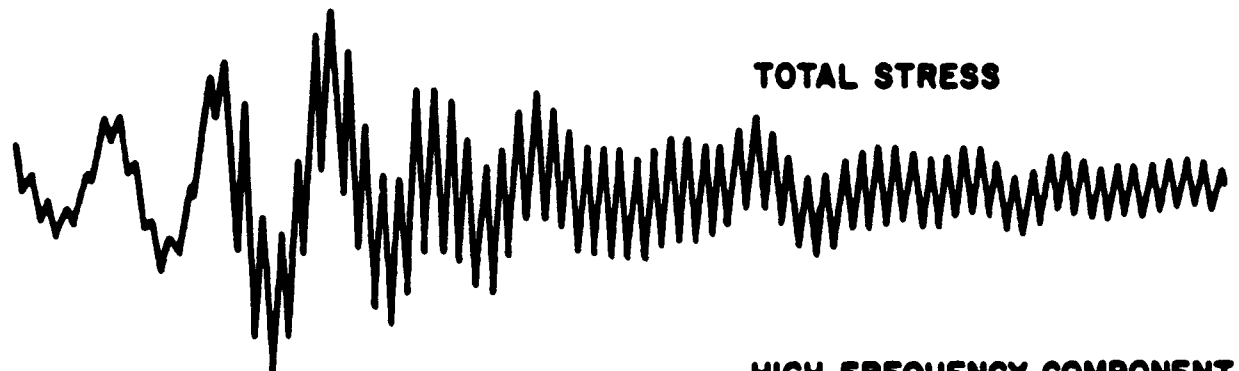
Figure B.1 Slamming Stress History Decomposition

APPENDIX C

SAMPLE OUTPUT FROM THE SCORES SEAKEEPING PROGRAM

THE UNIVERSITY OF MICHIGAN
DEPARTMENT OF NAVAL ARCHITECTURE AND MARINE ENGINEERING

SEAKEEPING PREDICTION PROGRAM (SPP-2.1) BY M.G. PARSONS

REFERENCE: RAFF, A. I., "PROGRAM SCORES - SHIP STRUCTURAL RESPONSE
            IN WAVES", SHIP STRUCTURES COMMITTEE REPORT SSC-230, 1972

RUN IDENTIFICATION:

INPUT VERIFICATION:

  1- WATERLINE LENGTH LWL (M)   =   161.28

  2- VESSEL DISPLACEMENT (TONNES)   =   8835.5

  3- VERTICAL CENTER OF GRAVITY (M)   =   7.10

  4- ROLL RADIUS OF GYRATION (M)   =   6.95

  5- FRACTION OF CRITICAL ROLL DAMPING   =   .1000

  6- SHIP SPEED (KNOTS)   =   20.00

  7- SHIP HEADING RELATIVE TO WAVES (DEG) =   135.00

  8- WATER TYPE   = SALT@15C

  9- ISSC TWO PARAMETER SPECTRUM EXCITATION

 10- SIGNIFICANT WAVE HEIGHT (M)   =   7.32

 11- CHARACTERISTIC WAVE PERIOD (S)   =   10.90

 12- LOWER FREQ.INTEGRATION LIMIT (R/S)   =   .26

 13- UPPER FREQ.INTEGRATION LIMIT (R/S)   =   1.70

STA.	BEAM[M]	AREA[M*M]	DRAFT[M]	WEIGHT[T]
0	.00	.00	.00	300.0
1	4.02	20.26	7.13	375.6
2	7.98	42.53	7.02	775.0
3	11.74	61.82	6.89	926.1
4	15.32	80.08	6.78	1324.4
5	16.73	92.16	6.55	1295.7
6	16.79	89.37	6.42	1320.0
7	16.2○	69.52	6.31	820.1
8	15.23	46.79	6.20	710.0
9	13.96	24.14	6.08	688.6
1○	12.46	7.45	5.96	300.0

THE UNIVERSITY OF MICHIGAN

DEPARTMENT OF NAVAL ARCHITECTURE AND MARINE ENGINEERING

SEAKEEPING PREDICTION PROGRAM (SPP-2.1) BY M.G. PARSONS

REFERENCE: RAFF, A. I., "PROGRAM SCORES - SHIP STRUCTURAL RESPONSE IN WAVES", SHIP STRUCTURES COMMITTEE REPORT SSC-230, 1972

RUN IDENTIFICATION:

MOTION NATURAL FREQUENCIES AND PERIODS:

HEAVE NATURAL FREQUENCY = 1.120 RAD/S   HEAVE NATURAL PERIOD = 5.61 SEC.

PITCH NATURAL FREQUENCY = 1.152 RAD/S   PITCH NATURAL PERIOD = 5.45 SEC.

ROLL NATURAL FREQUENCY = .412 RAD/S   ROLL NATURAL PERIOD = 15.26 SEC.

ROLL WAVE DAMPING   = 0.103E+03

ADDED VISCOUS ROLL DAMPING = 0.398E+04

SEAKEEPING RESPONSE RESULTS:

SHIP SPEED   = 20.0 KNOTS =10.29 M/S
WAVE ANGLE [WITH HEAD SEAS 180 DEG.]   =135.0 DEG.
ISSC TWO PARAMETER SPECTRUM - SIGN.HEIGHT = 7.32 M   CHAR. PERIOD = 10.90 S

NONDIMENSIONAL MOTION RESPONSE:

WAVE FREQ. R/S	ENCOUNT. FREQ. R/S	WAVE LENGTH M	HEAVE AMPL. ND	HEAVE PHASE DEG.	PITCH AMPL. ND	PITCH PHASE DEG.	ROLL AMPL. ND	ROLL PHASE DEG.
.260	.310	911.5	0.100E+01	179.9	0.723E+00	83.4	0.165E+01	-140.3
.340	.426	533.0	0.999E+00	179.9	0.736E+00	78.4	0.427E+01	125.5
.420	.551	349.3	0.995E+00	-179.9	0.747E+00	71.1	0.142E+01	54.2
.500	.685	246.5	0.101E+01	-179.5	0.747E+00	60.3	0.768E+00	37.2
.580	.830	183.2	0.110E+01	178.1	0.723E+00	43.8	0.495E+00	28.1
.660	.983	141.5	0.129E+01	158.9	0.626E+00	15.7	0.322E+00	21.4
.740	1.146	112.5	0.923E+00	109.0	0.349E+00	-20.9	0.186E+00	17.1
.820	1.319	91.6	0.223E+00	59.0	0.143E+00	-47.5	0.833E-01	17.0
.900	1.501	76.1	0.668E-01	-122.1	0.406E-01	-90.8	0.221E-01	43.8
.980	1.692	64.2	0.929E-01	-156.4	0.153E-01	165.3	0.178E-01	134.2
1.060	1.894	54.8	0.506E-01	-177.0	0.132E-01	114.1	0.183E-01	150.9
1.140	2.104	47.4	0.158E-01	153.6	0.602E-02	87.5	0.919E-02	155.9
1.220	2.324	41.4	0.547E-02	74.7	0.122E-02	45.5	0.170E-02	-176.8
1.300	2.554	36.5	0.392E-02	45.9	0.453E-03	-55.3	0.812E-03	-74.2
1.380	2.793	32.4	0.140E-02	48.6	0.367E-03	-19.9	0.239E-03	154.0
1.460	3.041	28.9	0.760E-03	-86.3	0.443E-03	-8.4	0.362E-03	160.4
1.540	3.299	26.0	0.158E-02	-99.3	0.135E-03	-83.1	0.584E-03	-107.1
1.620	3.567	23.5	0.449E-03	-113.2	0.276E-03	-172.5	0.494E-03	-139.9
1.700	3.844	21.3	0.873E-03	92.0	0.111E-03	155.0	0.550E-03	109.6

NONDIMENSIONAL MOMENT RESPONSE FOR RUN:

WAVE FREQ. R/S	ENCOUNT. FREQ. R/S	WAVE LENGTH M	VERTICAL MOMENT AMPL. ND	VERTICAL MOMENT PHASE DEG.	TRANS. MOMENT AMPL. ND	TRANS. MOMENT PHASE DEG.	TORS. MOMENT AMPL. ND	TORS. MOMENT PHASE DEG.
.260	.310	911.5	0.284E-03	7.3	0.115E-03	64.5	0.143E-03	-167.4
.340	.426	533.0	0.128E-02	2.6	0.220E-04	27.0	0.923E-03	119.4
.420	.551	349.3	0.329E-02	-.2	0.722E-03	84.0	0.572E-03	61.8
.500	.685	246.5	0.636E-02	-3.7	0.205E-02	71.1	0.451E-03	49.6
.580	.830	183.2	0.960E-02	-7.4	0.451E-02	64.1	0.324E-03	32.5
.660	.983	141.5	0.113E-01	-4.8	0.754E-02	59.1	0.217E-03	-18.5
.740	1.146	112.5	0.140E-01	5.5	0.987E-02	55.8	0.355E-03	-74.5
.820	1.319	91.6	0.152E-01	9.0	0.111E-01	56.3	0.563E-03	-91.8
.900	1.501	76.1	0.145E-01	8.1	0.103E-01	58.6	0.641E-03	-96.7
.980	1.692	64.2	0.926E-02	-2.3	0.759E-02	62.8	0.508E-03	-93.2
1.060	1.894	54.8	0.211E-02	-37.0	0.358E-02	70.4	0.250E-03	-65.9
1.140	2.104	47.4	0.323E-02	-179.9	0.571E-03	143.8	0.225E-03	5.8
1.220	2.324	41.4	0.363E-02	163.2	0.127E-02	-135.0	0.243E-03	24.9
1.300	2.554	36.5	0.136E-02	168.0	0.629E-03	160.7	0.120E-03	17.5
1.380	2.793	32.4	0.699E-03	-114.0	0.169E-02	103.3	0.565E-04	-19.7
1.460	3.041	28.9	0.619E-03	158.2	0.172E-02	105.0	0.855E-04	-4.2
1.540	3.299	26.0	0.151E-02	104.6	0.778E-03	93.9	0.493E-04	-6.6
1.620	3.567	23.5	0.457E-03	88.2	0.626E-03	5.6	0.996E-04	172.2
1.700	3.844	21.3	0.135E-02	-91.7	0.442E-03	-72.0	0.144E-03	121.6

AMPLITUDE RESPONSE SPECTRA:

FREQ R/S	WAVE AMP. M	HEAVE M	PITCH DEG.	ROLL DEG.	VERT. MOM. T-M	LAT. MOM. T-M	TORS. MOM. T-M
.260	.012	.012	.001	.005	0.188E+03	0.307E+02	0.478E+02
.340	3.654	3.648	.904	30.419	0.119E+07	0.352E+03	0.621E+06
.420	1C.376	10.263	6.148	22.114	0.224E+08	0.108E+07	0.677E+06
.500	9.598	9.757	11.418	12.086	0.773E+08	0.803E+07	0.390E+06
.580	6.500	7.867	13.135	6.159	0.120E+09	0.264E+08	0.136E+06
.660	4.060	6.734	10.321	2.724	0.104E+09	0.460E+08	0.381E+05
.740	2.520	2.146	3.140	.894	0.989E+08	0.489E+08	0.633E+05
.820	1.594	.080	.502	.171	0.737E+08	0.390E+08	0.101E+06
.900	1.035	.005	.038	.011	0.431E+08	0.221E+08	0.848E+05
.980	.691	.006	.005	.007	0.118E+08	0.794E+07	0.355E+05
1.060	.474	.001	.004	.007	0.421E+06	0.121E+07	0.589E+04
1.140	.332	0.000	.001	.002	0.692E+06	0.216E+05	0.337E+04
1.220	.238	0.000	0.000	0.000	0.625E+06	0.770E+05	0.281E+04
1.300	.174	0.000	0.000	0.000	0.648E+05	0.138E+05	0.499E+03
1.380	.130	0.000	0.000	0.000	0.126E+05	0.735E+05	0.828E+02
1.460	.098	0.000	0.000	0.000	0.750E+04	0.578E+05	0.143E+03
1.540	.075	0.000	0.000	0.000	0.344E+05	0.910E+04	0.366E+02
1.620	.059	0.000	0.000	0.000	0.245E+04	0.458E+04	0.116E+03
1.700	.046	0.000	0.000	0.000	0.167E+05	0.179E+04	0.191E+03

RESPONSE AMPLITUDE STATISTICS:

	M	M	DEG.	DEG.	T-M	T-M	T-M
R.M.S.	1.825	0.000	0.000	0.000	0.316E-37	0.316E-37	0.000E+00
AVE.	2.281	.000	.000	.000	0.105E-41	0.501E+04	0.519E+03
SIGNIF.	3.650	3.601	3.821	4.886	0.133E+05	0.802E+04	0.831E+03
AVE1/10	4.654	4.591	4.871	6.229	0.170E+05	0.102E+05	0.106E+04
DESIGN VALUE WITH N=1000 AND ALPHA=0.01					0.319E+05	0.192E+05	0.199E+04

APPENDIX D

USER MANUAL AND LISTING FOR THE CROSS-CORRELATION PROGRAM

USER'S MANUAL FOR CROSS-CORRELATION PROGRAM

MANCOR

(FOR THREE LOAD COMBINATIONS)

PROGRAMS AND MANUAL WRITTEN BY

MICHAEL C. JUE

FOR

DR. ALAA MANSOUR

MANSOUR ENGINEERING, INC.

JULY 20, 1992

D-1

ABSTRACT

.   This program takes data from complex transfer functions of
loads and calculates the coefficients used in a simple load
combination formula.

INTRODUCTION

The MANCOR program calculates root mean square values,
correlation coefficients and correlation factors, as well as the
combined stress. The program takes ship motion data in the
complex form of A + Bi for different wave frequencies and
calculates the necessary coefficients for the simplified formula,

STRESSC = C1*RMS1 + C2*KC2*RMS2 + C3*KC3*RMS3

where STRESSC is the combined stress; C's are conversion factors
which convert rms values to stress units; RMS1, RMS2, RMS3 are
RMS moments (or pressures); and KC2, KC3 are the calculated
correlation factors. Note: STRESS1 = C1 * RMS1. MANCOR was
designed to take any three loads which can be vertical moment,
lateral moment, and torsional moment or pressure data. This
program will only run when it is calculating a load combination
from exactly three individual loads. Additionally, the stress
ratios must be greater than 0.1. (i.e. R2=STRESS2/STRESS1 > 0.1
and R3=STRESS3/STRESS1 > 0.01)

MANCOR must be run once for each heading, speed, and point

on the ship (for pressure data or a ship section for moment data). The program can be run with any three loads, but the conversion factors (C1, C2, C3) must be adjusted to insure consistent units. Background information on the theory used in the computation of the correlation coefficients can be found in Mansour (1981,1990).

INPUT

Four datafiles are required to run MANCOR. One datafile is required for each of the three loads. An additional datafile with sea spectrum data is also required. The user also inputs the conversion factors C1, C2, and C3 at run time.

Each load datafile must be in the following form,

```
VERTICAL BENDING MOMENT
HEADING 45
WAVE
FREQ.       A          B
.20     .48E+03    .42E+04
.25     .16E+04    .10E+05
.30     .43E+04    .19E+05
.35     .97E+04    .32E+05
.40     .19E+05    .47E+05

...
4 lines of text
F10.2,2E10.2
```

The sea spectrum file must be in this format,

```
SEA SPECTRA -- GROUP 5
H1/3 =     14.378      METERS
WAVE        AVE.
FREQ        ORDINATE
0.2         10.6033
0.25         4.6042
0.3         18.0955
0.35        45.8864
0.4         53.6198
...
```

4 lines of text
F10.2, F10.4

Currently, the program is set to accept 34 data points in each file, if there are more or less data points then you must change the statement "PARAMETER (NPTS = 34)" accordingly and then re-compile the program.

The following files are examples which already have the proper format and are for an ABS tanker with 45 degree seas: VERT45A.DAT, HORZ45A.DAT, TORS45A.DAT, PRESS45A.DAT.

RUNNING MANCOR

Once all input files have been prepared compile and run MANCOR. The program will prompt you for the name of each load file, sea spectrum file, and output file. All character strings must be input with single quotes (i.e. 'VERT45A.DAT'). It will also ask you for the values of the conversion coefficients, C1, C2, C3. Input C1, C2, C3 as real numbers only.

OUTPUT

The output file will contain RMS values for each moment or pressure (RMS1, RMS2, RMS3), stress ratios (R2, R3), conversion coefficients (C1, C2, C3), correlation coefficients (RHO12, RHO13, RHO23), correlation factors (KC2, KC3), and the combined stress (STRESSC).

PROGRAMS

Each program is quite simple and can be altered to suit your

needs. A listing of MANCOR is included.

REFERENCES

1.   "An Introduction to Structural Reliability Theory", Mansour, Alaa E., Ship Structures Committee Report No. SSC-351, 1990.

2.   "Combining Extreme Environmental Loads for Reliability-Based Designs", Mansour, Alaa E., Proceedings of the Extreme Loads Response Symposium (SNAME), Arlington, VA, October 1981.

```
*   CALCULATES CROSS-CORRELATION COEFFICIENTS        *


* VARIABLES
***********************
* NPTS = NO. OF DIFFERENT FREQ.
* PROGRAM ORIGINALLY WRITTEN FOR V,H,P LATER ADAPTED FOR
*       ANY DATA.
* *V OR *1: VERTICAL OR FIRST DATA SET
* *H OR *2: HORIZONTAL OR SECOND DATA SET
* *P OR *3: PRESSURE OR THIRD DATA SET

* WVFREQ = WAVE FREQ
* RHOVH = VERT. VS. HORIZ. CROSS-CORRELATION COEFF.
* A*,B* :  A + B i
* STEP = FREQ INCREMENT
* INTGRAND = FUNCTION TO BE INTEGRATED
* SEASPEC = SEA SPECTRUM DATA
* NPTS = NUMBER OF DATA
* RMS* = ROOT MEAN SQUARE
* STRESSC = COMBINED RMS STRESS
* C1,2,3 = CONVERSION COEFFICIENTS
* KC2,3 = CORRELATION COEFF IN SIMPLIFIED FORMULA
* R2,3 = RATION VARIANCE/VARIANCE1
* FILE* = DATA FILES FOR FORCES
* SEAFILE = SEA SPECTRUM FILE
* OUTFILE = OUTPUT FILE
***********************
      PROGRAM MANCOR

      INTEGER NPTS, ERRCOD
      PARAMETER ( NPTS = 34 )

      REAL WVFREQ(NPTS), STEP

      REAL INTGRAND(NPTS)

      REAL AV(NPTS),BV(NPTS)
      REAL AH(NPTS),BH(NPTS)
      REAL AP(NPTS),BP(NPTS)

      REAL RHOVH, RHOVP, RHOHP
      REAL SEASPEC(NPTS)
      REAL RMSV, RMSH, RMSP
      REAL R2, R3
      REAL C1, C2, C3
      REAL KC2, KC3
      REAL STRESS1, STRESS2, STRESS3, STRESSC
      INTEGER QUIT

      CHARACTER*15 FILE1, FILE2, FILE3, SEAFILE, OUTFILE
      CHARACTER*80 COMMENT
*   FUNCTIONS
      REAL RHO
      EXTERNAL RHO

      REAL RMS
      EXTERNAL RMS

      PRINT*,'THREE LOAD COMBINED STRESS PROGRAM'
```

```
*    CALCULATES CROSS-CORRELATION COEFFICIENTS          *


* VARIABLES
************************
* NPTS = NO. OF DIFFERENT FREQ.
* PROGRAM ORIGINALLY WRITTEN FOR V,H,P LATER ADAPTED FOR
*       ANY DATA.
* *V OR *1: VERTICAL OR FIRST DATA SET
* *H OR *2: HORIZONTAL OR SECOND DATA SET
* *P OR *3: PRESSURE OR THIRD DATA SET

* WVFREQ = WAVE FREQ
* RHOVH = VERT. VS. HORIZ. CROSS-CORRELATION COEFF.
* A*,B* :  A + B i
* STEP = FREQ INCREMENT
* INTGRAND = FUNCTION TO BE INTEGRATED
* SEASPEC = SEA SPECTRUM DATA
* NPTS = NUMBER OF DATA
* RMS* = ROOT MEAN SQUARE
* STRESSC = COMBINED RMS STRESS
* C1,2,3 = CONVERSION COEFFICIENTS
* KC2,3 = CORRELATION COEFF IN SIMPLIFIED FORMULA
* R2,3 = RATION VARIANCE/VARIANCE1
* FILE* = DATA FILES FOR FORCES
* SEAFILE = SEA SPECTRUM FILE
* OUTFILE = OUTPUT FILE
************************
      PROGRAM CALOCOR

      INTEGER NPTS, ERRCOD
      PARAMETER ( NPTS = 34 )

      REAL WVFREQ(NPTS), STEP

      REAL INTGRAND(NPTS)

      REAL AV(NPTS),BV(NPTS)
      REAL AH(NPTS),BH(NPTS)
      REAL AP(NPTS),BP(NPTS)

      REAL RHOVH, RHOVP, RHOHP
      REAL SEASPEC(NPTS)
      REAL RMSV, RMSH, RMSP
      REAL R2, R3
      REAL C1, C2, C3
      REAL KC2, KC3
      REAL STRESS1, STRESS2, STRESS3, STRESSC
      INTEGER QUIT

      CHARACTER*15 FILE1, FILE2, FILE3, SEAFILE, OUTFILE
      CHARACTER*80 COMMENT
*  FUNCTIONS
      REAL RHO
      EXTERNAL RHO

      REAL RMS
      EXTERNAL RMS

      PRINT*,'THREE LOAD COMBINED STRESS PROGRAM'
```

```fortran
      PRINT*,'        WRITTEN BY'
      PRINT*,'        MICHAEL JUE'
      PRINT*,' '
      PRINT*,' '
      PRINT*,'        JUNE 22, 1992'
      PRINT*,' '
      PRINT*,'ARE FORCE OR MOMENT DATA FILES IN THE CORRECT FORMAT?'
      PRINT*,'4 HEADER LINES (A80)'
      PRINT*,'WAVE FREQ.,REAL PART, IMAGINARY PART'
      PRINT*,' F10.2, E10.2, E10.2'
      PRINT*,'PRESS 1 TO CONTINUE 0 TO STOP.'

      READ*, QUIT
      IF (QUIT .EQ. 0) STOP

      PRINT*,'ENTER CHARACTER STRINGS WITH QUOTES'
      PRINT*,'(i.e. ''VERT45A.DAT'')'
      PRINT*, 'NAME OF FIRST DATAFILE:  '
      READ *, FILE1
      PRINT*, 'NAME OF SECOND DATAFILE:  '
      READ *, FILE2
      PRINT*, 'NAME OF THIRD DATAFILE:  '
      READ *, FILE3
      PRINT*,'NAME OF SEA SPECTRUM FILE:  '
      READ*, SEAFILE
      PRINT*, 'NAME OF OUTPUT FILE:  '
      READ *, OUTFILE
      PRINT*, 'COMMENT LINE:  '
      READ *, COMMENT
      PRINT*,'ENTER CONVERSION COEFFICIENTS C1, C2, C3.'
      PRINT*, 'ENTER A VALUE FOR C1: '
      READ*, C1
      PRINT*, 'ENTER A VALUE FOR C2: '
      READ*, C2
      PRINT*, 'ENTER A VALUE FOR C3: '
      READ*, C3
C     FILE1 = 'VERT45A.DAT'
C     FILE2 = 'HORZ45A.DAT'
C     FILE3 = 'TORS45A.DAT'
C     SEAFILE = 'SEASPEC.DAT'
C     COMMENT = '45 DEG'
C     C1 = 1.
C     C2 = 1.
C     C3 = 1.

      OPEN(6,FILE=OUTFILE,FORM='FORMATTED',STATUS='NEW',
     c      IOSTAT=ERRCOD,ERR=1000)


*   GET DATA                *
      CALL GETSEA(NPTS, SEAFILE, SEASPEC, WVFREQ)

* GET PRESSURE FIRST BECAUSE FREQ IS ENCOUNTER FREQ. NOT WAVE FREQ
      CALL GETRAO(NPTS, FILE3, AP, BP,STEP, WVFREQ)
      CALL GETRAO(NPTS, FILE1, AV, BV, STEP, WVFREQ)
      CALL GETRAO(NPTS, FILE2, AH, BH, STEP, WVFREQ)

*   CALCULATE RMS AND R'S
      RMSV = RMS(NPTS,AV, BV, SEASPEC, STEP,INTGRAND)
      RMSH = RMS(NPTS,AH, BH, SEASPEC, STEP,INTGRAND)
```

```
        RMSP = RMS(NPTS,AP, BP, SEASPEC, STEP,INTGRAND)


*   CALCULATE CROSS COEFF                              *
        RHOVH = RHO(NPTS,RMSV,RMSH,AV,BV,AH,BH,SEASPEC,
     cSTEP,INTGRAND)
        RHOVP = RHO(NPTS,RMSV,RMSP,AV,BV,AP,BP,SEASPEC,
     cSTEP,INTGRAND)
        RHOHP = RHO(NPTS,RMSH,RMSP,AH,BH,AP,BP,SEASPEC,
     cSTEP,INTGRAND)


* CALCULATE KC'S
        STRESS1 = C1 * RMSV
        STRESS2 = C2 * RMSH
        STRESS3 = C3 * RMSP

        R2 = STRESS2/STRESS1
        R3 = STRESS3/STRESS1

        CALL CALCKC(R2, R3, RHOVH, RHOVP, RHOHP, KC2, KC3)

**********
* CALCULATE COMBINED STRESS USING
*   STRESSC = STRESS1 + KC2*STRESS2 + KC3*STRESS3
**********
        STRESSC = STRESS1 + KC2*STRESS2 + KC3*STRESS3

* WRITE TO OUTPUT FILE
        WRITE(6,'(3A15)') 'FILE1','FILE2','FILE3'
        WRITE(6,'(3A15)') FILE1, FILE2, FILE3
        WRITE(6,'(A80)') COMMENT
        WRITE(6,'(3A15)') 'C1','C2','C3'
        WRITE(6,'(3E15.4)') C1, C2, C3
        WRITE(6,'(3A15)') 'RMS1','RMS2','RMS3'
        WRITE(6,'(3E15.4)') RMSV,RMSH,RMSP
        WRITE(6,'(3A15)') 'STRESS1','STRESS2','STRESS3'
        WRITE(6,'(3E15.4)') STRESS1, STRESS2, STRESS3
        WRITE(6,'(3A15)')'RHO12','RHO13','RHO23'
        WRITE(6,'(3E15.4)') RHOVH,RHOVP,RHOHP
        WRITE(6,'(2A15)') 'R2','R3'
        WRITE(6,'(3E15.4)') R2,R3
        WRITE(6,'(2A15)') 'KC2','KC3'
        WRITE(6,'(2E15.4)') KC2,KC3
        WRITE(6,*) ' '
        WRITE(6,'(A50)') 'STRESSC = STRESS1 + KC2*STRESS2 + KC3*STRESS3'
        WRITE(6,'(A15,E15.4)') 'COMBINED STRESS',STRESSC

        CLOSE (6)

        PRINT*,'NORMAL TERMINATION'
        STOP
1000    PRINT*,'PROBLEM OPENING NEW FILE '//OUTFILE//'!!'
        STOP
        END


*********************************************************
*                    FUNCTIONS                          *
*********************************************************
```

```fortran
            REAL FUNCTION RHO(NPTS,RMS1,RMS2,A1,B1,A2,B2,
     cSEASPEC,STEP,INTGRAND)
**********
*  INTGRAND = FUNCTION TO BE INTEGRATED
*  INTEGRAL = INTEGRATED FUNCTION
*  RMS = ROOT MEAN SQUARE
********
            INTEGER I, NPTS
            REAL A1(NPTS), B1(NPTS), A2(NPTS), B2(NPTS)
            REAL SEASPEC(NPTS)
            REAL INTGRAND(NPTS)
            REAL STEP,RMS1,RMS2

            REAL SIN
            INTRINSIC SIN

            REAL COS
            INTRINSIC COS

            REAL INTGRATE

            INTGRATE = 0.

*   DO INTEGRAL PART
***   INTEGRAND = (A1 + i B1)*(A2 - i B2) * SEASPEC   ***
***              = (A1A2 + B1B2)SEASPEC + IMAGINARY PART
***   TAKE ONLY REAL PART

            DO 10 I = 1, NPTS
             INTGRAND(I) = (A1(I)*A2(I) + B1(I)*B2(I)) * SEASPEC(I)
10          CONTINUE

*   TRAPEZOIDAL RULE INTEGRATION
            DO 40 I= 1, NPTS-1
               INTGRATE = INTGRATE + (INTGRAND(I)+INTGRAND(I+1))/2 * STEP
40          CONTINUE

*   CALCULATE RHO
            RHO = INTGRATE/RMS1/RMS2

            RETURN
            END

*************************
*   ROOT MEAN SQUARE FUNCTION
*************************
            REAL FUNCTION RMS(NPTS,A, B, SEASPEC, STEP,INTGRAND)

            INTEGER I, NPTS
            REAL A(NPTS), B(NPTS), SEASPEC(NPTS), STEP
            REAL INTGRAND(NPTS)

            REAL SQRT
            INTRINSIC SQRT
            REAL INTGRATE

            INTGRATE = 0.

            DO 20 I = 1,NPTS
                INTGRAND(I)= (A(I)*A(I) + B(I)*B(I)) * SEASPEC(I)
```

```
20        CONTINUE

*  TRAPEZOIDAL RULE INTEGRATION
          DO 40 I= 1, NPTS-1
              INTGRATE = INTGRATE + (INTGRAND(I)+INTGRAND(I+1))/2 * STEP
40        CONTINUE

          RMS = SQRT(INTGRATE)

          RETURN
          END
**********************************************************
*                    SUBROUTINES                        *
**********************************************************

* GETS DATA
* SET UP TO READ 4 LINES OF TEXT BEFORE DATA
*
          SUBROU:     GETRAO(NPTS, INFILE, A, B,FREQSTEP,WVFREQ)

          INTEGER NPTS, I, ERRCOD
          REAL A(NPTS), B(NPTS), WVFREQ(NPTS)
          REAL FREQSTEP
          CHARACTER*80 TITLE
          CHARACTER*15 INFILE

          PRINT*,'OPENING INFILE '//INFILE

          OPEN(5,FILE=INFILE, FORM='FORMATTED', STATUS='OLD',
     +        IOSTAT=ERRCOD, ERR=2000)

* READ 4 LINE TEXT HEADER
          DO 10 I = 1,4
C             PRINT*,'READING HEADER'
              READ(5,'(A80)') TITLE
10        CONTINUE

* READ DATA
          DO 20 I = 1,NPTS
                  READ(5,1000) WVFREQ(I),A(I),B(I)
20        CONTINUE

* FREQSTEP TO BE USED LATER IN NUMERICAL INTEGRATION
          FREQSTEP = WVFREQ(2) - WVFREQ(1)

C1000     FORMAT (F10.2, E10.3, F10.1)
1000      FORMAT (F10.2, E10.2, E10.2)
          CLOSE (5)
          RETURN

2000      PRINT *, 'PROBLEM OPENING '//INFILE
          STOP
          END


******************************************
          SUBROUTINE GETSEA(NPTS, INFILE, SEASPEC, WVFREQ)

          INTEGER NPTS, I, ERRCOD
          REAL WVFREQ(NPTS), SEASPEC(NPTS)
          CHARACTER*80 TITLE
```

```fortran
        CHARACTER*15 INFILE

        PRINT*,'OPENING INFILE '//INFILE

        OPEN(5,FILE=INFILE, FORM='FORMATTED', STATUS='OLD',
     +    IOSTAT=ERRCOD, ERR=2000)

* READ 4 LINE TEXT HEADER
        DO 10 I = 1,4
C          PRINT*,'READING HEADER'
           READ(5,'(A80)') TITLE
10      CONTINUE

* READ DATA
        DO 20 I = 1,NPTS
                READ(5,1000) WVFREQ(I),SEASPEC(I)
20      CONTINUE

1000    FORMAT (F10.2, F10.4)

        CLOSE (5)
        RETURN

2000    PRINT *, 'PROBLEM OPENING '//INFILE
        STOP
        END


*********************************************
c*  THIS SUBROUTINE CALCULATES A COMBINED    *
c*   STRESS VALUE FROM THREE STRESSES        *
*********************************************
*   SIGMAC=A1*SIGMA1 + A2*KC2*SIGMA2 +       *
*                  + A3*KC3*SIGMA3           *
*   VARIABLES:
*       A1,A2,A3 = CONVERSION COEFFICIENTS
*       KC2, KC3 = CORRELATION COEFF.
*       R2 = SIGMA2/SIGMA1
*       R3 = SIGMA3/SIGMA1
*       RHO = CROSS CORRELATION COEFF.
*******************************************
*************************************************************

        SUBROUTINE CALCKC(R2,R3,RHO12,RHO13,RHO23, KC2,KC3)

        REAL KC2, KC3, R2, R3
        REAL RHO12, RHO13, RHO23
        REAL SIGMAC2, SIGMAC3
        REAL SQRT
        INTRINSIC SQRT

        SIGMAC2 = SQRT(1.0 + (1./R2)**2 + (R3/R2)**2
     c         + 2.0*RHO12/R2 + 2.0*RHO13*R3/(R2**2)
     c         + 2.0*RHO23*R3/R2)

        SIGMAC3 = SQRT(1.0 + (1./R3)**2 + (R2/R3)**2
     c         + 2.0*RHO12*R2/(R3**2) + 2.0*RHO13/R3
     c         + 2.0*RHO23*R2/R3)

        KC2 = (SIGMAC2 + 1.0 - (R3+1.)/R2)/2.0
        KC3 = (SIGMAC3 + 1.0 - (R2+1.)/R3)/2.0
```

```
RETURN
END
```

****

VERTICAL BENDING MOMENT
HEADING 45
WAVE

FREQ.	A	B
.20	.48E+03	.42E+04
.25	.16E+04	.10E+05
.30	.43E+04	.19E+05
.35	.97E+04	.32E+05
.40	.19E+05	.47E+05
.45	.31E+05	.61E+05
.50	.47E+05	.72E+05
.55	.62E+05	.74E+05
.60	.73E+05	.65E+05
.65	.76E+05	.45E+05
.70	.66E+05	.17E+05
.75	.44E+05	-.10E+05
.80	.15E+05	-.28E+05
.85	-.93E+04	-.31E+05
.90	-.20E+05	-.19E+05
.95	-.13E+05	-.15E+04
1.00	.34E+04	.86E+04
1.05	.13E+05	.56E+04
1.10	.72E+04	-.43E+04
1.15	-.59E+04	-.83E+04
1.20	-.93E+04	-.19E+04
1.25	.45E+03	.47E+04
1.30	.73E+04	.19E+04
1.35	.13E+04	-.29E+04
1.40	-.43E+04	.68E+03
1.45	.78E+03	.42E+04
1.50	.28E+04	-.15E+04
1.55	-.27E+04	-.34E+04
1.60	.94E+03	.34E+04
1.65	.53E+04	.20E+04
1.70	-.50E+04	-.28E+04
1.75	-.35E+04	.88E+03
1.80	.74E+04	-.11E+04
1.85	-.28E+04	-.57E+02

HORIZONTAL BENDING MOMENT
HEADING 45

WAVE FREQ	A	B
.20	.67E+03	-.25E+03
.25	.16E+04	-.64E+03
.30	.36E+04	-.14E+04
.35	.75E+04	-.25E+04
.40	.14E+05	-.39E+04
.45	.24E+05	-.54E+04
.50	.36E+05	-.65E+04
.55	.48E+05	-.64E+04
.60	.54E+05	-.47E+04
.65	.51E+05	-.21E+04
.70	.38E+05	-.19E+03
.75	.17E+05	.18E+03
.80	-.38E+04	-.10E+04
.85	-.13E+05	-.34E+04
.90	-.90E+04	-.40E+04
.95	.31E+04	-.24E+04
1.00	.13E+05	.13E+04
1.05	.96E+04	.46E+04
1.10	-.25E+04	.91E+03
1.15	-.84E+04	-.47E+04
1.20	-.22E+04	-.36E+04
1.25	.58E+04	.31E+04
1.30	.43E+04	.45E+04
1.35	-.31E+04	-.15E+04
1.40	-.45E+04	-.31E+04
1.45	.10E+04	.23E+04
1.50	.27E+04	.18E+04
1.55	-.12E+04	-.31E+04
1.60	-.82E+03	.12E+04
1.65	.15E+04	.44E+04
1.70	-.30E+04	-.41E+04
1.75	-.39E+03	-.36E+04
1.80	.65E+04	.50E+04
1.85	-.44E+04	.13E+04

PRESSURE DATA
HEADING 45
WAVE

FREQ	A	B
.19	.87E+00	-.91E-01
.23	.15E+01	-.17E+00
.27	.24E+01	-.27E+00
.31	.37E+01	-.38E+00
.34	.53E+01	-.50E+00
.38	.74E+01	-.71E+00
.41	.98E+01	-.11E+01
.44	.12E+02	-.20E+01
.47	.15E+02	-.36E+01
.50	.18E+02	-.59E+01
.52	.20E+02	-.91E+01
.55	.20E+02	-.13E+02
.57	.17E+02	-.17E+02
.59	.10E+02	-.23E+02
.61	.10E+01	-.30E+02
.62	-.57E+01	-.36E+02
.64	-.10E+02	-.32E+02
.65	-.21E+02	-.23E+02
.66	-.30E+02	-.17E+02
.67	-.34E+02	-.11E+02
.68	-.35E+02	-.73E+00
.68	-.35E+02	.12E+02
.69	-.32E+02	.25E+02
.69	-.23E+02	.36E+02
.69	-.72E+01	.42E+02
.69	.11E+02	.44E+02
.68	.28E+02	.38E+02
.68	.42E+02	.23E+02
.67	.51E+02	.27E+01
.66	.49E+02	-.20E+02
.65	.34E+02	-.42E+02
.64	.94E+01	-.56E+02
.62	-.19E+02	-.56E+02
.61	-.46E+02	-.39E+02

TORSIONAL BENDING MOMENT
HEADING 45
WAVE

FREQ	A	B
.20	.89E+02	-.57E+03
.25	.20E+03	-.13E+04
.30	.42E+03	-.26E+04
.35	.81E+03	-.46E+04
.40	.14E+04	-.71E+04
.45	.23E+04	-.10E+05
.50	.33E+04	-.13E+05
.55	.41E+04	-.16E+05
.60	.42E+04	-.18E+05
.65	.31E+04	-.18E+05
.70	.63E+03	-.16E+05
.75	-.26E+04	-.12E+05
.80	-.51E+04	-.68E+04
.85	-.55E+04	-.23E+04
.90	-.38E+04	.57E+03
.95	-.16E+04	.75E+03
1.00	.91E+02	-.18E+04
1.05	.15E+04	-.36E+04
1.10	.71E+03	-.22E+04
1.15	-.13E+04	.50E+02
1.20	-.16E+04	.80E+03
1.25	.15E+03	.16E+03
1.30	.15E+04	-.25E+03
1.35	.62E+03	.15E+03
1.40	-.70E+03	.42E+03
1.45	-.24E+03	.10E+03
1.50	.92E+03	-.49E+02
1.55	.38E+03	.19E+03
1.60	-.70E+03	.14E+03
1.65	-.45E+02	-.24E+03
1.70	.68E+03	-.12E+03
1.75	-.19E+03	.42E+03
1.80	-.23E+03	-.26E+02
1.85	.18E+03	-.51E+03

```
        FILE1            FILE2              FILE3
VERT45A.DAT     HORZ45A.DAT     PRESS45A.DAT
45 DEG, NOTE C3
            C1               C2                C3
    .1000E+01        .1000E+01         .1000E+04
          RMS1             RMS2              RMS3
    .2078E+06        .8806E+05         .5211E+02
       STRESS1          STRESS2           STRESS3
    .2078E+06        .8806E+05         .5211E+05
         RHO12            RHO13             RHO23
    .4277E+00        .2724E+00         .5161E+00
            R2               R3
    .4237E+00        .2507E+00
           KC2              KC3
    .6296E+00        .3741E+00


    STRESSC = STRESS1 + KC2*STRESS2 + KC3*STRESS3
COMBINED STRESS        .2828E+06
```

APPENDIX E

THE MANSOUR K CHARTS

KC3 VS RHO12
R2=.4,R3=.1,RHO23=.3

KC3 (vertical axis): 0.3, 0.2, 0.1, 0, -0.1, -0.2, -0.3, -0.4, -0.5

RHO12 (horizontal axis): 0.2, 0.3, 0.4, 0.5, 0.6

Legend: ∎ RHO13=.5 + RHO13=.6 ∗ RHO13=.7 ⊟ RHO13=.8
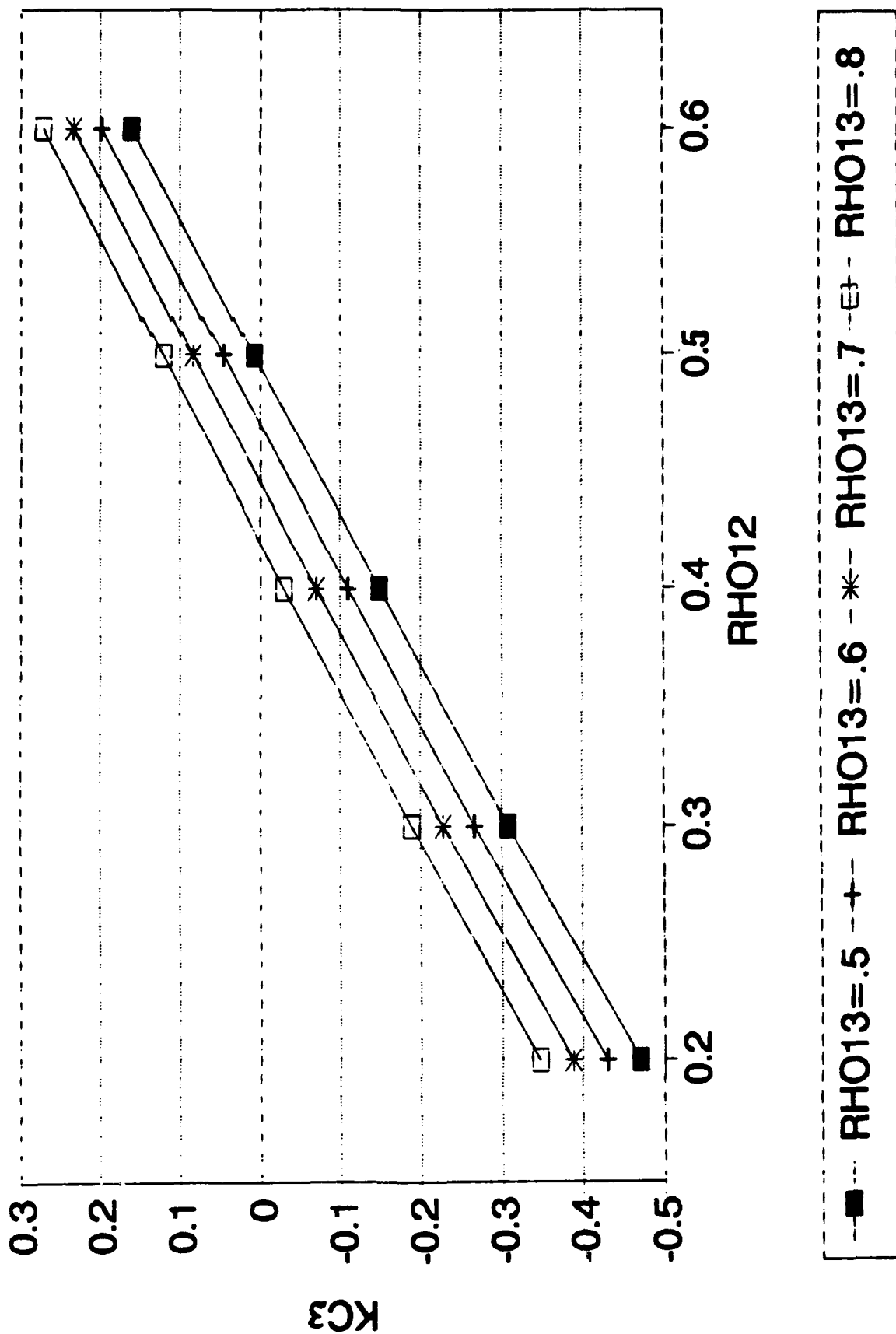
KC3 VS RHO12

R2=.4,R3=.3,RHO23=.3

Legend: -■- RHO13=.5 -+- RHO13=.6 -*- RHO13=.7 -□- RHO13=.8

X-axis: RHO12
Y-axis: KC3
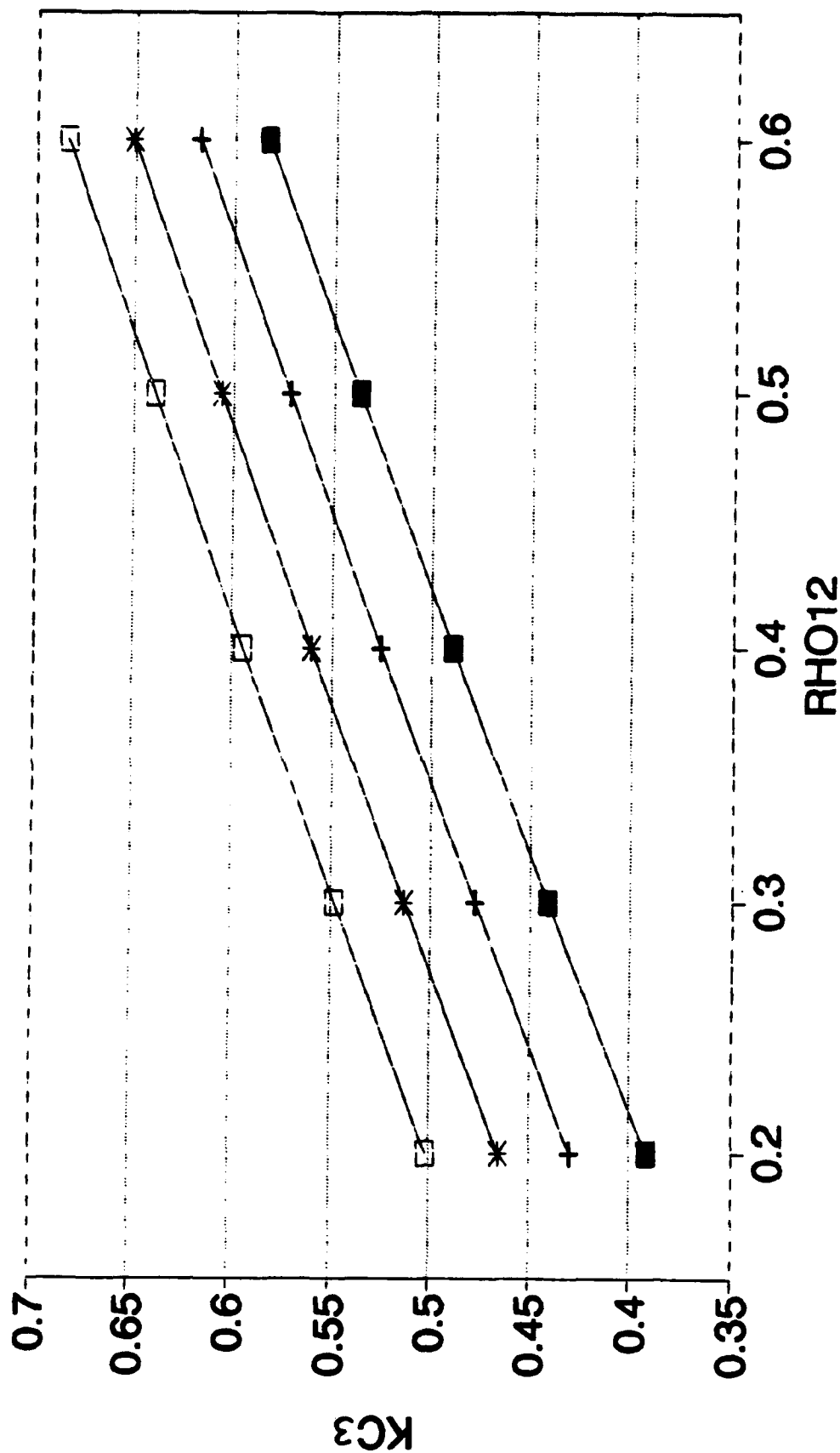
KC2 VS RHO12
R2=.4,R3=.5,RHO23=.3
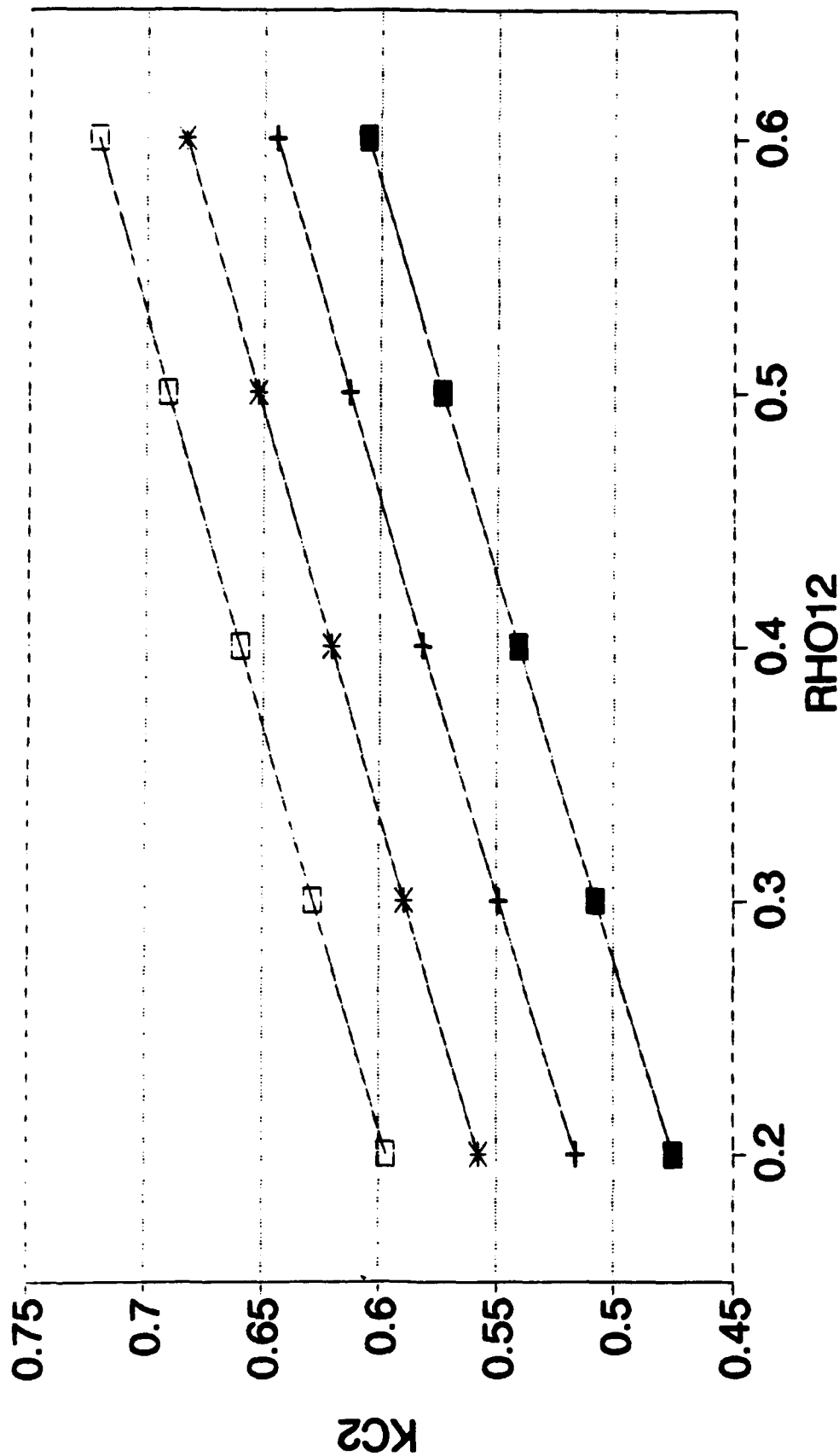
Legend: RHO13=.5, RHO13=.6, RHO13=.7, RHO13=.8

KC3 VS RHO12

R2=.4,R3=.5,RHO23=.3

KC3

RHO12

- ∎ - RHO13=.5 -+- RHO13=.6 - * - RHO13=.7 - ⊞ - RHO13=.8

E-4
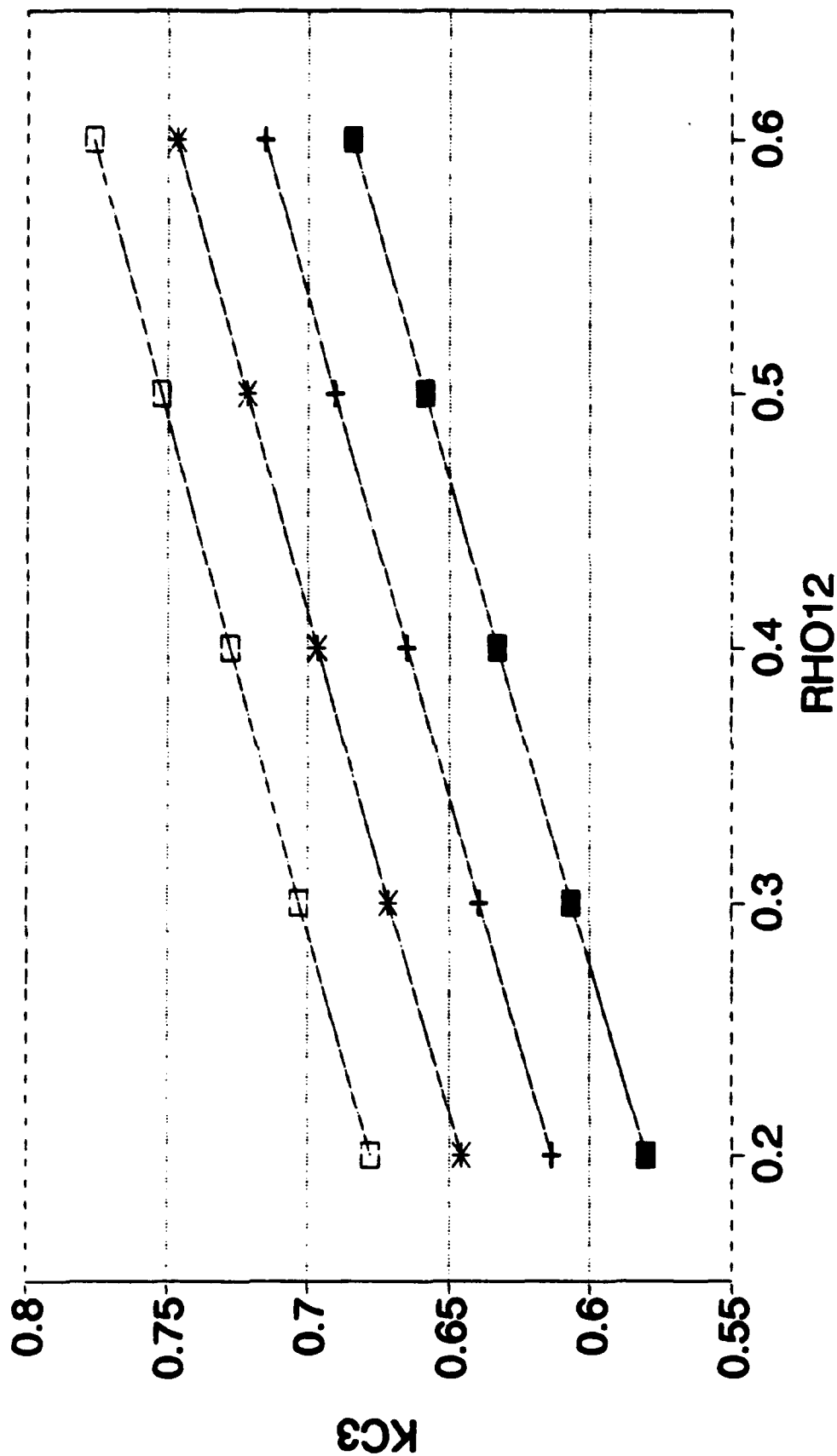
KC2 VS RHO12
R2=.6,R3=.1,RHO23=.3
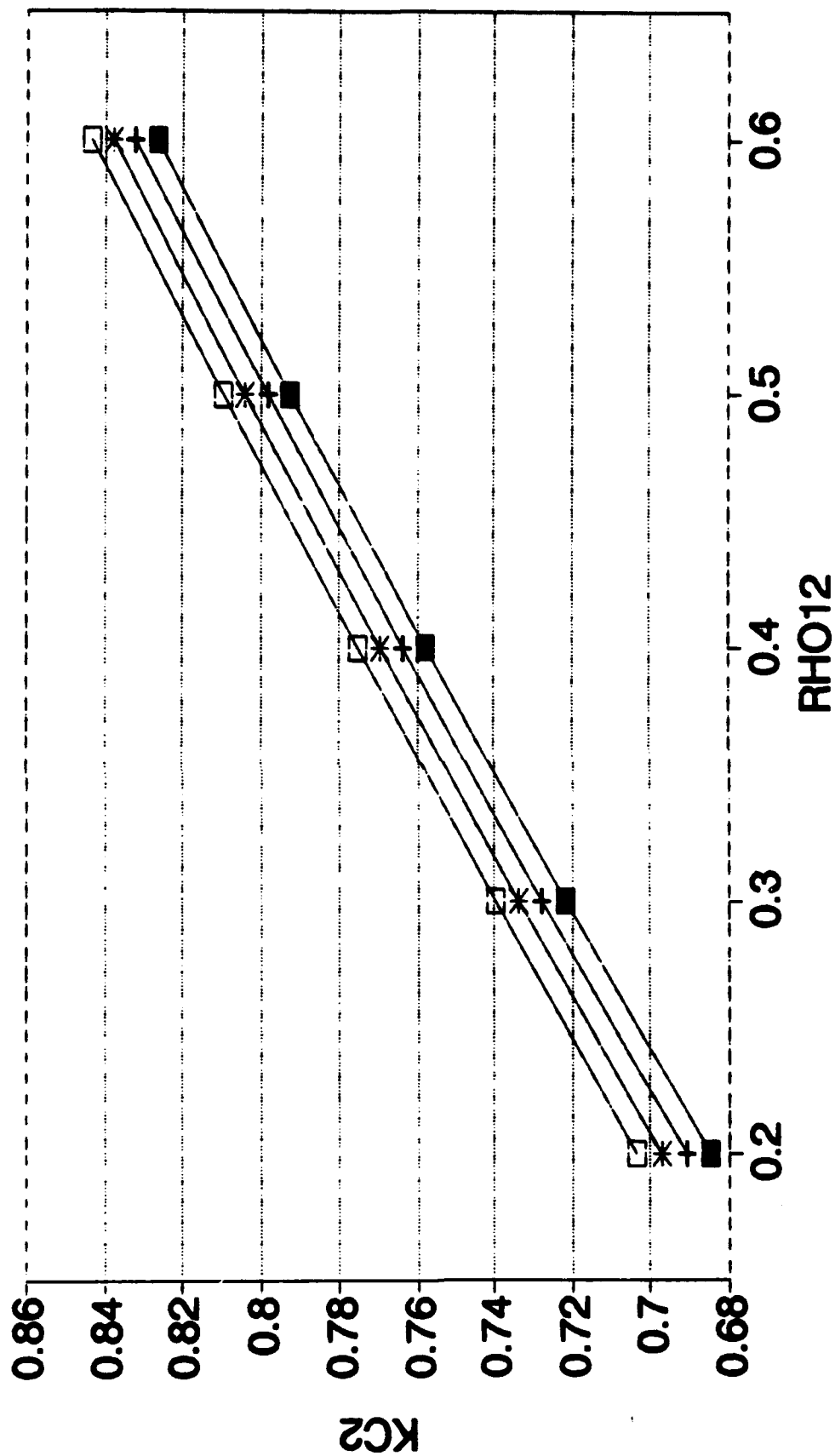
RHO13=.5 ─ + ─ RHO13=.6 ─ * ─ RHO13=.7 ─ E+ ─ RHO13=.8

RHO12

KC2

E-5

KC3 VS RHO12

R2=.6,R3=.1,RHO23=.3

Chart with x-axis labeled "RHO12" ranging from 0.2 to 0.6, and y-axis labeled "KC3" ranging from -0.9 to 0.1.

Legend:
- RHO13=.5
- RHO13=.6
- RHO13=.7
- RHO13=.8
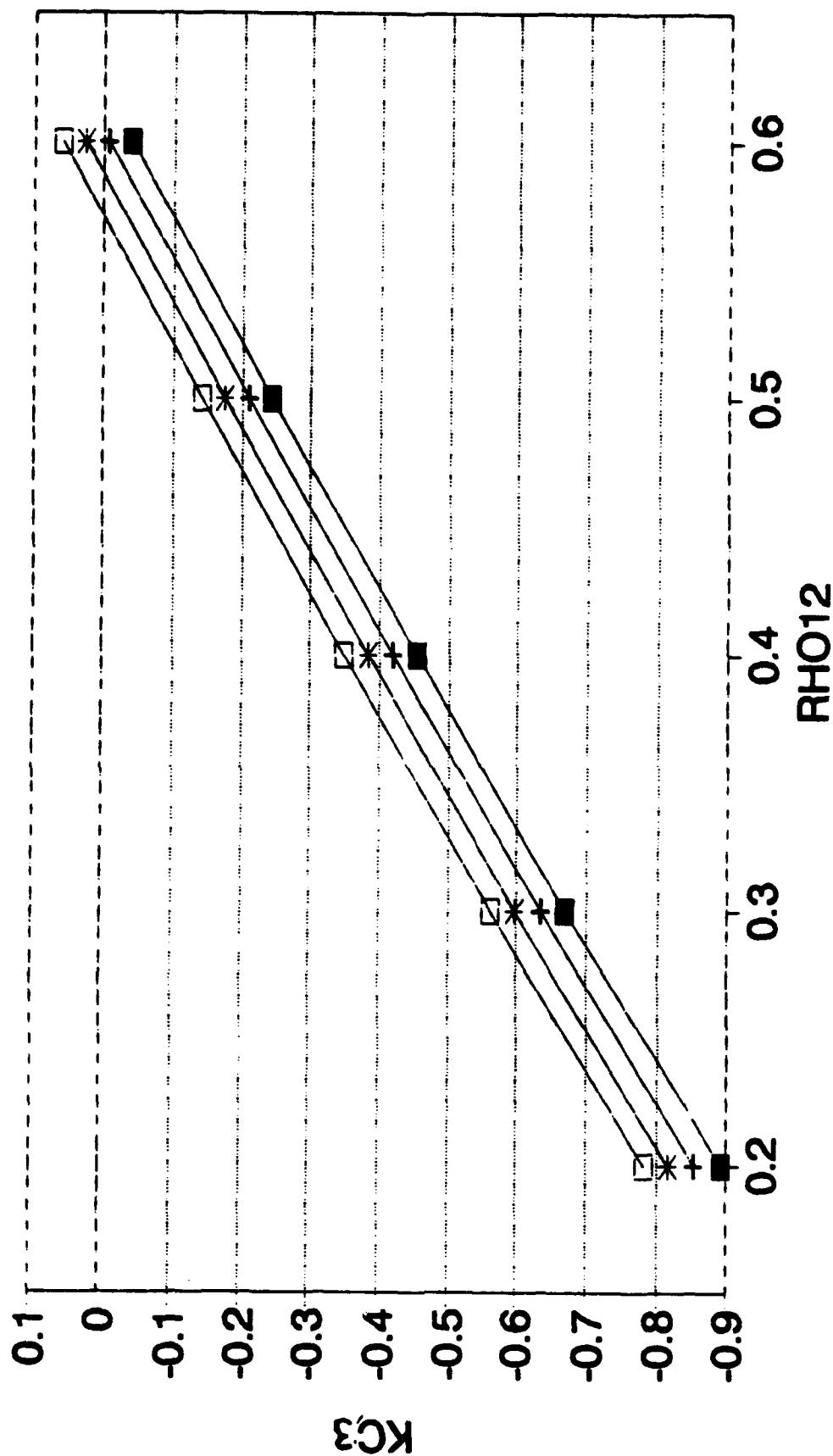
KC2 VS RHO12
R2=.6,R3=.3,RHO23=.3
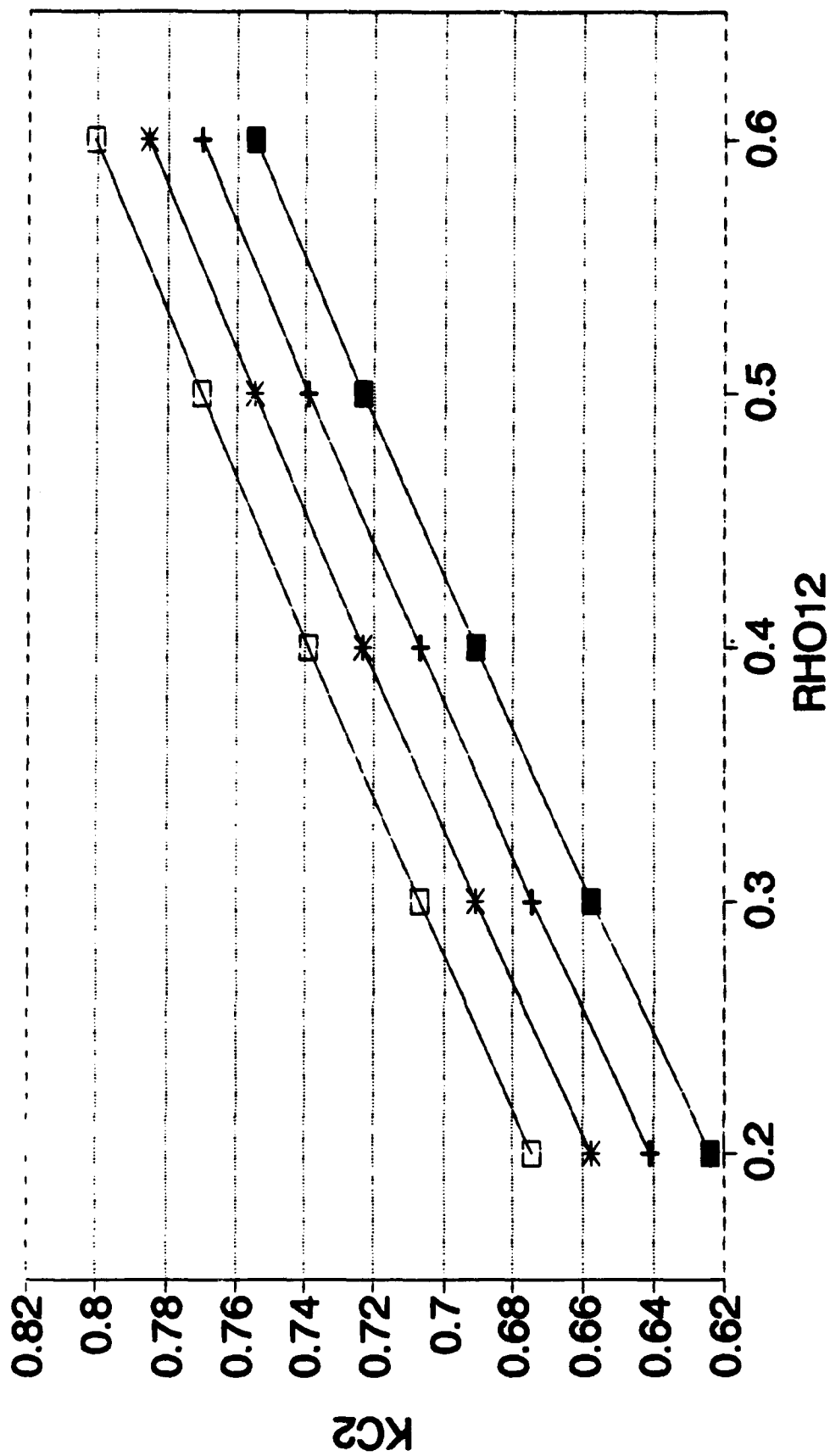
Legend: RHO13=.5 | RHO13=.6 * | RHO13=.7 | RHO13=.8 ■

KC3 VS RHO12
R2=.6,R3=.3,RHO23=.3

KC3

RHO12

RHO13=.5 RHO13=.6 RHO13=.7 RHO13=.8

KC2 VS RHO12
R2=.6,R3=.5,RHO23=.3

Legend: RHO13=.5, RHO13=.6, RHO13=.7, RHO13=.8

KC3 VS RHO12
R2=.6,R3=.5,RHO23=.3

RHO13=.5 RHO13=.6 RHO13=.7 RHO13=.8

KC2 VS RHO12
R2=.8,R3=.1,RHO23=.3

Legend: RHO13=.5 -+-   RHO13=.6 -*-   RHO13=.7 -⊞-   RHO13=.8

X-axis: RHO12
Y-axis: KC2
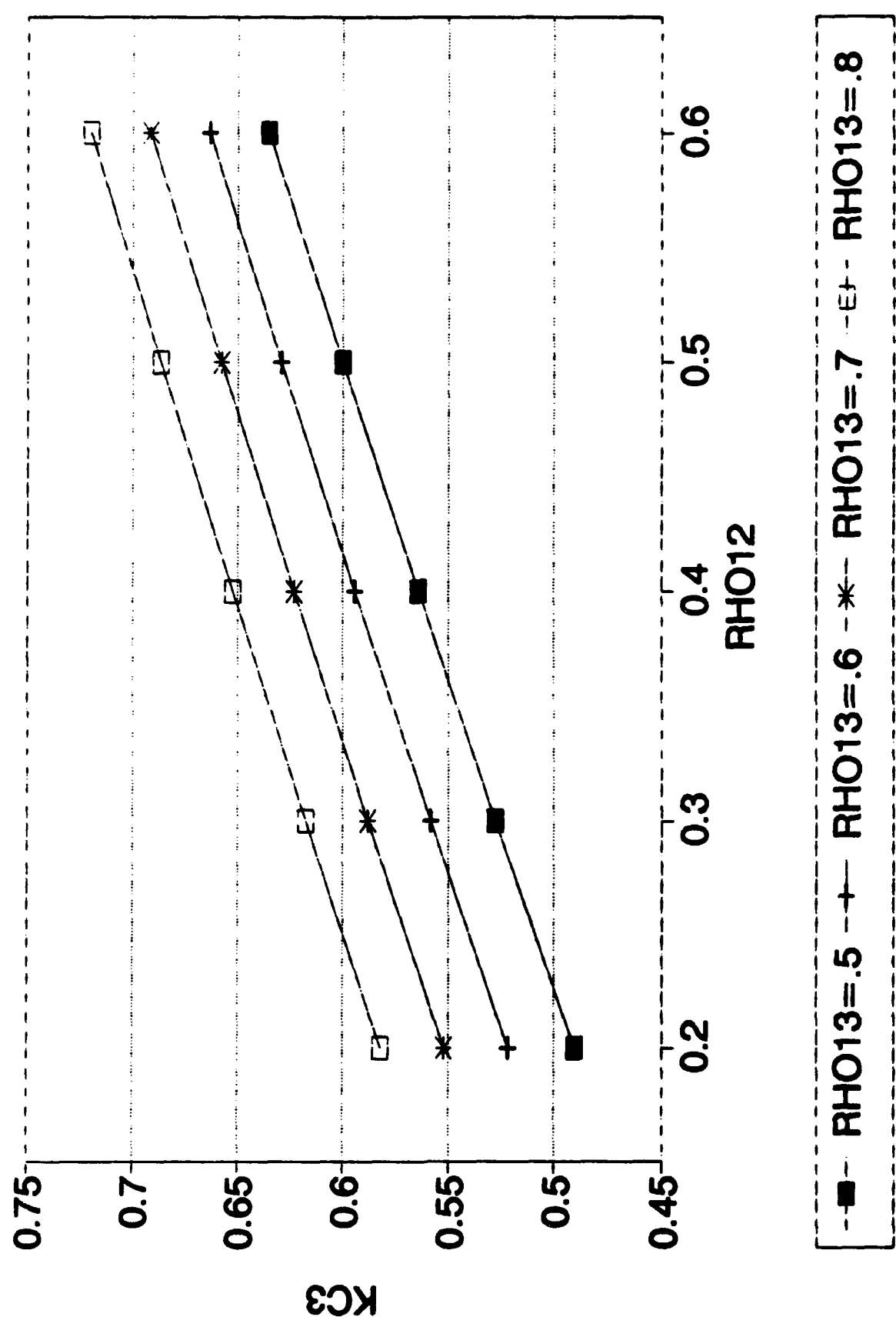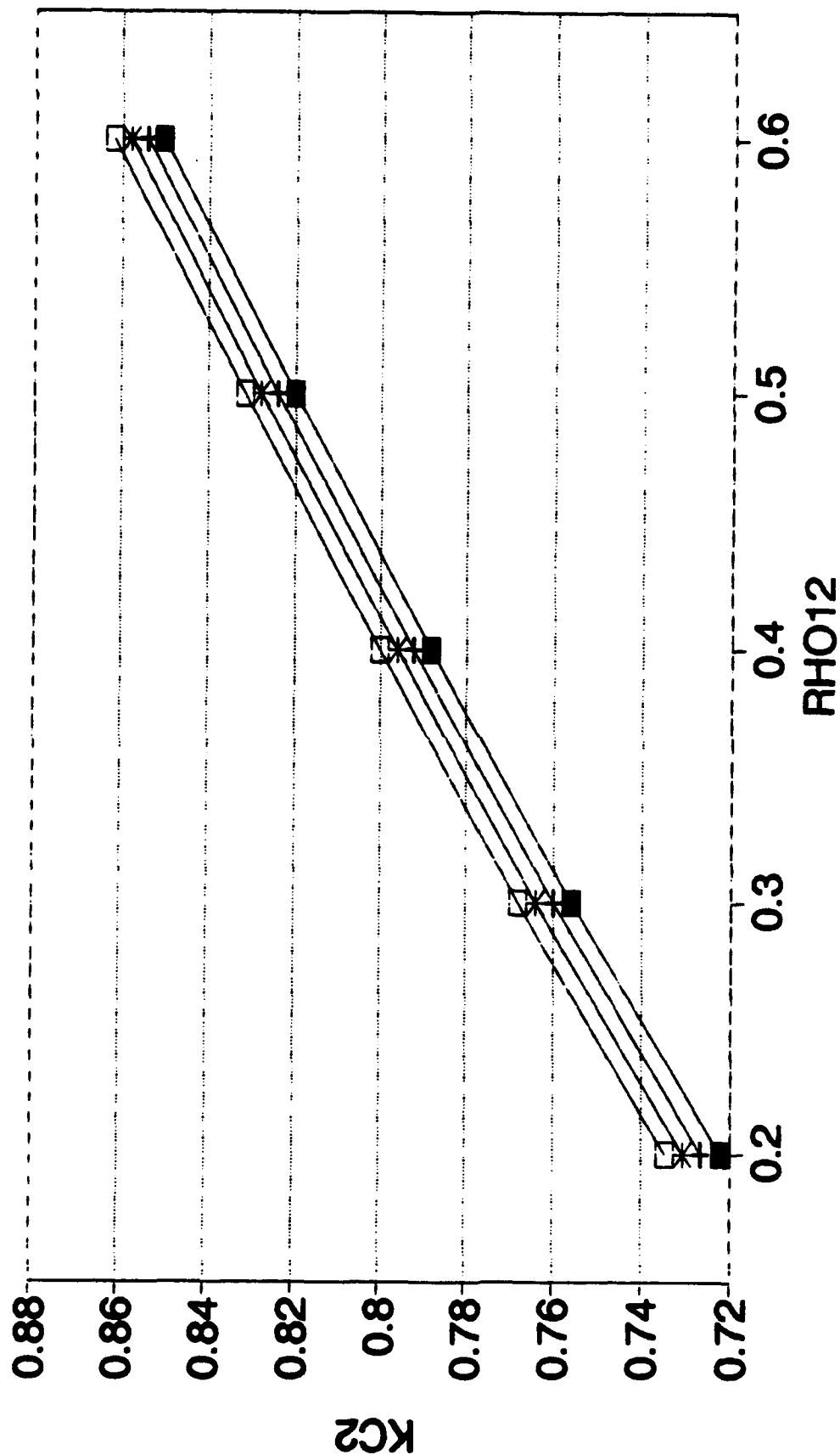
KC3 VS RHO12
R2=.8,R3=.1,RHO23=.3

RHO12

KC3
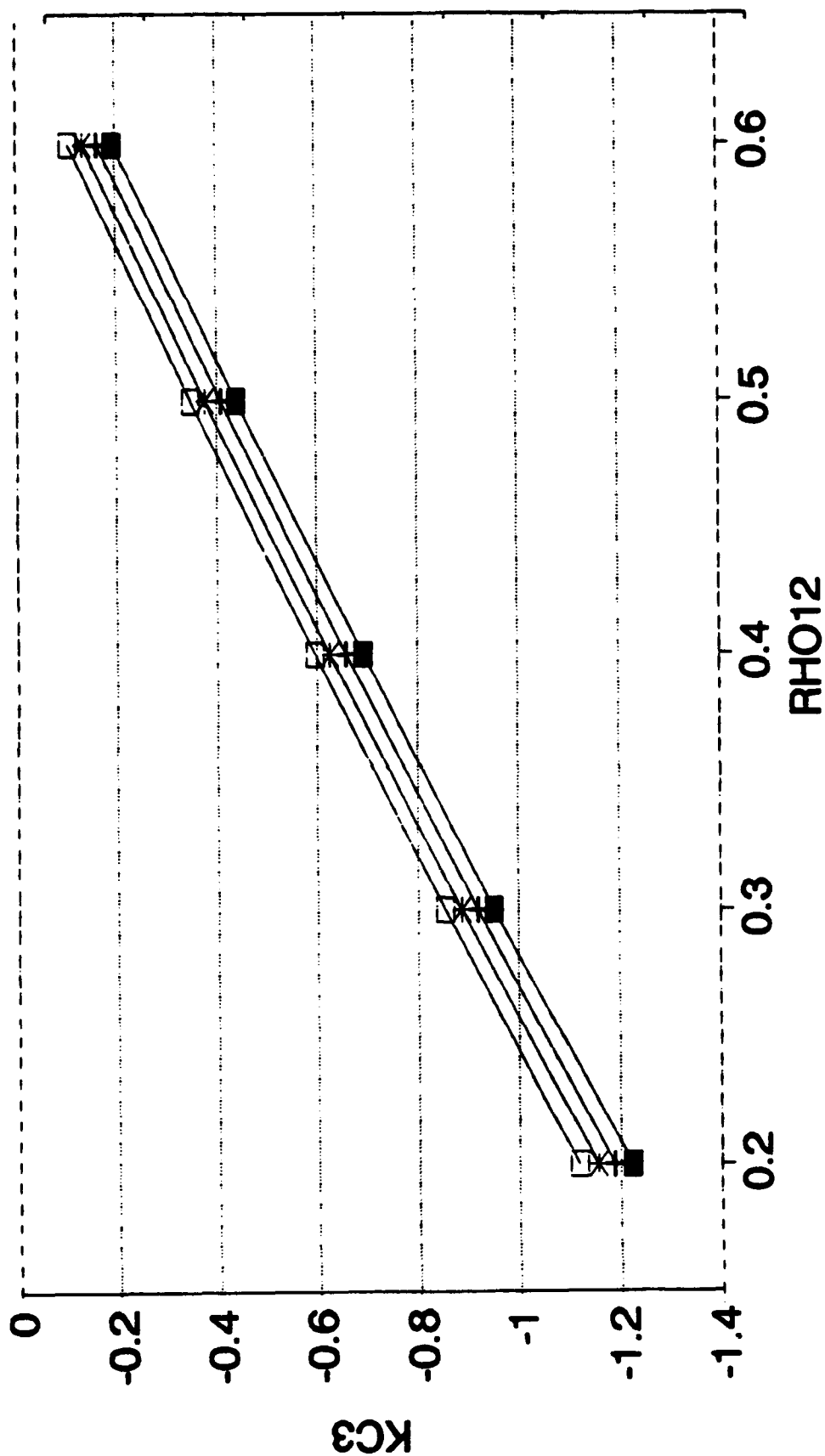
RHO13=.5 -+- RHO13=.6 -*- RHO13=.7 -⊟- RHO13=.8

KC2 VS RHO12
R2=.8,R3=.3,RHO23=.3

KC2 vs RHO12 plot with axes: y-axis KC2 (0.66 to 0.84), x-axis RHO12 (0.2 to 0.6). Legend: RHO13=.5, RHO13=.6, RHO13=.7, RHO13=.8
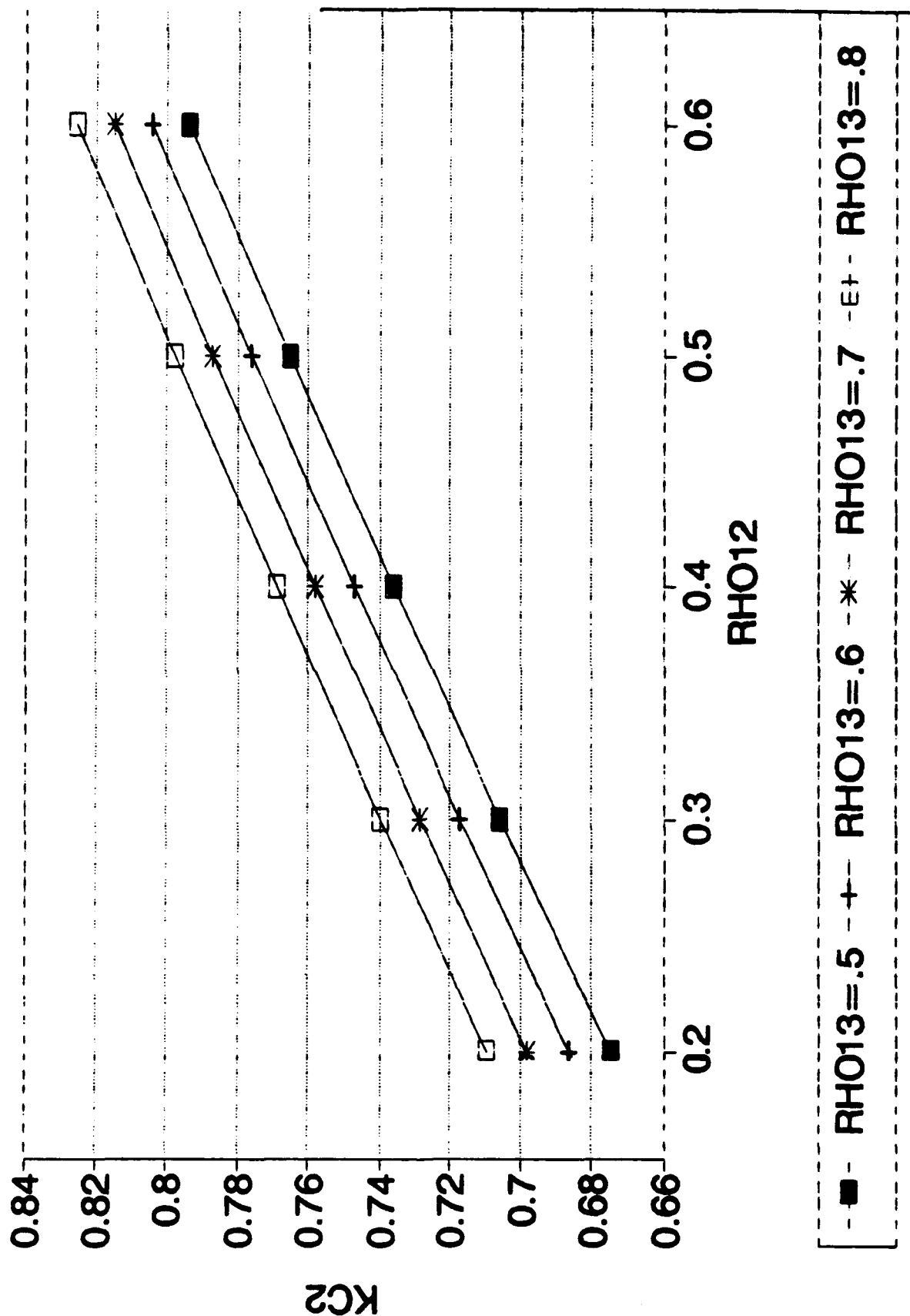
KC3 VS RHO12

P2=.8,R3=.3,RHO23=.3

Legend: RHO13=.5, RHO13=.6, RHO13=.7, RHO13=.8

X-axis: RHO12

Y-axis: KC3
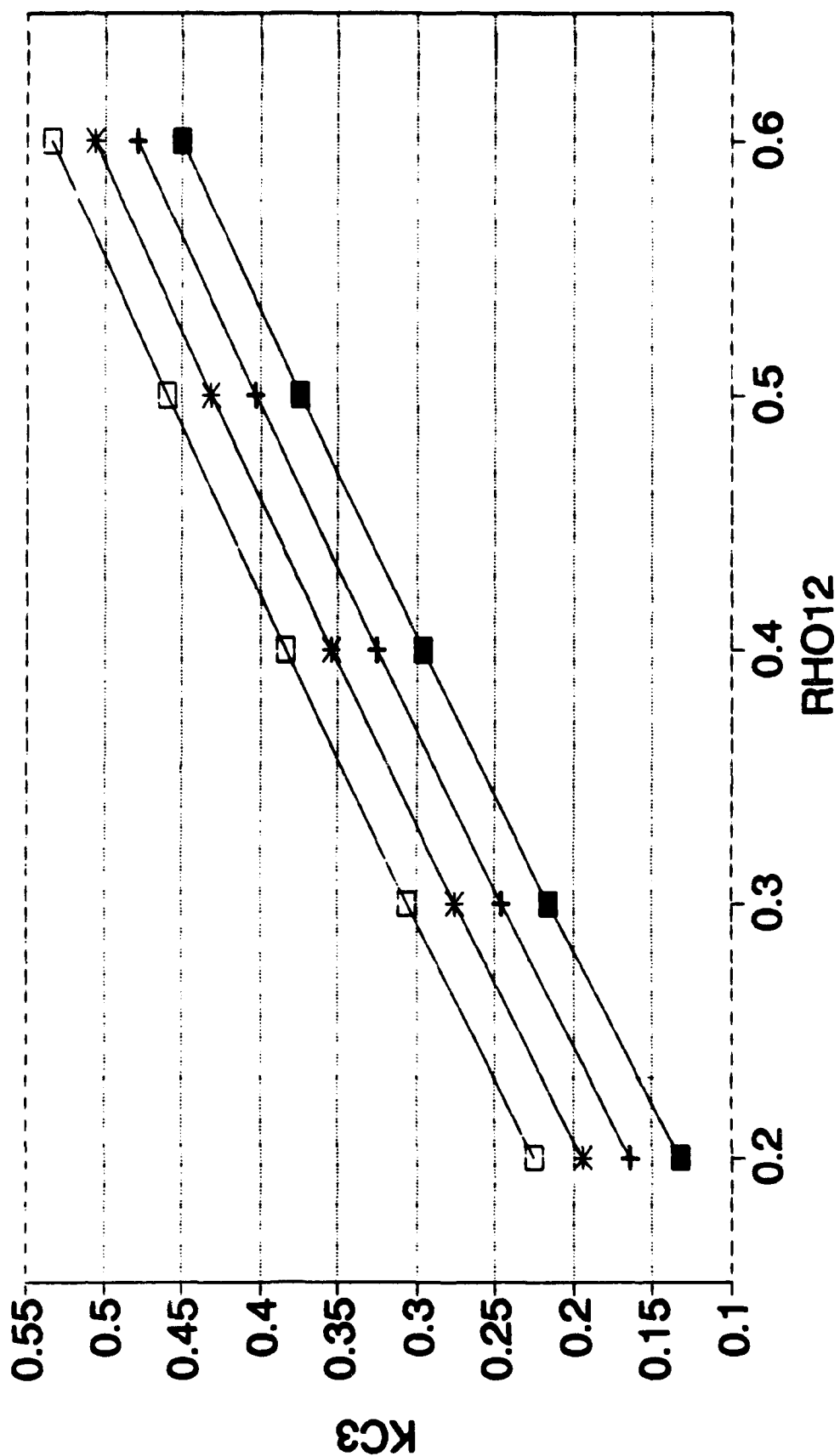
KC2 VS RHO12
R2=.8,R3=.5,RHO23=.3
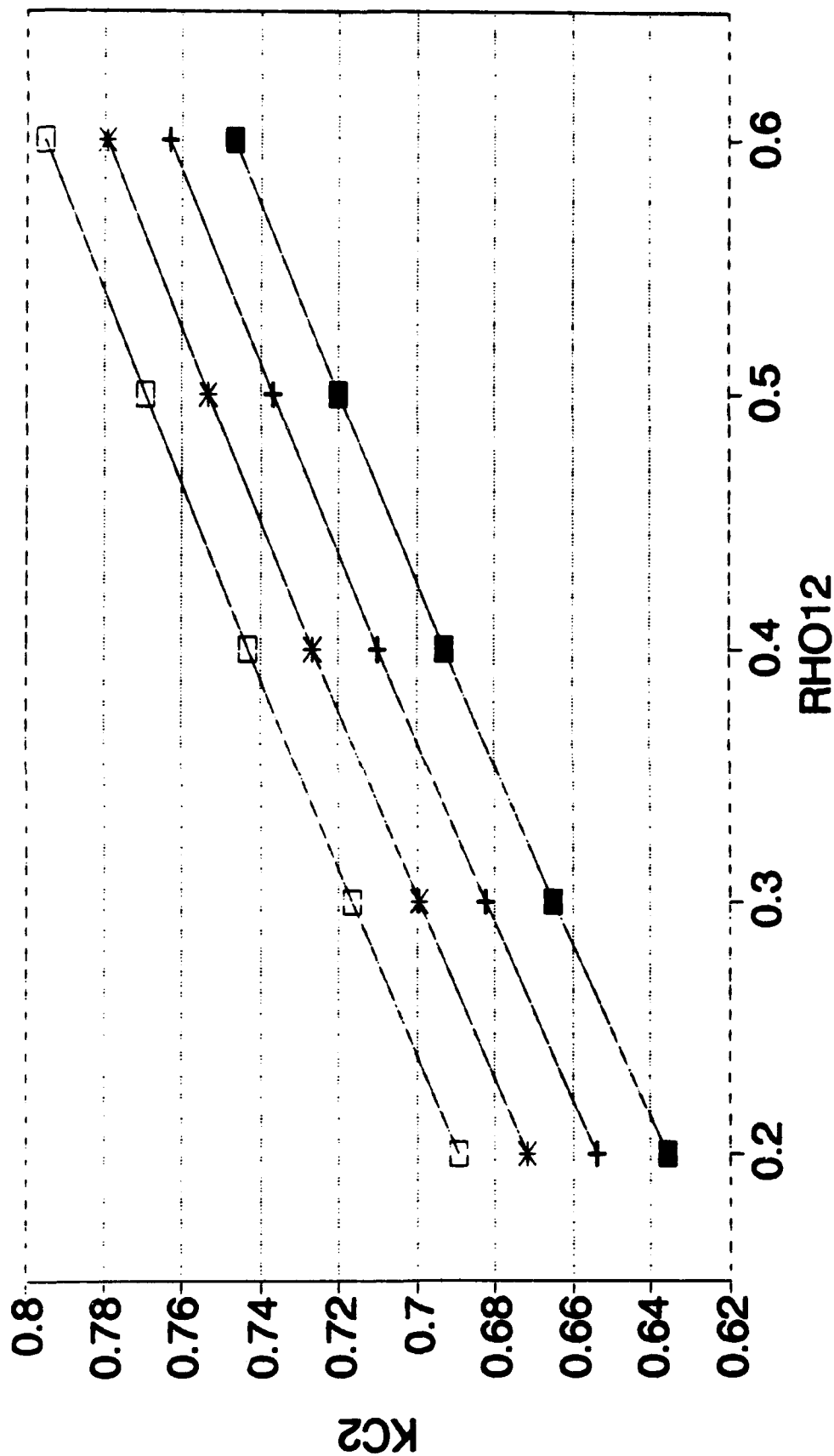
RHO13=.5 — + — RHO13=.6 — * — RHO13=.7 — □ — RHO13=.8

KC3 VS RHO12
R2=.8,R3=.5,RHO23=.3

- ■ - RHO13=.5   - + - RHO13=.6   - * - RHO13=.7   - □ - RHO13=.8

PAGE INTENTIONALLY BLANK

Project Technical Committee Members

The following persons were members of the committee that represented the Ship Structure Committee to the Contractor as resident subject matter experts. As such they performed technical review of the initial proposals to select the contractor, advised the contractor in cognizant matters pertaining to the contract of which the agencies were aware, and performed technical review of the work in progress and edited the final report.

Robert Sielski – Chairman   Naval Sea Systems Command

Alan Engle   Naval Sea Systems Command

Gary Larimer   U. S. Coast Guard

Robert Sedat   U. S. Coast Guard

Key Chang   U. S. Coast Guard

Fred Seibold   Maritime Administration

Richard Sonnenschein   Maritime Administration

Paul Gilmour   Maritime Administration

Patrick Naughton   Military Sealift Command

John Baxter   American Bureau of Shipping

Neil Pegg   Defence Research Establishment Atlantic, Canada

Yi Kwei Wen   University of Illinois

Mr. William Siekierka   Naval Sea Systems Command,
                                        Contracting Officer's
                                        Technical Representative

Mr. Alex Stavovy   National Academy of Science,
                                        Marine Board Liaison

CDR Mike Parmelee   U.S. Coast Guard, Executive Director
CDR Steve Sharpe   Ship Structure Committee

SHIP STRUCTURE COMMITTEE PUBLICATIONS

SSC-354   Structural Redundancy for Discrete and Continuous Systems by P. K. Das and J. F. Garside 1990

SSC-355   Relation of Inspection Findings to Fatigue Reliability by M. Shinozuka 1989

SSC-356   Fatigue Performance Under Multiaxial Load by Karl A. Stambaugh, Paul R. Van Mater, Jr., and William H. Munse 1990

SSC-357   Carbon Equivalence and Weldability of Microalloyed Steels by C. D. Lundin, T. P. S. Gill, C. Y. P. Qiao, Y. Wang, and K. K. Kang 1990

SSC-358   Structural Behavior After Fatigue by Brian N. Leis 1987

SSC-359   Hydrodynamic Hull Damping (Phase I) by V. Ankudinov 1987

SSC-360   Use of Fiber Reinforced Plastic in Marine Structures by Eric Greene 1990

SSC-361   Hull Strapping of Ships by Nedret S. Basar and Roderick B. Hulla 1990

SSC-362   Shipboard Wave Height Sensor by R. Atwater 1990

SSC-363   Uncertainties in Stress Analysis on Marine Structures by E. Nikolaidis and P. Kaplan 1991

SSC-364   Inelastic Deformation of Plate Panels by Eric Jennings, Kim Grubbs, Charles Zanis, and Louis Raymond 1991

SSC-365   Marine Structural Integrity Programs (MSIP) by Robert G. Bea 1992

SSC-366   Threshold Corrosion Fatigue of Welded Shipbuilding Steels by G. H. Reynolds and J. A. Todd 1992

SSC-367   Fatigue Technology Assessment and Strategies for Fatigue Avoidance in Marine Structures by C. C. Capanoglu 1993

SSC-368   Probability Based Ship Design Procedures: A Demonstration by A. Mansour, M. Lin, L. Hovem, A. Thayamballi 1993

SSC-369   Reduction of S-N Curves for Ship Structural Details by K. Stambaugh, D. Lesson, F. Lawrence, C-Y. Hou, and G. Banas 1993

SSC-370   Underwater Repair Procedures for Ship Hulls (Fatigue and Ductility of Underwater Wet Welds) by K. Grubbs and C. Zanis 1993

SSC-371   Establishment of a Uniform Format for Data Reporting of Structural Material Properties for Reliability Analysis by N. Pussegoda, L. Malik, and A. Dinovitzer 1993

None   Ship Structure Committee Publications – A Special Bibliography